Development of novel fertilizer manufacturing processes using human urine

Prepared by:
Caitlin Courtney
CRTCAI001

Supervised by:
Associate Professor Dyllon Randall

Degree of
Doctor of Philosophy (PhD)
Department of Civil Engineering
University of Cape Town December 2020

This research was financially supported by the Water Research Commission of South Africa, the National Research Foundation of South Africa, and the Royal Society (FLAIR fellowship awarded to Dyllon Randall). The financial support from the University of Cape Town, the Annette Campbell White Scholarship, and the David and Elaine Potter Fellowship are also gratefully acknowledged.

Declaration

I, Caitlin Courtney, know that plagiarism is wrong. Plagiarism is to use another's work and pretend that it is one's own. I hereby declare that the work on which this thesis based is my own original work, in both conception and execution and that neither the whole work nor any part of it has been, is being, or is to be submitted for another degree in this or any other university.

I have used the Harvard (UCT, Author-date) convention for citation and referencing. Each contribution to, and quotation in, this thesis proposal from the work(s) of other people has been attributed and has been cited, and referenced.

This thesis/dissertation has been submitted to Turnitin module (or an equivalent similarity and originality checking software. I confirm that my supervisor has seen my report and any concerns revealed by such have been resolved with my supervisor.

I have not allowed and will not allow anyone to copy my work with the intention of passing it off as their own work.

Signature Signed by candidate

Date: 10/09/2022

Acknowledgements

To my supervisor, Associate Professor Dyllon Randall. Thank you to replying to my email four years ago and taking a chance on me as a postgraduate student. I couldn't have asked for a more passionate and invested supervisor. You are a trail blazer in your field, and I am honoured to be your first PhD student. You have provided me with so many opportunities and have pushed me beyond my wildest dreams and for this I will always be grateful.

This research would not have been successful without the support of the Water Quality Lab team. Thank you, Njabulo Thela, and Hector Mafungwa as well as the numerous undergraduate and postgraduate students over the years that made the lab an enjoyable place to work even after many long hours.

To Charles Nicholas, Ameen Jackoet, Curwin Nomdoe thank you for all your technical assistance and help with building my reverse osmosis system and all its data logging components.

Thank you to Nico Fischer, Rachel Cupido, Miranda Waldron, and Cesarina Edmonds-Smith for all your help with XRD, SEM, and HPLC analysis.

Thank you to all the urine donors, unfortunately I can't thank you by name since donation was anonymous, but you know who you are.

Thank you to all my friends, who told people I was making pee-bricks when I wasn't…Heather, I'm looking at you. Camille, Brad, Shane, Carina, and Gerhard thanks for making the weekends so much fun after many long hours in the lab.

To my adopted family Tian, Susan, Harry, Jess, Johan, Karien, Marli, and Siegie. You guys are my home away from home. You have made me feel a part of the family from day one and supported and cheered me every step of the way. Thank you. I am so lucky to have you all in my life.

To my family, Greg, Jane, and Peter. Thank you for all your emotional and unwavering support. For telling me that I can achieve anything (even though you're my parents so you have to say that). Mom and Dad, you have provided me with every opportunity, my success would not have been possible without you. I am a strong independent woman in STEM because you told me I could be.

Ralph, you can't read this because you're a dog, but thank you for all the cuddles and for helping me through all the tough times. For taking me on walks when I was stressed and always providing a little serotonin boost by just existing. You deserve an honorary PhD in my eyes.

Finally, to my partner Niel, I've taken an unusual path. You've only ever been supportive. I am so grateful for my life with you. There aren't enough words for everything you've done. Thank you for being part of this PhD adventure with me. I also appreciate that you let me keep a urinal in our flat during COVID.

Publications list

I confirm that I have been granted permission by the University of Cape Town's Doctoral Degrees Board to include the following publications in my Ph.D. thesis, and where co-authorships are involved, my co-authors have agreed that I may include the publications:

Paper 1: Courtney, C. and Randall, D.G., 2021. Precipitation to remove calcium ions from stabilized human urine as a pre-treatment for reverse osmosis. Water Science and Technology, 84(12), pp.3755-3768.

Paper 2: Courtney, C., Brison, A., and Randall, D.G. 2021. Calcium removal from stabilized human urine by air and CO_2 bubbling. Water Research 202, 117467.

Paper 3: Courtney, C. and Randall, D.G. 2022. Concentrating stabilized urine with reverse osmosis: How does stabilization method and pre-treatment affect nutrient recovery, flux, and scaling? Water Research, 209, 117970.

Paper 4: Courtney, C and Randall, D. 2022. A hybrid nanofiltration and reverse osmosis process for urine treatment: Effect on urea recovery and purity. Water Research 222, 118851.

Paper 5: Courtney, C and Randall, D. 2022. Concentrating stabilized urine using eutectic freeze crystallization for liquid fertilizer production. Water Research 223, 119760.

Signature: _____ **Date:** 10/09/2022

Student Name: Caitlin Emily Courtney **Student Number:** CRTCAI001

Abstract

Over 20 years of research on how to integrate and normalize urine as a resource has been conducted, including topics such as source-separation, fertilizer effectivity, public perception, and logistics. Another important aspect is the urine treatment method and how resources are recovered. This is because urine is 97% water, making the logistics of using urine as a fertilizer challenging. In addition, without treatment, the major nitrogen source in urine (urea) breaks down to ammonia and is lost to the atmosphere. This thesis investigated the technical feasibility of using different membrane and freezing techniques to concentrate and recover nutrients from human urine. It assessed different stabilization methods (to prevent urea breakdown), pre-treatment techniques, and process configurations to produce fertilizer products with different compositions.

To prevent urea degradation and subsequent ammonia volatilization during the collection phase, urine was 'stabilized' by adding an acid (citric acid) or a base ($Ca(OH)_2$). The addition of $Ca(OH)_2$ resulted in a saturated solution which would scale the RO membrane during concentration. Paper 1 and Paper 2 investigated two pre-treatment methods and showed that chemical addition ($NaHCO_3$) and air bubbling can remove 85-98% of the excess calcium ions from the solution, thus significantly reducing potential RO membrane scaling during concentration. The calcium concentration in urine after stabilization varies based on urine composition. To minimize the addition of unwanted sodium ions, an equimolar dose of $NaHCO_3$ is required. In Paper 1 it was determined that this dose (± 5%) could be determined by using conductivity as a proxy for calcium concentrations to help determine the required chemical dosage. In Paper 2, a model was developed to better understand the mechanisms of CO_2 dissolution and $CaCO_3$ precipitation. This model was used to optimize the time required to precipitate the maximum $CaCO_3$ as well as the energy required to operate the air blower.

In Paper 3, acid and base-stabilized urine were both concentrated using RO, and the two stabilization methods were compared. It was determined that membrane processes are not ideal for urine stabilized with an acid. This was due to the potential crystallization of uric acid dihydrate crystals which resulted in membrane scaling during concentration. Both pre-treatment methods for $Ca(OH)_2$ stabilized urine were found to be equally effective at preventing membrane scaling and significantly improved flux and ion rejection. Air bubbling was chosen as the preferred pre-treatment method as it does not add additional ions (Na^+), it reduces the urine pH to within the operating range of most common RO membranes (2-11), and it sequesters CO_2 from the atmosphere. Reverse osmosis was successfully used to remove 60% of the water from real urine stabilized with $Ca(OH)_2$ and pre-treated with air bubbling. The process recovered 85.5% of the urea and 98% of the potassium in the brine stream. Water removal was further improved to 70% with 79.5% of the urea and 98% of the potassium being recovered in the brine stream. This process produced a fertilizer with an N content of 1.9% and a K content of 0.5%.

While RO is effective at concentrating stabilized urine, it also concentrates undesirable salts and pharmaceuticals together with desired fertilizer components. In Paper 4, the feasibility of nanofiltration (NF) as a pre-treatment to remove pharmaceuticals and salts was thus investigated. Two types of NF membranes were tested, a loose NF and a tight NF membrane. The NF permeate was then further concentrated with seawater RO membranes as described in Paper 3. A hybrid loose NF-RO configuration could remove 80% of water, more than 70% of the pharmaceuticals, 78% of the organics, and 44% of the total ions, however, urea recovery was only 56%. A tight NF-RO configuration could remove 80% of water, 90% of the organics, more than 99% of the pharmaceuticals, and 66% of the total ions, however, urea recovery was only 32.8%. Based on an economic analysis it is unlikely that the increased value of the product (due to increased purity) outweighs the additional cost of this pre-treatment step.

In Paper 5, eutectic freeze concentration (EFC) was investigated to further concentrate the RO brine (70% water removal), whilst simultaneously crystallizing undesirable salts, as this treatment method is not affected by membrane scaling. It was experimentally shown that at eutectic conditions, $Na_2SO_4 \cdot 10H_2O$ crystallizes simultaneously with ice. A theoretical mass balance of the RO-EFC process, including ice washing and recycle streams, showed that 77% of the urea and 96% of the potassium could be recovered with a 95% water removal. Over 98% of the phosphorus would be recovered as calcium phosphate during the urine stabilization step. The final liquid fertilizer would have a composition of 11.5% N and 3.5% K, and 3.5 kg of $Na_2SO_4 \cdot 10H_2O$ would theoretically be recovered from 1000 kg of urine. This research was the first to experimentally show that EFC can be used to concentrate human urine whilst simultaneously crystallizing salts.

A high-level economic analysis showed that RO treatment processes have the lowest energy requirements (16 kWh m^{-3}, 70% water removal), followed by freeze concentration (119-162 kWh m^{-3}, 70-95% water removal), and lastly evaporative processes (154 -198 kWh m^{-3}, >95% water removal) which required the most energy. The fertilizer produced can either be sold as a niche (home gardening) or bulk (large agricultural) fertilizer. The size of the niche fertilizer market is important when determining a preferred treatment method. Assuming a feed supply of 7.5m^3 urine per week, for a market size where only 0.14 m^3 per week of niche fertilizer can be sold, RO-EFC produced the product with the highest value at R73 000. Alternatively, if the market size was 2 m^3 per week, RO had the highest value product at R304 000.

Treatment methods that produce a product with a higher nutrient content are preferred as bulk fertilizers. When selling fertilizers in bulk high density nutrient content is important to reduce transportation costs. For example, transport of the RO fertilizer, 75 km to farmland, would account for 3.2% of the gross fertilizer value whilst only 0.8% of the fertilizer value for the RO-EFC. The feed volume of urine required to make sufficient fertilizer for a small 20 ha wine farm using the alkaline dehydration treatment is 145 m^3 which would take 19 weeks to collect from 8 shopping centers. This bulk fertilizer

has a value of R76 000 compared to 0.14 m^3 of niche RO-EFC fertilizer which has a potential value of R73 000. It would take less than a week to collect enough urine to produce the niche RO-EFC fertilizer. At this stage, focusing on the niche fertilizer market would be more profitable. It also indicates that urine collection and treatment need to become more mainstream and normalized before significant replacement of commercial synthetic fertilizers can be achieved.

A membrane process with a variety of configurations can be used to concentrate human urine to produce a liquid fertilizer. Each configuration produces a product with a different composition and a commercial fertilizer with a comparable composition for each product could be found at a local garden center in Cape Town. However, the preferred treatment choice will be dependent on several factors such as process CAPEX and OPEX, fertilizer intended use (ornamental plants versus edible crops), the market size, the associated fertilizer regulations, and the scale at which urine collection is conducted.

Overall, this work has shown that membrane processes can be used to concentrate stabilized urine whilst still achieving high urea (>79.5%) recovery and water removal (70%). This allows for significant scalability of urine treatment processes using RO membranes as this technology is already widely used to treat both brackish water and sea water at varying scales. However, not all urine stabilization methods are suitable for use before RO concentration. This research was the first to determine that acid stabilization results in the crystallization of uric acid dihydrate which would scale RO membranes and reduce efficiency. This research was also the first to show that EFC can be used to simultaneously crystallize ice and salts from real human urine that has been pre-concentrated with RO (70% water removal). The work also demonstrates how hybrid configurations, combining various urine concentration methods, can be used to produce products with different compositions and urea purity. Ultimately, this novel research makes a valuable contribution to the growing field of urine treatment and resource recovery.

Table of contents

List of figures

List of tables

CHAPTER 1: INTRODUCTION

CHAPTER 1: INTRODUCTION

Urine is rich in three key components required for fertilizer production: nitrogen (N), phosphorus (P), and potassium (K). As a result, significant research has been conducted over the past twenty years investigating the potential of using urine as a sustainable alternative to synthetic fertilizers as well as the processes required to make this feasible (Larsen et al., 2021b). Important considerations for this to happen include source separation and urine collection (Flanagan and Randall, 2018; Gundlach et al., 2021), urine-derived fertilizer effectivity (Martin et al., 2022), public perception (Simha et al., 2018), stabilization and disinfection (Herraiz-Carboné et al., 2021; Randall et al., 2016), transport logistics and economics (Chipako and Randall, 2020a), and technologies for nutrient recovery (Larsen et al., 2021b).

Producing fertilizers from urine provides a sustainable alternative to the current status quo for several reasons. Approximately 85% of the N in human urine is in the form of urea (Udert et al., 2006). Urea accounts for more than 50% of global N-fertilizer (Glibert et al., 2006) and an estimated 211 million tons were produced in 2019 (Heffer and Prud'homme, 2015). Synthetic urea production relies on a complex reaction between ammonia (NH_3) and carbon dioxide (CO_2) at high temperatures (150-200°C) and pressures (150-250 bar) (Meessen, 2014) requiring significant energy input (54 MJ kg-N^{-1}) (Patyk and Reinhardt, 1997). Furthermore, the feedstock for urea production, NH_3, is made using the Haber-Bosch process, which is responsible for 1.2% of global anthropogenic CO_2 emissions (Nørskov et al., 2016). Phosphorus is also essential for plant growth (Malhotra et al., 2018) and is mined from phosphate rock, a non-renewable source (Cordell et al., 2011). The majority (>70%) of global P is mined in Morocco (Jasinski, 2009) and Cordell (2013) warns that this could potentially result in food security risks. Furthermore, the phosphorus mining process is not without its environmental drawbacks. The process produces waste products (sludge) that can cause pollution and the accumulation of these products leads to storage problems, reduction of arable land, and the disfigurement of local landscapes (Hakkou et al., 2016).

Current population numbers could not be sustained without the food security provided by fertilizer-based agriculture (Smil, 2011), and with world populations expected to increase by 35% in the next 40 years, our dependency on fertilizer will only increase further (Stewart and Roberts, 2012). Whilst there has been extensive research to produce NH_3 under milder conditions with cleaner energy (Chen et al., 2020), recovering urea and phosphorus from urine could potentially provide a simpler alternative.

The dichotomy of fertilizer nutrients (specifically N and P) is that while they are both essential for plant life to thrive, they are also toxic to the environment when present in excess (Britto and Kronzucker, 2002), and can lead to hypoxia and eutrophication if they accumulate in water bodies. Wastewater treatment plants (WWTP) were designed to treat domestic wastewater and remove these 'pollutants' (N and P) such that the treated wastewater could be safely discharged back into the environment (Daigger, 2009). However, the majority of global wastewater (80%) is not treated adequately, nor reused (Connor et al., 2017). Furthermore, most of the N (56%) and P (63%) in domestic wastewater requiring treatment

are from the urine fraction, but the urine contributes only 1% of the total domestic wastewater volume (Höglund, 2001). Wastewater treatment plants using biological treatment efficiently remove N and P, however, they contribute approximately half of a WWTP's energy demand (Wilsenach and Van Loosdrecht, 2004). Maurer et al. (2003) estimate that WWTPs use 49 and 45 MJ/kg is required for denitrification and P-precipitation, respectively, and the N and P are usually not recovered. In addition, 35-50 L of drinking water per person per day is used for toilet-flushing, contributing up to 25% of a person's daily wastewater production (Höglund, 2001).

In the nineties, these aspects led to research on the concept of source-separation, whereby different fractions of domestic wastewater are collected separately at the source (Jönsson et al., 1997; Larsen and Gujer, 1996) such that they can be treated to recover different nutrients (Larsen et al., 2013) with many additional benefits. For example, Wilsenach and Van Loosdrecht (2004) estimated that if 75% of urine was source-separated, chemical sludge production at WWTPs would decrease by 30% and the capacity of the plant could increase by as much as 60%. In addition, WWTPs would also become net energy producers (Wilsenach and van Loosdrecht, 2006).

The development of viable source-separation methods such as waterless urinals (Flanagan and Randall, 2018) and no-mix toilets with dual plumbing (Gundlach et al., 2021), are helping advance the field of source separation and urine recycling. Public perception of urine recycling has also reported predominantly positive outlooks (Simha et al., 2018). Urine recycling projects have been conducted at a municipality level in Durban, South Africa (Mkhize et al., 2017) and Tanum, Sweden (Kvarnström et al., 2006), but it has not yet reached mainstream implementation. This is likely because urine is largely water (97%), and the cost of large-scale collection and transportation from urban to agricultural areas is not always economical (Chipako and Randall, 2020a). Whilst it is common to apply urine directly to land as a fertilizer in some rural communities (Udert and Wächter, 2012), on a commercial scale this would be more challenging. This has led to the investigation of a variety of methods (of varying complexity) to remove the water and concentrate urine. These methods include evaporation (Simha et al., 2020a; Udert and Wächter, 2012), freeze concentration (Lind et al., 2001; Randall and Nathoo, 2018), electrodialysis (Pronk et al., 2006b), membrane distillation (Zhao et al., 2013), forward osmosis (Ray et al., 2019; Volpin et al., 2019a), and reverse osmosis.

However, many of these technologies are still being tested at the laboratory scale or are being designed for treatment at the toilet/household level. Wald (2022) in the journal *Nature* wrote, "Separating pee from the rest of sewage could mitigate some difficult environmental problems and provide a sustainable source of fertilizer. But there are big obstacles to radically re-engineering one of the most basic aspects of life." This thesis aims to address these gaps by developing a novel integrated urine treatment process to produce liquid fertilizers.

REFERENCES

Britto, D.T. and Kronzucker, H.J. 2002. NH4+ toxicity in higher plants: a critical review. Journal of plant physiology 159(6), 567-584.

Chen, C., Zhu, X., Wen, X., Zhou, Y., Zhou, L., Li, H., Tao, L., Li, Q., Du, S., and Liu, T. 2020. Coupling N2 and CO2 in H2O to synthesize urea under ambient conditions. Nature Chemistry 12(8), 717-724.

Chipako, T. and Randall, D. 2020. Investigating the feasibility and logistics of a decentralized urine treatment and resource recovery system. Journal of Water Process Engineering 37, 101383.

Connor, R., Renata, A., Ortigara, C., Koncagül, E., Uhlenbrook, S., Lamizana-Diallo, B.M., Zadeh, S.M., Qadir, M., Kjellén, M. and Sjödin, J. 2017. The united nations world water development report 2017. wastewater: the untapped resource. The United Nations World Water Development Report, New York, USA.

Cordell, D. (2013) Source Separation and Decentralisation for Wastewater Management. Larsen, T.A., Udert, K.M. and Lienert, J. (eds), IWA Publishing, London, England.

Cordell, D., Rosemarin, A., Schröder, J. and Smit, A. 2011. Towards global phosphorus security: A systems framework for phosphorus recovery and reuse options. Chemosphere 84(6), 747-758.

Daigger, G.T. 2009. Evolving urban water and residuals management paradigms: Water reclamation and reuse, decentralization, and resource recovery. Water environment research 81(8), 809-823.

Flanagan, C.P. and Randall, D.G. 2018. Development of a novel nutrient recovery urinal for on-site fertilizer production. Journal of Environmental Chemical Engineering 6(5), 6344-6350.

Glibert, P.M., Harrison, J., Heil, C. and Seitzinger, S. 2006. Escalating worldwide use of urea–a global change contributing to coastal eutrophication. Biogeochemistry 77(3), 441-463.

Gundlach, J., Bryla, M., Larsen, T.A., Kristoferitsch, L., Gründl, H. and Holzner, M. 2021. Novel NoMix toilet concept for efficient separation of urine and feces and its design optimization using computational fluid mechanics. Journal of Building Engineering 33, 101500.

Hakkou, R., Benzaazoua, M. and Bussière, B. 2016. Valorization of phosphate waste rocks and sludge from the Moroccan phosphate mines: challenges and perspectives. Procedia Engineering 138, 110-118.

Heffer, P. and Prud'homme, M. 2015. Fertilizer outlook 2015–2019. 83rd IFA Annual Conference, Istanbul, Turkey. Istanbul, Turkey, 25-27 May.

Herraiz-Carboné, M., Cotillas, S., Lacasa, E., Cañizares, P., Rodrigo, M.A. and Sáez, C. 2021. Enhancement of UV disinfection of urine matrixes by electrochemical oxidation. Journal of Hazardous Materials 410, 124548.

Höglund, C. (2001) Evaluation of microbial health risks associated with the reuse of source-separated humna urine. Doctoral thesis, Bioteknologi, Stockholm.

Jasinski, S.M. 2009. Phosphate rock, mineral commodity summaries. US Geological Survey, January.

Jönsson, H., Stenström, T.-A., Svensson, J. and Sundin, A. 1997. Source separated urine-nutrient and heavy metal content, water saving and faecal contamination. Water science and technology 35(9), 145-152.

Kvarnström, E., Emilsson, K., Stintzing, A.R., Johansson, M., Jönsson, H., af Petersens, E., Schönning, C., Christensen, J., Hellström, D. and Qvarnström, L. (2006) Urine diversion: one step towards sustainable sanitation, EcoSanRes Programme.

Larsen, T.A. and Gujer, W. 1996. Separate management of anthropogenic nutrient solutions (human urine). Water Science and Technology 34(3-4), 87-94.

Larsen, T.A., Riechmann, M.E. and Udert, K.M. 2021. State of the art of urine treatment technologies: A critical review. Water Research X, 100114.

Larsen, T.A., Udert, K.M. and Lienert, J. (2013) Source separation and decentralization for wastewater management, IWA Publishing, London.

Lind, B.-B., Ban, Z. and Bydén, S. 2001. Volume reduction and concentration of nutrients in human urine. Ecological Engineering 16(4), 561-566.

Malhotra, H., Sharma, S. and Pandey, R. 2018. Plant nutrients and abiotic stress tolerance, pp. 171-190, Springer.

Martin, T.M., Esculier, F., Levavasseur, F. and Houot, S. 2022. Human urine-based fertilizers: A review. Critical Reviews in Environmental Science and Technology 52, 1-47.

Maurer, M., Schwegler, P. and Larsen, T.A. 2003. Nutrients in urine: energetic aspects of removal and recovery. Water Science and Technology 48(1), 37-46.

Meessen, J. 2014. Urea synthesis. Chemie Ingenieur Technik 86(12), 2180-2189.

Mkhize, N., Taylor, M., Udert, K.M., Gounden, T.G. and Buckley, C.A. 2017. Urine diversion dry toilets in eThekwini Municipality, South Africa: acceptance, use and maintenance through users' eyes. Journal of Water, sanitation and Hygiene for Development 7(1), 111-120.

Nørskov, J., Chen, J., Miranda, R., Fitzsimmons, T. and Stack, R. 2016 Sustainable Ammonia Synthesis–Exploring the scientific challenges associated with discovering alternative, sustainable processes for ammonia production, US DOE Office of Science, Washingto DC, USA.

Patyk, A. and Reinhardt, G.A. 1997. Düngemittel-Energie-und Stoffstrombilanzen, Springer.

Pronk, W., Palmquist, H., Biebow, M. and Boller, M. 2006. Nanofiltration for the separation of pharmaceuticals from nutrients in source-separated urine. Water Research 40(7), 1405-1412.

Randall, D.G., Krähenbühl, M., Köpping, I., Larsen, T.A. and Udert, K.M. 2016. A novel approach for stabilizing fresh urine by calcium hydroxide addition. Water Research 95, 361-369.

Randall, D.G. and Nathoo, J. 2018. Resource recovery by freezing: A thermodynamic comparison between a reverse osmosis brine, seawater and stored urine. Journal of Water Process Engineering 26, 242-249.

Ray, H., Perreault, F. and Boyer, T.H. 2019. Urea recovery from fresh human urine by forward osmosis and membrane distillation (FO–MD). Environmental Science: Water Research & Technology 5(11), 1993-2003.

Simha, P., Karlsson, C., Viskari, E.-L., Malila, R. and Vinnerås, B. 2020. Field testing a pilot-scale system for alkaline dehydration of source-separated human urine: a case study in Finland. Frontiers in Environmental Science 8, 168-178.

Simha, P., Lalander, C., Ramanathan, A., Vijayalakshmi, C., McConville, J.R., Vinnerås, B. and Ganesapillai, M. 2018. What do consumers think about recycling human urine as fertiliser? Perceptions and attitudes of a university community in South India. Water Research 143, 527-538.

Stewart, W. and Roberts, T. 2012. Food security and the role of fertilizer in supporting it. Procedia Engineering 46, 76-82.

Udert, K.M., Larsen, T.A. and Gujer, W. 2006. Fate of major compounds in source-separated urine. Water Science and Technology 54(11-12), 413-420.

Udert, K.M. and Wächter, M. 2012. Complete nutrient recovery from source-separated urine by nitrification and distillation. Water Research 46(2), 453-464.

Volpin, F., Chekli, L., Phuntsho, S., Ghaffour, N., Vrouwenvelder, J.S. and Shon, H.K. 2019. Optimisation of a forward osmosis and membrane distillation hybrid system for the treatment of source-separated urine. Separation and Purification Technology 212, 368-375.

Wald, C. 2022. The urine revolution: How recycling pee could help to save the world. Nature 602(7896), 202-206.

Wilsenach, J.A. and Van Loosdrecht, M.C.M. 2004. Effects of Separate Urine Collection on Advanced Nutrient Removal Processes. Environmental Science & Technology 38(4), 1208-1215.

Wilsenach, J.A. and van Loosdrecht, M.C.M. 2006. Integration of Processes to Treat Wastewater and Source-Separated Urine. Journal of Environmental Engineering 132(3), 331-341.

Zhao, Z.-P., Xu, L., Shang, X. and Chen, K. 2013. Water regeneration from human urine by vacuum membrane distillation and analysis of membrane fouling characteristics. Separation and Purification Technology 118, 369-376.

CHAPTER 2: LITERATURE REVIEW

CHAPTER 2: LITERATURE REVIEW

2.1 URINE CHEMISTRY

Apart from the three key fertilizer nutrients (N, P, and K), urine contains a variety of salts and organic compounds (Putnam, 1971) and has a complex chemistry. The composition of urine will vary due to diet, medication use, and water intake. Urine composition will also vary depending on if it is fresh or hydrolyzed. In fresh urine, 85% of the nitrogen is fixed in the form of urea, roughly 5% consists of ammonia, and the remainder of the nitrogen is in the form of amino acids; creatinine, hippuric acid, and uric acid (Ciba-Geigy, 1977). The term 'hydrolyzed' urine refers to urine in which urea hydrolysis occurred. Hydrolysis is the process whereby urea ($CO(NH_2)_2$) decomposes to ammonia (NH_3) and carbonic acid (H_2CO_3) as per Equation 2-1.

$$CO(NH_2)_2 + 2H_2O \rightarrow 2NH_3 + H_2CO_3 \qquad \text{(Equation 2-1)}$$

Hydrolysis can occur chemically or enzymatically. Chemical urea hydrolysis occurs at high temperatures (above 40°C) and extreme pH conditions (< 2 and >13) (Randall et al., 2022). Hydrolysis can also occur enzymatically via the enzyme urease which happens significantly quicker than chemical hydrolysis (Callahan et al., 2005). For example, the half-life of enzymatic urea hydrolysis is 0.02s, while it is 14 days for chemical urea hydrolysis at 65°C (pH > 12.5) (Senecal and Vinnerås, 2017). Numerous urease-producing bacteria have been found in human intestines (Mobley and Hausinger, 1989) and the urinary tract (McLean et al., 1988), helping drive the enzymatic urea hydrolysis process. Urease-producing bacteria are present in both faeces and urine and will cause urea hydrolysis to occur spontaneously (Hotta and Funamizu, 2008) if not inhibited.

Urea hydrolysis results in significant changes in composition when compared to fresh urine. The formation of NH_3 and H_2CO_3 results in an increase in pH to approximately 9 (Udert et al., 2003a). The ammonia formed during hydrolysis exists in equilibrium with ammonium ions as described by Equation 2-2, with a pKa of 9.25 at 25°C (Haynes et al., 2016). As the pH of the system increases, the speciation shifts towards NH_3 which is volatile and will be lost to the atmosphere, affecting overall N recovery potential.

$$NH_{3(aq)} + H_2O \leftrightarrow NH_{4(aq)}^{+} + OH^{-} \qquad \text{(Equation 2-2)}$$

The increased pH also promotes the precipitation of struvite ($NH_4MgPO_4 \cdot 6H_2O$) and hydroxyapatite ($Ca_{10}(PO_4)_6OH_2$) which can lead to scaling and blocking of pipes (Udert et al., 2003b). The increase in the concentration of buffering compounds, ammonia and bi-carbonate ions, also increases the alkalinity of the solution (Udert et al., 2006). An increase in alkalinity would increase the amount of acid required to reduce the pH (to prevent NH_3 volatilization). The high concentration of ammonia is also responsible for the malodor typically associated with hydrolyzed urine.

CHAPTER 2: LITERATURE REVIEW

2.2 URINE STABILIZATION

Stabilization refers to the process whereby urease activity is inhibited, thus preventing urea hydrolysis. Urease activity can be inhibited by several compounds and mechanisms, however, there are two main principles of inhibition: inactivation of the enzyme and inactivation of the urease-producing bacteria. The optimum pH for microbial activity of urease-producing bacteria is in the range of 6.8 - 8.7 (Mobley and Hausinger, 1989). Rektorschek et al. (1998) showed that at pH values below 3.5 and above 8.6 the metabolism of urease-producing Helicobacter pylori bacterium is irreversibly inhibited (Rektorschek et al., 1998). Acidification or alkalization could therefore provide a method for urine stabilization. The urease enzyme can also be inactivated in a few ways. Heavy metals can inactivate the enzyme by binding to the nickel ions or the thiol groups and preventing functionality (Behbehani et al., 2011; Krajewska, 2009). Alternatively, a strong oxidizing agent can be used to oxidize the enzyme's thiol groups to prevent functionality (Krajewska, 2011).

A review of the literature available on acidification, alkalization, chemical oxidations, and heavy metals as methods for urine stabilization is summarized in Table 1. Both acidification and alkalization were proven to be effective stabilization methods as long as the pH was decreased below 4 (Ray et al., 2018) or increased to above 11 with $Ca(OH)_2$ dosing (Randall et al., 2016). Base stabilization will result in the loss of any NH_3 present due to volatilization, however, NH_3 typically only accounts for 5% of total nitrogen in fresh urine (Putnam, 1971). Vasiljev et al. (2022) showed that base stabilization with MgO could be used to recover the initial ammonium ions as struvite while also retaining the urea. Zhang et al. (2013) showed that hydrogen peroxide (a strong oxidizer) was effective at inhibiting urea hydrolysis, however, increased doses were required if the urine was contaminated with faeces. Ozone was found to be ineffective because it decomposes and then no longer inhibits the urease (Zhang et al., 2013). Ray et al. (2018) found heavy metals to be ineffective at inhibiting urea hydrolysis due to interactions with compounds present in urine. Fluoride was precipitated as calcium fluoride, resulting in no inhibition. Silver and zinc nitrate were also ineffective due to interference caused by the high concentration of chloride in real urine. When choosing an appropriate stabilization method, it is important to consider the practicalities of implementation. Strong acids and bases such as HCl, NaOH, and CaO should be avoided as they are highly corrosive and have potential safety concerns (Protea Chemicals, 2017). Dosing of weak acids (such as vinegar) requires significant volumes (15 %v/v), which is both impractical and would dilute the urine further (Boncz et al., 2016). Liquid stabilizers (many acids, and hydrogen peroxide) would require pumping equipment to ensure accurate dosing which could be costly to implement at scale (Randall et al., 2016).

One promising method of acid stabilization is to use citric acid because it exists in a granular form and would therefore not require complicated dosing equipment. It is food grade, and therefore safe to handle (FDA, 2019). Ray et al. (2018) investigated adding citric acid to fresh urine along with 0.53 g L^{-1} Jack

bean urease and determined a minimum dose of 5.2 g L^{-1} was sufficient to inhibit hydrolysis over four hours.

However, the fact that citric acid is an organic acid could be problematic. Ebrahim and Randall (2019) observed that when 250mL/L vinegar, was added to urine, the formation of a bio-film appeared. Chen et al. (2015) demonstrated that organic acids, such as acetic acid, stimulate biofilm formation as they act as a metabolic signal for bacteria. It is hypothesized that as the organic acid is biodegraded the urease inhibition would decrease over time. It is also unclear how biofilm formation would affect any subsequent urine treatment process. Both factors require important consideration.

Calcium hydroxide was identified as a suitable option for base stabilization. Only a small dose of 10 g/L $Ca(OH)_2$ in urine is required to make a supersaturated solution (unlike with NaOH which requires 420 g L^{-1} to reach saturation) that results in a pH of 12.5 at 25°C (Randall et al., 2016). Urine spiked with urease and 2.5, 5, and 10 g/L Ca(OH)2 was stored for 27 days and in all cases, the pH remained above 11.5. Randall et al. (2016) advised using a dose of 10 g/L as this ensures $Ca(OH)_2$ will always be in excess, regardless of urine composition. In addition, urine stabilization with $Ca(OH)_2$ results in the precipitation of calcium phosphate (>98% P-recovery (Flanagan and Randall, 2018)) which has been shown to be an effective fertilizer (Meyer et al., 2018). An additional advantage of base stabilization is the potential for pathogen inactivation (Senecal et al., 2018). In wastewater treatment, it is also common practice to use an alkali dosing for pathogen inactivation (Girovich, 1996). Exposure to more than 30 minutes at a pH of 11.5 has been shown to reduce bacteria to negligible levels (Farrell et al., 1974) and inactivate poliovirus type 1 (Pancorbo et al., 1988) in wastewater.

Table 1: Summary of methods used to stabilize fresh unhydrolyzed urine.

Method	Stabilizer	Advised minimum dosage	Comment	Reference
Acidification	H_2SO_4	60 meq/L (2.94 g/L) 160 meq/L (7.84 g/L) 0.065 M (6.3 g/L)	Safety Hazard and dosing impracticalities (liquid).	(Hellström et al., 1999) (Ray et al., 2018) (Boncz et al., 2016)
	Acetic Acid	60 meq/L (3.6 g/L) 160 meq/L (9.6 g/L) 0.13 M (7.8 g/L)	Dosing impracticalities (liquid). Consideration of long-term storage and bacterial growth resulting in decreased efficacy.	(Hellström et al., 1999) (Ray et al., 2018) (Boncz et al., 2016)
	Vinegar (5-7% acetic acid)	175 mL vinegar/L (15% v/v) 34 meq/L (32.4mL vinegar/L)	Large dosing volumes are required, significantly adding to urine volume. The least effective, hydrolyzation started after 105 min.	(Boncz et al., 2016) (Ray et al., 2018)
	Citric Acid	81 meq/L (5.2 g/L)	Safe to handle, easy to dose, prevents precipitation, but consideration of long-term storage and bacterial growth resulting in decreased efficacy required.	(Ray et al., 2018)
Alkalization	$Ca(OH)_2$	10 g/L	Safe to handle, easy to dose, and produces a fertilizer product	(Randall et al., 2016)
	$CaCO_3$ (limestone)	140 g/L 2 g/L	A significant mass was required. Contradicting results to Randall et al., (2016). Had a saturation pH of 7.25 which was not sufficient to prevent urea hydrolysis.	(Boncz et al., 2016) (Randall et al., 2016)
	CaO	3.5 g/L	Results in an exothermic reaction which is both a safety hazard and has the potential to cause chemical urea hydrolysis.	(Randall et al., 2016)
	Ash	50 g/L 3 to 1 ratio of ash to urine	A significant mass was required. Only 64-90% N was retained as urea. Contradicting results to Boncz et al. (2016) Did not increase pH sufficiently to prevent hydrolysis	(Senecal and Vinnerås, 2017) (Boncz et al., 2016)
	NaOH	0.009 M (0.36 g/L)	To ensure efficacy a saturated solution is required. At 420 g/L the mass required is significant and impractical. See comments for CaO.	(Boncz et al., 2016)
Other	H_2O_2	30mM (1.02 g/L)	Dosing impracticalities	(Zhang et al., 2013)
	Ozone	Not effective		
	$Zn(NO_3)_2$, $AgNO_3$, & F	Not effective in real urine due to metal precipitation because of inhibitors reacting with various ions present in urine.		(Ray et al., 2018)

2.3 URINE COLLECTION

Urine treatment for subsequent resource recovery requires separate collection from feces. This can be done using either conventional urinals, fertilizer-producing urinals (Flanagan and Randall, 2018) or no-mix toilets (Figure 2-1). The toilets and urinals can either be plumbed into a building with separate pipes for urine and feces collection. In this case, urine would be collected and stored in large tanks housed in the building. Alternatively, the systems can be free-standing (not connected with plumbing) with built-in collection tanks. The urine can be treated in the collection tank/toilet system (Riechmann et al., 2021b; Simha et al., 2020a) or the urine can be manually decanted into a larger tank and treated elsewhere (Chipako and Randall, 2020a) . The method of urine collection will also impact how, or if, urine is stabilized.

A challenge with the plumbed system is pipe blockages due to the precipitation of phosphate-based compounds (Udert et al., 2003a). Plumbed systems require regular maintenance but blockages can be avoided with regular flushing with an acid, by installing urine pipes with a larger diameter and at a slope (Lienert and Larsen, 2007). Saetta et al. (2019) have also developed a real-time cyber-physical system that monitors pH and then doses acetic acid to prevent hydrolysis and subsequent blockages. Free-standing systems such as waterless urinals with collection tanks (Flanagan and Randall, 2018) and the Blue Diversion Autarky toilet are not affected by these problems (Sutherland et al., 2021). EAWAG, EOOS, and Laufen pioneered a novel, no-mix toilet design (called Save!) with the invention of the 'urine trap'(Figure 2-1B), where urine is separated using the well-known hydrological phenomenon called the teapot effect (Gundlach et al., 2021).

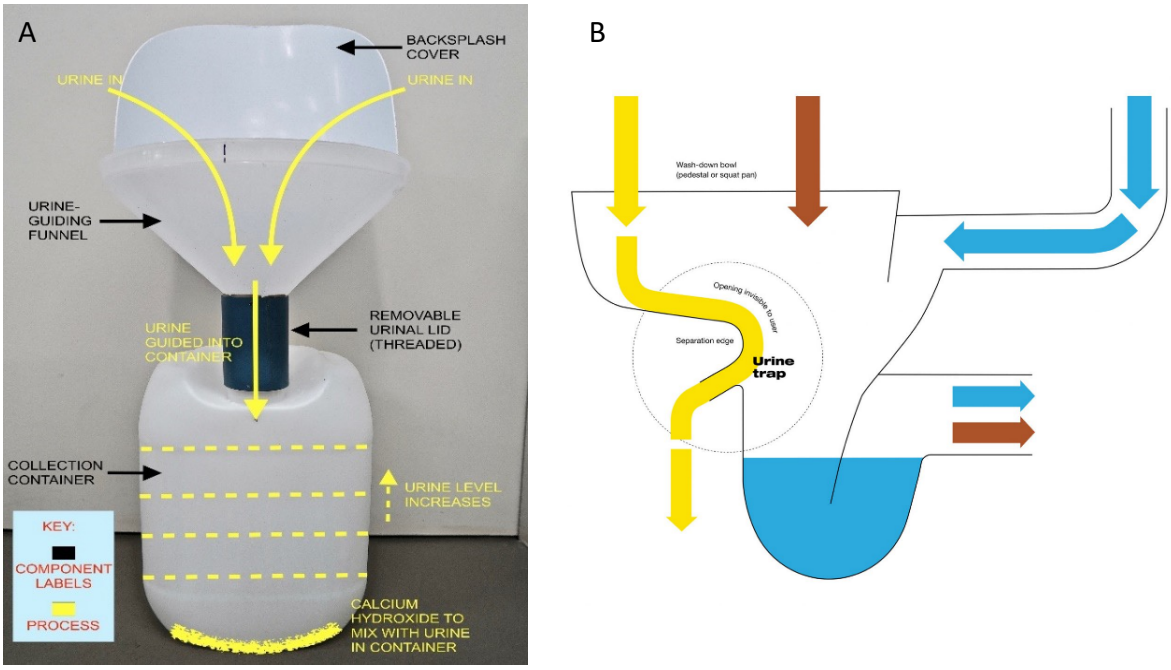

Figure 2-1: Fertilizer-producing waterless urinals (A) (Flanagan and Randall, 2018) and the save! no-mix, low-flush, Laufen toilet (copyright EOOS) (B).

Waterless urinals are advantageous as urine can be stabilized immediately upon collection. Flanagan and Randall (2018) developed a fertilizer-producing urinal that is pre-dosed with 10 g L^{-1} $Ca(OH)_2$ which simultaneously stabilizes the urine and precipitates calcium phosphate which can be used as a fertilizer (Meyer et al., 2018). Mufunde and Randall (2022) further advanced the fertilizer-producing urinal design to include a novel mixing mechanism that ensures effective stabilization and is activated by the user standing on a foot pedal whilst they urinate. In theory, this system could also be pre-dosed with an acid if that stabilization method is preferred. Urine collection systems can also be used for on-site treatment. Simha et al. (2020a) designed a dry sanitation system with a capacity of 30 L per day and Riechmann et al. (2021b) used the Blue Diversion Autarky toilet (Enssle and Udert, 2016) that has a treatment capacity of 10 users per day. These systems use no-mix toilets (such as the save!), the urine is diverted to a collection tank that has been pre-dosed with $Ca(OH)_2$ for stabilization and then the water is evaporated from the urine to produce a dry fertilizer.

2.4 CONCENTRATION METHODS

A multitude of methods for urine treatment and nutrient recovery have been identified and comprehensive reviews of these technologies have been conducted (Chipako and Randall, 2020b; Larsen et al., 2021b; Maurer et al., 2006). Water can be removed by two mechanisms: a phase change (evaporation or freezing) or using physical separation (membranes). The most well-studied concentrating technologies were reviewed to determine the most promising method to investigate further and are summarized in Figure 2-2. These processes specifically focus on volume reduction whilst aiming to maximize nutrient recovery and have previously been investigated in the context of either treating urine or other wastewaters.

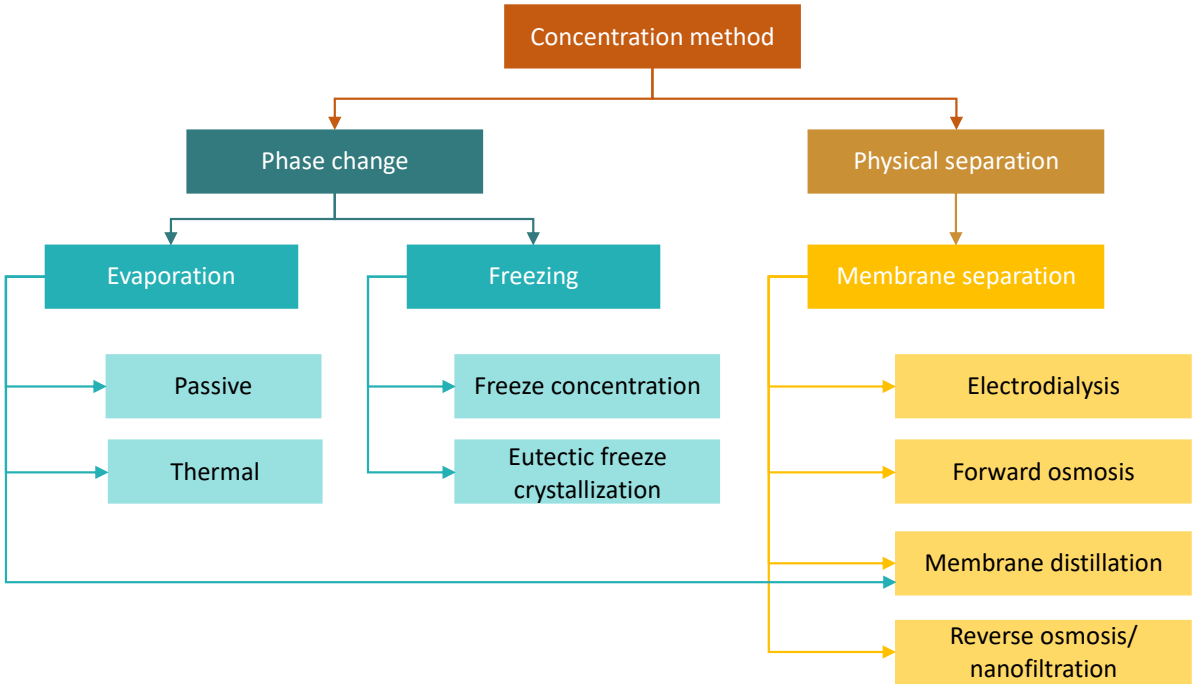

Figure 2-2: Various potential urine volume reduction methods, including variations within each method.

2.4.1 Evaporation

Evaporation refers to the process whereby the water in urine is converted to a vapor which can be condensed and recovered as pure water leaving behind a concentrated liquid. Concentration via evaporation can be achieved in varying degrees of complexity and energy intensity such as via convection with wind, using a solar still, or via vacuum distillation. A review of literature, summarized in Table 2, indicated a variety of outcomes based on the type of urine treated and evaporation method. However, in all cases high water removal (>90%), P and K, recovery is achievable, and it is possible to produce a solid fertilizer product. The points are :

Passive evaporation requires no external energy input but is extremely slow (0.95 L m^{-2} d^{-1}, (Antonini et al., 2012)) or requires a large surface area to increase the evaporation rate. Evaporation rates can be increased by using fans and a dehumidifier (1.2-3.1 L m^{-2} d^{-1},(Riechmann et al., 2021b)), and further increased by heating the air (30-40 L m^{-2} d^{-1}, (Simha et al., 2020a). However, these all come at the cost of increased energy input. For example, the energy consumption can be as high as 1320 kWh m^{-3} (Simha et al., 2020a). A distillation process can also be used with the advantage of being able to recover water as condensate, however, this should be operated under a vacuum to reduce the boiling point of water and therefore energy requirements (Udert and Wächter, 2012).

Evaporation of hydrolyzed urine results in a low nitrogen recovery (10%) (Bethune et al., 2014) due to the volatilization of ammonia gas. However, if the water vapor is recovered it is possible to strip the

ammonia gas present in the condensate to increase nitrogen recovery (Udert and Wächter, 2012). Alternatively, hydrolyzed urine can be acidified to prevent volatilization and improve nitrogen recovery (68%) (Antonini et al., 2012), but this requires significant acid addition due to the buffering capacity of hydrolyzed urine (Maurer et al., 2006). Acid (acetic acid) and base (calcium hydroxide) stabilization of fresh urine prior to evaporation increased nitrogen recovery to 100% (Boncz et al., 2016) and 98% (Riechmann et al., 2021b), respectively. A mix of alkaline MgO and co-substrates also had a high N-recovery (80%) raising the urine pH to 9.9 (Simha et al., 2021), the N-recovery was even higher (98%). Addition of MgO recovers volatile ammonia as struvite and evaporation occurred at a lower temperature (38°C versus 50°C) (Vasiljev et al., 2022) which lessened the potential for chemical urea hydrolysis. Nitrification of hydrolyzed urine, before evaporation, also showed high nitrogen recovery (97% recovery) (Udert and Wächter, 2012), but the loss of nitrogen during storage was not quantified.

Operating temperature will affect urea recovery due to chemical urea hydrolysis (Randall et al., 2022). Increasing the evaporation temperature from 35°C to 65°C reduced nitrogen recovery from 90 to 66% as a result of chemical urea hydrolysis (Senecal and Vinnerås, 2017). Furthermore, at 90°C, Simha et al. (2020a) only recovered 30% of the nitrogen.

Evaporation is well suited to treating urine at the household level, with the majority of evaporation systems designed to be used at a toilet scale. Simha et al. (2020a) designed a dry sanitation system with a capacity of 30 L per day and Riechmann et al. (2021b) used the Blue Diversion Autarky toilet (Enssle and Udert, 2016) which has a capacity of 10 users per day. Although, a distillation process does allow for an increase in scalability. Fumasoli et al. (2016) operated a pilot scale nitrification reactor (120 L) and distillation batch system (600 L).

Table 2: Summary of results from literature for the evaporation of urine, including the method of evaporation, the type of urine used, the operating temperature, water removal, pH, nutrient recovery, and evaporation rate.

Method	Urine type	Temp.	Water removed (%)	pH	Nutrient recovery (%)	Evap. Rate ($L\ m^{-2}\ d^{-1}$)	Reference
Passive (With air ventilation)	Stabilized: NaOH	± 25°C	97%	9	N – 34% P – 33% K – 78%	Slow	(Boncz et al., 2016)
	Stabilized: Acetic acid			<5	N – 100% P – 50% K – 100%		
Passive	Hydrolyzed	20°C	100%	9.2	N – 10%	1.5-8.5	(Bethune et al., 2014)
Solar still	Hydrolyzed then acidified	25-62°C	100%	4	N – 68%	0.95	(Antonini et al., 2012)
Air blowing	Stabilized ($Ca(OH)_2$)	12-24°C	96%	12-13	N-98% P – 92-96% K98%	1.2-3.1	(Riechmann et al., 2021b)
Thermal	Stabilized (wood ash)	35°C	95%	10.5	N – 90% P & K -100%	-	(Senecal and Vinnerås, 2017)
		65°C			N – 66% P & K -100%		
Thermal fan	Magnesium based substrates	38°C	>90%	9.6-10	N-98%	-	(Vasiljev et al., 2022)
	Stabilized (MgO and co-substrates)	50°C		9.9	N-80%	4.5	(Simha et al., 2021)
	Stabilized ($Ca(OH)_2$, wood ash)	90°C		>10	N – 30%	30-40	(Simha et al., 2020a)
	Wheat bran, wood ash, $Ca(OH)_2$, biochar, desert soil	60°C		>11	N- >90%		(Simha et al., 2020b)
Vacuum distillation	Hydrolyzed & nitrified	78°C	99.2%	4	N - 97% P & K -100%	Fast	(Udert and Wächter, 2012)

2.4.2 Freezing

Freeze concentration (FC) is a process where an aqueous salt solution is frozen to form crystalline ice that excludes the incorporation of non-water particles leaving behind a concentrated solution (Lind et al., 2001). Eutectic freeze concentration (EFC) is an extension of FC. At the eutectic point, the salt solution is saturated resulting in the crystallization of salts simultaneously with the formation of ice (Randall and Nathoo, 2015). Freeze processes are theoretically more energy efficient than evaporation because the latent heat of fusion is six times smaller than the latent heat of vaporization (Haynes et al., 2016) and there is no potential for chemical urea hydrolysis (Simha et al., 2020b). Literature on the freeze concentration of urine has shown promise and the results are summarized in Table 3. However, it is important to note that these are feasibility studies, and the aim was not to optimize nutrient recovery.

Lind et al. (2001) were able to recover over 80% of the nitrogen and phosphorus in 25% of the original volume using a freeze-thaw process. Gulyas et al. (2004) used a falling-film and stirred vessel freeze concentration system and Noe-Hays et al. (2021) studied block-freeze concentration. Both teams achieved comparable results. Noe-Hays et al. (2021) showed that a two-stage block freeze concentration process with recycle streams, had a theoretical N, P, and K recovery of 92% and 83% of the water would be removed. These studies used either fresh or hydrolyzed urine, however, no information was provided regarding ammonia losses due to volatilization. Moharramzadeh et al. (2022) concentrated stabilized urine using progressive freeze crystallization and recovered 59% of the urea with 80% water removal.

As for applying EFC to concentrate urine, there is only one theoretical study that investigated this method (Randall and Nathoo, 2018). However, EFC has been proven as a promising water treatment and salt recovery method for a variety of waste streams including seawater desalination (Mazli et al., 2020), hypersaline brines from mining (Lewis et al., 2010), reverse osmosis brine (Randall et al., 2011), and textile wastewater (Randall et al., 2014). It is therefore hypothesized that EFC could also potentially be used to concentrate human urine, recovering valuable salts. EFC is advantageous over traditional freeze concentration as the separation of the salts and ice is aided by gravity, whereby the ice floats to the surface and the salts sink to the bottom of the crystallizer (Genceli, 2008). It is also possible to remove different salts sequentially as their eutectic temperatures differ (Randall et al., 2011). Randall and Nathoo (2018) predicted that at a temperature of -27°C, 90% of the nitrogen from hydrolyzed urine could be recovered as ammonium chloride (NH_4Cl) and ammonium bicarbonate (NH_4HCO_3) using EFC. EFC is also most efficient when using concentrated streams as these streams are closer to the eutectic concentration (Randall and Nathoo, 2018).

Table 3: Nutrient recovery and volume reduction factor (VRF) for various freeze concentration processes of urine available in the literature.

Method	Urine type	Temp.	VRF	Recovery	Reference
Freeze-thaw	NS-RU	-14°C	4	>80% N & P	(Lind et al., 2001)
	Dilute (50%) NS-RU	-18°C	2.5	60% nutrient recovery	(Ganrot et al., 2007)
Freeze-concentration	NS-RU	-6 to -16°C	5	65% N, 50% P	(Gulyas et al., 2004)
	Urea-NaCl mixture	-4°C	2.8	Not stated	(Schmidt and Alleman, 2005)
Block freeze-concentration	H-RU	-6 and -13.5°C	3.3 5.8	80% nutrient retention 92% nutrient retention[c]	(Noe-Hays et al., 2021)
Progressive freeze concentration	S-SU[a]	-12°C	5	59% urea recovery	(Moharramzadeh et al., 2022)
Eutectic freeze crystallization[b]	H-SU	-27°C	-	90% N recovery- as NH_4Cl and NH_4HCO_3	(Randall and Nathoo, 2018)

NS-RU – Not stabilized real urine (the study did not indicate whether the urine had undergone urea hydrolysis), H-RU – hydrolyzed real urine, S-RU – stabilized real urine, H-SU – hydrolyzed synthetic urine, and S-SU – stabilized synthetic urine. [a]Stabilized with peracetic acid. [b]This was a thermodynamic simulation study. [c]Two-stage system incorporating iterative mass balance with recycle streams.

Noe-Hays et al. (2021) reported that for block freeze concentration only 14 kWh m^{-3}. However, this figure is misleading as this is only a theoretical energy requirement based on the energy required to freeze 1 kg of water. Gulyas et al. (2004) reported a higher energy demand using a NIRO freeze concentrator "W33" of 244 kWh m^{-3} of water removed for a 250 L hr^{-1} plant. Another NIRO freeze concentrator "W60" used to concentrate skim milk (196 kg hr^{-1}) had a measured energy consumption of 154.5 kWh m^{-3} water removed (Best and Vasavada, 1993a). Both energy measurements use slightly different conventions (feed processed versus water removed, information for the % water removed is required to convert between them).

2.4.3 Membrane processes

All membrane separation processes make use of a semi-permeable membrane through which water can pass, but dissolved solids are rejected, however, the driving force for each process differs. Figure 2-3 gives a summary of four different membrane processes. In general, concentrating hydrolyzed urine using a membrane process requires low pHs to reduce the concentration of NH_3 compared to NH_4^+ ions since NH_3 is both uncharged and volatile making it difficult to retain with membrane processes. This requires large amounts of acid for neutralization (Maurer et al., 2006) adding to operating costs.

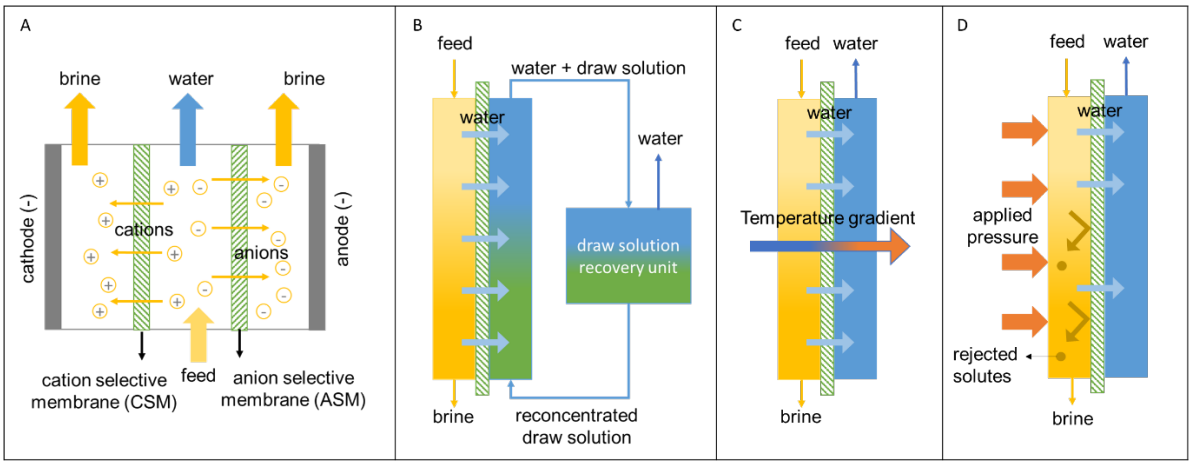

Figure 2-3: Membrane separation technologies; electrodialysis (A) adapted from (Pronk et al., 2006a), forward osmosis (B), membrane distillation (C), and pressure-driven membrane separation (D).

Electrodialysis

Electrodialysis (ED) uses an electrical potential difference and ion-selective membranes to separate ions from water (Figure 2-3A). The results of various ED studies are summarized in Table 4. De Paepe et al. (2018) achieved high water removals (80-85%) using ED on nitrified urine, however, up to 30% of the N, 60% of the P, and 30% of the K was lost in the ED process. Whilst Ledezma et al. (2017) were able to achieve a high N concentration factor (4.45) using a hybrid microbial electrolysis/electrodialysis cell, their overall N loss was 50%. Pronk et al. (2006a) observed that when concentrating hydrolyzed urine with ED, any further increase in water removal resulted in a decreased recovery of nutrients in the concentrate stream. This phenomenon is a result of ED being controlled by both electro-osmotic transport and osmotic water transport (Pronk et al., 2006a), which results in the backflow of ions from the concentrate to the water stream (Brewster et al., 2017). The high concentration factor achieved by De Paepe et al. (2018) is likely due to the urine being diluted up to 80%. These studies were all conducted with hydrolyzed or nitrified urine, therefore it is unclear what nutrient recoveries would be achieved for stabilized urine. Volpin et al. (2020) observed that a reverse ED process results in a fast diffusion of urea to the freshwater stream. As urea is uncharged it is unlikely to transport with the ions through the ion-selective membranes and would remain in the water stream resulting in low recoveries in the concentrate stream. Electrodialysis is therefore more suited for the concentration of hydrolyzed urine.

Energy requirements reported for ED vary. Dodd et al. (2008) reported an energy requirement of 97 kWh m^{-3} (Dodd et al., 2008). However, De Paepe et al. (2018) determined more conservative energy requirements of 4.3 kWh^{-3}. Jermakka et al. (2018) required 13 kWh $kg\text{-}N^{-1}$ recovered, which based on a 72% N recovery is approximately 103 kWh m^{-3} urine.

Table 4: Typical nutrient recovery and water removal for ED systems.

Process	Feed urine	Nutrient recovery (%)			Water removal	Reference
		N	P	K		
ED	Real, hydrolyzed		-		40-80%	(Pronk et al., 2006a)
ED	Nitrified – diluted	70	40	71	80%	(De Paepe et al., 2018)
MEC -ED	Synthetic, hydrolyzed	50	43	55	N.S.	(Ledezma et al., 2017)
EC-ED	Synthetic, hydrolyzed	72	39	79	N.S	(Jermakka et al., 2018)

MEC -microbial electrolysis cell, EC – electrolysis cell, N.S. – not stated.

Forward osmosis

Forward osmosis (FO) makes use of a difference in osmotic pressure between the feed (low osmotic pressure) and draw solution (DS) (high osmotic pressure) which draws water through a semi-permeable membrane. The water is then recovered from the draw solution which is then reused (Figure 2-3B). These processes are often used in conjunction with MD to recover water and re-concentrate the draw solution (Volpin et al., 2018). The literature on urine treatment using FO varies considerably and is generally limited to synthetic urine. In some cases, the aim was to concentrate urea in the urine (Volpin et al., 2019a; Zhang et al., 2014) whilst in others, the aim was to recover it in the draw solution (Ray et al., 2019; Volpin et al., 2019b). In addition, studies are often only conducted at low water recoveries (<15%) which makes it difficult to determine accurate recoveries at high concentration levels. Volpin et al. (2019b) recovered 50% of the N in the fertilizer draw solution, whilst Ray et al. (2019) recovered 10-20% of urea in the DS (which was to be further concentrated via membrane distillation). Zhang et al. (2014) were able to remove 70% of the water from fresh urine, however, urea rejection was <40%. Liu et al. (2016) note that any nutrients that are recovered in the DS would also accumulate after long-term operation as the DS is continually regenerated. Volpin et al. (2019a) observed that urea rejection could be improved by applying pressure to the DS, however, this results in decreased water flux. Whilst the energy requirements for FO are low (0.27 kWh m^{-3}, Iskander et al. (2017)), due to its low-pressure operation, depending on the method used to regenerate the DS the overall process energy consumption increases considerably (Moon and Lee, 2012). Forward osmosis in general has been slow to become established for industrial and commercial applications, despite over 15 years of research (Francis et al., 2020). Even more so, in the urine research field, there is a major gap in studies that conduct long-term operations (Larsen et al., 2021a).

Membrane distillation

Membrane distillation (MD) is a thermally driven separation process that uses a temperature gradient to vaporize water. The membrane is hydrophobic which prevents water from passing through but allows the vapor phase and other volatile compounds to migrate through (Figure 2-3C). Membrane distillation

is not suitable for stabilized urine as the temperature gradient required for water permeation is likely to lead to chemical urea hydrolysis. However, Ray et al. (2019) were able to recover 72-92% of the urea, although no information regarding potential losses due to urea hydrolysis was provided. Zhao et al. (2013) were only able to remove 32-49% of the water from fresh urine and they struggled with membrane fouling (urea was not measured). Khumalo et al. (2019) modified the membrane properties and saw improved water removal and nitrogen rejection but still struggled with fouling. As for energy demand, because MD requires water to be heated and vaporized the process can be energy intensive with energy demands in the range of 100 (Ullah et al., 2018) to 240 kWh m^{-3} (Winter et al., 2011). This is less than conventional evaporative processes (1320 kW m^{-3}, (Simha et al., 2020a)).

Pressure-driven membrane separation

Pressure-driven membrane processes such as reverse osmosis (RO) and nanofiltration (NF) make use of a pressure differential as a driving force to transport water through the semi-permeable membrane into the permeate (Figure 2-3C). Membrane filtration is a prominent technology used for the desalination of seawater and brackish water with reverse osmosis (RO) with approximately 20 000 plants around the world treating over 100 million m^3 day^{-1} (Jones et al., 2019). This shows that the process is both scalable and is a proven desalination technology. Nanofiltration (Pronk et al., 2006b) and reverse osmosis (Ek et al., 2006; Ray et al., 2020; Thörneby et al., 1999) membranes have shown promise as methods to concentrate urine (summarized in Table 5) and animal waste. However, published data investigating using stabilized urine is limited and does not provide an indication of the concentration potential, and possibility of fouling (Ray et al., 2020).

Membrane processes are often defined according to the rejection of various solutes which refers to how effectively a membrane retains the solutes in the brine stream. As this research focuses on stabilized urine, the rejection of urea rather than ammonia is key. Urea is a small uncharged particle, making it difficult to remove by size and charge exclusion (Yoon & Lueptow (2005)). Nanofiltration membranes typically have a low rejection of urea (less than 20%) and Pronk et al. (2006b) suggested that urea could be recovered in the permeate stream due to the low rejection rates. Urea rejection is improved with brackish water (BWRO) membranes and has been shown to be as high as 62% for acidified real fresh urine (Ray et al., 2020). There is currently no literature available on the rejection of urea for seawater (SWRO) membranes. However, as rejection increases with operating pressure (Bergman, 2007), it is likely that the high operating pressure of SWRO membranes (55 bar) would further improve urea rejection. Seawater RO membranes have a high rejection of P and K (above 98%) (Ek et al., 2006; Masse et al., 2008). However, for BWRO and NF membranes the range of results was much broader between studies. NF membranes provide limited rejection for monovalent ions such as potassium (Bergman, 2007) and the valency of phosphorus is pH dependent. Literature on potassium rejection

agrees with this, varying significantly from 43% to 88%, and appears to be membrane brand dependent. Additional limitations with the available research are that many studies used dead-end stirred cells (DESC) which do not mimic the crossflow that occurs in commercial RO/NF systems.

Reliable data regarding water recovery is only available for SWRO membranes and hydrolyzed urine or swine effluent. (Ek et al., 2006) recovered 80% of the water from acidified and hydrolyzed urine, however, the urine was dilute. Water removal is typically limited by operating pressure and initial total dissolved solids (TDS) concentration. Thörneby et al. (1999) found that when concentrating swine effluent, an increase in total dissolved solids (TDS) from 10 to 23 g/L reduced the water recovery from 85% to 60%. (Ek et al., 2006) reported a total energy requirement of 12 kWh m^{-3}, however commercial seawater RO desalination plants typically use 4-6 kWh m^{-3} (Abdelkareem et al., 2018). However, it has been shown that multi-stage RO processes can be used to achieve high water removals (70%) from seawater despite high TDS concentration (35 000 ppm) with relatively low energy requirements (3 kWh m^{-3}) (Ahunbay, 2019). Membranes can be prone to fouling, however, research by Ray et al. (2022) and Ek et al. (2006) showed that adequate pre-treatment with microfiltration can help reduce the potential for fouling.

Table 5: Range of nutrient recovery, and water removal for RO and NF membranes

Membrane	Urine	Pressure (bar)	Nutrient rejection (%)				Water removal	Reference
			Urea	NH_3	P	K		
SWRO	RU-Dilute-hydrolyzed	50	-	94	>98	-	80%	(Ek et al., 2006)
BWRO	Dilute synthetic WW	8	15-25	70-90	80-99	65-85	60%	(Yoon and Lueptow, 2005)
	RU-fresh	27.6	57	-	-	-	8%	(Ray et al., 2020)
Tight NF			42-54	-	-	-		
Loose NF	RU-Fresh	20	10-18	50-60	>98	60-80	-	(Pronk et al., 2006b)

2.4.4 Technology summary

Various urine concentration technologies were reviewed. Figure 2-4 summarizes the energy requirements and water removal percentages for each process. Energy consumption for urea production indicates the energy required for synthetic urea production based on an equivalent amount of urea present in 1 m^3 of urine. Similarly, for the WWTP category, this value is the energy required to treat the total N in 1 m^3 of urine if it were sent to a WWTP. Recovery of P and K is generally high for all processes as they are non-volatile so are not lost to the atmosphere and they are charged which makes it easier to reject them with a membrane process. Nitrogen recovery is heavily dependent on whether urine is hydrolyzed or stabilized as well as the solution pH. In general, all technologies were able to remove at least 70% of the water. However, only evaporative processes achieved complete water

removal. The disadvantage is that evaporative processes require the most energy, more than double the energy required to produce urea synthetically. Whilst FO has the lowest energy requirements, the energy required to recover the draw solution requires consideration. Furthermore, more research on the long-term operation of FO systems for urine treatment is still required (Larsen et al., 2021b).

The electrical requirements for ED varied significantly and it is therefore difficult to accurately determine the process energy requirements. As a result, the suitability of the process for stabilized urine is unclear. Freeze concentration had the second lowest energy requirements with RO requiring the least energy. Whilst there is a potential for RO membrane scaling, RO would be able to remove the bulk of the water from urine which could then be further concentrated by other technologies to reduce the overall energy requirements. RO was also suggested as a pre-treatment for both evaporation (Udert and Wächter, 2012) and EFC (Randall and Nathoo, 2018).

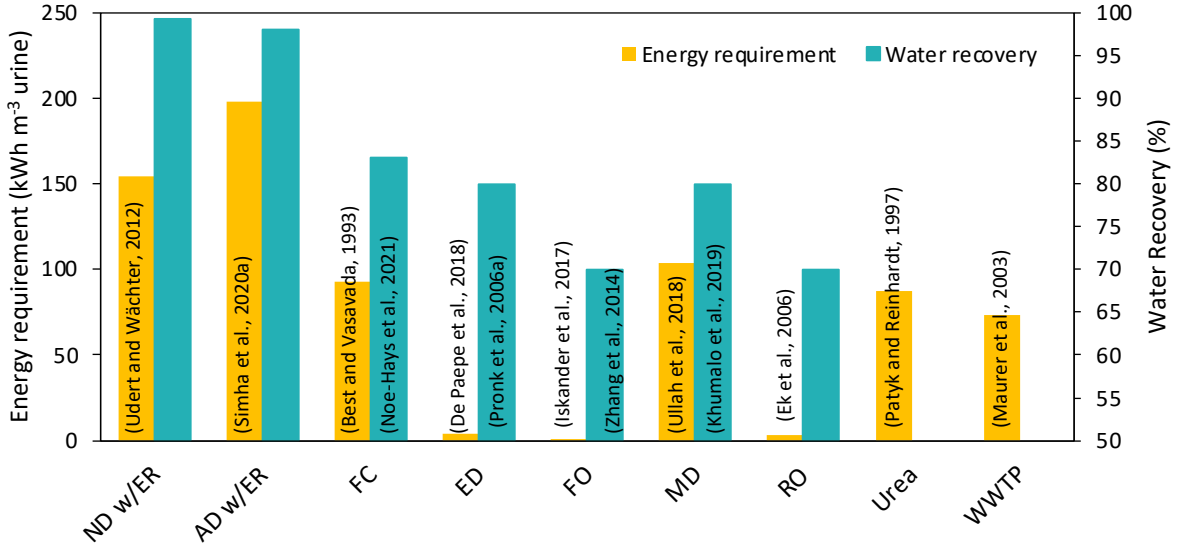

Figure 2-4: Energy requirements and water removal for different urine concentration technologies. Nitrification and distillation (ND) as well as alkaline dehydration (AD) include energy recovery.

2.5 MICROPOLLUTANTS

Urine is not necessarily sterile (Hilt et al., 2014), and whilst the majority of pathogens come from fecal contamination (Höglund et al., 2002), they can also come from urinary tract infections (Ferreira et al., 2010). Furthermore, up to 64% (±27%) of any pharmaceutical activate compounds (PhAC) consumed are excreted in urine (Lienert et al., 2007). Many urine treatment technologies concentrated the pathogens and PhACs present in urine with the fertilizer nutrients (NPK). If urine is to be used as a high-quality fertilizer for edible crops the removal of micropollutants requires consideration.

Pathogens: Storing acidified and alkalized urine has shown positive effects for pathogen inactivation but mixed results for degrading PhACs. Storage of urine at a high pH (>10.5) for 98, 15, and 4.2 days

at 20, 35, and 42°C respectively is required for the inactivation of pathogens and viruses (Senecal et al., 2018). Acidification to a pH less than 2 resulted in reduced concentrations of bacteria, however pH values between 2 and 7 showed increased bacterial concentrations (Hellström et al., 1999).

Pharmaceuticals and hormones: Storage at a pH of 10 for a year showed no significant reduction of four PhACs (Gajurel et al., 2007). Increasing the pH to 11 (6 months storage) resulted in a varying reduction from 10% (ibuprofen) to 80% (sulfadimidine) (Schürmann et al., 2012). No hormones were detected after dehydration of alkaline urine (Simha et al., 2020a). Storage at a pH of 4 for one year resulted in no significant reduction of PhACs (Gajurel et al., 2007). Decreasing the pH to 3 (6 months storage) resulted in a varying reduction from 10% (tramadol) to 80% (diclofenac) (Schürmann et al., 2012). Hormone reduction in urine stored at a pH of 2 for 6 weeks varied from 30-42% (Zanchetta et al., 2015).

The effect of pH, therefore, has a varying effect on the type of pharmaceutical being removed. Whilst extreme pH conditions (stabilization using acidification or alkalization) are sufficient for pathogen inactivation, it would not be a sufficient method to address the presence of all pharmaceuticals in urine.

A variety of other, more robust, micropollutant treatment techniques have been investigated for human urine. Granular activated carbon (GAC) has been shown to be effective at removing micropollutants (Köpping et al., 2020) from nitrified urine, however, urea is also absorbed by GAC and therefore would not be suitable for acid or base stabilized urine where the aim is to concentrate urea, as in this work. Advanced oxidation processes (AOP) (UV, ozone, hydrogen peroxide, or a combination) (Zhang et al., 2015) and plasma (Rodriguez et al., 2022) have shown promise as methods to remove PhACs from urine. These processes do not degrade the urea and could therefore be an effective pretreatment method for acid or base-stabilized urine. Although the high energy requirements of plasma (two orders greater the UV/H_2O_2) may reduce its desirability (Rodriguez et al., 2022). Electrolysis of fresh urine (Clark et al., 2021) and hydrodynamic cavitation (Thanekar et al., 2018) have also been shown to be effective at degrading PhACs. However, because these techniques (AOP, plasma, electrolysis, and hydrodynamic cavitation) are not adsorption processes, like with GAC, the PhACs are only broken down into other compounds and hence would still be present in the urine. The exact influence of the degraded compounds on the quality of the fertilizer product produced from stabilized urine would have to be further tested. Nanofiltration has shown a high rejection of pathogens (Patterson et al., 2012) and PhACs, but a low rejection of urea (Pronk et al., 2006b). In theory, the permeate, which would contain the majority of the urea and none of the pharmaceuticals, could then be further concentrated.

2.6 FERTILIZER QUALITY

Martin et al. (2022) conducted an in-depth review of studies investigating the effectivity of urine-based fertilizers (UBF) compared to synthetic fertilizers. In general, UBFs performed within a close range of

synthetic fertilizers. Simha et al. (2020a) recovered a dry UBF with an NPK ratio (weight percent) of 9.9:1.5:6 which has an almost identical NPK composition to a common South African rose and flower fertilizer 9.7:1.2:6.1 (Wonder, 2022). A concern with regards to UBFs is that urine also contains undesirable salts (Na^+, Cl^-, SO_4^{2-}). Salinity can affect soil structure and plant growth (Friedler et al., 2013) and therefore may impact the effectiveness of using an RO brine stream as a liquid fertilizer. For example, dry urine-based fertilizers recovered by Simha et al. (2020a) contained 4.6% Na^+ and 6.9% Cl^-. However, many mineral fertilizers such as NH_4Cl and KCl also contain chloride and are widely used. A local (South African) fertilizer, GroBest, has a Na^+ content of 0.25% (Makhro, 2022), which is lower. However, if N content is compared (UBF – 9.9% N, GroBest – 2.45%), four times as much GroBest would need to be applied for the same amount of N as the UBF, increasing the Na^+ added to 1%.

To ensure optimum plant growth, application rates might need to be varied based on crop sensitivity to salinity (Mnkeni et al., 2008), and irrigation and soil drainage should be considered (Guizani et al., 2016). Salts can be flushed during rainfall and irrigation (Guizani et al., 2016), but fertilizer application would need to be monitored in arid regions and soils with poor drainage. Hydrolyzed urine has been previously applied as a fertilizer for beetroots (salt tolerant) and carrots (salt sensitive) and yields peaked at an application rate of 800 kg N ha^{-1} for the beetroots compared to 50 kg N ha-1 for the carrots (Mnkeni et al., 2008). It is important to note that the ratio of N:Na used in this study was 1:1.2, whereas the fertilizer produced by Simha et al. (2020a) was at a ratio of 1:0.46. This indicates that the concentration of salts in UBFs are likely to only be a concern if nutrient content (NPK) in the product is proportionally low. Human urine is expected to acidify the soil, however, in cases where acidic soil requires $Ca(OH)_2$ application of an alkaline UBF would be beneficial (Martin et al., 2022). The use of acid-stabilized UBFs would in theory further increase soil acidification. Different urine treatment methods recover nutrients and salts in varying ratios. Therefore, the final product would need to be tested on a variety of plants with different salt tolerances to determine its effectiveness.

2.7 URINE PRE-TREATMENT

Reverse osmosis (RO) is an effective method to concentrate solutions, however, RO membranes can show a decline in productivity if scaling occurs (Greenlee et al., 2010). Scaling refers to the process where inorganics precipitate out of solution and deposit on the membrane forming a ‘scale’ (Kumar et al., 2006). Urine stabilized with $Ca(OH)_2$ is saturated with calcium (Randall et al., 2016) and could cause scaling in the form of calcium compounds. In addition, RO membranes have high CO_2 permeability (Mitsoyannis and Saravacos, 1977) and any dissolution of CO_2 in stabilized urine will form carbonate ions (CO_3^{2-}) due to the high pH. The excess calcium ions would react with the carbonate to form $CaCO_3$. As $CaCO_3$ is a sparingly soluble salt (14.25 mg L-1 at 25°C in water(Haynes et al.,

2016)) it will easily precipitate and likely result in scaling. A pre-treatment method for $Ca(OH)_2$ stabilized urine to remove excess calcium ions (Ca^{+2}) is therefore advised. Air bubbling (85% Ca^{+2} removal) (Lisitsin et al., 2008); (Hasson et al., 2011); CO_2 bubbling (99% Ca^{+2} removal) (Velts et al., 2011), and sodium carbonate (Na_2CO_3) fluidized bed reactor (95% Ca^{+2} removal) (Mahasti et al., 2017) have all been proven as effective methods to precipitate $CaCO_3$ from calcium rich waters. These methods could potentially be used as a pre-treatment step before the RO concentration process of stabilized urine.

2.8 PROPOSED TREATMENT OPTIONS

Based on the available literature, membrane separation (RO, NF, or a hybrid) was determined to have the most promise for concentrating stabilized urine. However, pre-treatment may be required based on the urine stabilization method used because of potential membrane scaling. In addition, depending on the extent of water removal, further concentration via eutectic freeze concentration may be beneficial. Based on the above, there are a variety of potential process combinations for the treatment of stabilized urine, as shown in Figure 2-5. These will result in product streams with different compositions. The operating and capital costs of each treatment will also differ. An economic analysis can then be used to determine if there is a market for any of the fertilizer compositions produced and whether production would be economically feasible.

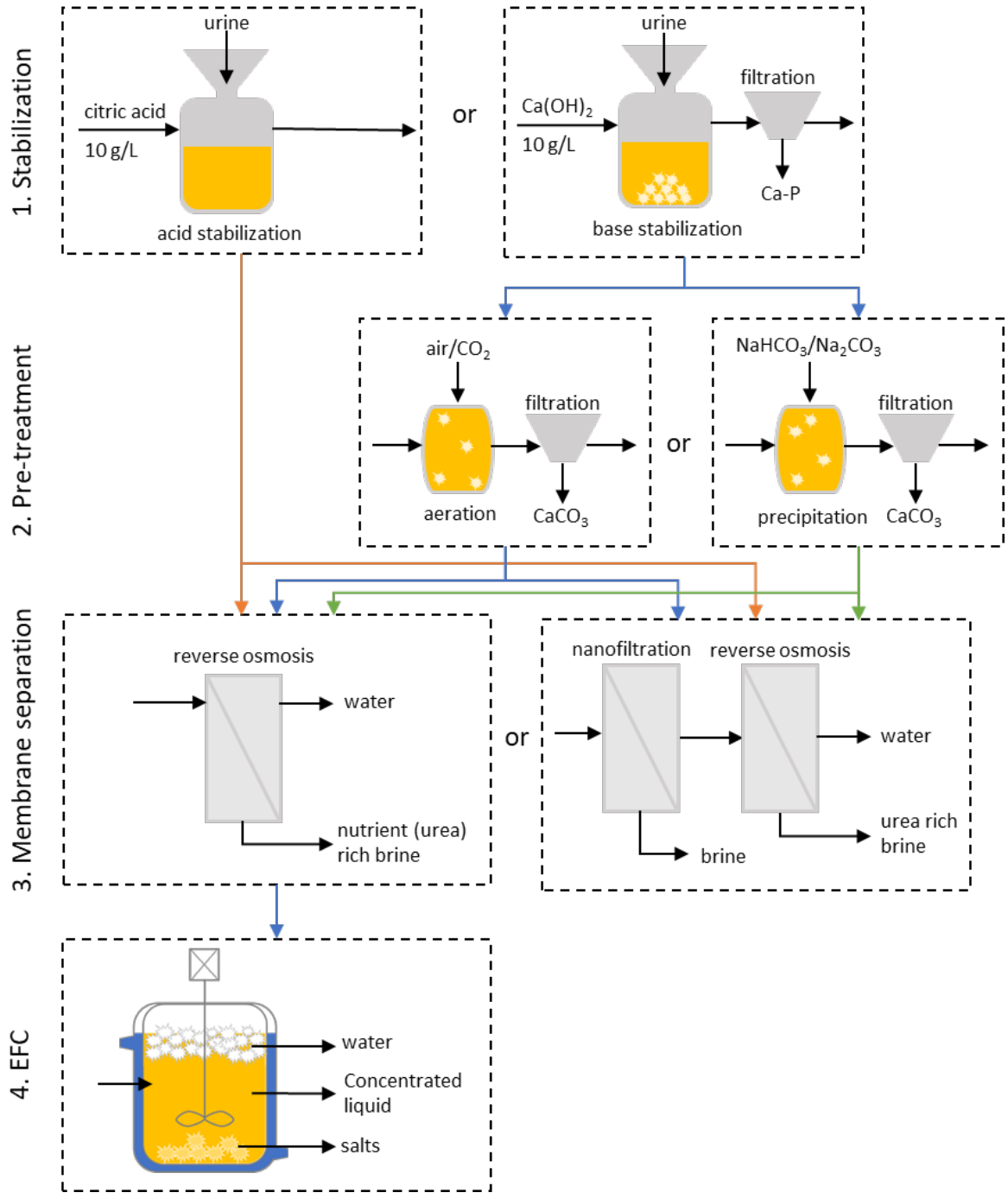

Figure 2-5: Proposed integrated treatment process options to concentrate urine stabilized with $Ca(OH)_2$ or citric acid, including ore-treatment, membrane separation, and eutectic freeze crystallization.

2.9 RESEARCH OUTLINE

2.9.1 Problem statement

Whilst urine could provide a sustainable alternative to synthetic fertilizer its implementation is still widely at the lab scale. A major barrier to commercial implementation is that urine is 97% water which makes it expensive to transport. However, while there are established urine concentration technologies that have high water removal capabilities (distillation, alkaline dehydration), they are often designed to be used at a household level and many require significantly more energy than simply treating urine at a WWTP. Reverse osmosis could potentially provide a scalable, more energy-efficient option, but, depending on the type of urine stabilization used, membrane scaling can occur.

2.9.2 Overall aims

Previous research has been conducted on various urine volume reduction technologies and stabilization methods. However, no researcher has looked at producing a liquid fertilizer concentrate from stabilized urine using reverse osmosis, which is often used to desalinate wastewater streams. The objective of this research was therefore to develop an integrated urine treatment process that concentrates stabilized urine while also recovering valuable nutrients. The integrated process considered the method of urine stabilization, whether pre-treatment was required, the membrane process configuration, and whether EFC could be used to further concentrate the product RO brine stream. By comparing the various process configurations, an optimized configuration for water removal and nutrient recovery was determined. The overarching objectives were to:

1. Determine whether the chemical addition of carbonate ions ($NaHCO_3$, or Na_2CO_3) to urine stabilized with $Ca(OH)_2$ is a feasible and effective method to remove the scaling pre-cursor ions Ca^{2+} (as $CaCO_3$) such that they cannot later scale a reverse osmosis membrane.
2. Determine whether aeration (air or CO_2 bubbling) could be used as an alternative pre-treatment method to chemical addition to prevent adding unwanted Na^+ ions, whilst still removing the Ca^{2+} scaling pre-curser ion as $CaCO_3$.
3. Determine whether RO in combination with urine stabilization and pre-treatment can be used to produce a nutrient-rich concentrate, whilst simultaneously removing at least 60% of the water from urine.
4. Determine whether a hybrid NF-RO process can be used to recover a purer concentrated urea-rich stream by removing undesirable salts and pharmaceuticals.
5. Determine whether eutectic freeze crystallization can be used to further concentrate urine after reverse osmosis treatment.

6. Conduct a high-level economic analysis assessing the overall energy requirements and the value of the products in the niche and bulk fertilizer markets considering nutrient recovery and water removal of the different process configurations.

2.10 SCOPE AND KNOWLEDGE CONTRIBUTION

2.10.1 Scope and limitations

This research was confined to a laboratory-scale investigation and focused on determining the proof of concept and technical feasibility of different urine treatment options. All experiments were conducted in triplicate with synthetic urine (ensuring consistent composition) and then the results were confirmed with real human urine. Only three different types of membranes (SWRO, loose NF, and tight NF) were investigated and only one brand of membrane from each category was tested as the aim was to determine technical feasibility rather than to optimize the process. Investigation into the rejection of PhAC using NF was limited to only six PhACs. Pharmaceutical rejection using NF membranes is well researched and the core aim was to investigate how NF impacted urea purity and recovery. Whilst EFC can theoretically be used to crystallize multiple salts from urine, only the crystallization of one salt ($Na_2SO_4 \cdot H_2O$) was investigated. Based on the experimental results, areas that require further in-depth research to optimize the process were identified. A high-level economic analysis was also conducted. This analysis did not include the equipment CAPEX though as the treatment plant only exists at a laboratory scale. The economic analysis was limited to the energy requirements of different treatment methods and the potential value of the products produced. The core scope of the analysis was to assess two different fertilizer markets (niche and cbulk) and determine which market UBFs would be best suited for in terms of potential profit. The scope of this analysis was limited to one system boundary, a decentralized urine treatment model.

2.10.2 Novel aspects

There is currently no literature on the concentration of stabilized human urine (with $Ca(OH)_2$) using RO or NF membranes. This may be due to the scaling potential caused by the high calcium ion concentration in urine stabilized with $Ca(OH)_2$. This research was the first to assess the feasibility of two potential pre-treatment options (air/CO_2 bubbling and Na_2CO_3/$NaHCO_3$) for stabilized urine, considering not only their potential for calcium removal but also the downstream effects on the RO/NF membrane process.

This research also expanded on the use of RO and NF for urine treatment in a multitude of ways:

1. The experimental setup used a crossflow cell rather than a dead-end stirred cell, which more accurately mimics a full-scale RO or NF operation.
2. Different pre-treatment methods to prevent RO scaling were investigated and a model was developed to explain the pre-treatment process with air and CO_2 while considering urine's unique chemistry. The model was also used to optimize the process.
3. Urea rejections for SWRO membranes operating at high pressure were determined for the first time using synthetic urine and real urine.
4. High water removals (up to 70%) for real urine concentration with RO were also determined for the first time.
5. Previous research focused on hydrolyzed or dilute human urine, whilst this work focused on stabilized and undiluted human urine for high nitrogen recoveries. Furthermore, research to date on urine concentration using freezing techniques has been limited to freeze concentration and not EFC. This work was the first to successfully show that human urine can be further concentrated using EFC that had been pre-concentrated using RO, thus offering a novel urine concentration and treatment process.

REFERENCES

Abdelkareem, M.A., Assad, M.E.H., Sayed, E.T. and Soudan, B. 2018. Recent progress in the use of renewable energy sources to power water desalination plants. Desalination 435, 97-113.

Ahunbay, M.G. 2019. Achieving high water recovery at low pressure in reverse osmosis processes for seawater desalination. Desalination 465, 58-68.

Antonini, S., Nguyen, P.T., Arnold, U., Eichert, T. and Clemens, J. 2012. Solar thermal evaporation of human urine for nitrogen and phosphorus recovery in Vietnam. Science of The Total Environment 414, 592-599.

Behbehani, G.R., Saboury, A., Taherkhani, A., Barzegar, L. and Mollaagazade, A. 2011. A thermodynamic study on the binding of mercury and silver ions to urease. Journal of thermal analysis and calorimetry 105(3), 1081-1086.

Bergman, R. 2007. Reverse osmosis and nanofiltration, 2nd edition, American Water Works Association, Colorado, USA.

Best, D. and Vasavada, K. 1993 Freeze concentration of dairy products Phase 2: Final report, Dairy Research Foundation, Illinois, USA.

Bethune, D.N., Chu, A. and Ryan, M.C. 2014. Passive evaporation of source-separated urine from dry toilets: a lab study. Journal of Water, Sanitation and Hygiene for Development 4(4), 654-662.

Boncz, M.A., Formagini, E.L., Arima, F.X. and Paulo, P.L. 2016.. Methods for stabilising and concentrating human urine for use as a fertilizer. P13th IWA Specialized Conference on Small Water and Wastewater Systems. Athens, Greece, 14-16 September.

Brewster, E.T., Jermakka, J., Freguia, S. and Batstone, D.J. 2017. Modelling recovery of ammonium from urine by electro-concentration in a 3-chamber cell. Water research 124, 210-218.

Chen, Y., Gozzi, K., Yan, F. and Chai, Y. 2015. Acetic acid acts as a volatile signal to stimulate bacterial biofilm formation. mBio Americal Society for Microbiology 6(3).

Chipako, T. and Randall, D. 2020a. Investigating the feasibility and logistics of a decentralized urine treatment and resource recovery system. Journal of Water Process Engineering 37, 101383.

Chipako, T. and Randall, D. 2020b. Urine treatment technologies and the importance of pH. Journal of Environmental Chemical Engineering, 103622.

Clark, J.A., Yang, Y., Ramos, N.C. and Hillhouse, H.W. 2021. Selective oxidation of pharmaceuticals and suppression of perchlorate formation during electrolysis of fresh human urine. Water Research 198, 117106.

De Paepe, J., Lindeboom, R.E., Vanoppen, M., De Paepe, K., Demey, D., Coessens, W., Lamaze, B., Verliefde, A.R., Clauwaert, P. and Vlaeminck, S.E. 2018. Refinery and concentration of nutrients from urine with electrodialysis enabled by upstream precipitation and nitrification. Water research 144, 76-86.

Dodd, M.C., Zuleeg, S., Gunten, U.v. and Pronk, W. 2008. Ozonation of Source-Separated Urine for Resource Recovery and Waste Minimization: Process Modeling, Reaction Chemistry, and Operational Considerations. Environmental Science & Technology 42(24), 9329-9337.

Ebrahim, W. and Randall, D. 2019. Implications of different toilet flushing solutions on the precipitation potential of urine. Journal of Water Process Engineering 31, 100847.

Ek, M., Bergström, R., Bjurhem, J.E., Björlenius, B. and Hellström, D. 2006. Concentration of nutrients from urine and reject water from anaerobically digested sludge. Water Science and Technology 54, 437-444.

Enssle, S. and Udert, K. 2016. The Autarky toilet–a modular approach for integrated on-site treatment of wastewater, urine and faeces through stream separation at the source. P 13th IWA Specialized Conference on Small Water and Wastewater Systems. Athens, Greece, 14-16 September.

Farrell, J.B., Smith Jr, J.E., Hathaway, S.W. and Dean, R.B. 1974. Lime stabilization of primary sludges. Journal (Water Pollution Control Federation), 113-122.

FDA, U. 2019. Code of Federal Regulations Title 21 Volume 3: 21CFR184.1033.

Ferreira, L., Sánchez-Juanes, F., González-Ávila, M., Cembrero-Fuciños, D., Herrero-Hernández, A., González-Buitrago, J.M. and Muñoz-Bellido, J.L. 2010. Direct identification of urinary tract pathogens from urine samples by matrix-assisted laser desorption ionization-time of flight mass spectrometry. Journal of clinical microbiology 48(6), 2110-2115.

Flanagan, C.P. and Randall, D.G. 2018. Development of a novel nutrient recovery urinal for on-site fertilizer production. Journal of Environmental Chemical Engineering 6(5), 6344-6350.

Francis, L., Ogunbiyi, O., Saththasivam, J., Lawler, J. and Liu, Z. 2020. A comprehensive review of forward osmosis and niche applications. Environmental Science: Water Research & Technology 6(8), 1986-2015.

Friedler, E., Butler, D. and Alfiya, Y. 2013. Source separation and decentralization for wastewater management. Larsen, T.A., Udert, K.M. and Lienert, J. (eds), pp. 241-257, IWA Publishing, London.

Fumasoli, A., Etter, B., Sterkele, B., Morgenroth, E. and Udert, K.M. 2016. Operating a pilot-scale nitrification/distillation plant for complete nutrient recovery from urine. Water Science and Technology 73(1), 215-222.

Gajurel, D.R., Gulyas, H., Reich, M. and Otterpohl, R. 2007. Behavior of four selected pharmaceuticals during long-time storage of yellow water, Brazil.

Ganrot, Z., Dave, G. and Nilsson, E. 2007. Recovery of N and P from human urine by freezing, struvite precipitation and adsorption to zeolite and active carbon. Bioresource technology 98(16), 3112-3121.

Genceli, F.E. 2008. Scaling-up Eutectic Freeze Crystallization. PhD Thesis, Technical University of Delft, The Netherlands.

Girovich, M.J. 1996. Biosolids treatment and management: Processes for beneficial use, CRC Press, Florida, USA.

Greenlee, L.F., Testa, F., Lawler, D.F., Freeman, B.D. and Moulin, P. 2010. The effect of antiscalant addition on calcium carbonate precipitation for a simplified synthetic brackish water reverse osmosis concentrate. Water research 44(9), 2957-2969.

Guizani, M., Fujii, T., Hijikata, N. and Funamizu, N. 2016. Salt removal from soil during rainy season of semi-arid climate following an assumed salt accumulation from previous cultivations fertilized with urine. Euro-Mediterranean Journal for Environmental Integration 1(1), 1-11.

Gulyas, H., Bruhn, P., Furmanska, M., Hartrampf, K., Kot, K., Luttenberg, B., Mahmood, Z., Stelmaszewska, K. and Otterpohl, R. 2004. Freeze concentration for enrichment of nutrients in yellow water from no-mix toilets. Water Science and Technology 50(6), 61-68.

Gundlach, J., Bryla, M., Larsen, T.A., Kristoferitsch, L., Gründl, H. and Holzner, M. 2021. Novel NoMix toilet concept for efficient separation of urine and feces and its design optimization using computational fluid mechanics. Journal of Building Engineering 33, 101500.

Hasson, D., Segev, R., Lisitsin, D., Liberman, B. and Semiat, R. 2011. High recovery brackish water desalination process devoid of precipitation chemicals. Desalination 283, 80-88.

Haynes, W.M., Lide, D.R. and Bruno, T.J. 2016. CRC handbook of chemistry and physics, 95th edition, CRC Press, Florida, USA.

Hellström, D., Johansson, E. and Grennberg, K. 1999. Storage of human urine: acidification as a method to inhibit decomposition of urea. Ecological Engineering 12(3), 253-269.

Hilt, E.E., McKinley, K., Pearce, M.M., Rosenfeld, A.B., Zilliox, M.J., Mueller, E.R., Brubaker, L., Gai, X., Wolfe, A.J. and Schreckenberger, P.C. 2014. Urine is not sterile: use of enhanced urine culture techniques to detect resident bacterial flora in the adult female bladder. Journal of clinical microbiology 52(3), 871-876.

Höglund, C., Ashbolt, N., Stenström, T.A. and Svensson, L. 2002. Viral persistence in source-separated human urine. Advances in Environmental Research 6(3), 265-275.

Iskander, S.M., Zou, S., Brazil, B., Novak, J.T. and He, Z. 2017. Energy consumption by forward osmosis treatment of landfill leachate for water recovery. Waste Management 63, 284-291.

Jermakka, J., Brewster, E.T., Ledezma, P. and Freguia, S. 2018. Electro-concentration for chemical-free nitrogen capture as solid ammonium bicarbonate. Separation and Purification Technology 203, 48-55.

Jones, E., Qadir, M., van Vliet, M.T., Smakhtin, V. and Kang, S.-m. 2019. The state of desalination and brine production: A global outlook. Science of the Total Environment 657, 1343-1356.

Khumalo, N., Nthunya, L., Derese, S., Motsa, M., Verliefde, A., Kuvarega, A., Mamba, B.B., Mhlanga, S. and Dlamini, D.S. 2019. Water recovery from hydrolysed human urine samples via direct contact membrane distillation using PVDF/PTFE membrane. Separation and Purification Technology 211, 610-617.

Köpping, I., McArdell, C.S., Borowska, E., Böhler, M.A. and Udert, K.M. 2020. Removal of pharmaceuticals from nitrified urine by adsorption on granular activated carbon. Water research X 9, 100057.

Krajewska, B. 2009. Ureases I. Functional, catalytic and kinetic properties: A review. Journal of Molecular Catalysis B: Enzymatic 59(1), 9-21.

Krajewska, B. 2011. Hydrogen peroxide-induced inactivation of urease: Mechanism, kinetics and inhibitory potency. Journal of Molecular Catalysis B: Enzymatic 68(3), 262-269.

Kumar, M., Adham, S.S. and Pearce, W.R. 2006. Investigation of seawater reverse osmosis fouling and its relationship to pretreatment type. Environmental science & technology 40(6), 2037-2044.

Larsen, T.A., Gruendl, H. and Binz, C. 2021a. The potential contribution of urine source separation to the SDG agenda–A review of the progress so far and future development options. Environmental Science: Water Research & Technology.

Larsen, T.A., Riechmann, M.E. and Udert, K.M. 2021b. State of the art of urine treatment technologies: A critical review. Water Research X, 100114.

Ledezma, P., Jermakka, J., Keller, J. and Freguia, S. 2017. Recovering nitrogen as a solid without chemical dosing: bio-electroconcentration for recovery of nutrients from urine. Environmental Science & Technology Letters 4(3), 119-124.

Lewis, A.E., Nathoo, J., Thomsen, K., Kramer, H., Witkamp, G., Reddy, S. and Randall, D.G. 2010. Design of a Eutectic Freeze Crystallization process for multicomponent waste water stream. Chemical Engineering Research and Design 88(9), 1290-1296.

Lienert, J., Bürki, T. and Escher, B.I. 2007. Reducing micropollutants with source control: substance flow analysis of 212 pharmaceuticals in faeces and urine. Water Science and Technology 56(5), 87-96.

Lienert, J. and Larsen, T.A. 2007. Pilot projects in bathrooms: A new challenge for wastewater professionals. Water Practice and Technology 2(3), 1-14.

Lind, B.-B., Ban, Z. and Bydén, S. 2001. Volume reduction and concentration of nutrients in human urine. Ecological Engineering 16(4), 561-566.

Lisitsin, D., Hasson, D. and Semiat, R. 2008. The potential of CO2 stripping for pretreating brackish and wastewater desalination feeds. Desalination 222(1-3), 50-58.

Liu, Q., Liu, C., Zhao, L., Ma, W., Liu, H. and Ma, J. 2016. Integrated forward osmosis-membrane distillation process for human urine treatment. Water research 91, 45-54.

Mahasti, N.N., Shih, Y.-J., Vu, X.-T. and Huang, Y.H. 2017. Removal of calcium hardness from solution by fluidized-bed homogeneous crystallization (FBHC) process. Journal of the Taiwan Institute of Chemical Engineers 78, 378-385.

Makhro. 2022. GroBest Liquid Fish Fertilizer Label [Online]. Available: https://makhro.co.za/wp-content/uploads/2021/03/Grobest-Label_compressed.pdf [Accessed 24 Agust 2022].

Martin, T.M., Esculier, F., Levavasseur, F. and Houot, S. 2022. Human urine-based fertilizers: A review. Critical Reviews in Environmental Science and Technology 52, 1-47.

Masse, L., Massé, D.I. and Pellerin, Y. 2008. The effect of pH on the separation of manure nutrients with reverse osmosis membranes. Journal of Membrane Science 325(2), 914-919.

Maurer, M., Pronk, W. and Larsen, T.A. 2006. Treatment processes for source-separated urine. Water Research 40(17), 3151-3166.

Maurer, M., Schwegler, P. and Larsen, T.A. 2003. Nutrients in urine: energetic aspects of removal and recovery. Water Science and Technology 48(1), 37-46.

Mazli, W., Samsuri, S. and Amran, N. 2020. Study of progressive freeze concentration and eutectic freeze crystallization technique for salt recovery. IOP Conference Series: Materials Science and Engineering. Kuala Lumpur, Malayasia, 30-31 October. IOP Publishing. 012167.

Meyer, G., Frossard, E., Mäder, P., Nanzer, S., Randall, D.G., Udert, K.M. and Oberson, A. 2018. Water soluble phosphate fertilizers for crops grown in calcareous soils–an outdated paradigm for recycled phosphorus fertilizers? Plant and soil 424(1-2), 367-388.

Mitsoyannis, E. and Saravacos, G.D. 1977. Precipitation of calcium carbonate on reverse osmosis membranes. Desalination 21(3), 235-240.

Mnkeni, P.N., Kutu, F.R., Muchaonyerwa, P. and Austin, L.M. 2008. Evaluation of human urine as a source of nutrients for selected vegetables and maize under tunnel house conditions in the Eastern Cape, South Africa. Waste management & research 26(2), 132-139.

Mobley, H. and Hausinger, R. 1989. Microbial ureases: significance, regulation, and molecular characterization. Microbiological reviews 53(1), 85-108.

Moharramzadeh, S., Ong, S.K., Alleman, J. and Cetin, K.S. 2022. Stabilization and concentration of nitrogen in synthetic urine with peracetic acid and progressive freeze concentration. Journal of Environmental Chemical Engineering, 107768.

Moon, A.S. and Lee, M. 2012. Energy consumption in forward osmosis desalination compared to other desalination techniques. International Journal of Chemical and Molecular Engineering 6(5), 427-429.

Mufunde, T. and Randall, D. 2022. A novel mixing mechanism for effective stabilisation of urea in urinals for subsequent nutrient recovery. South African Journal of Chemical Engineering 42, 42-52.

Noe-Hays, A., Homeyer, R.J., Davis, A.P. and Love, N.G. 2021. Advancing the Design and Operating Conditions for Block Freeze Concentration of Urine-Derived Fertilizer. ACS ES&T Engineering 2(3), 446-455.

Pancorbo, O.C., Bitton, G., Farrah, S.R., Gifford, G.E. and Overman, A.R. 1988. Poliovirus retention in soil columns after application of chemical-and polyelectrolyte-conditioned dewatered sludges. Appl. Environ. Microbiol. 54(1), 118-123.

Patterson, C., Anderson, A., Sinha, R., Muhammad, N. and Pearson, D. 2012. Nanofiltration membranes for removal of color and pathogens in small public drinking water sources. Journal of Environmental Engineering 138(1), 48-57.

Patyk, A. and Reinhardt, G.A. 1997. Düngemittel-Energie-und Stoffstrombilanzen, Springer.

Pronk, W., Biebow, M. and Boller, M. 2006a. Electrodialysis for Recovering Salts from a Urine Solution Containing Micropollutants. Environmental Science & Technology 40(7), 2414-2420.

Pronk, W., Palmquist, H., Biebow, M. and Boller, M. 2006b. Nanofiltration for the separation of pharmaceuticals from nutrients in source-separated urine. Water Research 40(7), 1405-1412.

Protea Chemicals 2017 Safety Data Sheet: Sodium Hydroxide. Chemicals, P. (ed), South Africa.

Putnam, D.F. 1971 Composition and concentrative properties of human urine, p. 112, NASA, Washington, D.C.

Randall, D., Nathoo, J. and Lewis, A. 2011. A case study for treating a reverse osmosis brine using Eutectic Freeze Crystallization—Approaching a zero waste process. Desalination 266(1-3), 256-262.

Randall, D., Zinn, C. and Lewis, A.E. 2014. Treatment of textile wastewaters using eutectic freeze crystallization. Water science and technology 70(4), 736-741.

Randall, D.G., Brison, A. and Udert, K.M. 2022. High temperatures and CO2 dissolution can cause nitrogen losses from urine stabilized with base. Frontiers in Environmental Science 10.

Randall, D.G., Krähenbühl, M., Köpping, I., Larsen, T.A. and Udert, K.M. 2016. A novel approach for stabilizing fresh urine by calcium hydroxide addition. Water Research 95, 361-369.

Randall, D.G. and Nathoo, J. 2015. A succinct review of the treatment of Reverse Osmosis brines using Freeze Crystallization. Journal of Water Process Engineering 8, 186-194.

Randall, D.G. and Nathoo, J. 2018. Resource recovery by freezing: A thermodynamic comparison between a reverse osmosis brine, seawater and stored urine. Journal of Water Process Engineering 26, 242-249.

Ray, H., Perreault, F. and Boyer, T. 2022. Ammonia recovery and fouling mitigation of hydrolyzed human urine treated by nanofiltration and reverse osmosis. Environmental Science: Water Research & Technology 8(2), 429-442.

Ray, H., Perreault, F. and Boyer, T.H. 2019. Urea recovery from fresh human urine by forward osmosis and membrane distillation (FO–MD). Environmental Science: Water Research & Technology 5(11), 1993-2003.

Ray, H., Perreault, F. and Boyer, T.H. 2020. Rejection of nitrogen species in real fresh and hydrolyzed human urine by reverse osmosis and nanofiltration. Journal of Environmental Chemical Engineering, 103993.

Ray, H., Saetta, D. and Boyer, T.H. 2018. Characterization of urea hydrolysis in fresh human urine and inhibition by chemical addition. Environmental Science: Water Research & Technology 4(1), 87-98.

Rektorschek, M., Weeks, D., Sachs, G. and Melchers, K. 1998. Influence of pH on metabolism and urease activity of Helicobacter pylori. Gastroenterology 115(3), 628-641.

Riechmann, M.E., Ndwandwe, B., Greenwood, E.E., Reynaert, E., Morgenroth, E. and Udert, K.M. 2021. On-site urine treatment combining Ca(OH)2 dissolution and dehydration with ambient air. Water research X 13, 100124.

Rodriguez, M., Luque, S., Alvarez, J. and Coca, J. 2000. A comparative study of reverse osmosis and freeze concentration for the removal of valeric acid from wastewaters. Desalination 127(1), 1-11.

Saetta, D., Padda, A., Li, X., Leyva, C., Mirchandani, P.B., Boscovic, D. and Boyer, T.H. 2019. Real-time monitoring and control of urea hydrolysis in cyber-enabled nonwater urinal system. Environmental science & technology 53(6), 3187-3197.

Schmidt, J.M. and Alleman, J.E. 2005. Urine Processing for Water Recovery via Freeze Concentration. SAE Transactions 114, 477-484.

Schürmann, B., Everding, W., Montag, D. and Pinnekamp, J. 2012. Fate of pharmaceuticals and bacteria in stored urine during precipitation and drying of struvite. Water Science and Technology 65(10), 1774-1780.

Senecal, J., Nordin, A., Simha, P. and Vinnerås, B. 2018. Hygiene aspect of treating human urine by alkaline dehydration. Water Research 144, 474-481.

Senecal, J. and Vinnerås, B. 2017. Urea stabilisation and concentration for urine-diverting dry toilets: Urine dehydration in ash. Science of The Total Environment 586, 650-657.

Simha, P., Friedrich, C., Randall, D.G. and Vinnerås, B. 2021. Alkaline dehydration of human urine collected in source-separated sanitation systems using Magnesium Oxide. Frontiers in Environmental Science 8, 9.

Simha, P., Karlsson, C., Viskari, E.-L., Malila, R. and Vinnerås, B. 2020a. Field testing a pilot-scale system for alkaline dehydration of source-separated human urine: a case study in Finland. Frontiers in Environmental Science 8, 168-178.

Simha, P., Lalander, C., Nordin, A. and Vinnerås, B. 2020b. Alkaline dehydration of source-separated fresh human urine: Preliminary insights into using different dehydration temperature and media. Science of the Total Environment 733, 139313.

Sutherland, C., Reynaert, E., Dhlamini, S., Magwaza, F., Lienert, J., Riechmann, M.E., Buthelezi, S., Khumalo, D., Morgenroth, E. and Udert, K.M. 2021. Socio-technical analysis of a sanitation innovation in a peri-urban household in Durban, South Africa. Science of the Total Environment 755, 143284.

Thanekar, P., Panda, M. and Gogate, P.R. 2018. Degradation of carbamazepine using hydrodynamic cavitation combined with advanced oxidation processes. Ultrasonics sonochemistry 40, 567-576.

Thörneby, L., Persson, K. and Trägårdh, G. 1999. Treatment of Liquid Effluents from Dairy Cattle and Pigs using Reverse Osmosis. Journal of Agricultural Engineering Research 73(2), 159-170.

Udert, K.M., Larsen, T.A., Biebow, M. and Gujer, W. 2003. Urea hydrolysis and precipitation dynamics in a urine-collecting system. Water Research 37(11), 2571-2582.

Udert, K.M. and Wächter, M. 2012. Complete nutrient recovery from source-separated urine by nitrification and distillation. Water Research 46(2), 453-464.

Ullah, R., Khraisheh, M., Esteves, R.J., McLeskey Jr, J.T., AlGhouti, M., Gad-el-Hak, M. and Tafreshi, H.V. 2018. Energy efficiency of direct contact membrane distillation. Desalination 433, 56-67.

Vasiljev, A., Simha, P., Demisse, N., Karlsson, C., Randall, D.G. and Vinnerås, B. 2022. Drying fresh human urine in magnesium-doped alkaline substrates: Capture of free ammonia, inhibition of enzymatic urea hydrolysis & minimisation of chemical urea hydrolysis. Chemical Engineering Journal 428, 131026.

Velts, O., Uibu, M., Kallas, J. and Kuusik, R. 2011. CO2 mineral trapping: Modeling of calcium carbonate precipitation in a semi-batch reactor. Energy Procedia 4, 771-778.

Volpin, F., Chekli, L., Phuntsho, S., Ghaffour, N., Vrouwenvelder, J.S. and Shon, H.K. 2019a. Optimisation of a forward osmosis and membrane distillation hybrid system for the treatment of source-separated urine. Separation and Purification Technology 212, 368-375.

Volpin, F., Fons, E., Chekli, L., Kim, J.E., Jang, A. and Shon, H.K. 2018. Hybrid forward osmosis-reverse osmosis for wastewater reuse and seawater desalination: Understanding the optimal feed solution to minimise fouling. Process Safety and Environmental Protection 117, 523-532.

Volpin, F., Heo, H., Hasan Johir, M.A., Cho, J., Phuntsho, S. and Shon, H.K. 2019b. Techno-economic feasibility of recovering phosphorus, nitrogen and water from dilute human urine via forward osmosis. Water Research 150, 47-55.

Volpin, F., Woo, Y.C., Kim, H., Freguia, S., Jeong, N., Choi, J.-S., Cho, J., Phuntsho, S. and Shon, H.K. 2020. Energy recovery through reverse electrodialysis: Harnessing the salinity gradient from the flushing of human urine. Water research 186, 116320.

Winter, D., Koschikowski, J. and Wieghaus, M. 2011. Desalination using membrane distillation: Experimental studies on full scale spiral wound modules. Journal of Membrane Science 375(1-2), 104-112.

Wonder. 2022. Wonder: Fertilizers [Online]. Available: https://wonder.co.za/product_type/fertiliser/?prod_id=600 [Accessed 11 August 2022].

Yoon, Y. and Lueptow, R.M. 2005. Reverse osmosis membrane rejection for ersatz space mission wastewaters. Water Research 39(14), 3298-3308.

Zanchetta, P.G., Heringer, O., Scherer, R., Pacheco, H.P., Gonçalves, R. and Pena, A. 2015. Evaluation of storage and evaporation in the removal efficiency of D-norgestrel and progesterone in human urine. Environmental monitoring and assessment 187(10), 1-8.

Zhang, J., She, Q., Chang, V.W., Tang, C.Y. and Webster, R.D. 2014. Mining nutrients (N, K, P) from urban source-separated urine by forward osmosis dewatering. Environmental science & technology 48(6), 3386-3394.

Zhang, R., Sun, P., Boyer, T.H., Zhao, L. and Huang, C.-H. 2015. Degradation of pharmaceuticals and metabolite in synthetic human urine by UV, UV/H2O2, and UV/PDS. Environmental science & technology 49(5), 3056-3066.

Zhang, Y., Li, Z., Zhao, Y., Chen, S. and Mahmood, I.B. 2013. Stabilization of source-separated human urine by chemical oxidation. Water Science and Technology 67(9), 1901.

Zhao, Z.-P., Xu, L., Shang, X. and Chen, K. 2013. Water regeneration from human urine by vacuum membrane distillation and analysis of membrane fouling characteristics. Separation and Purification Technology 118, 369-376.

CHAPTER 3: THEORY

Chapter 3: Theory

3.1 REVERSE OSMOSIS AND NANOFILTRATION

3.1.1 Separation mechanisms

Reverse osmosis and nanofiltration make use of slightly different mechanisms that allow water to pass through the membrane while solutes are rejected when pressure is applied to the system. Reverse osmosis membranes do not have distinct pores (Greenlee et al., 2009) and therefore have much slower permeation than NF membranes (Van der Bruggen et al., 2003). Solute-liquid separation is governed by solution diffusion whereby water molecules are absorbed into the membrane surface and then they permeate through the membrane by diffusion through the nonporous surface layer (Mazid, 1984).

Nanofiltration makes use of two mechanisms for solute rejection: steric hindrance (sieving) and the Donnan potential (charge effects) (Bergman, 2007). The sieving separates compounds based on their size in relation to the membrane's pore size, which is characterized by a molecular weight cut-off or the molecular weight of a solute that will be 90% retained by the membrane. For NF membranes, this is 250-2000 Daltons (Greenlee et al., 2009). The Donnan potential is an electrical potential phenomenon created as negative ions are repelled by the surface of the membrane (Greenlee et al., 2009). The electric potential between the membrane and the bulk solution allows ions to be rejected even though they are smaller than the NF membrane pore sizes (Van der Bruggen et al., 2003). Nanofiltration typically has a high rejection of divalent ions but a poor rejection of monovalent ions as the rejection of divalent ions is determined by Donnan exclusion, whereas because monovalent ions have weak electrostatic repulsion their rejection is controlled by steric hindrance (Suhalim et al., 2022).

3.1.2 Fundamentals of RO and NF operation

This section describes the equations used to determine the efficiency of RO and NF systems. Water recovery is typically defined as the volume percentage of the influent recovered as permeate (Kucera, 2015). However, as the aim of this study was to concentrate urine rather than recover water it shall be referred to as ‘water removal’. The concentration or volume reduction factor is the ratio between the initial and final (concentrate) volume.

Permeate flux is described by Equation 3-1 and is usually measured as the permeate flow rate per membrane area. The water transport coefficient is unique for each membrane and it can vary with pH and temperature (Kucera, 2015). Water permeation will only occur when the feed pressure exceeds the solution's osmotic pressure. The driving force for flux is the difference between the applied pressure and solution osmotic pressure. For thermodynamically ideal solutions, the osmotic pressure is described by Equation 3-2, (Greenlee et al., 2009). As the solution is concentrated, the osmotic pressure increases, resulting in a decrease in flux. Whilst diffusion of solutes through the membrane is possible, the mass transfer rate is much slower than that of water (Bergman, 2007) and is defined by Equation 3-3.

CHAPTER 3: THEORY

Rejection is used to describe the percentage of an influent solute that is retained by the membrane (Equation 3-4). Solution rejection increases with increasing applied pressure (Bergman, 2007). Solution flux increases with applied pressure; however, solute flux remains relatively constant. This results in an increased calculated solute rejection because progressively more solution permeates relative to the salt (Kucera, 2015). Concentration polarization is a phenomenon that can result in decreased rejection. It is defined as the occurrence of increased solute concentration at the membrane surface relative to the bulk solution (Bergman, 2007).

Flux:

$$J_w = K_w(\Delta P - \Delta\pi) = \frac{Q_p}{A} \qquad \text{(Equation 3-1)}$$

Where:

J_w = Permeate flux (L m^{-2} hr^{-1})

K_w = water transport coefficient (L m^{-2} bar^{-1})

ΔP = the pressure difference across the membrane (bar)

$\Delta\pi$ = the osmotic pressure difference between the feed and permeate (bar)

Osmotic pressure:

$$\pi = CRT \qquad \text{(Equation 3-2)}$$

Where:

C = the total ion concentration (mols L^{-1})

R = the ideal gas constant (L bar mol^{-1} K^{-1})

T = the solution temperature (K^{-1})

Dissolved solute flux:

$$J_s = K_s(C_m - C_p) \qquad \text{(Equation 3-3)}$$

Where:

K_s = solute mass transfer coefficient (m hr^{-1})

C_m = the solute concentration at the membrane surface (g L^{-1})

C_p = the solute concentration in the permeate (g L^{-1})

Rejection:

$$R_x = \left(1 - {}^{C_{x,p}}\!/_{C_{x,f}}\right) \times 100\% \qquad \text{(Equation 3-4)}$$

Where:

$C_{x,p}$ = the concentration in the permeate (g L^{-1})

$C_{x,f}$ = the concentration in the feed (g L^{-1})

3.1.3 Fouling and scaling

RO and NF membranes can often show a decline in productivity over time. This can be attributed to either fouling or scaling because of the deposition of solids on the membrane surface. During the concentration process, inorganics precipitate out of the solution and deposit on the membrane forming a 'scale' (Kumar et al., 2006). Multiple mechanisms cause fouling including; pore clogging, adsorption of feed components, chemical interaction between the membrane and solutes in the feed, bacterial growth, and gel formation (Goosen et al., 2005). Potential fouling and scaling components include suspended solids (organic & inorganic), dissolved organic matter, dissolved solids (precipitation of sparingly soluble salts as concentration increases), and biological organisms (Amiri and Samiei, 2007). Upen et al. (2000) advise that bacterial adhesion is one of the most serious forms of fouling and can be very difficult to remove. The potential for fouling can be reduced in several ways such as pre-treatment, changing operational variables, and cleaning.

Pre-treatment: Kumar et al. (2006) observed that particulate matter greater than 1 µm caused the most fouling on high pressure SWRO membranes. However, they further noted that pre-treatment using 0.1 µm microfiltration had the most significant impact on fouling reduction. For stable filtration performance, Franks et al. (2009) advise a suspended solids concentration of less than 0.5 ppm.

Operational variables: Increasing the feed velocity has also been shown to reduce the potential of scaling/ solute build-up by increasing turbulence at the membrane surface (Amiri and Samiei, 2007). Increased turbulence and flux can also be achieved by increasing feed spacer thickness (Sablani et al., 2002). Franks et al. (2009) found that with increasing feed spacer thickness, cleaning-in-place (CIP) requirements were reduced. An antiscalant can be used to increase the concentration at which scaling components precipitate (Bergman, 2007).

Cleaning: In the case that it is too late for fouling prevention, it is possible to remove any fouling or scaling with a chemical CIP, which works by dissolving, dislodging, or breaking down the fouling/scaling component (Bergman, 2007).

3.2 FREEZE CRYSTALLIZATION

3.2.1 Crystallization

Crystallization occurs as a result of a phase change where a crystalline solid forms from a solution (Myerson, 2002). Crystallization can only occur when a solution is supersaturated (described by Equation 3-5 and Equation 3-6). Supersaturation is the thermodynamic driving force for crystallization (Löffelmann and Mersmann, 2002). However, a metastable state exists where supersaturation or supercooling alone may not be sufficient for crystallization to occur (Mullin, 2001). Before crystallization occurs there must be a certain number of nuclei or seeds present that act as centers of crystallization (Mullin, 2001). Figure 3-1 shows the metastable zone width (MSZW). This region shows the maximum a solution can be supercooled before spontaneous nucleation will occur (Beckmann, 2013). Seed crystals can be added to a supersaturated or supercooled solution to act as a point of nucleation and promote crystallization (Myerson, 2002).

Supersaturation:

$$S = \frac{C}{C_{eq}} \qquad \text{(Equation 3-5)}$$

Where:

C = solute concentration (mol L^{-1})

C_{eq} = equilibrium solute concentration (mol L^{-1})

Supercooling (cooling crystallization):

$$S = T - T^{*} \qquad \text{(Equation 3-6)}$$

Where:

T = is the liquid temperature (°C)

T^{*} = is the equilibrium temperature (°C)

3.2.2 Ice crystallization

As a solution is cooled the temperature decreases until ice crystallization occurs (either spontaneously or by adding ice seeds). The ice crystallization temperature (ICT) refers to the temperature at which the first ice crystals form (Figure 3-1:A). An enthalpy change occurs during crystallization, known as the heat of crystallization (Myerson, 2002) and results in an increase in the solution temperature. The temperature to which the solution increases is referred to as the ice equilibrium temperature (IET). The solution temperature will only decrease if further heat is removed from the solution using cooling. The ICT of a solution will vary based on a solution's metastable zone width (MSZW) and whether ice seeds

were added, whilst the IET is fixed for a certain solution composition. Thermodynamic models cannot be used to determine the MSZW of a solution and only predict the IET of a solution. The MSZW for a given solution is dependent on several factors including liquid volume, cooling rate, and temperature difference between the liquid and chiller (Randall et al., 2012).

3.2.3 Eutectic freeze crystallization

The operating principle of EFC is described in Figure 3-1:B. The initial solution concentration will either be to the left or right of the eutectic concentration (C_E). When a solution (1), with a concentration less than C_E, is cooled ice will form first (2) (Randall and Nathoo, 2015). During slow ice crystal formation, dissolved solutes are excluded from the ice crystal structure and remain concentrated in the liquid (Lind et al., 2001). As the solution is further cooled and more ice forms, the liquid becomes more concentrated, and this process is known as freeze concentration. If the solution is cooled further and sufficient ice forms the solution will reach C_E. If a solution at the C_E concentration is cooled further, both ice and salt will crystallize, this is known as the eutectic point (Van der Ham et al., 1999).

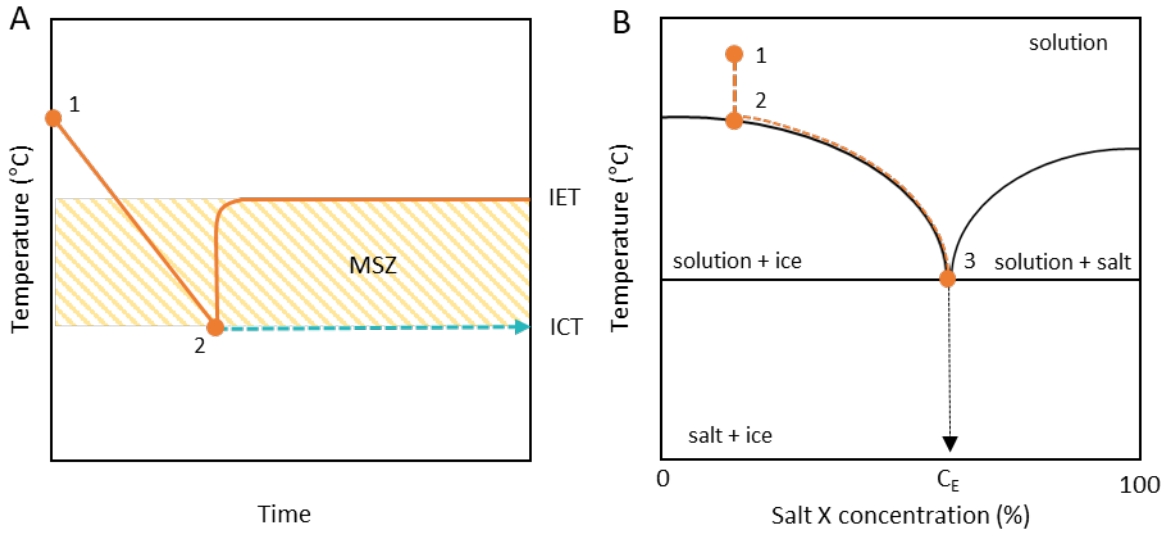

Figure 3-1: Temperature profile of a liquid as it is cooled from point 1 and when ice crystallization begins at point 2 (A), and a binary phase diagram for a water and salt X solution where the orange line depicts how the concentration of salt X increases during a freeze concentration process, adapted from (Randall and Nathoo, 2015) (B).

REFERENCES

Amiri, M.C. and Samiei, M. 2007. Enhancing permeate flux in a RO plant by controlling membrane fouling. Desalination 207(1), 361-369.

Beckmann, W. 2013. Crystallization: Basic concepts and industrial applications, John Wiley & Sons.

Bergman, R. 2007. Reverse osmosis and nanofiltration, 2nd edition, American Water Works Association, Colorado, USA.

Franks, R., Bartels, C. and Nagghappan, L. 2009. Performance of a reverse osmosis system when reclaiming high pH-high temperature wastewater. American Water Works Association Membrane Technology Conference. Memphis, USA, 15-18 March. 1-16.

Goosen, M., Sablani, S., Al-Hinai, H., Al-Obeidani, S., Al-Belushi, R. and Jackson, a. 2005. Fouling of reverse osmosis and ultrafiltration membranes: a critical review. Separation science and technology 39(10), 2261-2297.

Greenlee, L.F., Lawler, D.F., Freeman, B.D., Marrot, B. and Moulin, P. 2009. Reverse osmosis desalination: Water sources, technology, and today's challenges. Water Research 43(9), 2317-2348.

Kucera, J. 2015. Reverse osmosis: industrial processes and applications, 3rd Edition, John Wiley & Sons, New York.

Kumar, M., Adham, S.S. and Pearce, W.R. 2006. Investigation of seawater reverse osmosis fouling and its relationship to pretreatment type. Environmental science & technology 40(6), 2037-2044.

Lind, B.-B., Ban, Z. and Bydén, S. 2001. Volume reduction and concentration of nutrients in human urine. Ecological Engineering 16(4), 561-566.

Löffelmann, M. and Mersmann, A. 2002. How to measure supersaturation? Chemical Engineering Science 57(20), 4301-4310.

Mazid, M. 1984. Mechanisms of transport through reverse osmosis membranes. Separation Science and Technology 19(6-7), 357-373.

Mullin, J.W. 2001. Crystallization, 4th edition, Butterworth-Heinemann, Oxford, UK.

Myerson, A. 2002. Handbook of industrial crystallization, Butterworth-Heinemann.

Randall, D., Nathoo, J., Genceli-Güner, F., Kramer, H., Witkamp, G.-J. and Lewis, A. 2012. Determination of the metastable ice zone for a sodium sulphate system. Chemical engineering science 77, 184-188.

Randall, D.G. and Nathoo, J. 2015. A succinct review of the treatment of Reverse Osmosis brines using Freeze Crystallization. Journal of Water Process Engineering 8, 186-194.

Sablani, S.S., Goosen, M.F., Al-Belushi, R. and Gerardos, V. 2002. Influence of spacer thickness on permeate flux in spiral-wound seawater reverse osmosis systems. Desalination 146(1-3), 225-230.

Suhalim, N.S., Kasim, N., Mahmoudi, E., Shamsudin, I.J., Mohammad, A.W., Mohamed Zuki, F. and Jamari, N.L.-A. 2022. Rejection Mechanism of Ionic Solute Removal by Nanofiltration Membranes: An Overview. Nanomaterials 12(3), 437.

Upen, J., Barwada, S.J., Coker, S. and Terry, A. 2000. Winning the battle against biofouling of reverse osmosis membranes. Desalination and Water Reuse 10(2), 53-58.

Van der Bruggen, B., Vandecasteele, C., Van Gestel, T., Doyen, W. and Leysen, R. 2003. A review of pressure-driven membrane processes in wastewater treatment and drinking water production. Environmental progress 22(1), 46-56.

Van der Ham, F., Witkamp, G., De Graauw, J. and Van Rosmalen, G. 1999. Eutectic freeze crystallization simultaneous formation and separation of two solid phases. Journal of crystal growth 198, 744-748.

CHAPTER 4: GENERAL METHODS

CHAPTER 4: GENERAL METHODS

The over-arching aim of this research was to develop an integrated treatment process to concentrate urine whilst maximizing the recovery of key nutrients (N, P, K). This chapter covers the general and recurring methods that were used throughout this research, including the method for urine collection, make-up methodology and composition for synthetic urine, thermodynamic modeling, and analytical methods. Additional experimental conditions and equipment are described in more detail in the relevant chapters.

4.1 URINE COLLECTION AND STABILIZATION

4.1.1 Real urine

All real urine used throughout this work was collected anonymously from men and women working and studying in the New Engineering Building at the University of Cape Town. The majority of urine used throughout this research was stabilized with 10 g L^{-1} $Ca(OH)_2$ (Randall et al., 2016). The urine was collected in novel fertilizer-producing urinals, developed by Flanagan and Randall (2018), which were pre-dosed with the appropriate amount of $Ca(OH)_2$ (98%, Kimix, South Africa). The urinals were manually mixed twice daily during the collection phase by gently swirling the container contents. This ensured a homogenous solution pH above 12. After collection, the urine was stored in sealed 25 L containers and used within one month of collection. All urine was filtered (1,2µm, Ahlstrom-Munksjö, Helsinki, Finland) to remove excess $Ca(OH)_2$ and other precipitates before experiments were conducted. Due to COVID-19, the limited presence of students and staff on campus made it difficult to collect sufficient volumes of urine with the same composition, hence many experiments using real urine had different compositions. Detailed urine compositions from each experiment are available in the relevant Appendix for each chapter ((Table B-1, Table C-1, Table D-1, and Table E-1).

4.1.2 Synthetic urine

The composition of real urine can vary significantly. Synthetic urine is therefore useful because the composition can be kept constant throughout experiments. In addition, the modeling software (described in detail below) used throughout this research does not include many of the organics present in urine (other than urea) in its database. Therefore, a synthetic urine recipe was developed without organics such that those experimental results could be directly compared to the thermodynamic model. Table 6 details the synthetic urine recipe. The synthetic recipe was developed based on average ion concentrations in urine observed in literature and was composed of salts recommended by (Pronk et al., 2006b). However, some salts were replaced by acetate salts (ammonium acetate, and sodium acetate) to mimic the organic content and pH of real fresh urine more closely. The synthetic urine recipe was based on “fresh” urine to which the relevant stabilizer was added and then treated as per the real urine.

Table 6: Recipe for fresh synthetic urine in g L^{-1}, pH = 5.7.

Compound		Concentration (g L^{-1})	Purity (%)	Supplier
Urea	$CO(NH_2)_2$	13.0	99.5	Sigma Aldrich
Sodium chloride	NaCl	3.65	99.0	Sigma Aldrich
Potassium chloride	KCl	3.87	99.0	Sigma Aldrich
Sodium dihydrogen phosphate	NaH_2PO_4	1.38	99.0	Sigma Aldrich
Sodium sulfate	Na_2SO_4	1.43	97.0	Sigma Aldrich
Ammonium acetate	CH_3OONH_4	2.24	98.0	Sigma Aldrich
Calcium chloride dihydrate	$CaCl_2{\cdot}2H_2O$	0.56	100	Kimix
Magnesium chloride	$MgCl_2$	0.24	98.0	Sigma Aldrich
Sodium Acetate	NaC_2H_3O	1.00	98.0	Kimic

4.2 THERMODYNAMIC MODELING

All thermodynamic modeling was conducted using OLI Stream Analyzer (OLI Systems Inc, 2022). The Mixed Solvent Electrolyte (MSE) database was used as this is not limited by the ionic strength of the solution. Thermodynamic properties of aqueous species are calculated based on the revised Helgeson-Kirkham-Flowers (HKF) framework and the activity coefficients for complex high ionic strength solutions (like urine) are based on the combined work of Bromley, Zemaitis, Pitzer, Debye–Huckel (Lewis et al., 2010). Analysis of an aqueous stream should have a balance of anions and cations. Simply inputting the concentrations of the ions measured in urine does not always result in the cations and anions balancing as it is not analytically possible to measure every species in urine, and accurately. Therefore, directly inputting the urine recipe based on the salts used ensured the cations and anions were balanced.

4.3 ANALYTICAL METHODS

4.3.1 Liquid Analysis

Colorimetric methods were used to determine the concentration of urea, total ammoniacal nitrogen (TAN), PO_4-P, Mg^{2+}, $Ca^{2+,}$ SO_4^{2-}, Cl^-, and K^+, where required. This process was automated with a GalleryTM Discrete Analyzer (ThermoFisher Scientific, Massachusetts) using standard methods of the equipment. The samples were diluted, and the pH was adjusted (with dilute HCl, 0.01M) to between 7 and 8 to prevent ammonia volatilization where necessary. The concentration of sodium ions was determined using inductively coupled plasma optical emission spectrometry (5900 SVDV, Agilent, USA). The chemical oxygen demand (COD) of a sample was measured with medium-range reagent

vials (HI94754B-25, Hanna, Johannesburg) and a multiparameter photometer (H183399, Hanna, Johannesburg). The COD was used as a proxy for the concentration of organics (Li and Liu, 2018). Solids could also be analyzed for specific ions by redissolving a known mass in 100 mL of de-ionized water. All liquid samples were analyzed within 30 minutes of sampling.

4.3.2 Scanning electron microscope

Scanning electron microscopy (SEM) (FEI Nova SEM 230, FEI, USA) was used to analyze the $CaCO_3$ crystal morphology in Chapter 5 and the RO membrane surface in Chapter 7. The SEM was equipped with an Oxford X-Max dispersive X-ray spectroscopy (EDS) detector (Oxford Instruments, England) which was used to characterize precipitates on the membrane surface using elemental analysis. The analysis was carried out on the Oxford INCA software.

4.3.3 X-ray diffraction

X-ray diffraction (XRD) analysis was conducted in Chapter 5 and Chapter 6, to confirm the precipitation of $CaCO_3$, using a D8 advanced diffractometer (Bruker, Germany) which was outfitted with a position-sensitive detector (LYNXEYE) and Bragg Brentano geometry was used for the analysis. Power to the Co anode was set at 35 kV and 40 mA. A range of 20° to 120° (d^{-1} = 0.19 to 0.97 Å-1) with a 0.017° step size (0.84 seconds per step) was used to acquire the diffraction patterns. The ICDD database (PDF4+, released 2020) was used to compare the diffraction patterns to the reference data files.

REFERENCES

Flanagan, C.P., and Randall, D.G. 2018. Development of a novel nutrient recovery urinal for on-site fertilizer production. Journal of Environmental Chemical Engineering 6(5), 6344-6350.

Lewis, A.E., Nathoo, J., Thomsen, K., Kramer, H., Witkamp, G., Reddy, S. and Randall, D.G. 2010. Design of a Eutectic Freeze Crystallization process for multicomponent wastewater stream. Chemical Engineering Research and Design 88(9), 1290-1296.

Li, D. and Liu, S. 2018. Water quality monitoring and management: basis, technology, and case studies, Academic Press, Massachusetts, USA.

OLI Systems Inc. 2022. OLI Stream Analyzer, version 11.0, OLI Systems Inc, New Jersey, USA.

Pronk, W., Palmquist, H., Biebow, M. and Boller, M. 2006. Nanofiltration for the separation of pharmaceuticals from nutrients in source-separated urine. Water Research 40(7), 1405-1412.

Randall, D.G., Krähenbühl, M., Köpping, I., Larsen, T.A. and Udert, K.M. 2016. A novel approach for stabilizing fresh urine by calcium hydroxide addition. Water Research 95, 361-369.

CHAPTER 5: CHEMICAL ADDITION PRE-TREATMENT

CHAPTER 5: CHEMICAL ADDITION PRE-TREATMENT

This chapter is based on the published work from Paper 1 titled: Precipitation to remove calcium ions from stabilized human urine as a pre-treatment for reverse osmosis.

5.1 INTRODUCTION

There are two common barriers to implementing RO technology: brine management and disposal (Bond and Veerapaneni, 2007), and membrane scaling (Greenlee et al., 2009). In the case of urine concentration, the brine would be the product (liquid fertilizer) and the permeate could be used as a recycled water source (Chipako and Randall, 2020a). Membrane scaling is a process where solid precipitates build up on the membrane surface once their solubility limit has been reached (Kucera, 2015). This results in decreased permeate flux, and overall operating efficiency, and can also shorten the life span of membranes (Rahardianto et al., 2007). Common scaling compounds include $CaCO_3$, $Mg(OH)_2$, $CaSO_4$, $SrSO_4$, $BaSO_4$, CaF_2 and SiO_2 (Sutzkover-Gutman and Hasson, 2010) and Ca_3PO_4 (Antony et al., 2011). In terms of scaling components, $CaCO_3$ is the most common problematic for both seawater and brackish water RO systems (Greenlee et al., 2009) as it is almost insoluble (14.25 mg L^{-1} at 25°C in water (Haynes et al., 2016)).

Urine contains many scaling precursor ions (Ca^{2+}, SO_4^{2-}, Mg^{2+}, and PO_4^{3-}). In addition, to prevent enzymatic urea hydrolysis, urine can be stabilized by adding $Ca(OH)_2$ in excess (Randall et al., 2016) which results in a further increase in the concentration of Ca^{2+} ions (1000 – 1400 mg L^{-1}) (Randall et al., 2016). Urine stabilized with $Ca(OH)_2$ is saturated with respect to $Ca(OH)_2$ and which would precipitate on the membrane surface as the solution is concentrated resulting in scaling.

The application of chemicals that result in a pH increase and ultimately precipitate undesirable salts is a widely known pre-treatment technique for RO systems (Sheikholeslami and Bright, 2002). Calcium hydroxide can be used to reduce water hardness by increasing the pH, allowing any inorganic carbon and magnesium present to be precipitated as $CaCO_3$ and $Mg(OH)_2$ via Equations 5-1 and Equation 5-2. It is also common to remove the remaining calcium ions with Na_2CO_3 softening (Ayoub et al., 2019), which results in further $CaCO_3$ precipitation via Equation 5-3. Stabilization with $Ca(OH)_2$ is also advantageous as it results in the precipitation of another scaling compound, calcium phosphate (Flanagan and Randall, 2018), which can also be recovered and used as a fertilizer (Meyer et al., 2018).

$$Ca(OH)_2 + HCO_3^- \rightarrow CaCO_{3(s)} + H_2O + OH^- \quad \text{(Equation 5-1)}$$

$$Ca(OH)_2 + Mg^{2+} \rightarrow Mg(OH)_{2(s)} + Ca^{2+} \quad \text{(Equation 5-2)}$$

$$Na_2CO_3 + Ca^{+2} \rightarrow CaCO_{3(s)} + 2Na^+ \quad \text{(Equation 5-3)}$$

Research on the concentration of urine using RO is limited to hydrolyzed urine (Ek et al., 2006) and no studies that this author is aware of have been conducted with $Ca(OH)_2$ stabilized urine. This may be

because of the high membrane scaling potential. A pre-treatment step to reduce the calcium concentration is therefore required. A chemical antiscalant could also be used to minimize $CaCO_3$ scaling potential as they work by inhibiting crystal formation (Antony et al., 2011). However, their effectiveness is limited with increasing $CaCO_3$ saturation indices and precipitation may still occur (Greenlee et al., 2010).

Whilst Na_2CO_3 addition has been widely shown as a method to remove excess calcium from hard waters (Ayoub et al., 2019; Mahasti et al., 2017), it was hypothesized that $NaHCO_3$ could also be used to precipitate excess calcium from human urine stabilized with $Ca(OH)_2$. This would be advantageous as at \$150 ton^{-1} (compared to \$250 ton^{-1} for Na_2CO_3), $NaHCO_3$ is significantly cheaper than Na_2CO_3 (Alibaba.com, 2021). In addition, dosing $NaHCO_3$ would only add one sodium ion (Equation 5-4) instead of two ions as with Na_2CO_3 (Equation 5-3), thus minimizing the total dissolved solids (TDS) of the solution. This is important, as the extent of water removal and flux in an RO system is directly proportional to the TDS (Bergman, 2007).

$$NaHCO_3 + Ca^{2+} \rightarrow Na^+ + H^+ + CaCO_3 \qquad \text{(Equation 5-4)}$$

The calcium concentration in stabilized urine varies based on urine composition (Randall et al., 2016). The minimum required dose of a carbonate salt would therefore also vary based on the urine composition. The dosing method could be achieved via either a fixed dose that covers a wide range of typical urine compositions, or an exact dose based on the calcium concentration of a given composition of urine. An exact dose is advantageous as it minimizes reagent costs as well as the addition of undesirable sodium ions. Alternatively, it should be investigated if pH or conductivity could potentially be used as a proxy to indicate complete $CaCO_3$ precipitation and therefore be used to determine the required dosage of the carbonate salt without having to measure the calcium concentration.

The aim of this chapter was therefore to:

1. Determine the feasibility of using bicarbonate and carbonate salts such as $NaHCO_3$ or Na_2CO_3 as a method to remove excess calcium ions from stabilized human urine, prior to a RO process.
2. Investigate how the addition of these salts affected the conductivity and pH of the solution and whether one of these parameters could be used as a proxy for the calcium concentration to determine the required salt dosage.
3. Compare the effectiveness of a once-off fixed dose and an exact dose based on different urine compositions and determine the most suitable dosing method.

5.2 MATERIALS AND METHODS

5.2.1 Experimental conditions

A variety of experimental conditions were examined to compare the efficacy of $NaHCO_3$ and Na_2CO_3 but also to determine the most cost-effective method to control the dosing. This was achieved by assessing how a once-off fixed dose and an exact dose affect the calcium concentration, pH, and conductivity. Each experiment was repeated in triplicate and Table 7 below summarizes the experimental conditions. The term carbonate salt is used interchangeably throughout to refer to both bicarbonate and carbonate salts.

Table 7: Experimental conditions for different experiments.

Exp. #	Urine comp.	Dose (mmol L^{-1})	Reactant	Aim
A1	U1	5, 10, 15, 20, 25, 30	$NaHCO_3$	To compare $NaHCO_3$ and Na_2CO_3 in terms of calcium removed, solids formed, pH, and conductivity.
A2	U1		Na_2CO_3	
A3	Synth		$NaHCO_3$	
B1	U1-U5 Synth	40	$NaHCO_3$	Determine the effect of a once-off dose on varying urine compositions.
*C1	U2	32.4	$NaHCO_3$	Determine the effect of an exact dose based on the initial measured calcium concentration.
	U3	31.7		
	U4	57.9		
	U5	38.6		
	Synth	32.9		
D1	Synth	2.0 (Every 45 s)	NaHCO3	Determine if conductivity could be used as a proxy for the calcium concentration.

**During experiment C1, the U1 container accidentally broke and the remaining urine sample was lost.*

Incremental dosing

Samples of stabilized, filtered (1.2 µm) urine were added to six 100 mL volumetric flasks. An additional 50 mL of the urine sample was further filtered to 0.45 µm (ClearRight, Cape Town, South Africa) and the pH (H15221, Hanna, Johannesburg, South Africa), temperature, conductivity (H15321, Hanna, Johannesburg, South Africa), and calcium concentration was measured. A 1 M solution of either $NaHCO_3$ or Na_2CO_3 (Sigma-Aldrich) was used for each experiment. A volume of 0.5 mL was added to the first flask, 1 mL to the second, 1.5 mL to the third, and so on. The lid of the volumetric flask was replaced to seal the mixture. It was then mixed with a magnetic stirrer (F-13, Freed Electric, Israel) for 45 minutes to ensure the reaction had run to completion. Once the reaction was complete, each sample was filtered to 0.45 µm. The filtered solids were dried in an oven at 100°C for 24 hours before being weighed. The pH, conductivity, and temperature of the filtered liquid were remeasured at the end of each experiment.

To determine if conductivity could be used as a proxy for the calcium concentration, the 1 M $NaHCO_3$ solution was dosed in 45s increments (0.4 mL per dose) to 200 mL of synthetic stabilized urine. The solution was continuously mixed, and the conductivity was recorded every 45 seconds.

Once-off and exact dosing

To determine the amount of $NaHCO_3$ required for the once-off dose, five different urine compositions were collected plus one synthetic urine composition. Each sample was stabilized with $Ca(OH)_2$ and the calcium concentrations of the solutions were measured. To increase the sample size, the calcium concentration of three additional stabilized urine compositions from this work and literature (Flanagan and Randall, 2018; Randall et al., 2016) were also evaluated. The average calcium concentration of these 8 compositions was determined to be 31.9 ± 8.6 mmol L^{-1}. The once-off dose was then calculated as the average plus one standard deviation, which was rounded to 40 mmol of $NaHCO_3$ L^{-1}. This equates to a 4 mL dose per 100 mL of urine. Overdosing by one standard deviation ensures enough carbonate ions would be added for a wide range of changing urine compositions. For the exact dosing method, the volume for a 1 M $NaHCO_3$ solution required was calculated based on the measured initial calcium concentration.

5.2.2 Thermodynamic modeling

A thermodynamic model was used to simulate the addition of Na_2CO_3 and $NaHCO_3$ and compared to the experimental results. After confirming that the model was an accurate representation of the experimental results it was used to determine if three other carbonate-forming compounds ($KHCO_3$, NH_4HCO_3, and $MgCO_3$) could be used as alternative compounds to $NaHCO_3$. Where possible, bicarbonate compounds were chosen over carbonate compounds as they introduced fewer additional cations to the solution.

5.3 RESULTS AND DISCUSSION

5.3.1 $NaHCO_3$ and Na_2CO_3 incremental addition

The addition of either $NaHCO_3$ or Na_2CO_3 had the same effect on the remaining calcium concentration and the mass of solids formed as shown in Figure 5-1A and Figure 5-1B. The calcium removed was >99.6% for both $NaHCO_3$ and Na_2CO_3. This is greater than the 92% calcium removal achieved by Mahasti et al. (2017) using Na_2CO_3 in a fluidized-bed homogeneous crystallization process and the same as achieved by Ayoub et al. (2019) who used a combination of NaOH and Na_2CO_3 addition. In addition, the number of moles of calcium removed was proportionate to the number of moles of

$NaHCO_3$ or Na_2CO_3 added. This suggests that the addition of the reagent in excess is not required and that the reaction follows theoretical stoichiometry, unlike with struvite precipitation (Altinbaş et al., 2002). The mass of solids formed deviated slightly from the theoretical value from 15 mmol L^{-1} onwards. The XRD analysis confirmed the formation of a pure $CaCO_3$ solid. Deviations in the mass of solids formed could not be explained via XRD. However, it was hypothesized that it may be due to the formation of small amounts of amorphous compounds such as monohydrate calcite ($CaCO_3$·H2O) and ikaite ($CaCO_3 \cdot 6H_2O$).

For Na_2CO_3, the conductivity remains relatively stable until 20 mmol L^{-1} and then increases, whilst for $NaHCO_3$ a continuous decrease in conductivity is observed (Figure 5-1C). This was expected as every mole of Na_2CO_3 adds two moles of Na^+ ions compared to one mole if $NaHCO_3$ is dosed. For Na_2CO_3 this results in no net increase in cations until all the Ca^{2+} is precipitated, after which there is an increase in conductivity. Whereas with $NaHCO_3$ addition, there is a net decrease in cations (-1) until all the Ca^{2+} is precipitated. Therefore, the conductivity decreases until all the $CaCO_3$ is precipitated and, if sufficient $NaHCO_3$ is added, the conductivity should begin to increase again.

For experiments with Na_2CO_3 dosing, the pH remained relatively constant whilst for $NaHCO_3$ dosing a decrease in pH was observed. The equilibrium constant for the HCO_3^-/CO_3^{2-} carbonate system is 10.33 (Haynes et al., 2016). Therefore, at a pH above 10.33 the formation of CO_3^{2-} is favored. When $NaHCO_3$ is added, the salt dissociates to form Na+ and HCO_3- ions. Because the pH of stabilized urine is approximately 12.45, the speciation of HCO_3^- shifts to $CO_3^{2-,}$ and H^+ ions are released. When Na_2CO_3 is added it dissociates to $2Na^+$ and CO_3^{2-} and no shift in the carbonate ion speciation is observed. The H+ ions from $NaHCO_3$ addition result in a decrease in pH which does not occur with Na_2CO_3 addition. In both cases, after 30 mmol L^{-1} (and once the calcium concentration was at a minimum) addition of either Na_2CO_3 or $NaHCO_3$, the pH remained above 11. This is the pH threshold for enzymatic urea hydrolysis (Randall et al., 2016) and it indicates that the urine would still be stabilized.

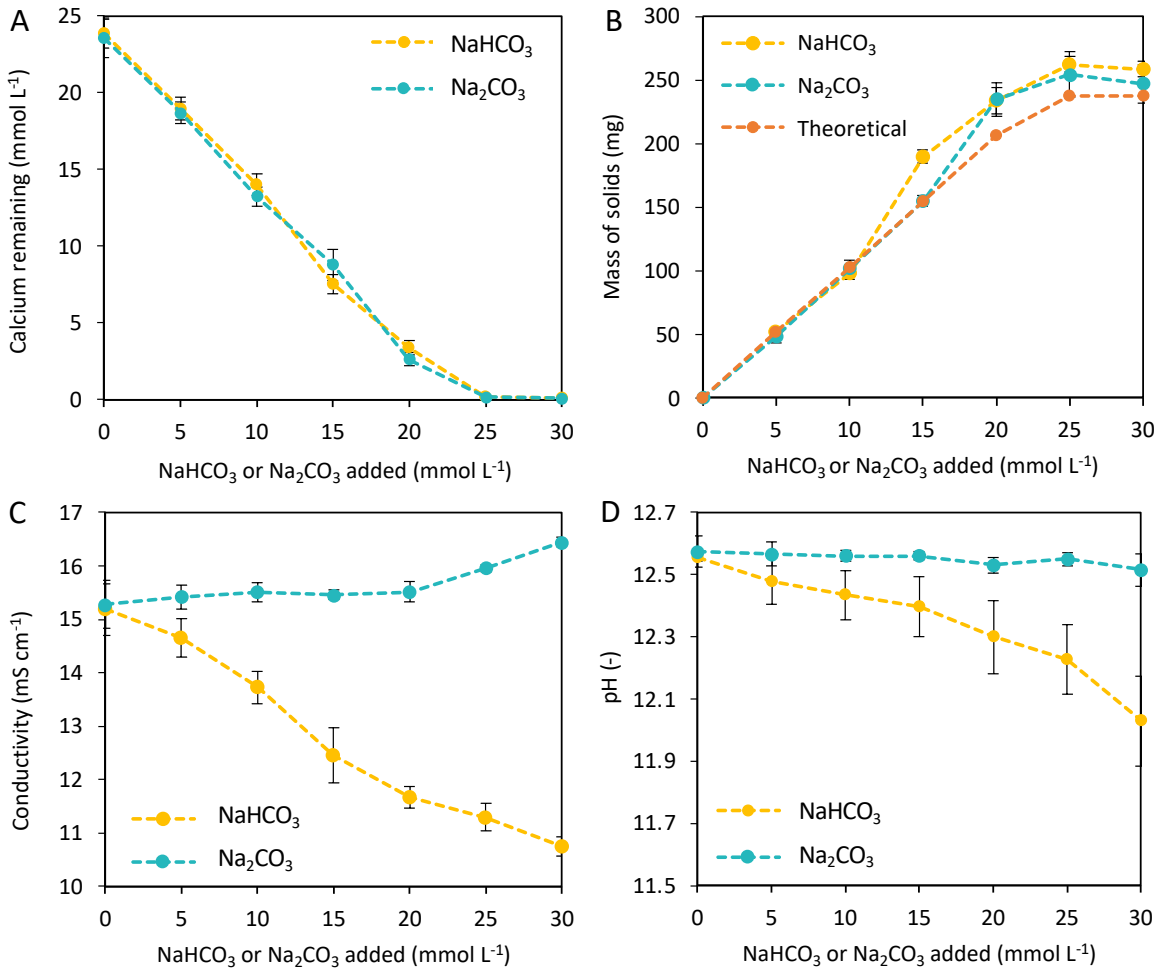

Figure 5-1: Comparison of the incremental addition of either $NaHCO_3$ or Na_2CO_3 and its effect on the calcium concentration (A), the mass of solids formed (B), the conductivity (C), and the solution pH (D) for synthetic urine. Where the theoretical solid mass represents the mass of solids formed based on $CaCO_3$ formation.

5.3.2 Simulation vs. experimental results

Figure 5-2 compares the modelled and experimental results. With regards to the calcium concentration (Figure 5-2A), a comparison of the experimental and simulated results shows an identical trend. However, the absolute value for calcium differs. This may be due to the simulation overestimating the initial calcium concentration. The experimentally measured mass of solids (up to 25 mmol L^{-1} of $NaHCO_3$ added) is slightly higher than the value predicted by the simulation (Figure 5-2B). It is hypothesized that this is due to the formation of amorphous $CaCO_3$ compounds under those conditions. The conductivity and pH predicted by the simulation (Figure 5-2C and Figure 5-2D) are a good fit and have a Nash-Sutcliff model efficiency (NSE) coefficient of 0.93 and 0.99, respectively. This indicates that the model simulates the experimental data accurately and can be used with confidence to predict the results for different urine compositions as well as different carbonate salts. For Na_2CO_3 addition, the simulated results show a similar trend for pH. With regards to conductivity for both $NaHCO_3$ and

Na_2CO_3, there are two observable gradients with the change in gradient occurring approximately at the minimum calcium concentration. This suggests that conductivity could potentially be used as a proxy to determine the required $NaHCO_3$ or Na_2CO_3 dose. As $NaHCO_3$ addition was shown to be as effective as Na_2CO_3 all further experiments were conducted with $NaHCO_3$ addition only. $NaHCO_3$ was chosen as the preferred salt because it is cheaper and adds less unwanted sodium ions.

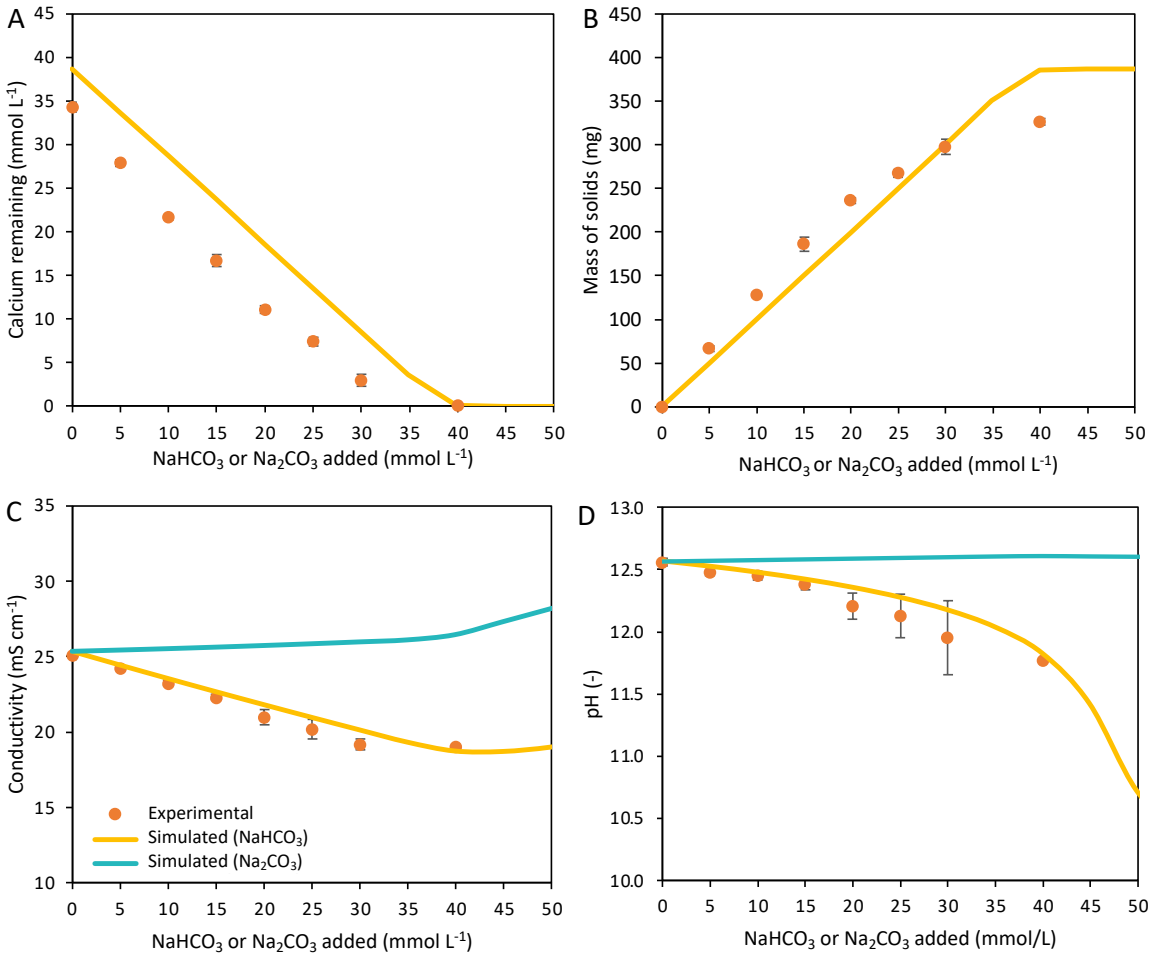

Figure 5-2: Comparison of experimental ($NaHCO_3$) and simulated ($NaHCO_3$ and Na_2CO_3) results for the calcium concentration (A), the mass of solids formed (B), conductivity (C), and pH (D). The simulated Na_2CO_3 results overlap with the simulated $NaHCO_3$ results in (A) and (B).

5.3.3 Once-off dosing for varying urine compositions

Figure 5-3A compares the initial and final calcium concentration for six different urine compositions each dosed with a fixed concentration of 40 mmol L^{-1} $NaHCO_3$. For five out of six of the urine compositions, a dose of 40 mmol L^{-1} was sufficient to remove more than 99.5% of the calcium with a final calcium concentration of less than 0.072 mmol L^{-1}. However, urine composition four had an abnormally high initial calcium concentration (53 mmol L^{-1}), and therefore the fixed-dose was not

sufficient and only 83% of the calcium was removed. The mass of solids formed (Figure 5-3B) was comparable to the theoretical value.

Figure 5-3C shows the change in conductivity compared to the initial calcium concentration. As the dose of $NaHCO_3$ was added to each urine composition a fixed change in conductivity was expected. However, in some cases (composition 4) not all the calcium was precipitated and therefore there was potential for a further drop in conductivity. However, in other cases (composition 1), significantly more $NaHCO_3$ was added than required. The additional Na^+ ions would therefore have contributed to the conductivity increasing above the minimum. Whilst all urine samples received a fixed dose of $NaHCO_3$, the final pH differed significantly between compositions. This may be due to the varying concentration of organics present in the urine that affect the buffering capacity of each composition. This indicates that pH would not be a good proxy for determining the correct dosage for calcium removal.

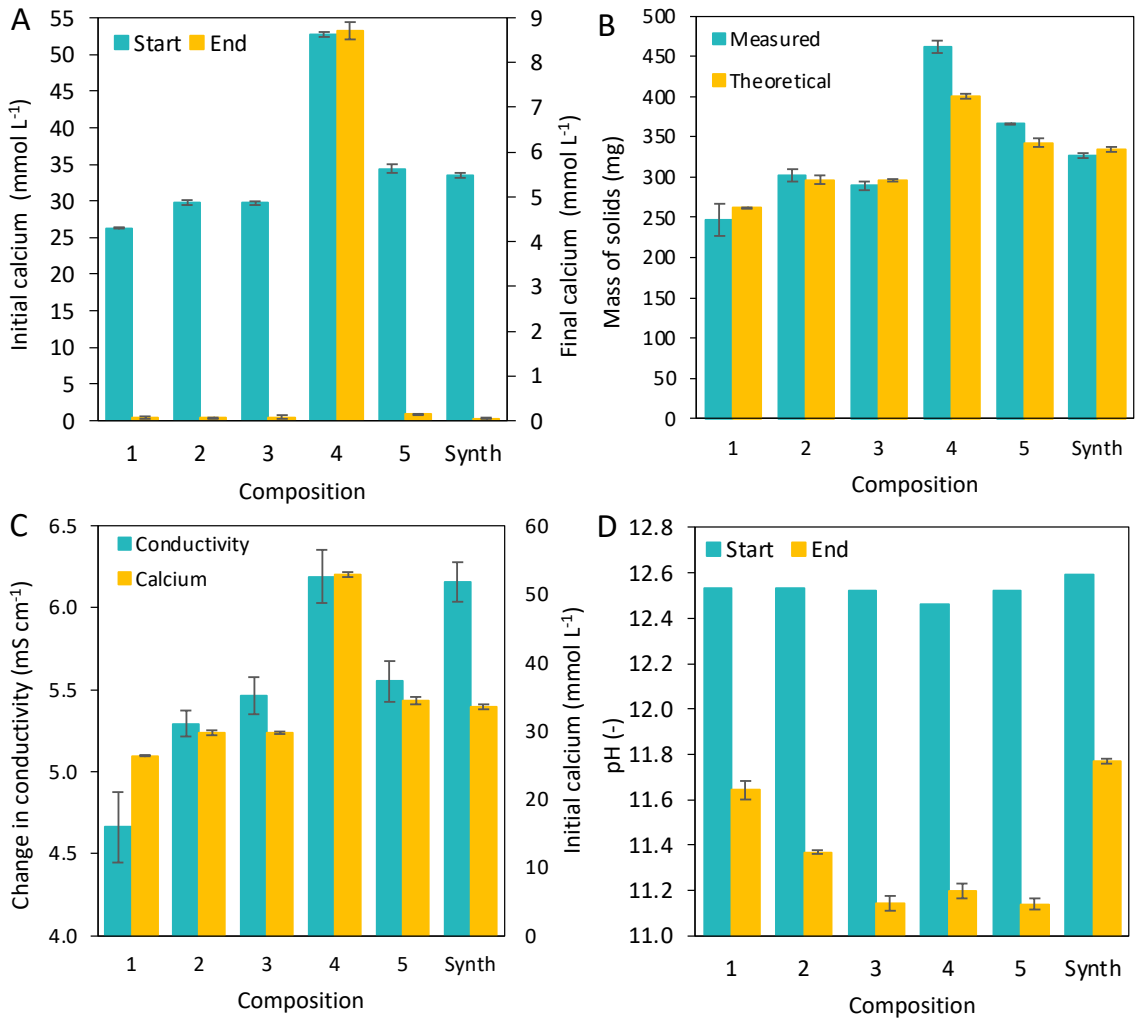

Figure 5-3: Comparison of how the composition of the urine affects the start and end calcium concentration (A), the measured and theoretical mass of solids formed (B), the change in conductivity compared to the initial calcium concentration (C), and the start and end pH (D), for a fixed dose of 40 mmol L^{-1} of $NaHCO_3$.

5.3.4 Exact dosing for varying urine compositions

In all cases, the calcium removed using an exact dose (see Table 7 for values) was greater than 95% (Figure 5-4A). The final calcium concentration varied from 0.8 to 1.6 mmol L^{-1}. Although the percentage removal was still high, the final calcium concentration for the exact dose was higher than the fixed-dose (maximum final calcium concentration of 0.072 mmol L^{-1}). This may be due to slightly underdosing because of measurement error in the initial calcium concentration. However, it is also possible that without the additional CO_3^{2-} ions added with a fixed dose that the reaction driving force, according to Le Chatelier's principle, is limited. To overcome both potential measurement error and the reaction driving force, the exact dose was increased by 5% to ensure maximum calcium removal as deviations in the calcium measurement varied as much as 4.2%.

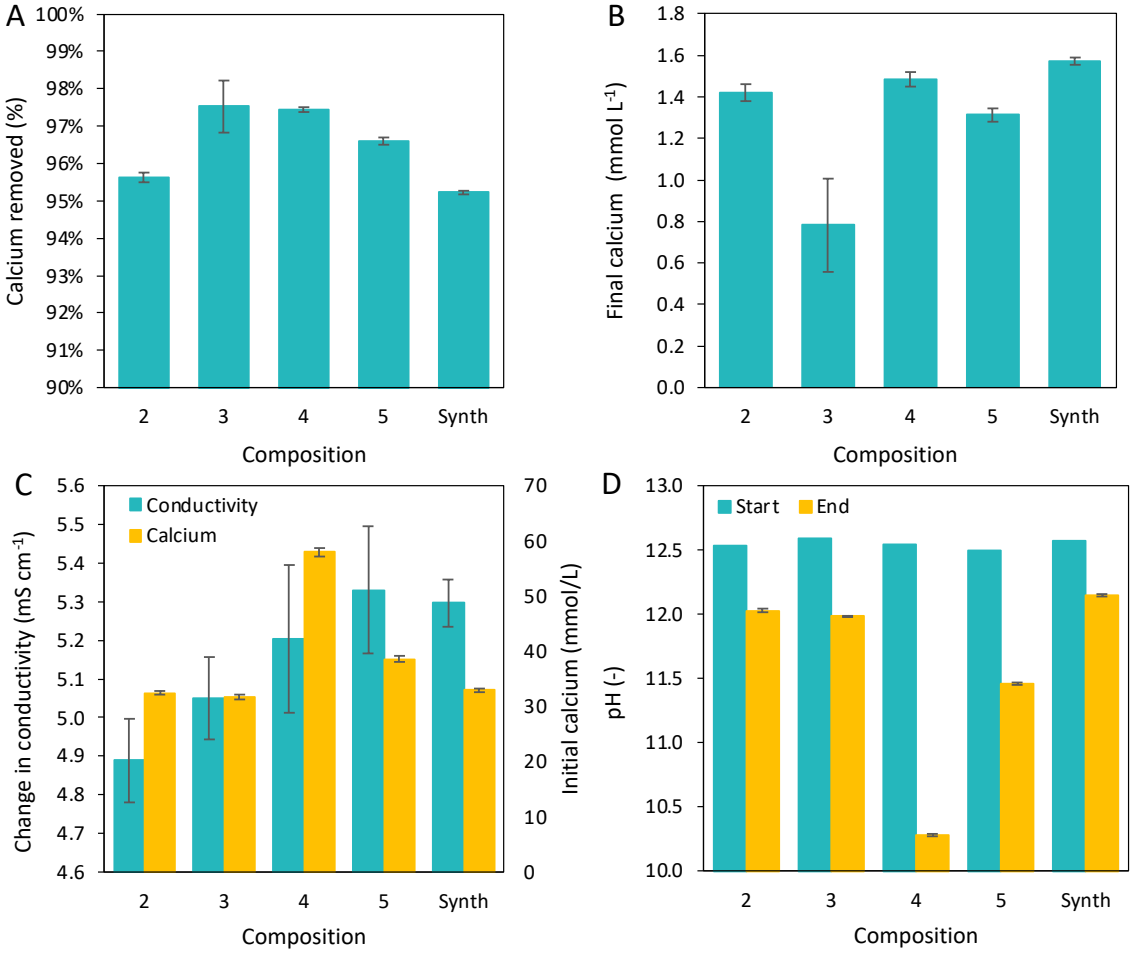

Figure 5-4: Comparison of how the composition of the urine affects the percentage of calcium removed (A), the final calcium concentration (B), the change in conductivity compared to the initial calcium concentration (C), and the start and end pH (D), where the $NaHCO_3$ dosed is calculated based on the start calcium concentration.

A direct correlation between the change in conductivity and the initial calcium concentration was expected with an exact dose. However, the change in conductivity is relatively constant at Δ5.55±0.6

mS cm^{-1}. With regards to pH, the final pH (Figure 5-4D) differs significantly based on urine composition, thus again confirming that the buffer capacity of the solution varies based on urine composition. Therefore, pH is not a good parameter to use to control chemical dosing. It should be noted that for the five urine compositions tested, after an exact dose of $NaHCO_3$, the final pH was always greater than 11 (Figure 5-4D). Typical pH operating conditions for RO and NF membranes are between 2 and 11 (Greenlee et al., 2009). The final pH after $NaHCO_3$ treatment falls outside this advised membrane operating range. The long-term effects on the membrane's lifespan and efficiency should therefore be considered and confirmed experimentally.

5.3.5 Conductivity as a proxy for calcium concentration

Conductivity was measured while $NaHCO_3$ was dosed in 45-second increments and compared to a simulation of the same process for synthetic urine (Figure 5-5A). This method is possible because the reaction occurs almost instantaneously after $NaHCO_3$ addition and equilibrium is reached within 45s before the next dose of $NaHCO_3$ was added. Figure 5B shows the change in conductivity per mmol L^{-1} of $NaHCO_3$ added. The initial conductivity measured experimentally was lower than the simulated value. This may be because the simulation predicted an initial calcium concentration of 38.5 mmol L^{-1} whilst experimentally only 33.5 mmol L^{-1} was measured. Based on the initial calcium an exact dose of $NaHCO_3$ would be 38.5 mmol L^{-1} for the simulation and 33.5 mmol L^{-1} for the experiment (indicated by the vertical dashed lines in Figure 5-5A). There is a change in the slope of the conductivity (Figure 5-5A) which aligns with the exact dose of $NaHCO_3$ required to precipitate all the calcium. It was therefore hypothesized that this change in slope could be used as a proxy for the calcium concentration.

The criteria for dosing would be that the change in conductivity would be measured after each incremental dose. The first measured change in conductivity would be used as a reference. Once the change in conductivity reached 50% of the reference value, dosing would stop. This dose (actual dose) was then compared to the exact dose based on the initial Ca^{2+} concentration. Based on the simulation, 3.5% more $NaHCO_3$ would have been dosed than required, and experimentally 5.9% more $NaHCO_3$ would be dosed than required. However, it was determined that even for a known calcium concentration the exact dose should be increased slightly (in this case a 5% increase was chosen) to account for various forms of error. The end calcium concentration measured experimentally using this method was 0.03 mmol L^{-1} which is equivalent to a 99.9% calcium removal. These results show that using conductivity as a proxy for calcium concentration would provide an accurate dose that is comparable to using an exact dosing method based on measuring the initial calcium concentration.

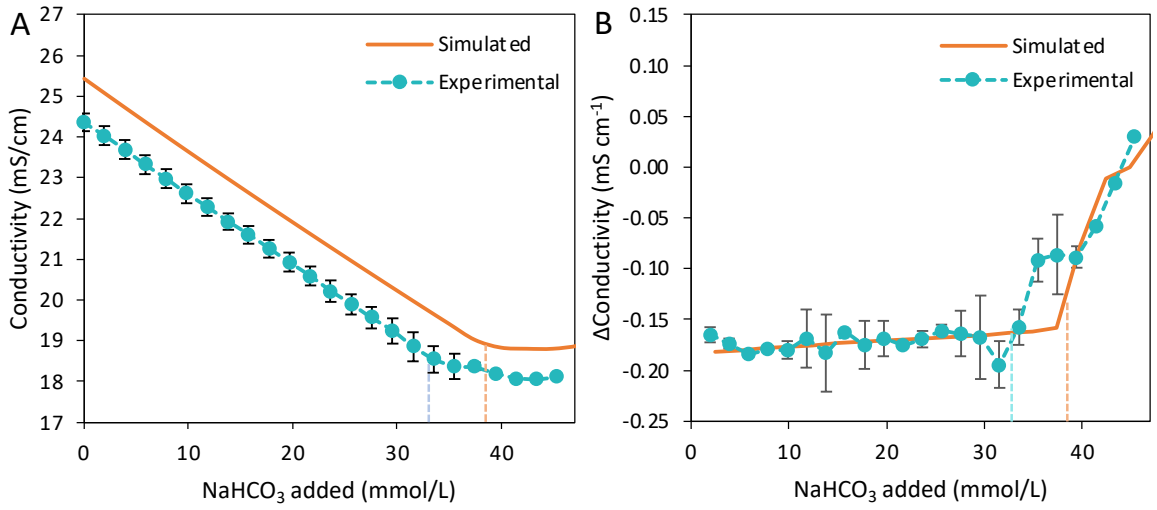

Figure 5-5: Experimental and simulation of the conductivity as a function of $NaHCO_3$ added (A), and the change in conductivity per mmol L^{-1} of $NaHCO_3$ added (B). Where the vertical dashed lines indicated the exact dose of $NaHCO_3$ required.

5.3.6 Comparison of dosing methods

As the composition of urine varies so will the dose of $NaHCO_3$ required to remove the maximum amount of Ca^{2+} ions, whilst also minimizing additional Na^+ ions in the product stream. Three dosing methods were investigated: a once-off fixed dose based on the average calcium concentration of seven different urine compositions plus one standard deviation, an exact dose calculated by measuring the calcium concentration in the specific urine composition requiring treatment, and finally, dosing in fixed increments and using a change in conductivity as a proxy to determine when to stop dosing.

A once-off fixed dose is the simplest method; however, it can result in up to 25% more $NaHCO_3$ being added to the solution than required. This would increase operating costs and may have downstream limitations on the water recovery possible with RO due to the additional Na^+ ions. It is also important to consider that any outlying urine compositions would not be adequately treated and could result in potential RO membrane scaling. Furthermore, the unnecessary Na^+ ions could be problematic if the product stream is to be used as a liquid fertilizer as many plants do not tolerate high concentrations of Na^+ ions (Zhu, 2001).

To provide an exact dose, the calcium concentration of each batch of urine would have to be measured. This can be achieved in multiple ways including, colorimetric methods (complexometric Ethylenediaminetetraacetate (EDTA) titration (Baird, 2017)), ion chromatography, or using a calcium ion selective electrode (ISE). Whilst ISEs are simple to operate they are prone to interference from other ions such as Na+, K+, and Mg2+, which are present in urine (Mettler-Toledo AG, 2010). Further research to confirm the accuracy of ISEs when testing urine is therefore required. Many colorimetric methods and ion chromatography require expensive laboratory equipment and would not always be

economical. However, complexometric titration is simple and could be done on-site as it requires only basic laboratory equipment and skill. It is therefore the preferred calcium measurement option.

Using conductivity measurements as a proxy for the calcium concentration provides an accurate dosing method. However, the $NaHCO_3$ would need to be dissolved in water such that it could be dosed via a dosing pump. Whereas with the other two methods the dosing salt could simply be weighed and mixed into the batch of collected urine. Table 8 summarizes the advantages and disadvantageous of each method. Both the exact dosing method and using conductivity as a proxy are preferred to a fixed dose as they minimize chemical use and overall operating costs. Both methods are comparably accurate and therefore the design choice may be based on a preference for complete automation or manual operation.

Table 8: Comparison of the advantages and disadvantages of three different dosing techniques.

Method	Advantages	Disadvantages
Fixed dose	Simple and does not require any additional equipment or operator skill.	More $NaHCO_3$ is used than required thus increasing operating costs. Urine compositions with abnormally high calcium concentrations would not have complete calcium removal.
Calcium testing	Reagent costs are minimized.	Requires an operator on-site for regular calcium measurements.
Conductivity as a proxy	Reagent costs are minimized. Automated system	The system would require $NaHCO_3$ to be dissolved in water and dosed via a dosing pump.

The final pH of urine after an exact dose of $NaHCO_3$ is likely to be above 11 and therefore outside the design range for most commercial RO membranes. To reduce the pH to within the RO membrane operating pH range, either additional $NaHCO_3$ could be dosed to a lower pH, or an acid could be added. Modeling of synthetic urine showed that an additional 11.4 mmol L-1 $NaHCO_3$ or 4.7 mmol L-1 H_2SO_4 would be required to reduce the pH to 10.5. Whilst simply dosing $NaHCO_3$ to a fixed pH is the simplest option, it is advised that H_2SO_4 should rather be added to adjust the pH as this minimizes the additional ions added. This reduces the impact on the solution's osmotic pressure and downstream concentration using RO.

5.3.7 Alternative carbonate salts and cost considerations

Adding carbonate ions to stabilized urine removes excess calcium by $CaCO_3$ precipitation. These can be added in forms other than $NaHCO_3$, such as $KHCO_3$, NH_4HCO_3, and $MgCO_3$. These four options were compared via a simulation in terms of calcium removal, pH, conductivity, and cost as shown in Figure 5-6. All four options provided equal removal of calcium ions. With regards to pH, $KHCO_3$ results

in an identical pH change as $NaHCO_3$. The addition of NH_4HCO_3 results in the largest pH decrease due to the addition of ammonium ions. The pKa for the NH_3/NH_4^+ system is 9.25 (Haynes et al., 2016) and therefore pH values above 9.25 will favor the formation of NH_3, which does not initially contribute to conductivity. However, as the pH drops below 9.25, equilibrium favors NH_4^+ ion formation, thus resulting in an increase in the conductivity. The addition of $MgCO_3$ results in both the precipitation of $CaCO_3$ and brucite ($Mg(OH)_2$) and therefore explains both the decrease in pH (due to the precipitation of OH^- ions) and the steeper decrease in conductivity.

The total dosing chemical cost to treat 1 m^3 of stabilized urine is a function of the chemical cost and the chemical dose required (Figure 5-6D). The most expensive option is $KHCO_3$ (\$3.4 m^{-3} urine) followed by $MgCO_3$ (\$1.6 m^{-3} urine), NH_4HCO_3 (\$0.53 m^{-3} urine) and $NaHCO_3$ (\$0.49 m^{-3} urine), the cheapest option (Figure 5-6D). Whilst all the carbonate salts provided equal calcium removal, both $MgCO_3$ and $KHCO_3$ are significantly more expensive and therefore would not be favorable. When dosing with $NaHCO_3$ if the high pH is shown to affect the operation of the RO/NF membranes, the additional H_2SO_4 required to decrease the pH to 10.5 would increase the operating cost to \$ 0.56 m^{-3} urine.

At \$0.03 m^{-3} urine less, NH_4HCO_3 could potentially provide an alternative to the slightly more expensive $NaHCO_3$ and H_2SO_4 combination. It resulted in an approximate final pH (with an exact dose) of 9.5, which is well within the operating pH range of many RO and NF membranes. At a pH of 9.5 equilibrium favors ammoniacal nitrogen in the form of ammonia rather than ammonium. Air pollution due to ammonia emissions (Sutton et al., 2020) should also, therefore, be considered. Importantly, if NH_4HCO_3 was used for pre-treatment, conductivity measurements would not be a viable proxy for the calcium concentration and an exact dose would need to be determined via measurement of the calcium concentration. This is because the dose of NH_4HCO_3 that results in a minimum in conductivity does not align with complete calcium removal. Both $NaHCO_3$ and NH_4HCO_3 should be tested as a pre-treatment step for an RO system to determine the most suitable dosing chemical.

A desktop feasibility study for the concentration of source-separated urine using RO (assuming 80% water removal) determined that the concentrated liquid fertilizer would need to be sold at \$1.57 L^{-1} for the business model to break even after 5 years (Chipako and Randall, 2020a), however, the market value was much higher (\$10.5 L^{-1}). The cost of chemical addition pre-treatment (chemical cost only) would not have a significant impact on the business model developed by Chipako and Randall (2020a) as it would require the break-even sales price to be increased by only 0.13% to maintain a 5-year break-even period.

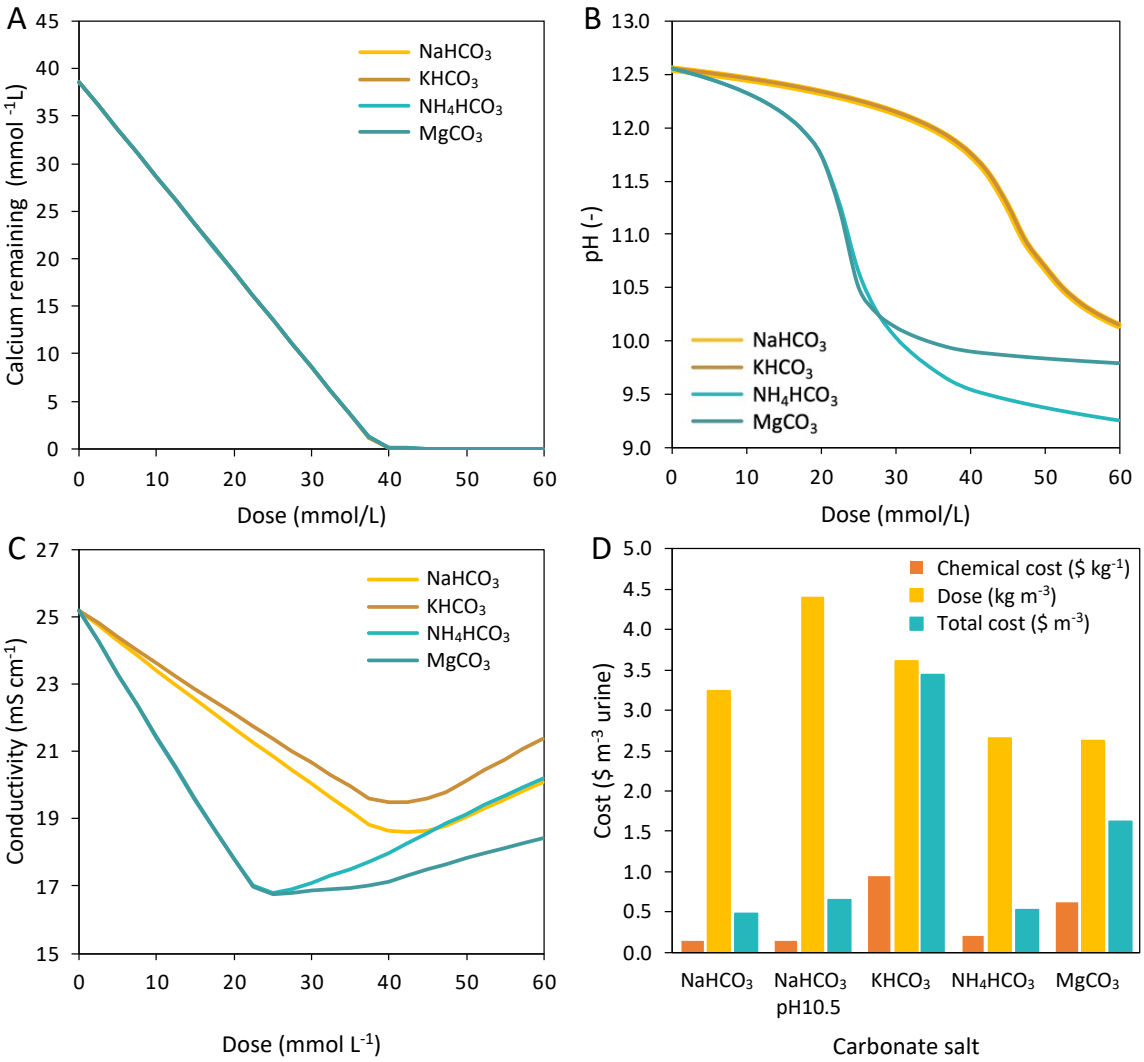

Figure 5-6: The simulated effect of the addition of NaHCO3, KHCO3, NH4HCO3, and MgCO3 to Ca(OH)2 stabilized urine on the calcium concentration (A), pH (B), conductivity (C), and cost (D). The cost includes the reactant cost, the dose required, and the overall cost to treat 1 m3 of urine. All compounds overlap in (A) and NaHCO3 and KHCO3 overlap in (B).

5.4 CONCLUSIONS

The addition of carbonate salts to urine stabilized with $Ca(OH)_2$ was shown to be a simple and effective method to reduce the concentration of calcium ions and the scaling potential of RO membranes. Both $NaHCO_3$ and Na_2CO_3 addition were shown experimentally to reduce the calcium concentration in $Ca(OH)_2$ stabilized urine to at least 0.18 mmol L^{-1}. $NaHCO_3$ is preferred over Na_2CO_3 as it is cheaper, adds half the amount of Na^+ ions, and results in a change in the measured conductivity which can then possibly be used as a proxy for the calcium concentration. Dosing either of these salts would also effectively prevent enzymatic urea hydrolysis from occurring because a high operating pH (>11) would be maintained. It was found that the pH buffering capacity of urine varies with composition and pH could therefore not be used as a proxy for the calcium concentration. However, when dosing $NaHCO_3$

there was a correlation between calcium concertation and conductivity. It was shown experimentally that conductivity could be used as a proxy for the calcium concentration and would only require 3.2 to 5.9% additional $NaHCO_3$.

It is advised that either complexometric titration, to determine the initial calcium concentration, or using conductivity as a proxy for calcium concentration should be used to determine the exact dose of $NaHCO_3$ required. This will minimize chemical costs and the addition of undesirable Na^+ ions. Should the operating pH of the membrane process be lower than 11, then H_2SO_4 should be dosed to correct the pH. Whilst simply dosing additional $NaHCO_3$ to a fixed pH is simpler, the addition of H_2SO_4 would minimize the number of additional ions added.

Modelling of the experiments was shown to be accurate and used to simulate the addition of other carbonate salts. Excess calcium can also be removed by dosing other carbonate salts such as $KHCO_3$, NH_4HCO_3, and $MgCO_3$. Whilst K^+ ions from $KHCO_3$ are more desirable than Na^+ ions and $MgCO_3$ results in the lowest TDS, these two options were significantly more expensive and therefore not favored. Ammonium bicarbonate (\$0.53 m^{-3} urine) was comparable in cost to $NaHCO_3$ (\$0.49 m^{-3} urine) and would result in a solution pH within the operating range of most RO or NF membranes and extra N would be added to the stream instead of Na^+ ions. It is advised that both $NaHCO_3$ and NH_4HCO_3 addition be assessed as a pre-treatment method for an RO system to determine the preferred dosing chemical. The concentration of $Ca(OH)_2$ stabilized urine using reverse osmosis without pre-treatment is likely to cause significant membrane scaling that would render the process economically unfeasible. However, the addition of a bicarbonate salt ($NaHCO_3$ or NH_4HCO_3) has been proven to be a quick, simple, and cost-effective method to reduce the scaling potential of $Ca(OH)_2$ stabilized urine.

REFERENCES

Alibaba.com. 2021. Taian Health Chemical Co., LTD [Online]. Available: https://healthchemical.en.alibaba.com/?spm=a2700.shop_plser.88.16 [Accessed 12 March 2021].

Altinbaş, M., Yangin, C. and Ozturk, I. 2002. Struvite precipitation from anaerobically treated municipal and landfill wastewaters. Water Science and Technology 46(9), 271-278.

Antony, A., Low, J.H., Gray, S., Childress, A.E., Le-Clech, P. and Leslie, G. 2011. Scale formation and control in high pressure membrane water treatment systems: A review. Journal of membrane science 383(1-2), 1-16.

Ayoub, G.M., Korban, L., Al-Hindi, M. and Zayyat, R. 2019. Brackish Water Desalination: An Effective Pretreatment Process for Reverse Osmosis Systems. Water, Air, & Soil Pollution 230(10), 1-12.

Baird, R.B. 2017. Standard Methods for the Examination of Water and Wastewater, 23rd Edition, Water Environment Federation, American Public Health Association, , Colorado, USA.

Bergman, R. 2007. Reverse osmosis and nanofiltration, 2nd edition, American Water Works Association, Colorado, USA.

Bond, R. and Veerapaneni, S. 2007. Zero liquid discharge for inland desalination, AWWA Research Foundation, Colorado, USA.

Chipako, T. and Randall, D. 2020. Investigating the feasibility and logistics of a decentralized urine treatment and resource recovery system. Journal of Water Process Engineering 37, 101383.

Ek, M., Bergström, R., Bjurhem, J.E., Björlenius, B. and Hellström, D. 2006. Concentration of nutrients from urine and reject water from anaerobically digested sludge. Water Science and Technology 54, 437-444.

Flanagan, C.P. and Randall, D.G. 2018. Development of a novel nutrient recovery urinal for on-site fertilizer production. Journal of Environmental Chemical Engineering 6(5), 6344-6350.

Greenlee, L.F., Lawler, D.F., Freeman, B.D., Marrot, B. and Moulin, P. 2009. Reverse osmosis desalination: Water sources, technology, and today's challenges. Water Research 43(9), 2317-2348.

Greenlee, L.F., Testa, F., Lawler, D.F., Freeman, B.D. and Moulin, P. 2010. The effect of antiscalant addition on calcium carbonate precipitation for a simplified synthetic brackish water reverse osmosis concentrate. Water research 44(9), 2957-2969.

Haynes, W.M., Lide, D.R. and Bruno, T.J. (2016) CRC handbook of chemistry and physics, 95th edition, CRC Press, Florida, USA.

Kucera, J. 2015. Reverse osmosis: industrial processes and applications, 3rd Edition, John Wiley & Sons, New York.

Lewis, A.E., Nathoo, J., Thomsen, K., Kramer, H., Witkamp, G., Reddy, S. and Randall, D.G. 2010. Design of a Eutectic Freeze Crystallization process for multicomponent waste water stream. Chemical Engineering Research and Design 88(9), 1290-1296.

Li, D. and Liu, S. 2018. Water quality monitoring and management: basis, technology and case studies, Academic Press.

Mahasti, N.N., Shih, Y.-J., Vu, X.-T. and Huang, Y.H. 2017. Removal of calcium hardness from solution by fluidized-bed homogeneous crystallization (FBHC) process. Journal of the Taiwan Institute of Chemical Engineers 78, 378-385.

Mettler-Toledo AG 2010 perfectION Guidebook: Combination Calcium Electrode, Mettler-Toledo, Switzerland.

Meyer, G., Frossard, E., Mäder, P., Nanzer, S., Randall, D.G., Udert, K.M. and Oberson, A. 2018. Water soluble phosphate fertilizers for crops grown in calcareous soils–an outdated paradigm for recycled phosphorus fertilizers? Plant and soil 424(1-2), 367-388.

OLI Systems Inc. 2022. OLI Stream Analyzer, version 11.0, OLI Systems Inc, New Jersey, USA.

Pronk, W., Palmquist, H., Biebow, M. and Boller, M. 2006. Nanofiltration for the separation of pharmaceuticals from nutrients in source-separated urine. Water Research 40(7), 1405-1412.

Rahardianto, A., Gao, J., Gabelich, C.J., Williams, M.D. and Cohen, Y. 2007. High recovery membrane desalting of low-salinity brackish water: Integration of accelerated precipitation softening with membrane RO. Journal of Membrane Science 289(1-2), 123-137.

Randall, D.G., Krähenbühl, M., Köpping, I., Larsen, T.A. and Udert, K.M. 2016. A novel approach for stabilizing fresh urine by calcium hydroxide addition. Water Research 95, 361-369.

Sheikholeslami, R. and Bright, J. 2002. Silica and metals removal by pretreatment to prevent fouling of reverse osmosis membranes. Desalination 143(3), 255-267.

Sutton, M.A., Van Dijk, N., Levy, P.E., Jones, M.R., Leith, I.D., Sheppard, L.J., Leeson, S., Sim Tang, Y., Stephens, A. and Braban, C.F. 2020. Alkaline air: changing perspectives on nitrogen and air pollution in an ammonia-rich world. Philosophical Transactions of the Royal Society A 378(2183), 20190315.

Sutzkover-Gutman, I. and Hasson, D. 2010. Feed water pretreatment for desalination plants. Desalination 264(3), 289-296.

Zhu, J.-K. 2001. Plant salt tolerance. Trends in plant science 6(2), 66-71.

CHAPTER 6: AERATION PRE-TREATMENT

CHAPTER 6: AERATION PRE-TREATMENT

This chapter is based on the published work from Paper 2 titled: Calcium removal from stabilized human urine by air and CO_2 bubbling

6.1 INTRODUCTION

In the previous chapter, the need for a pre-treatment method for urine stabilized with $Ca(OH)_2$ prior to concentration with reverse osmosis (RO) was established. Whilst chemical dosing is a quick and simple pre-treatment method it may not be the optimal pre-treatment option. The pH of $NaHCO_3$ addition was above 11. The operating pH for most commercial polyamide and cellulose acetate membranes is between 2 and 11. Acid addition to lower the pH would therefore be required to increase the longevity of the membrane life-span (Franks et al., 2009), further complicating the pre-treatment process. It is also important to consider the greenhouse gas emissions associated with the production of $NaHCO_3$ and the effects of the additional added Na^+ ions.

Understanding the reactions that occur between stabilized urine and the atmosphere is important, as this can help explain why membrane scaling might occur. Scaling can happen in two ways: solutes precipitate when their solubility limit is reached during concentration, or a reaction occurs that produces an insoluble compound. For example, Mitsoyannis and Saravacos (1977) observed experimentally that RO membranes have a high CO_2 permeability. In the case of $Ca(OH)_2$ stabilized urine, the dissolution of CO_2 from the air into urine would form carbonate (CO_3^{2-}) ions due to the high pH of stabilized urine, as described by Equations 6-1 to 6-3. The excess Ca^{2+} ions added during this stabilization method would react with the CO_3^{2-} ion to form $CaCO_3$ as described in Equation 6-4. As $CaCO_3$ is a sparingly soluble salt (14.25 mg L^{-1} at 25°C in water (Haynes et al., 2016)) it will precipitate and form a $CaCO_3$ scale on the membrane surface.

$$CO_{2(g)} + H_2O \leftrightarrow H_2CO_{3(aq)} \quad \text{(Equation 6-1)}$$

$$H_2CO_3 \leftrightarrow HCO_3^- + H^+ \quad \text{(Equation 6-2)}$$

$$HCO_3^- \leftrightarrow CO_3^{2-} + H^+ \quad \text{(Equation 6-3)}$$

$$Ca^{2+}{}_{(aq)} + CO_{3(aq)}^{2-} \leftrightarrow CaCO_{3(s)} \quad \text{(Equation 6-4)}$$

The same reaction that causes membrane scaling could also be taken advantage of as a pre-treatment method. Air bubbling has been shown as an effective method to reduce the calcium concentration in brackish water as a pre-treatment step for RO (Hasson et al., 2011; Lisitsin et al., 2008; Touati et al., 2018). The process works by producing $CaCO_3$ as governed by Equations 6-1 to 6-4. Researchers have also shown that bubbling pure CO_2 through a $Ca(OH)_2$ solution can reduce the concentration of calcium in the solution (Altiner, 2018; Bang et al., 2011). Hasson and co-workers (Hasson et al., 2011) were able to reduce the calcium concentration in brackish water by 70% to 213 mg L^{-1} in 2 hours with air

bubbling, enabling an increase in water recovery in an RO treatment process from 78% to 90%. Bang and co-workers (Bang et al., 2011) were able to reduce the concentration of calcium in a 0.1 M $Ca(OH)_2$ slurry to 320 mg L^{-1} via bubbling with pure CO_2 at 0.1 L min^{-1}.

In the case of stabilized urine using $Ca(OH)_2$, the addition of air or CO_2 would theoretically reduce the concentration of calcium in the solution while also decreasing the pH. The lower pH would thus be beneficial for prolonging the lifespan of the RO membrane. However, Randall and co-workers (Randall et al., 2016) showed that a pH above 11 is required to prevent enzymatic urea hydrolysis. It is not clear to what extent enzymatic urea hydrolysis could occur after a pH drop below 11 during air or CO_2 bubbling. In addition, any urea hydrolysis that might occur at lower pH values would be converted to free ammonia, which is easily stripped during air bubbling (Campos et al., 2013), thus resulting in nitrogen loss.

Many studies have investigated methods to increase the rate of $CaCO_3$ precipitation. The overall process happens in two steps: the dissolution of CO_2 (Equation 6-1) and the formation of $CaCO_3$ (Equation 6-4). Increasing the feed flow rate of air/CO_2 increases the rate of CO_2 dissolution. Altiner (2018) and Bang and co-workers (Bang et al., 2011) investigated the carbonation of a $Ca(OH)_2$ (lime) slurry. Altiner (2018) showed that increasing the CO_2 flow rate decreased the reaction time. However, at CO_2 flow rates above 3 L min^{-1}, there was no significant decrease in reaction time observed. In addition, Altiner (2018) observed that an increased CO_2 flow rate from 0.3 to 1.0 L min^{-1} reduced the amount of CO_2 reacted from 27% to 12%. It was hypothesized that this occurs because at certain flowrates the formation of $CaCO_3$ becomes the limiting factor rather than the rate of CO_2 dissolution. Understanding the mechanisms involved in CO_2 dissolution and $CaCO_3$ formation is important to optimize the aeration system.

The aim of this chapter was to:

1. Investigate the feasibility of using air or CO_2 bubbling as a method to remove calcium from stabilized urine as a pre-treatment step for RO. As there are many benefits to stabilizing urine with $Ca(OH)_2$, it was deemed important to find an effective pre-treatment step to ensure that downstream RO processes would not be impacted by the scaling potential of this treatment method.
2. Determine if a simulation could be used to better understand how the operating parameters (flow rate and gaseous CO_2 concentration) affected the kinetics of $CaCO_3$ precipitation in stabilized urine.
3. Determine if a decrease in the stabilized urine's pH would result in enzymatic urea hydrolysis.
4. Estimate, using a simulation, the potential recovery rates of a RO process using this pre-treatment step and calculated the preliminary operating costs of the treatment process.

6.2 MATERIALS AND METHODS

6.2.1 Experimental conditions

A variety of experimental conditions were examined to determine their effect on the rate and extent of calcium removal. Table 9 summarizes the experimental conditions and aims for each experiment. All experiments were run in triplicate. Urine compositions are however not consistent between experimental conditions due to limitations in urine collection and storage time.

Table 9: Experimental conditions for different CO_2 bubbling experiments.

Exp. #	Urine composition	Flowrate (L min^{-1})	CO_2 conc. (%)	Aim
A1	U1	1.5	0.04	To compare the rate of calcium removal as a function of flow rate.
A2	U4	3.0		
A3	U4	6.0		
A4	U3	9.0		
C1	U1	1.5	1.0	To compare the rate of calcium removal as a function of CO_2 concentration.
C2	U1		100	
U1	U5	3.0	0.04	To compare the rate of calcium removal as a function of CO_2 concentration.

Where: A – air; C – CO_2 and U – urea.

6.2.2 Air and CO_2 bubbling procedure

Approximately 1 L of filtered, stabilized urine was weighed and then added to a 1 L jacketed reaction vessel (GlassChem, Stellenbosch, South Africa), which was open to the atmosphere. The desired temperature was kept constant via a recirculation chiller (MM series, Polyscience, Illinois, USA) using tap water as the coolant. The solution was continuously mixed throughout the experiment with an overhead mechanical stirrer (Hei-TORQUE Core, Heidolph Instruments, Schwabach, Germany) at 550 rpm. A Rushton impeller was used to ensure all solids present remained suspended for the duration of the experiment. The equipment was also continuously weighed using a precision scale to account for any evaporation (Radwag PS 4500.X.2 precision scale, Radom, Poland). A pH-temperature probe (H1 5221, Hanna, Johannesburg, South Africa) was fixed in the reaction vessel for continuous measurements and to track the extent of the reaction. A 4-point calibration (4.01, 7.01, 10.01, and 12.45) of the pH probe was conducted before each experiment. Air (ACO-003, Resun, Shenzhen, China) and 1% and 100% CO_2 gas (Afrox, Cape Town, South Africa) were bubbled through the urine at various flowrates (see Table 2), which were measured and controlled with a variable flowmeter (LT-08A01-MV 0.5-10 L min^{-1}, Wet Technologies, Strand, South Africa). An air stone (A-002, Daro, Cape Town, South Africa) was used to reduce the bubble size and ensure more even bubble distribution.

The air/CO_2 bubbling time varied based on the experimental conditions. At the start of each experiment, a foam formed. To prevent the foam from overflowing from the reaction vessel the air flow rate was increased incrementally (proportionally for each flowrate) for the first 90 minutes of the experiment. For the air bubbling, when the solution pH reached 8.6 ± 0.1 the reaction was determined to be complete, and the air feed was switched off. The exception was for experiment U1, where air bubbling was continued for an additional 18 hours after the pH reached 8.6 to determine the effect on urea loss. For 1% CO_2, the reaction was determined to be complete when the measured calcium concentration remained constant for 2 hours. The 100% CO_2 experiment was run for 8 hours. The pH was measured in 5 min intervals for experiments A1-A4 and U1, every 1 minute for C1, and every 1 second for C2. Samples were taken periodically throughout the experiment to measure the calcium concentration. At the end of each experiment, the liquid was filtered. The solids were collected on filter paper with a pore size of 1.2 µm (Ahlstrom-Munksjö, Helsinki, Finland) and dried at 105ºC for 3 hours. The solids were analyzed to confirm if $CaCO_3$ had formed. After each experiment, all the equipment was cleaned with a 0.08 M HCl solution to remove any precipitates that had formed and then rinsed thoroughly with tap water.

6.2.3 Gas-transfer and precipitation model

The bubbling of air/CO_2 through stabilized urine was modelled using a precipitation model developed and defined in detail by Udert (Udert, 2002), and further updated by Brison (Brison, 2016), using Aquasim (Reichert, 1994). The model makes use of solubility equilibria, complex formation reactions, and acid-base reactions to calculate a state of thermodynamic equilibrium. The rate at which calcium is converted to $CaCO_3$ is dependent on a multitude of factors including the concentration of calcium and carbonate ions, the air/CO_2 flow rate, temperature, mass transfer of gas, etc. The rate of $CaCO_3$ precipitation/Ca^{2+} removal used in this model is described by Equation 6-5 (Kazmierczak et al., 1982), where: X_{CaCO_3} are the moles of $CaCO_3$ precipitated, k_{CaCO_3} is the rate constant for $CaCO_3$ precipitation [d^{-1}], (Ca^{2+}) and (CO_3^{2-}) are the activities of calcium and carbonate ions [mol L^{-1}] which is a function of their concentration, $pK_{s,CaCO3}$ is the solubility product of $CaCO_3$, and V is the liquid volume in the reactor [L]. The rate of formation of $CaCO_3$ is therefore directly proportional to the concentration of Ca^{+2} and CO_3^{-2} ions and the precipitation rate constant.

$$\frac{dX_{CaCO_3}}{dt} = k_{CaCO_3}\left[\{(Ca^{2+}) \cdot (CO_3^{-2})\}^{1/2} - 10^{(-pK_{s,CaCO3}/2)}\right] \cdot V \qquad \text{(Equation 6-5)}$$

The rate of CO_2 dissolution was modelled using Equation 6-6 (adapted from (Udert et al., 2003b)), where: Q_{air} is the air/CO_2 flowrate [L d^{-1}], V is the liquid volume in the reactor [L], C_{CO2} is the concentration of CO_2 in the inlet air flow [mol L^{-1}], S_{CO_2} is the CO_2 concentration in the liquid phase

[mol L^{-1}], $K_L a_{CO_2}$ is the mass transfer coefficient [d^{-1}], and H_{CO_2} is the Henry constant for CO_2 in water [$mol_g\ mol_{aq}^{-1}$]. It was assumed that Henry's constant for CO_2 in water can also be applied to urine.

$$V \cdot \frac{dS_{CO_2}}{dt} = Q_{air} \cdot (C_{CO_2} - H_{CO_2} \cdot S_{CO_2}) \cdot \left\{1 - \exp\left(-\frac{K_L a_{CO_2} \cdot V}{H_{CO_2} \cdot Q_{air}}\right)\right\} \qquad \text{(Equation6-6)}$$

These two dynamic processes, as well as enzymatic urea hydrolysis and ammonia volatilization, were considered and adjusted to accurately simulate the bubbling air/CO_2 through stabilized urine. In this work, chemical urea hydrolysis was not considered as the operating temperature of experiments conducted was less than 25°C and the rate of urea loss would have been negligible (Warner, 1942). The dissociation constants for carbonic acid and bicarbonate were adjusted to account for the urine's salinity and temperature as determined by Millero et al. (2006). In addition, creatinine was added to the model to account for the amino acids present in urine (Putnam, 1971). The experimental data were used to fit the model and calibrate the unknown parameters (k_{CaCO_3} and $K_L a_{CO_2}$). Processes could then be switched on and off in the model to determine their effect. Once the simulation was determined to be an accurate representation of the experimental data, a multitude of different operating conditions were investigated to determine the most cost-efficient operating parameters. The Nash-Sutcliff model efficiency (NSE) coefficient was used to determine the accuracy of the model. Additional information regarding the model improvements (Figure C-5) and how differences in the urine composition affect the pH and calcium concentration (Figure C-6) can be found in Appendix C.

6.2.4 Thermodynamic modeling

To simulate the removal of water, the mass of solids formed and the effect on the scaling index (SI) of different species, simulations were conducted using OLI Stream Analyzer (OLI Systems Inc, 2022). Where SI=Log(IAP/Ksp), IAP is the ionic activity product, and Ksp is the solubility product. The Mixed Solvent Electrolyte (MSE) model was used since it has no limitation on the ionic strength of a solution. The aerated urine was simulated by adding CO_2 to a stabilized urine solution until a pH of 8.5 was reached. The solids were then removed from the stream to mimic filtration and then different amounts of water removal were simulated. This mimicked what would happen in a RO process.

6.3 RESULTS

6.3.1 Effect of air flowrate and CO_2 concentration on the pH and calcium concentration

The rate at which the pH and calcium concentration change with time for different flow rates of air is shown in Figure 6-1. The faster the air flow rate, the quicker the pH and calcium concentration decreased. However, the marginal decrease in reaction time from a flow rate of 1.5 to 3 L min^{-1} was

much greater than from 6 to 9 L min^{-1}. Figure 6-1B shows two distinct regions where the calcium concentration decreases and then remains constant. The 9 L min^{-1} flow rate resulted in a pH of 8.5 and a concentration of 78 mg Ca^{2+} L^{-1} after 6 hours. The final calcium concentration ranged from 18 to 179 mg L^{-1}. The deviation in the 1.5 L min^{-1} pH curve was due to a build-up of calcite on the pH probe overnight, the probe was cleaned and re-calibrated at 20 hours.

The experimentally determined pH and calcium concentration, as a function of time for varying CO_2 concentration between 0.04 to 100%, are shown in Figure 6-1C and Figure 6-1D, with the time in Log hours. Increasing the CO_2 concentration decreased the time required to reach the system's equilibrium pH from over 24 hours with air to 1 hour with 1% CO_2 and 5 minutes for 100% CO_2. The concentration of CO_2 that will dissolve in a liquid is governed by Henry's Law. Therefore, an increase in CO_2 concentration in the air also defined the equilibrium pH. The time required to reach a minimum calcium concentration was reduced to 1 hour for 1% CO_2. However, for 100% CO_2 there no significant calcium removal was observed. The reason for this is explained in section 4.2.

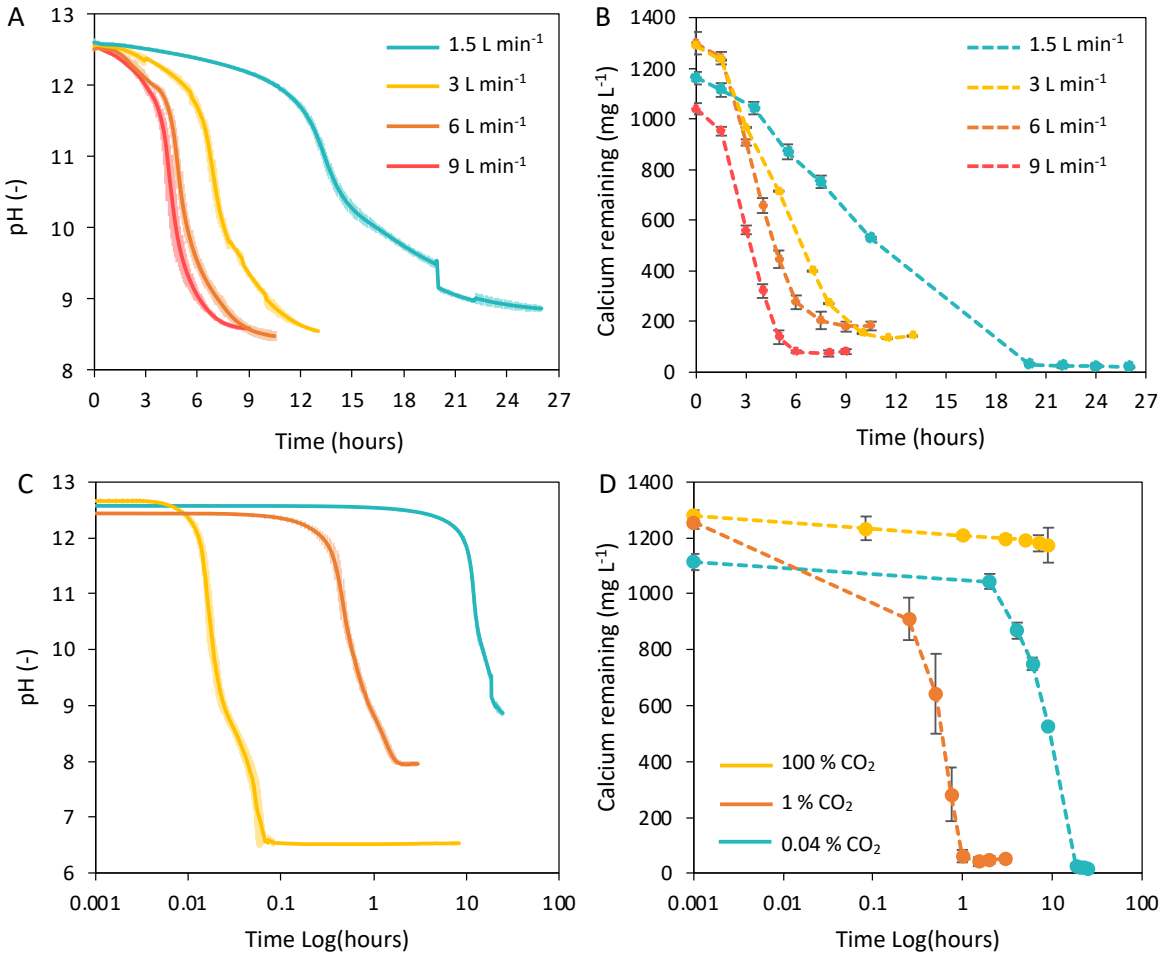

Figure 6-1: Experimentally determined pH (A) and remaining calcium concentration (B) vs time for air flowrates of 1.5, 3, 6, and 9 L min^{-1}. Experimentally determined pH (C), and remaining calcium concentration (D) for a flow rate of 1.5 L min^{-1} and CO_2 concentration of 0.04%, 1%, and 100%. The lighter shading for the pH curves shows the fluctuation in the pH readings between each experimental run (triplicates).

6.3.2 Urea stability

Figure 6-2A shows that the concentration of urea remained constant throughout the 30 hours of air bubbling, of which for more than 24 hours the pH was below the minimum threshold pH of 11, thus indicating that no significant urea loss had occurred during the experiment. The concentration of free and saline ammonia decreased at the start of the experiment as it was stripped from the solution (Figure 6-2B). Stabilized urine will have an initial concentration of ammonia. However, the concentration is typically less than 400 mg L^{-1} (Figure 6-2) and is significantly less than the concentration present in hydrolyzed urine. The concentration of ammonia after the initial stripping process remained constant, further indicating that urea hydrolysis did not occur.

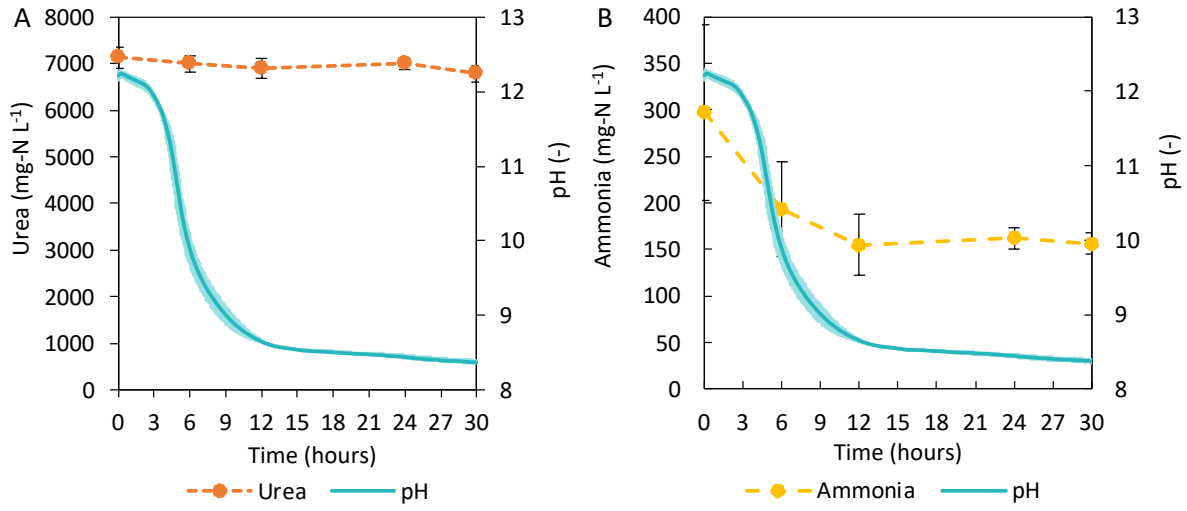

Figure 6-2: Urea concentration (A), ammonia concentration (B), and pH over 30 hours with an air flow rate of 3 L min^{-1}.

6.3.3 Analysis of precipitates

The precipitate was analyzed via SEM and XRD, both of which confirmed the sample to be calcium carbonate. The XRD analysis indicated that no other crystalline phase was present. No calcium hydroxide was present in the precipitant. The crystal morphology can be determined from SEM imagery which can be found in Appendix C. SEM showed that the particles exist in a cube-like formation with a size range of approximately 2-5 µm (Figure C-3). The regular cubic formation indicates that the calcium carbonate is in the form of calcite (Siva et al., 2017), which is in agreement with the XRD analysis.

6.3.4 Model fit

A comparison of the experimental and simulated pH and calcium data for 0.04% CO_2 (A and B), 1% CO_2 (C and D), and 100% CO_2 (E and F) is shown in Figure 6-3. Comparison of the experimental and simulated data and model calibration for different air flow rates can be found in Figure C-4 in Appendix C.

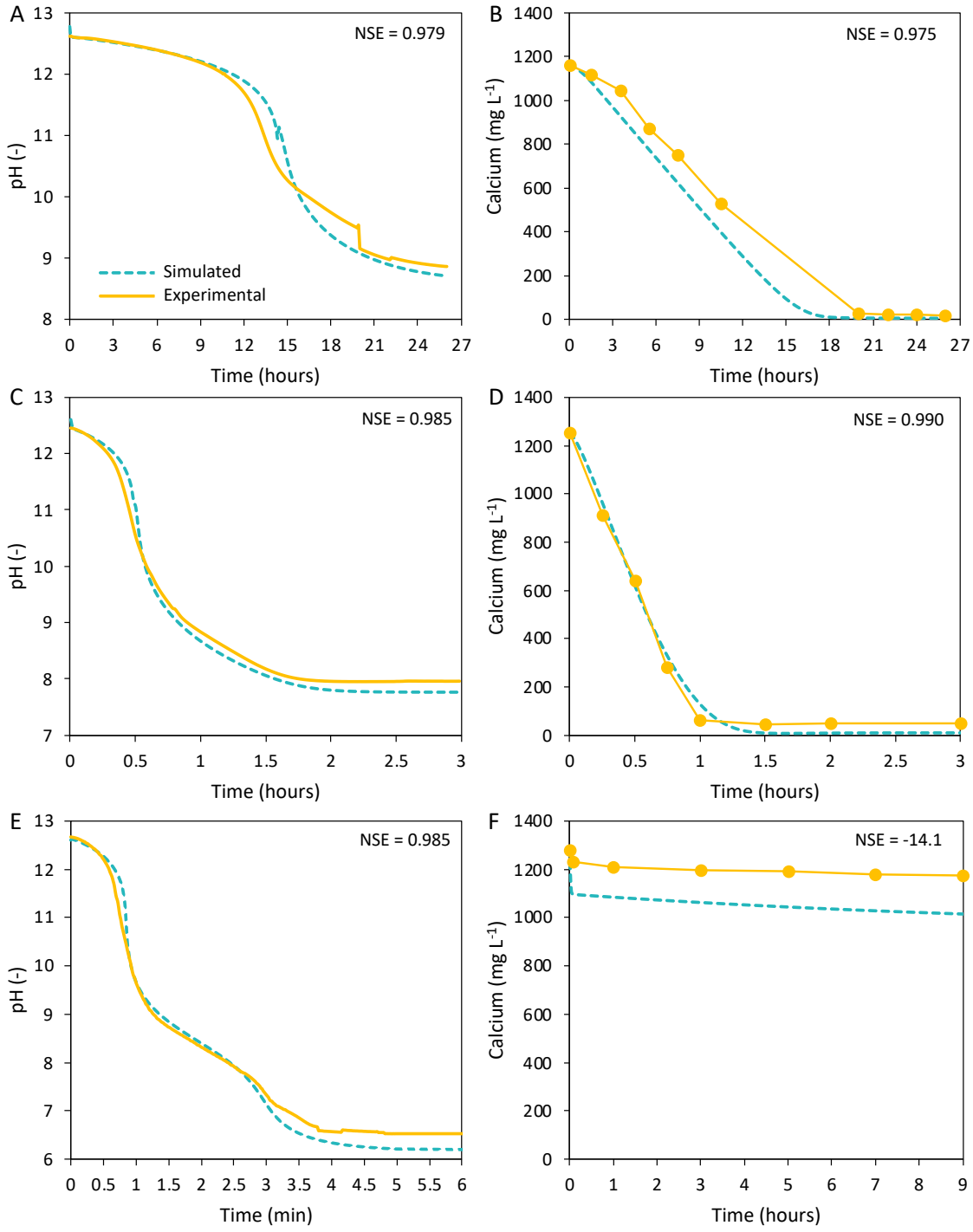

Figure 6-3: Comparison of simulated (- - -) and experimental (—) results for a flowrate of 1.5 L min^{-1} and a CO_2 concentration of 0.04% (A, B), 1% (C, D), and 100% (E, F) where A, C, and E compare pH and B, D and F compare the remaining calcium concentration.

In all cases, the model captured the pH curve well with a Nash-Sutcliff model efficiency (NSE) coefficient greater than 0.96. The model also captured the calcium concentration well with an NSE coefficient greater than 0.95 for all cases, except for the 100% CO_2 curve where the NSE coefficient was -14. In this case, the model captures the trend where the calcium concentration decreases slightly in the first five minutes and then remains relatively constant but not the absolute values (Figure 6-3D).

6.3.5 Scaling potential after treatment

The treated stabilized urine will be saturated with respect to $CaCO_3$ after aerating it with air/CO_2. As stated earlier, $CaCO_3$ is a common scaling component. Therefore, it was important to determine how the $CaCO_3$ present after air/CO_2 bubbling would affect the operation of an RO process. A simulation of how the scaling index (SI) of $CaCO_3$ increases as water is removed (concentrated by RO) for different urine compositions was therefore conducted, shown in Figure 6-4A. Approximately 85% water removal could be achieved before a $CaCO_3$ SI of 1.2 is reached. Urine composition does not have a significant impact on the scaling index. Figure 6-4B shows the relationship between temperature and SI as water is removed. Water removal was simulated at 20, 25, and 30°C, assuming air bubbling took place at 20°C followed by water removal at 25°C (20/25) and 15°C (20/15). Water removal at temperatures between 20 and 30°C does not result in a significant variation in the scaling index. If water removal occurs at a higher temperature than the air bubbling step, the solution is initially under-saturated with respect to $CaCO_3$ and over-saturated if water removal occurs at a lower temperature than air bubbling. However, as water is removed, the difference in scaling index converges to the same value regardless of composition and water removal temperature.

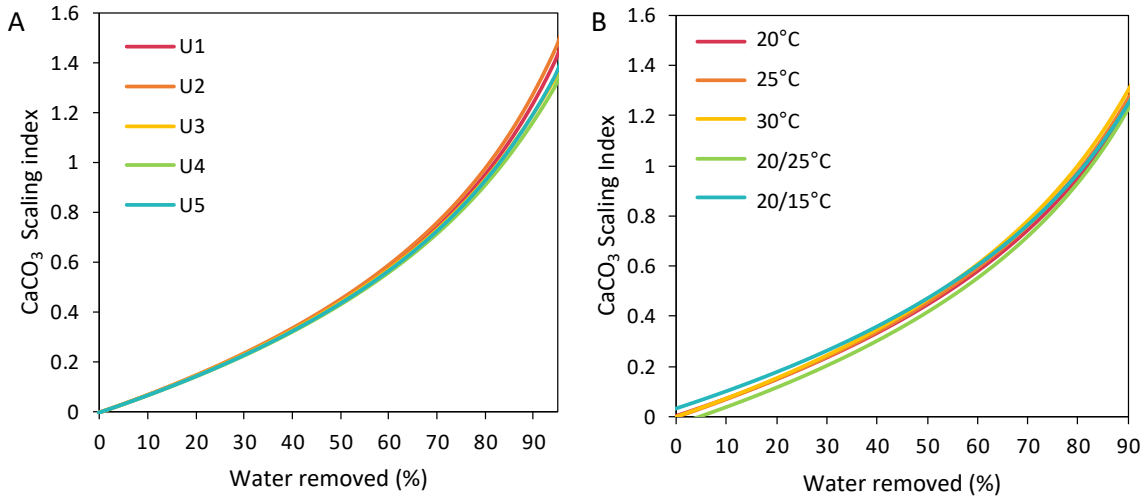

Figure 6-4: (A) CaCO3 scaling index as a function of water removal for five different urine compositions, (B) the effect of temperature on the $CaCO_3$ scaling index as a function of water removal, where the water is removed at 20°C, 25°C, and 30°C, the solution is aerated at 20°C and the water is removed at 25°C, the solution is aerated at 20°C and the water is removed at 15°C.

6.4 DISCUSSION

6.4.1 Model Interpretation

With 100% CO_2, the pH reached equilibrium after 5 minutes. With the available flowmeter, it was not possible to accurately measure a low enough CO_2 flow rate to determine how 100% CO_2 would affect the rate of calcium precipitation. Therefore, an accurate precipitation rate constant for 100% CO_2 could not be determined via the model. The model predicted that the precipitation rate constant for air and 1% CO_2 was 139 d^{-1} and 584 d^{-1}, respectively. El Fil and Manzola (2003) coupled air bubbling with seeding (0.1 mg L^{-1}) in geothermal waters and they determined the precipitation rate constant to be 138 d^{-1}. This value is in agreement with this work. Velts et al. (2011) investigated 5% CO_2 bubbling in an aqueous $Ca(OH)_2$ solution and determined a precipitation rate constant of 777 d^{-1}. Whilst this work did not use a seeding technique and used 1% CO_2 rather than 5 %, the precipitation rate constants are comparable. Based on the NSE coefficients, it was determined that the model is sufficiently accurate to explain the underlying mechanisms occurring during the air/CO_2 bubbling process. Furthermore, the integrated model can be adapted to model urine evaporation processes, microbial-induced calcium carbonate precipitation, and various kinetic aspects related to urine treatment, and other wastewater systems.

6.4.2 Understanding the processes involved

The model assumed that CO_2 dissolution, $CaCO_3$ precipitation, and ammonia stripping were occurring, and that the urea hydrolysis was negligible. Figure 6-5A shows how the pH is affected if there is no CO_2 dissolution. Figure 6-5B shows the pH and calcium concentration assuming no $CaCO_3$ precipitated. Figure 6-5C shows the pH and total ammoniacal nitrogen (TAN) assuming there was no ammonia stripping and Figure 6-5D shows the pH and TAN assuming 0.2 mol d^{-1} of urea hydrolysis was occurring. From Figure 6-5A, it is evident that CO_2 dissolution is the main controller of pH. However, $CaCO_3$ precipitation and ammonia stripping will also affect the equilibrium pH, but to a lesser extent. Figure 6-5B shows that if no $CaCO_3$ precipitation occurs, the pH will still decrease due to the addition of CO_2. However, the equilibrium pH would be slightly higher due to the build-up of carbonate ions that did not precipitate. Figure 6-5C shows that without ammonia stripping, the ammonia concentration would remain constant until a pH of 9.25, this is the dissociation constant at which ammonia protonates to form ammonium, resulting in a slight decrease in ammonia concentration. The model predicts that if urea hydrolysis was occurring, there would be an increase in the ammonia concentration observed.

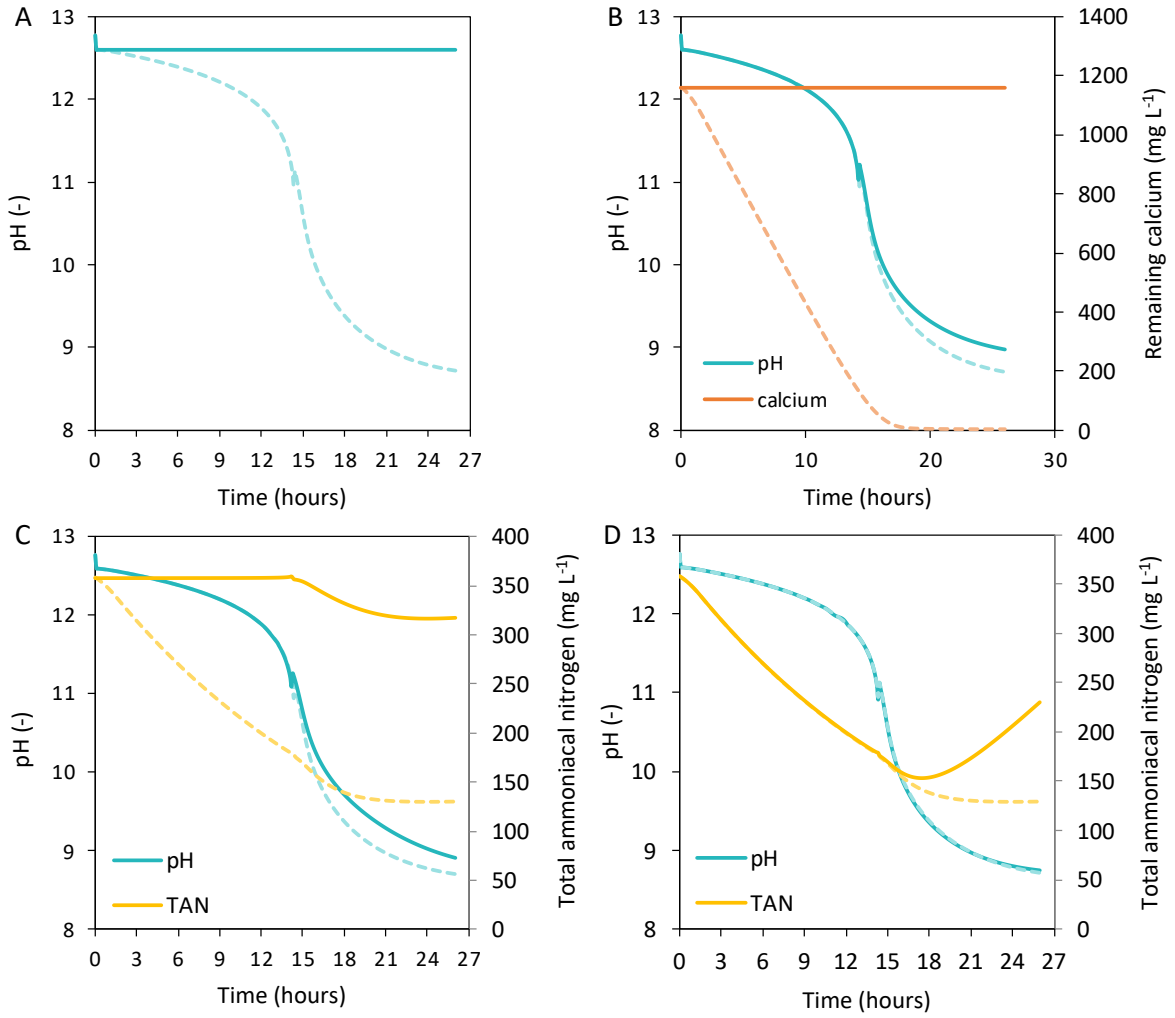

Figure 6-5: Comparison of the simulation with all processes on (- - -) and the effect of neglecting individual processes (—), where CO_2 dissolution is turned off (A), $CaCO_3$ precipitation is turned off (B), ammonia stripping is turned off (C), and urea hydrolysis of 0.2 mol d^{-1} (D).

The rate of CO_2 dissolution (Equation 6) is directly linked to three variables: the concentration of CO_2 in the air, the air flow rate (for a given reactor size), and the mass transfer coefficient. For each flow rate, there will be a limiting value for the mass transfer coefficient where the exponent term tends to zero. The concentration of carbonate ions is directly linked to the pH of a solution, as the pH decreases below the salinity-adjusted carbonate dissociation constant (9.35 (Millero et al., 2006)), the percentage of inorganic carbon in the form of CO_3^{-2} will decrease, thus reducing the driving force for the formation of $CaCO_3$ as per Equation 5. This explains the two distinct regions observed in Figure 6-1B. If CO_2 dissolves too quickly, the pH will decrease below the carbonate dissociation constant before any $CaCO_3$ can precipitate, as observed with 100% CO_2 experimental data. In the work of (Altiner, 2018; Bang et al., 2011), bubbling 100% CO_2 through a $Ca(OH)_2$ slurry was investigated. In this case, the precipitation of $CaCO_3$ was observed and the calcium concentration was reduced from 20 000 to 160 mg L^{-1} (Bang et al., 2011). The dissolution of excess $Ca(OH)_2$ in the slurry acted as a buffer to maintain a high pH

and thus, ensured that the inorganic carbon remained in the form of carbonate thereby providing a driving force for the precipitation reaction. In this current work, no excess $Ca(OH)_2$ was present to counter the pH decrease. Therefore, if the pH decrease occurs faster than the precipitation reaction, the extent of calcium removal would be limited.

Figure 6-6 compares how different air flow rates affect the pH and calcium concentration, for a given reactor size, and assuming that the mass transfer coefficient is not limiting. The mass transfer can be improved via mixing (Lisitsin et al., 2008) or decreasing bubble size (Altiner, 2018; Bang et al., 2011) to maximize surface area and bubble retention time. At low flow rates and CO_2 concentrations, the rate of CO_2 dissolution is the rate-limiting step for $CaCO_3$ precipitation. The precipitation rate is faster than the addition of CO_3^{-2} ions to the system. Once the maximum CO_2 dissolution rate is achieved, the formation of CaCO3 becomes the rate-limiting step. This is evident in Figure 6-6B, where, at flowrates greater than 5 L min-1, there is no significant increase in the rate at which calcium is removed. The rate of $CaCO_3$ formation could be increased by increasing the operating temperature, which would decrease the $K_{sp,CaCO_3}$ (Stumm and Morgan, 1996) or by adding seeds, which would increase the k_{CaCO_3} (El Fil and Manzola, 2003; Song et al., 2006). The results ultimately show that it is important to have a rate of CO_3^{2-} formation greater than the precipitation rate of $CaCO_3$, but the CO_2 dissolution rate should be small enough to allow for substantial calcium removal before the buffer capacity of the solution is depleted.

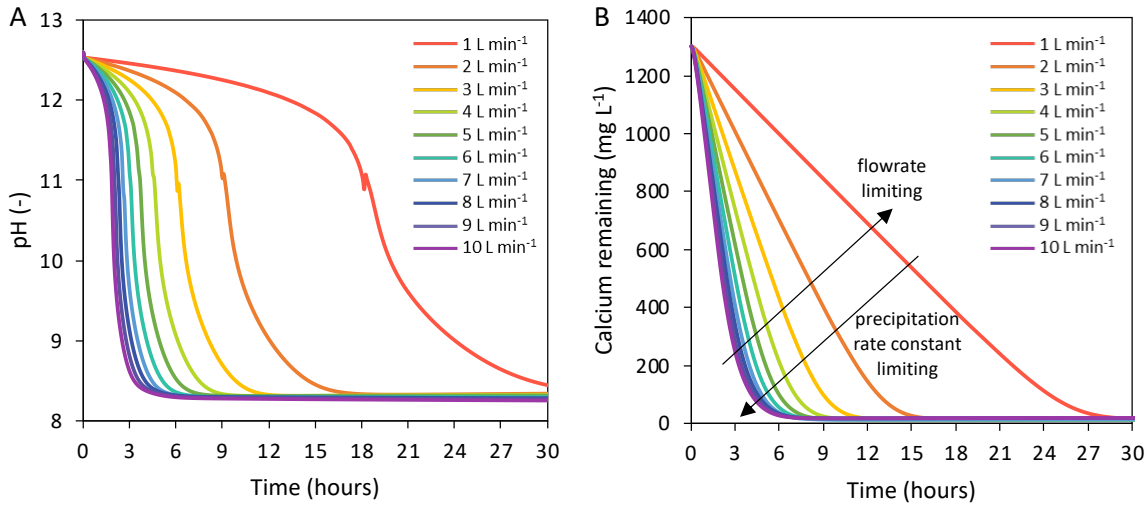

Figure 6-6: Effect of varying air flow rate from1 to 10 L min^{-1} on the pH (A), and calcium (B) assuming maximum gas mass transfer.

6.4.3 Urea stability during air bubbling

After air bubbling, the pH of the treated urine was 8.5 and thus below the threshold value of 11 (Randall et al., 2016), which inhibits enzymatic urea hydrolysis. However, no significant hydrolysis occurred.

This is likely because of the following reasons. There was a low concentration of urease or urease-producing bacteria present. At pH values below 3.5 and above 8.6 the metabolism of urease-producing Helicobacter pylori bacterium is irreversibly inhibited (Rektorschek et al., 1998), this phenomenon may potentially be inhibiting the activity of the urease-producing bacteria present in urine, even after a pH decrease is observed. In addition, all experiments were conducted at a temperature of ~20°C, which is too low for chemical hydrolysis to occur (Callahan et al., 2005). As the air/CO_2 bubbling would occur continuously, and directly before RO as a pre-treatment step, it is unlikely that hydrolysis would occur and affect the recovery of urea.

6.4.4 Implications for a reverse osmosis process

Simulation of water removal via RO after treatment with air/CO_2 bubbling showed that although the aerated urine is saturated with respect to $CaCO_3$, scaling caused by $CaCO_3$ might be delayed. Rahardianto et al. (2008) observed that up to a SI of 1.2 $CaCO_3$ membrane scaling was undetected. This occurs at a water removal of approximately 85%. Figure C-7 in Appendix C, further confirms the importance of the pre-treatment step by displaying the difference in the amounts of solids formed during water removal. For the treated urine, the simulation shows that only a small mass of solids would precipitate (< 60 mg) up to a water removal of 90%. This is significantly less than stabilized urine. For 1 L of urine, at a water removal of 50%, 1.07 g of solids would precipitate. This would cause significant membrane scaling. The potential risk of scaling could also be further reduced by adding an antiscalant, but this might reduce the quality of the product produced. This means that stabilizing fresh urine to first produce calcium phosphate and then bubbling CO_2/air through the treated urine to reduce the calcium concentration in the solution could provide an effective pre-treatment method for RO. In addition, the bubbling of air into stabilized urine could also provide an innovative method to sequester CO_2 (Aguilar, 2012). For example, approximately 1.32 kg CO_2 could be sequestered per m^3 of stabilized urine (this will vary based on the initial calcium concentration though).

6.4.5 Design and economic considerations

Air bubbling cost vs. operating time

The power required for the air blower to treat 1 m^3 of urine is a function of the air bubbling time and blower power (kW). The operating time was calculated from Figure 6-6B and was determined as the time required for 95% calcium removal for each air flow rate. The blower power requirements were calculated according to Sierra (Sierra et al., 2008) and increased with increasing air flow rate, with detailed calculations provided in Appendix C. Figure 6-7A compares the total cost and operating times required for each air flow rate. As the air flow rate increases, the marginal decrease in operating time

also decreases. Therefore, the optimum air flow rate is approximately 4 L min^{-1} L^{-1} urine, after which the marginal increase in cost outweighs the marginal decrease in operating time. At an air flow rate of 4 L min^{-1} L^{-1} urine, the air bubbling would cost \$0.65 m^{-3} and would require an operating time of approximately 7.6 hours.

Air vs. CO_2 enriched gas

Figure 6-7B compares the cost and operating time for different CO_2 concentrations at optimum operating conditions. Whilst the required operating time is significantly decreased by increasing the CO_2 concentration, the cost is 2.35 times more when compared to air bubbling. As CO_2 costs \$ 0.97 per kg (Air Liquide, Cape Town), even if CO_2 is 100% efficient, approximately 1.3 kg of CO_2 is required per m^3 of urine resulting in a minimum cost of \$1.27 m^{-3} urine, which is double the cost of air bubbling. Further information regarding how flow rate and operating time impact the costing for CO_2 can be found in Figure C-8. An additional advantage of air bubbling to remove excess calcium is that it can be used to sequester CO_2 directly from the atmosphere (Aguilar, 2012). The cost of the power requirements for air bubbling would require the break-even sales price (\$ 1.57 L^{-1}) of the niche fertilizer product to be increased by 0.2%, based on the economic analysis conducted by Chipako and Randall (2020a).

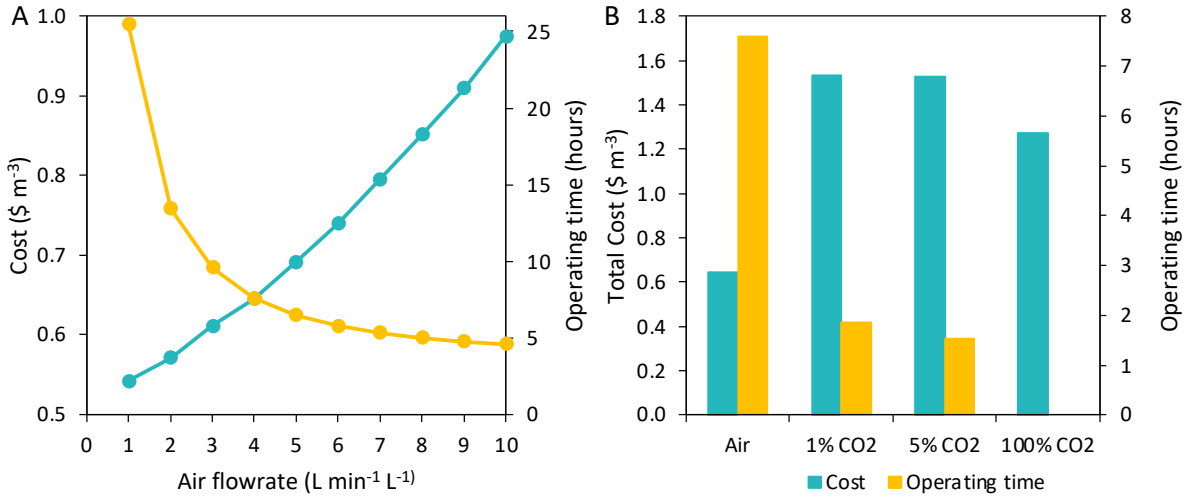

Figure 6-7: Cost and operating time as a function of air flow rate varying from 1 to 10 L min^{-1} L^{-1} (A), cost and operating time as a function of CO_2 concentration for the most cost-efficient flow rate (B).

6.5 CONCLUSIONS

It was shown experimentally that air bubbling is an effective method for removing calcium ions from urine stabilized with calcium hydroxide, removing between 85-98% of the calcium depending on the initial calcium concentration, flow rate, and operating time.

CHAPTER 6: AERATION PRE-TREATMENT

It was determined that the rate of CO_2 dissolution is the key process controlling the pH of the solution, and ultimately the calcium is removed as solid $CaCO_3$. At low flow rates, CO_2 dissolution was the rate-limiting step whilst at high flow rates and/or high CO_2 concentrations, the fast pH decrease limited the precipitation of $CaCO_3$.

It was also shown that even though the pH of the solution had dropped below the threshold pH for enzymatic urea hydrolysis to occur (<11), no urea hydrolysis was detected, most likely because the urease-producing bacteria had been inhibited at the high initial pH values (>12.5) and the reaction time was too fast.

Through simulations, it was shown that after pre-treatment with air bubbling, 85% of the water could be removed from the urine before $CaCO_3$ scaling would be detected. However, the exact nature of membrane scaling for the proposed process needs to be investigated further experimentally and in a full-scale RO system.

The cost of using air enriched with CO_2 was more than double compared to using an air blower. Whilst using higher concentrations of CO_2 resulted in a significant decrease in operating time, it did not justify the overall operating cost. The optimum operating condition was determined to be an air flow rate of 4 L min^{-1} L^{-1} urine and an operating time of 7.6 hours. At these conditions, 95% of the calcium could be removed for a cost of \$0.65 m^{-3} (R11 m^{-3}). This represents only 0.2% of the break-even sales price (\$1.57/ R27 L^{-1}) of a liquid fertilizer product that could be produced in a RO system.

REFERENCES

Aguilar, M.J. 2012. Urine as a CO_2 absorbent. Journal of Hazardous Materials 213-214, 502-504.

Altiner, M. 2018. Influences of CO_2 Bubbling Types on Preparation of Calcite Nanoparticles by Carbonation Process. Periodica Polytechnica Chemical Engineering 62(2), 209-214.

Bang, J.-H., Jang, Y.N., Kim, W., Song, K.S., Jeon, C.W., Chae, S.C., Lee, S.-W., Park, S.-J. and Lee, M.G. 2011. Precipitation of calcium carbonate by carbon dioxide microbubbles. Chemical engineering journal 174(1), 413-420.

Brison, A. 2016. Understanding the processes involved during the stabilization of urine with calcium hydroxide, MSc. Thesis. ETH Zürich Zürich

Callahan, B.P., Yuan, Y. and Wolfenden, R. 2005. The Burden Borne by Urease. Journal of the American Chemical Society 127(31), 10828-10829.

Campos, J.C., Moura, D., Costa, A.P., Yokoyama, L., Araujo, F.V.d.F., Cammarota, M.C. and Cardillo, L. 2013. Evaluation of pH, alkalinity and temperature during air stripping process for ammonia removal from landfill leachate. Journal of Environmental Science and Health, Part A 48(9), 1105-1113.

Chipako, T. and Randall, D. 2020. Investigating the feasibility and logistics of a decentralized urine treatment and resource recovery system. Journal of Water Process Engineering 37, 101383.

El Fil, H. and Manzola, A. 2003. Decarbonation of geothermal waters by seeding with aragonite crystals coupled with air bubbling. Applied geochemistry 18(8), 1137-1148.

Franks, R., Bartels, C. and Nagghappan, L. 2009. Performance of a reverse osmosis system when reclaiming high pH-high temperature wastewater. American Water Works Association Membrane Technology Conference. Memphis, USA, 15-18 March. 1-16.

Hasson, D., Segev, R., Lisitsin, D., Liberman, B. and Semiat, R. 2011. High recovery brackish water desalination process devoid of precipitation chemicals. Desalination 283, 80-88.

Haynes, W.M., Lide, D.R. and Bruno, T.J. 2016. CRC handbook of chemistry and physics, 95th edition, CRC Press, Florida, USA.

Kazmierczak, T., Tomson, M. and Nancollas, G. 1982. Crystal growth of calcium carbonate. A controlled composition kinetic study. The Journal of Physical Chemistry 86(1), 103-107.

Lisitsin, D., Hasson, D. and Semiat, R. 2008. The potential of CO2 stripping for pretreating brackish and wastewater desalination feeds. Desalination 222(1-3), 50-58.

Millero, F.J., Graham, T.B., Huang, F., Bustos-Serrano, H. and Pierrot, D. 2006. Dissociation constants of carbonic acid in seawater as a function of salinity and temperature. Marine Chemistry 100(1-2), 80-94.

Mitsoyannis, E. and Saravacos, G.D. 1977. Precipitation of calcium carbonate on reverse osmosis membranes. Desalination 21(3), 235-240.

OLI Systems Inc. 2022. OLI Stream Analyzer, version 11.0, OLI Systems Inc, New Jersey, USA.

Putnam, D.F. 1971 Composition and concentrative properties of human urine, p. 112, NASA, Washington, D.C.

Rahardianto, A., McCool, B.C. and Cohen, Y. 2008. Reverse osmosis desalting of inland brackish water of high gypsum scaling propensity: kinetics and mitigation of membrane mineral scaling. Environmental science & technology 42(12), 4292-4297.

Randall, D.G., Krähenbühl, M., Köpping, I., Larsen, T.A. and Udert, K.M. 2016. A novel approach for stabilizing fresh urine by calcium hydroxide addition. Water Research 95, 361-369.

Reichert, P. 1994. AQUASIM-A tool for simulation and data analysis of aquatic systems. Water Science and Technology 30(2), 21.

Rektorschek, M., Weeks, D., Sachs, G. and Melchers, K. 1998. Influence of pH on metabolism and urease activity of Helicobacter pylori. Gastroenterology 115(3), 628-641.

Sierra, E., Acién, F., Fernández, J., García, J., González, C. and Molina, E. 2008. Characterization of a flat plate photobioreactor for the production of microalgae. Chemical Engineering Journal 138(1-3), 136-147.

Siva, T., Muralidharan, S., Sathiyanarayanan, S., Manikandan, E. and Jayachandran, M. 2017. Enhanced polymer induced precipitation of polymorphous in calcium carbonate: calcite aragonite vaterite phases. Journal of Inorganic and Organometallic Polymers and Materials 27(3), 770-778.

Song, Y., Weidler, P.G., Berg, U., Nüesch, R. and Donnert, D. 2006. Calcite-seeded crystallization of calcium phosphate for phosphorus recovery. Chemosphere 63(2), 236-243.

Stumm, W. and Morgan, J.J. (1996) Aquatic chemistry: chemical equilibria and rates in natural waters, John Wiley & Sons, New York.

Touati, K., Cherif, H., Kammoun, N., Jendoubi, M. and Elfil, H. 2018. Inhibition of calcium carbonate scaling by precipitation using secondary nucleation coupled to degassing with atmospheric air. Journal of water process engineering 22, 258-264.

Udert, K. 2002. The fate of phosphorus and nitrogen in source-separated urine, PhD thesis. Swiss Federal Institute of Technology, Zurich, Switzerland.

Udert, K.M., Larsen, T.A. and Gujer, W. 2003. Estimating the precipitation potential in urine-collecting systems. Water Research 37(11), 2667-2677.

Velts, O., Uibu, M., Kallas, J. and Kuusik, R. 2011. CO2 mineral trapping: Modeling of calcium carbonate precipitation in a semi-batch reactor. Energy Procedia 4, 771-778.

Warner, R.C. 1942. The kinetics of the hydrolysis of urea and of arginine. Journal of Biological Chemistry 142(2), 705-723.

CHAPTER 7: CONCENTRATION USING REVERSE OSMOSIS

CHAPTER 7: CONCENTRATION USING REVERSE OSMOSIS

This chapter is based on the published work in Paper 3 titled: Concentrating stabilized urine with reverse osmosis: How does stabilization method and pre-treatment affect nutrient recovery, flux, and scaling?

7.1 INTRODUCTION

Reverse osmosis (RO) has been identified as a promising, yet understudied, concentration technique because it is energy efficient when compared to other urine concentration methods (Udert and Wächter, 2012). Reverse osmosis is also used widely to desalinate seawater (Greenlee et al., 2009) and urine has a similar total dissolved solids (TDS) concentration (30 – 40 g L^{-1}) to that of seawater. It is to this author's best knowledge, only two RO studies with real human urine have been conducted (Ek et al., 2006; Ray et al., 2020).

In the first study, Ek et al. (2006) removed 80% of the water from hydrolyzed urine using a high-pressure seawater reverse osmosis (SWRO) membrane. However, this study was conducted using dilute and hydrolyzed urine with H_2SO_4 addition to reduce the pH and improve ammonia rejection. As the urine was dilute it is unclear if similar water removal is realistic for stabilization of fresh urine. The study used hydrolyzed urine and therefore rejection of nitrogen using a SWRO membrane is only for ammonia/ammonium and not urea. In the second study, Ray et al. (2020) investigated urea rejection with brackish water RO membranes (27 bar) using real urine stabilized with NaOH (Rejection -50%, pH = 12.5) and acetic acid (Rejection-62%, pH = 5). The limitation of this study was that experiments were conducted with a dead-end stirred cell, which does not accurately mimic the cross-flow that occurs in commercial RO/NF systems. In addition, rejection was calculated at a water removal of only 8%. This provides limited insight into how the rejection of different salts and urea would be affected as the feed concentration increases. Finally, no permeate flux data was presented, therefore it was not possible to draw conclusions on whether any scaling or fouling occurred or what possible volume reductions are achievable. This is critical for the design of full-scale RO processes for higher water removals and concentrations. There is currently also no literature available on the rejection of urea using seawater RO (SWRO) membranes, which operate at higher pressures (55 bar compared to 27 bar).

This research focuses on urine stabilized with $Ca(OH)_2$ or citric acid. In Chapter 5 and Chapter 6, the potential for the $Ca(OH)_2$ to cause membrane scaling was discussed and two pre-treatment methods (chemical addition and aeration) for removing calcium ions from urine stabilized with $Ca(OH)_2$ were investigated. However, their effectivity for preventing RO membrane scaling has not yet been tested during the concentration of stabilized urine. The pre-treated solutions have varying pH values (approximately 8.5 after air bubbling, 9.5 after NH_4HCO_3 addition, and 12 after $NaHCO_3$ addition), which may also influence the ion rejection through the RO membranes. Stabilizing urine by acidification would in theory not require a pre-treatment and all ions would remain dissolved in the

urine. Therefore, all NPK nutrients could be theoretically recovered in the brine stream during acid stabilization, unlike with base stabilization, where P is removed via filtration as solid calcium phosphate. The chosen stabilization method will also affect the osmotic pressure of the feed stream, which will influence the permeate flux and the potential volume reduction.

No studies have investigated urine stabilized specifically with $Ca(OH)_2$ or citric acid and high water removals (~60%) using RO systems. Importantly, the method of stabilization will also impact feed osmotic pressure, pH, and membrane permeability if scaling occurs. It is therefore important to consider membrane flux in conjunction with ion rejection. The main aim of this work was therefore to determine the preferred stabilization method (acidification or alkalization) to concentrate human urine using a SWRO membrane for maximum nutrient recovery. Specifically, the work aimed to:

1. Investigate, using synthetic urine, whether air bubbling, $NaHCO_3$ or NH_4HCO_3 addition are effective pre-treatment RO methods for $Ca(OH)_2$ stabilized urine. Based on flux and ion rejection, determine a preferred pre-treatment RO method, and compare the results to synthetic urine stabilized with citric acid.
2. Investigate which stabilization method (alkalinization or acidification) gives the highest nutrient recoveries and how the stabilization method affects flux, ion rejection, and scaling/fouling, for real urine.

7.2 MATERIALS AND METHODS

7.2.1 Urine stabilization and pre-treatment

Urine was stabilized with either 10 g L^{-1} $Ca(OH)_2$ or 7.8 g L^{-1} citric acid (this was the amount required to reduce the urine pH to below 3.5 at which bacterial inactivation would occur (Rektorschek et al., 1998)). Urine stabilized with $Ca(OH)_2$ was pre-treated with an exact dose of either $NaHCO_3$, $NaHCO_3$, or air was bubbled through the urine until a pH < 8.7 was reached. A detailed method for chemical dosing is given in Section D.2 and the method for air bubbling is given in Section D.1. Whilst a 1.2 μm pore size filtration is sufficient to remove excess undissolved $Ca(OH)_2$ before air bubbling a smaller pore size microfiltration is required as pre-treatment to prevent scaling before RO. Post air bubbling all urine was filtered with 0.45 μm pore size filter paper (CHM Lab Group, Spain).

7.2.2 Membranes and equipment setup

A Dow-Filmtec SW30 membrane was used for all experiments. A SWRO membrane was chosen as there is currently no available data on the urea rejection characteristics of SWRO membranes. In addition, this membrane was used in a previous urine concentration study by Ek et al. (2006). The

complete membrane filtration equipment consisted of a feed tank that was temperature controlled with a chiller (HH-25, Jeiotech, South Korea) and water circulation. The feed was circulated through a cross-flow (CF) cell (SEPA CF, Sterlitech, USA) using a high-pressure pump (M-03S, Hydra-cell, Minneapolis, USA). The CF cell housed the flat sheet membrane with an active area of 140 cm^2. The brine flow rate was measured with a flow meter (LZT-1002G, 1-7 L min^{-1}, Wet Technologies, Strand, South Africa). The permeate stream was collected and continuously weighed on a digital mass balance (PS 8100.X.2, Radwag, Poland) to determine the permeate flux. The pressure (PT100R-13-LU2-H1131, Turck, Germany), temperature and conductivity (Mettler-Toledo, USA), and pH (H1 5221, Hanna, Johannesburg, South Africa) of the permeate and brine were also continuously measured.

7.2.3 Experimental conditions

Table 10 summarizes the type of urine, pre-treatment, and operating conditions used for each experiment. Synthetic urine was used to determine the effect of the stabilization method and pre-treatment on the key operating parameters (volume reduction factor, flux, rejection, scaling/fouling). The optimum pre-treatment method for $Ca(OH)_2$ stabilized urine and urine stabilized with citric acid was compared with real urine to obtain more realistic results and whether or not fouling occurred due to the presence of organics in the urine.

Table 10: Summary of experimental conditions including stabilization, pre-treatment, membrane, and operating pressure.

Experiment	Urine Type	Stabilization	Pre-treatment	Membrane	Operating pressure
Stabilization Method	Synthetic	$Ca(OH)_2$	None Air bubbling $NaHCO_3$ NH_4HCO_3	SW30	55 bar
		Citric acid	None		
Real Urine	Real	$Ca(OH)_2$	Air bubbling	SW30	55 bar
		Citric acid	None		

7.2.4 Experimental procedure

A new flat sheet membrane was used for each experiment and pre-soaked in de-ionized water for at least 30 minutes before an experiment commenced. Before each experiment, de-ionized water was also circulated through the system at atmospheric pressure. The pressure in the system was then slowly increased to the desired operating pressure and the de-ionized water was circulated at 55 bar for 30 minutes. For each experiment, the starting volume was 5 L. The start volume was chosen to ensure each experiment could be completed in one day and, whilst in theory, the solution could have been concentrated further, the experiment was stopped at 60% water removal due to a minimum liquid volume (2 L) in the feed tank being required to protect the pump. For synthetic urine stabilized with

$Ca(OH)_2$ and real urine stabilized with citric acid, the experiment was stopped at 50% water removal due to a significant decline in flux. The feed flow rate was 6.4 L min^{-1} which corresponds to a tangential velocity of 0.58 m s^{-1}. After each experiment, the membrane was removed and dried. The system was then flushed with tap water and cleaned with a dilute HCl solution ($2 < pH < 3$) to remove any potential scaling components in the system.

7.3 RESULTS AND DISCUSSION

7.3.1 Effectiveness of pre-treatment methods for base stabilized synthetic urine

Urine stabilized with $Ca(OH)_2$ is likely to cause significant membrane scaling if concentrated using RO. Three potential pre-treatment methods; air bubbling, $NaHCO_3$ addition, or NH_4HCO_3 addition were investigated to reduce the membrane scaling. The urea and potassium rejection, normalized permeate flux, and permeate conductivity as a function of the volume reduction factor (VRF) are shown in Figure 7-1. Phosphorus is precipitated during base stabilization and is therefore not detectable in the feed stream.

As expected, with $Ca(OH)_2$ stabilized urine without pre-treatment there was an immediate, steep, decline in permeate flux (Figure 7-1C) caused by membrane scaling. This was confirmed visually as a white powder covering the active membrane surface and via SEM and EDS (Figure D-6). The EDS detected no carbon present in the white powder and the ratio of calcium to oxygen suggests that the scaling component was $Ca(OH)_2$. The rejection of urea and K were both poor and showed a significant decline upon concentration (Figure 7-1A and Figure 7-1B). The concentration of other ions in the permeate was also significant, resulting in high permeate conductivity that was similar to the initial feed conductivity at a VRF of 2. Ray et al. (2020) also investigated urea rejection at a pH (12.5, with a BWRO membrane) outside the designed membrane operating range (2-11). However, their deviation in rejection was much smaller than observed in this study. This may be because they used NaOH to raise the pH which would not have resulted in prolific scaling, as with $Ca(OH)_2$. This is because NaOH is much more soluble.

Comparing the three pre-treatment options, with regard to permeate flux (Figure 7-1C), it is evident that all pre-treatment methods equally reduced membrane scaling. In order of increasing permeate conductivity and decreasing urea and K rejection, air bubbling provided the highest rejection followed by NH_4HCO_3 addition, and then $NaHCO_3$ addition as pre-treatment methods. Urea rejection remained constant across all pre-treatment methods with a maximum decline of 8% with increasing VRF. At a VRF of 2.5, 79%, 77%, and 74% of the urea was recovered in the brine for the air, NH_4HCO_3 and $NaHCO_3$ pre-treated alkalinized urine respectively. Potassium rejection was greater than 95% and K recovery in the brine at a VRF of 2.5 was also greater than 95% in all cases. For all pre-treatment

methods, permeate conductivity increased with increasing VRF, again indicating a decline in salt rejection with increasing water recovery.

In addition, pre-treatment with $NaHCO_3$ resulted in a solution with a pH of approximately 11.85, which is above the upper membrane pH operating limit of 11. Long-term operation at high pH values can lead to a membrane swelling effect and increased passage of sodium ions (Franks et al., 2009) and most likely urea, as observed with the $Ca(OH)_2$ stream and the higher conductivity of the $NaHCO_3$ permeate. Whilst, pre-treatment with NH_4HCO_3 results in the addition of NH_4^+ ions, which are more favorable than Na^+ ions with regard to fertilizers, ammonia emissions should be considered as this has both safety and environmental implications (Skjøth et al., 2008). At least 20% of the ammonia was lost through volatilization. Whilst all pre-treatment methods provide an adequate reduction in scaling, the most suitable pre-treatment method is air bubbling. This process can be slow though (Chapter 6), but it provides a high rejection of the key nutrients urea and K and does not add additional undesired ions such as sodium. This method also does not pose any health and safety implications as with NH_4HCO_3 dosing, whilst simultaneously sequestering CO_2 from the atmosphere.

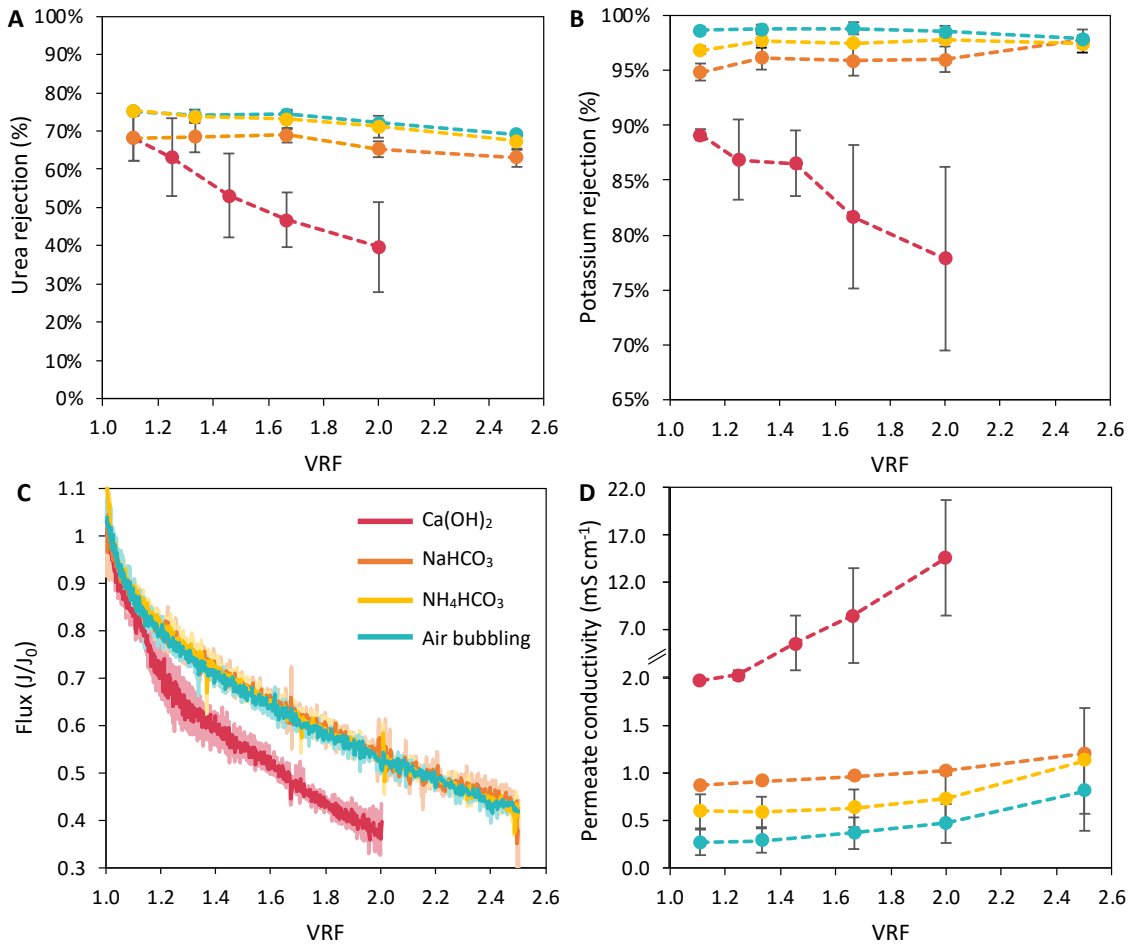

Figure 7-1: Urea rejection (A), potassium rejection (B), normalized permeate flux (C), and permeate conductivity (D) for synthetic urine stabilized with $Ca(OH)_2$ and then pre-treated with either $NaHCO_3$, NH_4HCO_3, or air bubbling as a function of VRF.

7.3.2 Comparison of acid and base stabilization for real and synthetic urine

Synthetic and real urine was stabilized with citric acid or $Ca(OH)_2$ and then pre-treated with air bubbling. The stabilized solutions were then concentrated to a VRF of 2.5 (except for real urine stabilized with citric acid where the experiment was stopped at a VRF of 2 due to a significant flux decline). The urea, P, and K rejections and normalized permeate flux are shown in Figure 7-2. With regards to ion rejection, in all cases, the rejection rates for acidified urine were higher than for base stabilized urine. Interestingly, there appears to be a correlation between urea rejection and feed pH (Figure D-11). In addition, rejection rates for real urine were higher than in synthetic urine. This was also observed by Pronk et al. (2006b) in a study that used nanofiltration to remove pharmaceuticals from real and synthetic urine. This was hypothesized to be either due to the formation of a fouling layer which then acts as a secondary membrane (Schäfer et al., 2002) or due to the organic matrix of the natural substances in urine (uric, oxalic, and proteins) (Boyce, 1968). These matrices would increase the compound size and therefore ion rejections. Whilst fouling was observed for the acidified urine (Figure D-7), it was not observed for base stabilized urine (Figure D-7), therefore the formation of a secondary 'membrane' seems unlikely.

For both citric acid and air bubbling (real urine), urea rejection decreased by less than 0.5% up to a VRF of 2. This increased to 2.4% at a VRF of 2.5 for stabilized urine pre-treated with air bubbling. Urea rejection was 90.7% for real acidified urine and 82.5% for real air bubbled urine (VRF=2.5). High rejection of P (for acidified urine; > 99.4%) and K (> 98%) was achieved for both stabilization methods. With regards to flux, the addition of citric acid to stabilize the urine results in an increase in osmotic pressure and therefore a smaller initial absolute flux (Figure D-3). This may have implications for the extent of water recovery as the osmotic pressure increases. The flux decline for acidified real urine was steeper than for air-bubbled real urine (Figure 7-2D). Visual inspection of the membranes showed the formation of visible brown fouling of the membrane for acidified urine. Analysis of the air bubbled (real urine) membrane surface via SEM (Figure D-7B) showed minimal scaling with only a small number of organic solids present. The presence of inorganic (Figure D-7C) and organic compounds (Figure D-7C) on the citric acid (real urine) treated membrane surface was much larger. Organics are observed to be more soluble at higher pH values (Franks et al., 2009), which could explain why organic fouling was observed with the acidified urine but not with base-stabilized urine.

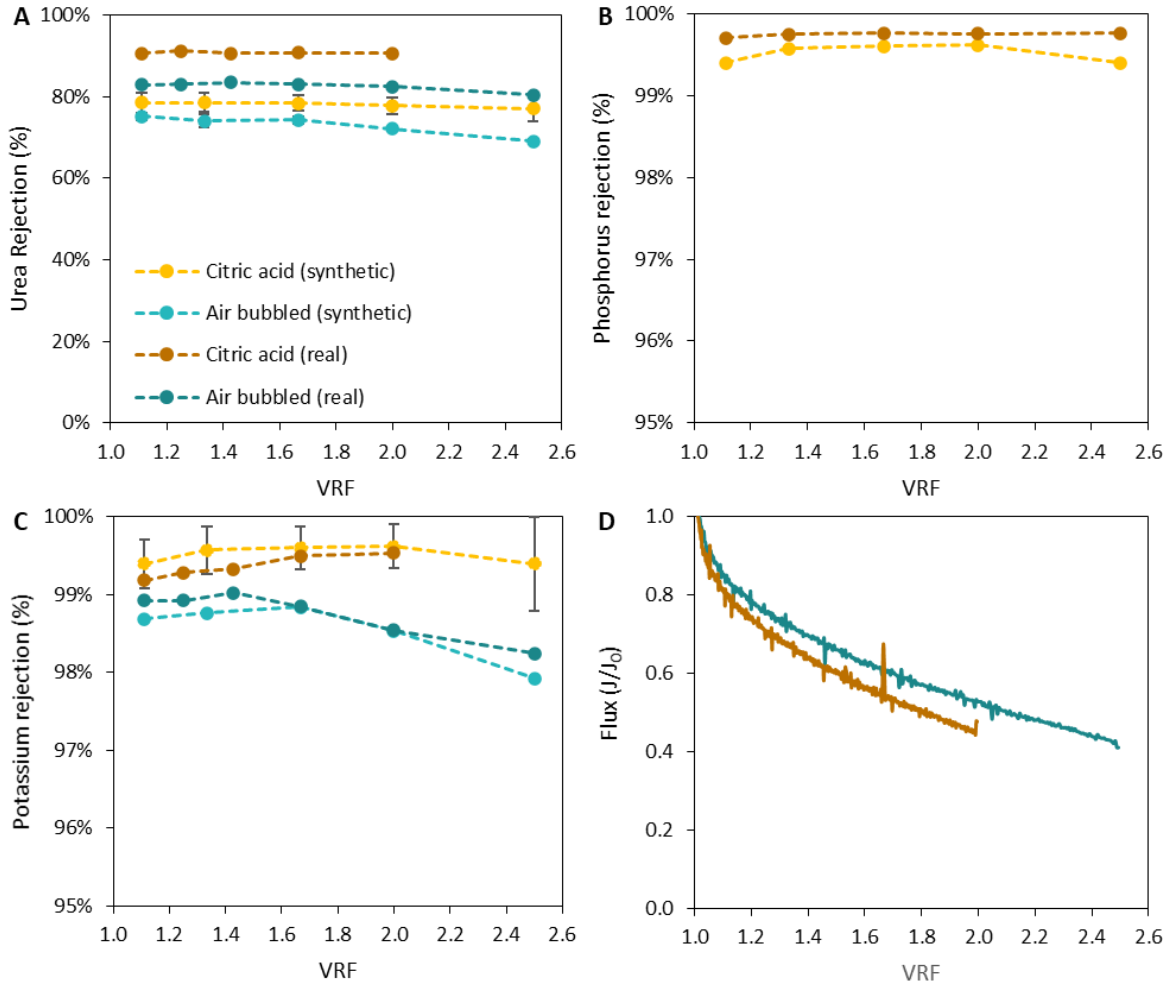

Figure 7-2: Urea rejection (A), phosphorus rejection (B), potassium rejection (C), normalized permeate flux (D) for real and synthetic urine stabilized with citric acid or stabilized with $Ca(OH)_2$ and then pre-treated with air bubbling, as a function of volume reduction factor (VRF).

7.3.3 Formation of solids during acid stabilization and further concentration

Base stabilized urine was dosed with $Ca(OH)_2$ in excess which resulted in a solid mixture of calcium phosphate, magnesium hydroxide and undissolved $Ca(OH)_2$. The solid mixture was allowed to settle before filtration. Filtration (filter pore size of 1.2 µm) of the supernatant of this mixture resulted in minimal blocking of the filter paper. However, filtering a well-mixed solution caused significant blocking of the filter paper, as expected. During the stabilization of real urine with citric acid, the formation of red crystals was observed. As with the base stabilized urine, the solids in the acid stabilized urine were also allowed to settle before filtration. However, in this case, when filtering the supernatant, the filter paper was still quickly blocked. Filtration of the settled crystals also caused significant blocking of the filter paper. Figure D-8 in Appendix D shows all four filter papers after filtration. The red crystals were identified as uric acid dihydrate (Figure D-9). Uric acid compounds have a decreasing solubility with decreasing pH (Wang and Königsberger, 1998) and would explain their formation in the

acidified but not in basic urine. Furthermore, many other compounds can form from acidified urine as typical kidney stones which would also lead to membrane scaling during RO concentration (Frassetto and Kohlstadt, 2011). Both Ek et al. (2006) and Ray et al. (2020) investigated the RO of acidified urine, however, those studies were conducted at pHs of 6 and 5, respectively which may not have been low enough to cause precipitation of uric acid dihydrate. Alternatively, the lack of solid formation may be due to differences in urine composition.

During the concentration of real urine with RO that had been stabilized with citric acid, a dark red/brown substance began to form on the walls of the feed tank. Visual inspection of the RO membrane at the end of the experiment also showed visible formation of a brown scaling/fouling on the membrane surface and this was confirmed by the observed flux decline (Figure 7-2D). Whilst analysis of the membrane surface and the brown substance from the tank wall via EDS could not confirm what the compound was, there was a high weight percent of carbon (C) and oxygen (O), which suggest that it is an organic substance. The molar ratio of C:O of the substance on the membrane and tank walls was also the same, which confirms that this is likely the same compound that forms as the acidified urine is concentrated by RO. It is also expected that during the long-term operation of an RO system to concentrate stabilized urine treated with citric acid; significant biological growth will occur as a result of the addition of an extra carbon source for acid-tolerant bacteria. This would lead to excessive bio-fouling of the RO membrane.

These results have implications for the treatment and concentration of human urine using RO. It implies that RO should ideally not be used to concentrate acidified urine because these components cannot be easily removed as with base stabilized urine by chemical addition (de-supersaturation of the major precipitating cation or anion). Furthermore, the pH of the acidified urine cannot be further decreased (as with base stabilized urine) since this will be outside the lower recommended pH operating range of the membranes. It is recommended that dehydration by evaporation be used instead to concentrate acidified urine as the process does not entail membranes and subsequent issues with scaling and bio-fouling.

7.3.4 Nutrient recovery during concentration using reverse osmosis

In terms of nutrient recovery, Figure 7-3 compares the overall NPK recovery from acid and base-stabilized real urine after 50% water removal by RO. The shaded region in nitrogen recovery represents the portion of N recovered as total ammoniacal nitrogen (TAN). During base stabilization, 99.8% of the P is precipitated as calcium phosphate and recovered as a solid. This has been shown to be an effective solid calcium phosphate-based fertilizer (Meyer et al., 2018). After air bubbling and concentration (VRF = 2) using RO, 86.1 % of the N (urea + TAN = 9.45 g-N L^{-1}), and 99.2% of the K (2.83 g L^{-1}) is recovered in the brine stream. The concentration of acid stabilized urine results in a

recovery of 99.9% of the P (0.88 g L^{-1}), 99.6% of the K (2.86 g L^{-1}), and 93.7% of the N (urea + TAN = 10.73 g L^{-1}). Final concentrations will vary based on the initial urine compositions though. Urea recovery in acidified urine was only slightly higher than for basic urine (89.2% vs. 93.6%), however, the TAN recovery in acidified urine is much higher (97.4% vs. 18.6%). This is due to ammonia stripping during the air bubbling pre-treatment as well as poor rejection of TAN in RO because the solution pH favored the formation of NH_3 over NH_4^+, which is easier to reject. A detailed mass balance for both the acidified (Figure D-5) and base stabilized (Figure D-4) urine can be found in Appendix D. Whilst acidification results in a higher recovery of nutrients, the associated issues with observed membrane fouling are problematic and would likely increase during long-term operation. Therefore, base stabilized urine pre-treated with air bubbling was determined to be the preferred urine concentration method.

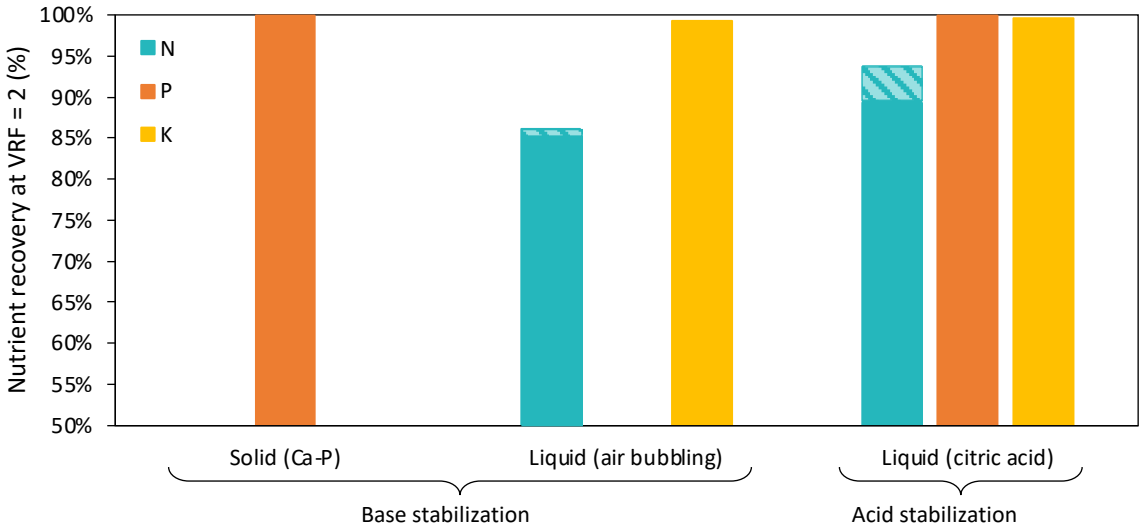

Figure 7-3: Nutrient recovery of nitrogen (urea-N and TAN), phosphorus, and potassium for real urine stabilized with $Ca(OH)_2$ and pre-treated with air bubbling and real urine stabilized with citric acid. The shaded region indicates the percentage of N recovered as TAN.

7.3.5 Further concentration

This Chapter only investigated concentrating stabilized urine up to 60%. Maximizing water removal is important to reduce the costs of transporting the final liquid fertilizer product (Maurer et al., 2006). As urine has a TDS concentration similar to seawater (high osmotic pressure) the water recovery may be limited due to the pressure limits of the membrane, to limit energy consumption, or to limit salt (and urea) passage to the permeate due to concentration polarization (Dupont, 2021). However, new SWRO membranes have been developed to operate at pressures up to 120 bar (Dupont, 2020). Alternatively, RO membranes could be used in conjunction with other water removal technologies such as evaporation (Simha et al., 2020b), membrane distillation (MD) (Volpin et al., 2019a), or freeze concentration (Randall and Nathoo, 2018). Base stabilization of fresh urine followed by pre-treatment with air

bubbling was determined to be the most promising treatment train before RO to optimize nutrient recovery and operation. Whilst Ek et al. (2006) reported an energy requirement of 12 kWh m^{-3} (80% water recovery, VRF = 5) to concentrate dilute urine, the typical energy consumption for a real-scale SWRO plant (including pre and post-treatment) ranges from 4 - 6 kWh m^{-3} feed (Abdelkareem et al., 2018). In Chapter 6 the energy require for air bubbling was calculated to be 10 kWh m^{-3}. Assuming 6 kWh m^{-3} for RO, the air bubbling would therefore account for two-thirds of the process's energy requirements. This is not unusual as aeration at wastewater treatment plants can account for up to 50% of total energy consumption (Wilsenach and Van Loosdrecht, 2004). Converting to a per kg-N basis (calculated in Appendix A), the combined air bubbling and RO process would require 11.5 MJ $kg\text{-}N^{-1}$. This energy requirement is significantly less than those reported by Patyk and Reinhardt (1997) and (Maurer et al., 2003) for the production of synthetic urea and treatment of N in domestic wastewater, respectively.

7.3.6 Effect of flush water

This research only investigated urine collected from waterless urinals that had been pre-dosed with either citric acid or $Ca(OH)_2$. However, the RO treatment process could be used to concentrate urine recovered from other collection methods where dilution occurs with flush water. For example, plumbed systems such as the Save! source separating toilet still requires small amounts of flush water to keep pipes clean and prevent scaling. This results in additional dilution and in regions where water is extremely hard (high concentrations of Ca^{2+} and Mg^{2+} ions) it would affect the urine chemistry.

With regards to diluting collected urine, larger volumes of urine would require treatment and hence the capital and operating cost of the RO system would increase. However, this would also be the case for all urine treatment technologies. In terms of urine chemistry, the effect of additional Ca^{2+} and Mg^{2+} from the flush water, which are scaling pre-cursor ions, may also result in membrane scaling, if not pre-treated. In Section 7.3.3, acid stabilization prior to RO was determined to be unsuitable due to the precipitation of uric acid dihydrate crystals and an organic compound. Whilst dilution by hard tap water may delay the precipitation of these compounds, it is likely that they will still form as the urine is concentrated using RO. In the case of flush water dilution for base stabilized urine, the addition of $Ca(OH)_2$ would act as a softening process and would precipitate the additional Mg^{2+} ions as $Mg(OH)_2$. The additional Ca^{2+} ions from the flush water would also be removed during the air bubbling/chemical addition pre-treatment step as $CaCO_3$. Urine collection (with base stabilization) that results in dilution from tap-water would therefore not be a concern for the operation of an RO system but would increase the capital and operating costs

7.4 CONCLUSIONS

Pre-treatment of base ($Ca(OH)_2$) stabilized urine with air bubbling, $NaHCO_3$ addition, or NH_4HCO_3 addition are all sufficient methods to reduce the potential for RO membrane scaling. However, air bubbling was determined to be the preferred pre-treatment method as it added no additional ions to the solution, resulted in a feed pH of 8.0-8.5, which is within the operating range of most commercial RO membranes, and achieved high nutrient recoveries in the brine stream.

Acidified urine resulted in a higher recovery of key NPK nutrients but the permeate flux was lower due to increased feed osmotic pressure from the acid addition and significant scaling on the RO membrane. The results from this work showed that RO should not ideally be used to concentrate acidified urine because the acidification of fresh urine results in the formation of uric acid dihydrate crystals and further concentration results in the formation of an unidentified organic compound. Neither of these could be removed by filtration or air bubbling as with base stabilized urine. Therefore, concentrating acidified urine would be best achieved using an evaporation process.

In this study, 60% of the water was removed from pre-treated base stabilized urine using RO, producing a liquid concentrate with 11.2 g-N L^{-1} (1.8% N) and 3.66 g-K L^{-1} (0.35% K) and a separate solid phosphate-based fertilizer. The process recovered approximately 86% of the urea, 99% of the potassium in the RO brine stream, and more than 99% of the phosphorus in the solid fertilizer.

This research also highlights the importance of using real urine to validate results. Had only synthetic urine been used, the formation of uric acid dihydrate crystals and the organic foulant would not have been identified. In addition, the rejection of urea differed significantly for real and synthetic urine. The use of synthetic urine to allow for consistency and repeatability is valuable, however, real urine should always be used when designing treatment processes.

It is recommended that the integrated urine concentration process be tested at a pilot scale and that higher water recoveries (> 60%) be investigated. In addition, a detailed economic analysis of the process and products produced should also be conducted along with crop field trials of the fertilizers produced.

REFERENCES

Abdelkareem, M.A., Assad, M.E.H., Sayed, E.T. and Soudan, B. 2018. Recent progress in the use of renewable energy sources to power water desalination plants. Desalination 435, 97-113.

Boyce, W.H. 1968. Organic matrix of human urinary concretions. The American journal of medicine 45(5), 673-683.

Dupont. 2020. DuPont™ XUS180808 Reverse Osmosis Element: Product Data Sheet [Online]. Dupont. Available: https://www.dupont.com/content/dam/dupont/amer/us/en/water-solutions/public/documents/en/45-D01736-en.pdf [Accessed 15/09/2021].

Dupont. 2021. FilmTec™ Reverse Osmosis Membranes Technical Manual [Online]. Available: https://www.dupont.com/content/dam/dupont/amer/us/en/water-solutions/public/documents/en/45-D01504-en.pdf [Accessed 15/09/2021].

Ek, M., Bergström, R., Bjurhem, J.E., Björlenius, B. and Hellström, D. 2006. Concentration of nutrients from urine and reject water from anaerobically digested sludge. Water Science and Technology 54, 437-444.

Franks, R., Bartels, C. and Nagghappan, L. 2009. Performance of a reverse osmosis system when reclaiming high pH-high temperature wastewater. American Water Works Association Membrane Technology Conference. Memphis, USA, 15-18 March. 1-16.

Frassetto, L. and Kohlstadt, I. 2011. Treatment and prevention of kidney stones: an update. American family physician 84(11), 1234-1242.

Greenlee, L.F., Lawler, D.F., Freeman, B.D., Marrot, B. and Moulin, P. 2009. Reverse osmosis desalination: Water sources, technology, and today's challenges. Water Research 43(9), 2317-2348.

Maurer, M., Pronk, W. and Larsen, T.A. 2006. Treatment processes for source-separated urine. Water Research 40(17), 3151-3166.

Maurer, M., Schwegler, P. and Larsen, T.A. 2003. Nutrients in urine: energetic aspects of removal and recovery. Water Science and Technology 48(1), 37-46.

Meyer, G., Frossard, E., Mäder, P., Nanzer, S., Randall, D.G., Udert, K.M. and Oberson, A. 2018. Water soluble phosphate fertilizers for crops grown in calcareous soils–an outdated paradigm for recycled phosphorus fertilizers? Plant and soil 424(1-2), 367-388.

Patyk, A. and Reinhardt, G.A. 1997. Düngemittel-Energie-und Stoffstrombilanzen, Springer.

Pronk, W., Palmquist, H., Biebow, M. and Boller, M. 2006. Nanofiltration for the separation of pharmaceuticals from nutrients in source-separated urine. Water Research 40(7), 1405-1412.

Randall, D.G. and Nathoo, J. 2018. Resource recovery by freezing: A thermodynamic comparison between a reverse osmosis brine, seawater and stored urine. Journal of Water Process Engineering 26, 242-249.

Ray, H., Perreault, F. and Boyer, T.H. 2020. Rejection of nitrogen species in real fresh and hydrolyzed human urine by reverse osmosis and nanofiltration. Journal of Environmental Chemical Engineering, 103993.

Rektorschek, M., Weeks, D., Sachs, G. and Melchers, K. 1998. Influence of pH on metabolism and urease activity of Helicobacter pylori. Gastroenterology 115(3), 628-641.

Schäfer, A., Mastrup, M. and Jensen, R.L. 2002. Particle interactions and removal of trace contaminants from water and wastewaters. Desalination 147(1-3), 243-250.

Simha, P., Lalander, C., Nordin, A. and Vinnerås, B. 2020. Alkaline dehydration of source-separated fresh human urine: Preliminary insights into using different dehydration temperature and media. Science of the Total Environment 733, 139313.

Skjøth, C.A., Ellermann, T., Hertel, O., Gyldenkærne, S. and Mikkelsen, M.H. 2008. Footprints on ammonia concentrations from environmental regulations. Journal of the Air & Waste Management Association 58(9), 1158-1165.

Udert, K.M. and Wächter, M. 2012. Complete nutrient recovery from source-separated urine by nitrification and distillation. Water Research 46(2), 453-464.

Volpin, F., Chekli, L., Phuntsho, S., Ghaffour, N., Vrouwenvelder, J.S. and Shon, H.K. 2019. Optimisation of a forward osmosis and membrane distillation hybrid system for the treatment of source-separated urine. Separation and Purification Technology 212, 368-375.

Wang, Z. and Königsberger, E. 1998. Solubility equilibria in the uric acid–sodium urate–water system. Thermochimica acta 310(1-2), 237-242.

Wilsenach, J.A. and Van Loosdrecht, M.C.M. 2004. Effects of Separate Urine Collection on Advanced Nutrient Removal Processes. Environmental Science & Technology 38(4), 1208-1215.

CHAPTER 8: HYBRID NANOFILTRATION PROCESS

CHAPTER 8: HYBRID NANOFILTRATION PROCESS

This chapter is based on the published work in Paper 4 titled: A hybrid nanofiltration and reverse osmosis process for urine treatment: Effect on urea recovery and purity

8.1 INTRODUCTION

Limited research into urine concentration using reverse osmosis (RO) was likely due to the high potential for membrane scaling and poor urea rejection. In Chapter 7 it was shown that operation at high pressure (55 bar) using a seawater reverse osmosis (SWRO) membrane can be used to improve urea rejection. In addition, pre-treatment of $Ca(OH)_2$ stabilized urine with either aeration or chemical addition was shown to be effective at reducing membrane scaling. However, air bubbling was chosen as the preferred pre-treatment method. Urine was concentrated by at least a factor of 2.5, whilst also recovering 86% of the urea in the brine stream.

There are, however, limitations with a process that only uses RO to concentrate urine. Urine is not necessarily sterile (Hilt et al., 2014) and pathogens can be present from urinary tract infections (Ferreira et al., 2010). Furthermore, up to 64% (±27%) of any pharmaceutical activate compounds (PhAC) consumed are excreted in urine (Lienert et al., 2007). Urine also contains many other undesirable salts and organics. Nanofiltration has shown a high rejection of pathogens (Patterson et al., 2012) and PhACs (Pronk et al., 2006b). Therefore, as SWRO membranes provide even better rejection than NF membranes it results in the salts, organics, and any PhACs present in the urine being concentrated along with the valuable fertilizer nutrients. Whilst crops fertilized with urine have comparable yields to those treated with synthetic fertilizers (Pandorf et al., 2018), application rates need to be adjusted based on a crop's salt sensitivity to maximize yield (Mnkeni et al., 2008). Crop uptake of PhACs also requires consideration, and any safety concerns could be avoided by limiting urine-derived fertilizer use to non-food-related agriculture such as flower farming. However, salt tolerance would still need to be considered, which could potentially limit the commercial appeal of urine-derived fertilizers. A method to recover a purer urea stream that still contains other key fertilizer nutrients could therefore increase the value of the final fertilizer product or be used to produce alternative urea-based products (Marepula et al., 2021).

In Chapter 2, a variety of treatment methods to remove pharmaceuticals were discussed. Some methods, such as GAC are not suitable for stabilized urine as it absorbs urea along with the PhACs. Other methods did not physically remove the PhACs but degraded them to other compounds (the effects of which are not known). One promising method was nanofiltration (NF) which has been widely researched in the context of water (Foureaux et al., 2019), but only one study (to this author's knowledge) has investigated NF for pharmaceutical removal in the context of urine (Pronk et al., 2006b). Pronk et al. (2006b) observed that NF of unhydrolyzed urine resulted in poor urea rejection (< 20%), whilst PhACs were

retained in the brine stream. They suggested that NF could be used to rather recover urea in the permeate stream. Nanofiltration membranes are generally classified as either loose or tight membranes (Schäfer and Fane, 2021). Nanofiltration membranes provide good rejection of divalent ions, but they have limited rejection capacity for monovalent ions (Bergman, 2007). However, tight NF membranes provide a higher rejection of monovalent ions (Thamaraiselvan et al., 2018). Tight NF membranes also improve urea rejection (46-58% urea rejection, NF90, (Ray et al., 2020)) compared to loose NF membranes (10-20%, NF270 (Pronk et al., 2006b)). A loose NF membrane could potentially be used as pre-treatment to remove PhACs from urine, whilst a tight NF membrane could be used to remove undesirable salts in addition to PhACs, thus resulting in a purer urea product stream. However, the lower urea recovery in the permeate stream (due to the higher rejection capabilities of tight NF membranes) would need to be considered. The permeate stream could then be concentrated further using seawater RO to produce a concentrated and purified urea product stream.

The recovery and purity of urea in the permeate will also be affected by the extent of the volume reduction factor (VRF) (amount of water removed as permeate). Many rejection studies are limited to a VRF of 2.5 (water removal of 60%). At high VRFs the feed becomes increasingly concentrated and there is the potential for concentration polarization, which reduces rejection capacity (Bergman, 2007). It is therefore important to assess salt rejection and urea recoveries at high VRFs.

The aim of this work was therefore to determine if a hybrid NF and RO process could be used to recover urea from urine in a purer form by removing undesirable salts, organics, and PhACs. This was achieved by:

1. Determining the rejection capabilities of loose and tight NF membranes with regards to urea, undesirable salts, organics, and pharmaceuticals.
2. Comparing how urea and salt rejection are affected as the VRF increases.
3. Assessing the overall recovery and purity of urea when the NF permeate was further concentrated with a seawater RO membrane.

8.2 MATERIALS AND METHODS

8.2.1 Urine collection and preparation

Both real and synthetic urine stabilized with $Ca(OH)_2$ were pre-treated with air bubbling following the method described in Appendix D to remove excess calcium ions. All urine was filtered with 0.45 μm pore size filter paper (CHM Lab Group, Spain) after air bubbling and before NF. Detailed compositions of the real urine are available in Table E-1.

8.2.2 Pharmaceutical dosing

Six different pharmaceuticals, three acidic and three basic of varying molecular weight were chosen to compare the rejection capacity of tight and loose NF membranes. The properties of each pharmaceutical compound are summarized below in Table 11. Each pharmaceutical was dosed at 100 mg L^{-1}. Whilst this concentration is higher than measured in real urine it was chosen to ensure that at least 99% rejection could be accurately measured based on the method detection limit (MDL). The PhACs are costly, and the ones used in this study were all donations. The stock of Tenofovir and Stavudine was unfortunately not sufficient for use in experiments with real urine.

Table 11: Characteristics of salicylic acid, paracetamol, stavudine, lamivudine, tenofovir, chlorpheniramine maleate.

Pharmaceutical	Classification	Dissociation constant (pKa)	$LogK_{ow}$[a]	Molecular weight (g mol^{-1})
Salicylic acid	Anti-inflammatory	2.79[a] (acid)	2.26	138
Acetaminophen	Analgesic, antipyretic	9.46[a] (base)	0.46	151
Stavudine	HIV treatment	9.95[a] (base)	-0.73	224
Lamivudine	HIV and HepB treatment	4.3[b] (acid)	-1.4	229
Tenofovir	HIV treatment	1.35[a] (acid)	-1.5	287
Chlorpheniramine maleate	Relieves allergy symptom	9.47[a] (base)	3.74	391

[a]*(Wishart et al., 2022),* [b]*(Eyni et al., 2018).*

8.2.3 Membranes and equipment setup

The equipment setup used in this chapter is the same used in Chapter 7, Section 7.2.2. The following FilmTec membranes were used; NF270, NF90, and SW30. The NF270 is considered a loose NF membrane, the NF90 is a tight NF membrane, and the SW30 membrane is typically used for seawater desalination.

8.2.4 Experimental conditions and methods

All membranes were prepared by pre-soaking in de-ionized water for at least 24 hours. De-ionized water was then circulated through the system at 35 bar (55 bar for the SW30) for at least 2 hours to compact the membrane and ensure steady flux. The feed flow rate was 6.8 L min^{-1} (maximum feed flow rate advised by the equipment supplier) which corresponds to a tangential velocity of 1.09 m s^{-1}. This was repeated for the feed solution and a new membrane was used for each experimental run. The

concentration of pharmaceuticals was measured in the feed solution before and after the circulation period to determine if any adsorption to the membrane had occurred.

A high operating pressure (35 bar) was chosen for the NF membrane experiments to ensure sufficient driving force to overcome the osmotic pressure of urine. The effect of membrane operating pressure on urea and ion rejection was investigated and the results are shown in Figure E-2.For the NF experiments, enough permeate was collected to achieve a VRF of 5 (80% water removal) for the NF270 membrane due to a minimum liquid volume requirement in the feed tank to protect the pump and a VRF of 4 (75% water removal) for the NF90 membrane due to flux decline caused by the increased concentration of the feed. Pharmaceutical rejection was analyzed at a VRF of 2 (water removal of 50%) for consistent comparison. The permeate collected from the NF90 (real urine) experiment was further concentrated using a SW30 membrane at 55 bar. Due to the poor purification properties of the NF270 membrane, it was determined that further concentration of the permeate from these experiments was not feasible. Both real and synthetic urine was used for each experimental condition.

To calculate the urea purity of a stream the concentration of urea in the stream was first analyzed. The water from 100 mL of the stream was evaporated at 30°C (to prevent urea hydrolysis) and the mass of dried solids was then weighed. A known mass of the dried sample was then re-dissolved in de-ionized water and the urea was re-measured to confirm no hydrolysis had occurred. The urea purity was then calculated as the mass of urea as a percentage of the total dissolved solids. The concentration of ammonia was less than 1% of the measured ions in all samples tested for purity. Therefore, it was determined that any ammonia loss during drying would not significantly contribute to the urea purity calculations.

8.2.5 Pharmaceutical analysis

Pharmaceuticals were measured using an Agilent 1220 Infinity liquid chromatograph (Agilent Technology Inc., Switzerland) equipped with an Agilent Poroshel 120 C18 column (4.3 cm x 50 mm x 2.7µm). Chromatographic separations were performed at 35°C using 15 mM phosphate buffer pH 3.25 (A) and acetonitrile (B) as mobile phase with gradient elution at a flow rate of 0.8 mL/min. Detection of all the components was carried out at 210 nm and completed within 15 minutes.

8.3 RESULTS AND DISCUSSION

8.3.1 Pharmaceutical rejection

Figure 8-1 compares the rejection of six PhACs by the NF90 and NF270 membranes, the molecular weight (MW) of the PhACs increases from left to right. The tight NF90 membrane provided high rejections of pharmaceuticals (>98%) while for the NF270 membrane, at least 73% of all the PhACs were rejected. These results were agreeable with those of Pronk et al. (2006b) for PhACs with similar MWs. Tenofovir appeared to have degraded in the synthetic stabilized urine (pH 7.0), which could explain the high rejection (99%) achieved in comparison to the other two acidic pharmaceuticals which had lower rejections compared to the basic compounds (for the NF270 membrane). Although tenofovir was not present in the real urine experiments, it is likely that a similar high rejection would have been observed due to the degradation. For the NF270 there was no observable trend between rejection and MW. There was no significant difference in the concentrations of the pharmaceuticals before and after membrane equilibration. It is therefore unlikely that significant membrane adsorption occurred.

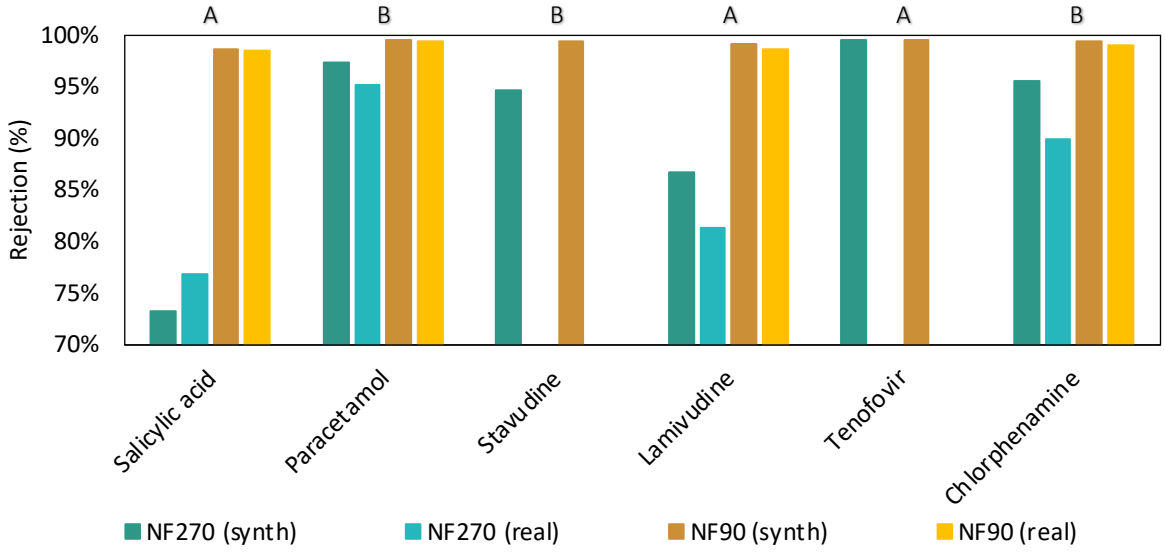

Figure 8-1: Pharmaceutical rejection for NF90 and NF270 membranes for both real and synthetic urine at a VRF of 2. Pharmaceuticals are presented in increasing molecular weights. Limited availability of stavudine and tenofovir resulted in their exclusion from the experiments with real urine. Compounds are labelled either A or B to denote whether they are acidic (A) or basic (B).

It is likely that other membrane characteristics such as surface charge and solution pH played a role in rejection. Pronk et al. (2006b) showed that, for basic compounds, rejection decreases with increasing pH due to increased absorption of the positively charged compound to the negatively charged membrane with the reverse occurring for acidic compounds. Real urine dosed with PhACs has a pH of 8.0 compared to 7.0 for synthetic urine. This would explain why the rejection of basic compounds was lower in real urine compared to synthetic urine. It is likely that a similar trend would have been observed

with stavudine in real urine. These aspects should be investigated further in future work though. Alternatively, rejection may be influenced by differences in the osmotic pressure of real and synthetic urine caused by the rejection of organics (Pronk et al., 2006b). In general, both the NF90 and NF270 membrane are suitable for the removal of a broad spectrum of PhACs.

8.3.2 Urea purification using nanofiltration

To determine if a purer urea stream could be recovered from urine using NF, the urea, ion, and COD rejection were measured as a function of volume reduction factor (VRF), shown in Figure 8-2. Where VRF is the ratio of the starting volume to the brine volume remaining. Urea typically consists of 37 ± 4% of the TDS in urine (this will vary based on urine composition). For the loose NF270 membrane, urea rejection was low (less than 10%) and decreased further as more permeate was recovered. The rejection rates for real and synthetic urine were in a similar range to those achieved by Pronk et al. (2006b) using the same membrane. For the synthetic urine experiments, 77.6% of the urea was recovered in the permeate, at an 80% water removal. Flux decline due to fouling was observed for real urine, as such, only 75% of the water could be recovered as permeate. However, the urea recovery in the permeate is comparable with synthetic urine (Figure 8-2B). Rejection of monovalent ions by the NF270 membrane was poor (< 55%) which can be observed by the high conductivity in the permeate (6 – 12 mS cm^{-1}) as shown in Figure 8-2C. Rejection of ions was comparable for real and synthetic urine, the differences in permeate conductivity are due to the differences in initial conductivity of the two streams. The NF270 provided > 70% rejection of organic compounds measured as COD. At a VRF of 4, 46% of the ions, and 78% of the COD was removed. This increased the urea purity from 37 to 56%.

The urea rejection rates for the tight NF90 membrane were higher than for the NF270 membrane and decreased with increasing permeate recovery. These results agreed with those of Ray et al. (2020), who observed a urea rejection of approximately 55% for real fresh urine at a VRF of 1.1. Urea rejection by the NF90 membrane increased significantly (20%) between synthetic and real urine. Pronk et al. (2006b) hypothesized that this phenomenon could be attributed to the formation of organic matrices that increased the size of urea and thus increased rejection. The NF90 provided high rejection of ions resulting in a permeate conductivity of < 0.6 mS cm^{-1} for real urine (Figure 8-2C). The rejection of COD was greater than 95%. At a water removal (permeate) of 75%(for real urine), 48% of the urea was recovered, 90% of the COD was removed, and 97% of the ions were removed, resulting in increased urea purity from 37% to 89%. Concentrating the NF permeate stream using SWRO membranes would further decrease the recovery of urea since approximately 14% of the total urea is lost using a SWRO membrane (Chapter 7).

Due to the poor rejection of salts by the NF270 membrane, only further concentration of the NF90 permeate using RO was investigated. However, the NF270 membrane is advantageous as it has a higher permeate flux and lower urea rejection compared to the NF90 membrane. This results in a smaller NF setup being required and increased urea recovery in the permeate. However, the low rejection of monovalent ions (< 55% compared to > 80% for divalent ions) does not significantly improve the urea purity. Replacement of monovalent ions with divalent ions using ion exchange resins would increase their rejection and thus result in a purer urea stream. Hilal et al. (2015a) exchanged up to 80% of the chloride ions with sulfate ions (depending on dose and contact time) in seawater. Hilal et al. (2015b) further observed that permeate flux using an NF90 membrane increased from 4 to 11 L m-2

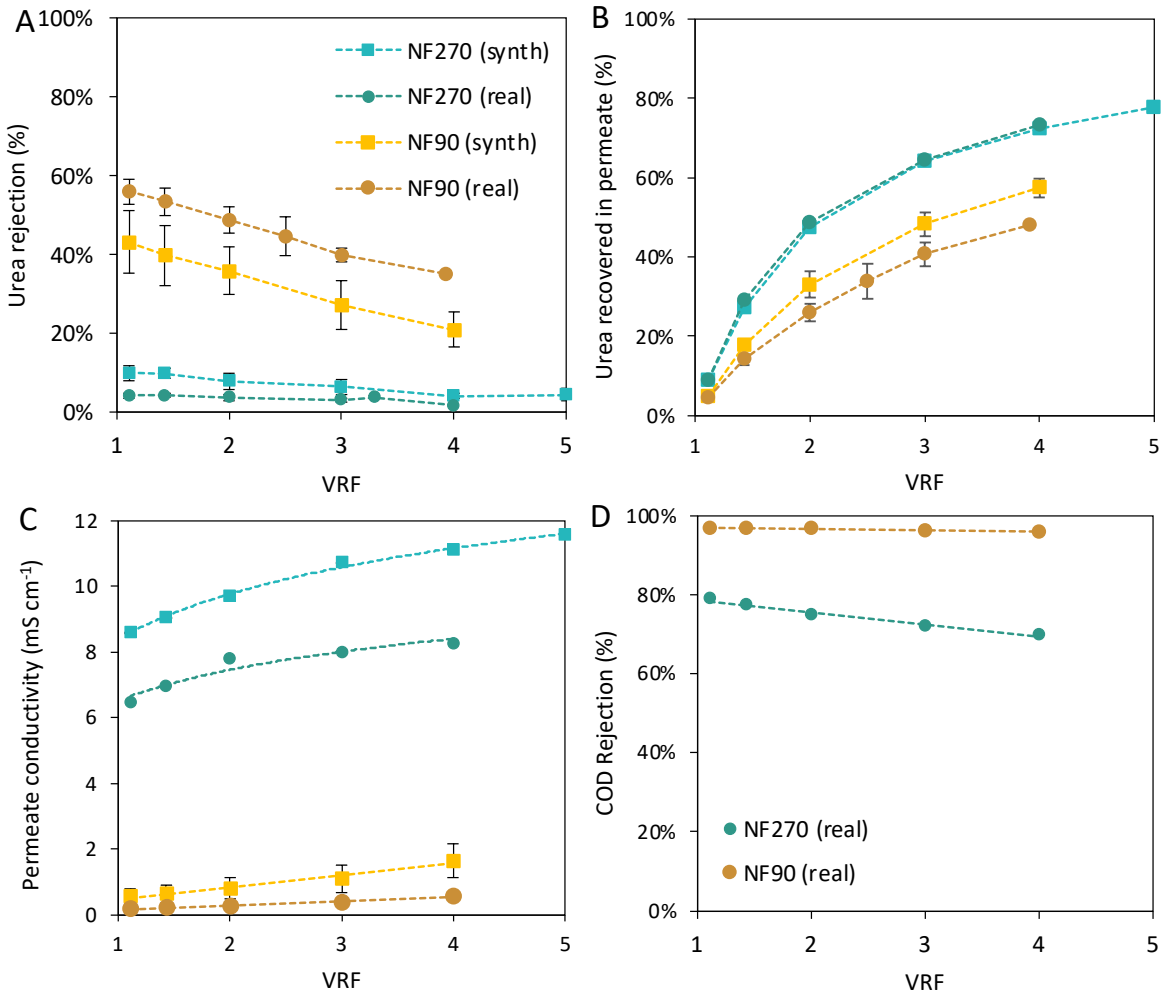

h-1 after seawater was treated with ion exchange. An ion exchange pre-treatment step should therefore be further investigated for this integrated urine treatment process.

Figure 8-2: Comparison of the NF270 and NF90 membranes, for both real and synthetic urine in terms of urea rejection (A), urea recovery in the permeate (B), total ion rejection (C), and COD rejection for real urine (D).

8.3.3 Further concentration of NF permeate using RO

Whilst NF can be used to improve the purity of urine by removing organics, undesirable salts, and PhACs, these membranes do not sufficiently reduce the volume of the stream. Further concentration using RO is therefore still required for transportation of the final product to be economically feasible. The NF90 permeate from real urine was further concentrated to a volume reduction factor of 2.5 and the urea rejection was monitored (Figure 8-3A). The VRF was limited due to the volume of permeate available and the minimum liquid volume required in the feed tank. The relationship between VRF and urea rejection was then used to predict urea recovery and purity if the permeate was concentrated beyond a VRF of 2.5 (Figure 8-3B). Rejection of urea for both real and synthetic permeate was consistent. This was expected as the majority of organics present in real urine are removed during the NF pre-treatment and can therefore no longer influence urea rejection as hypothesized by Pronk et al. (2006b). Higher urea rejection by the NF90 membrane for real urine compared to synthetic urine results in lower urea recovery in the permeate and therefore lower overall recovery as the permeate is further concentrated using SWRO. The purity of synthetic urine was also slightly higher than real urine due to

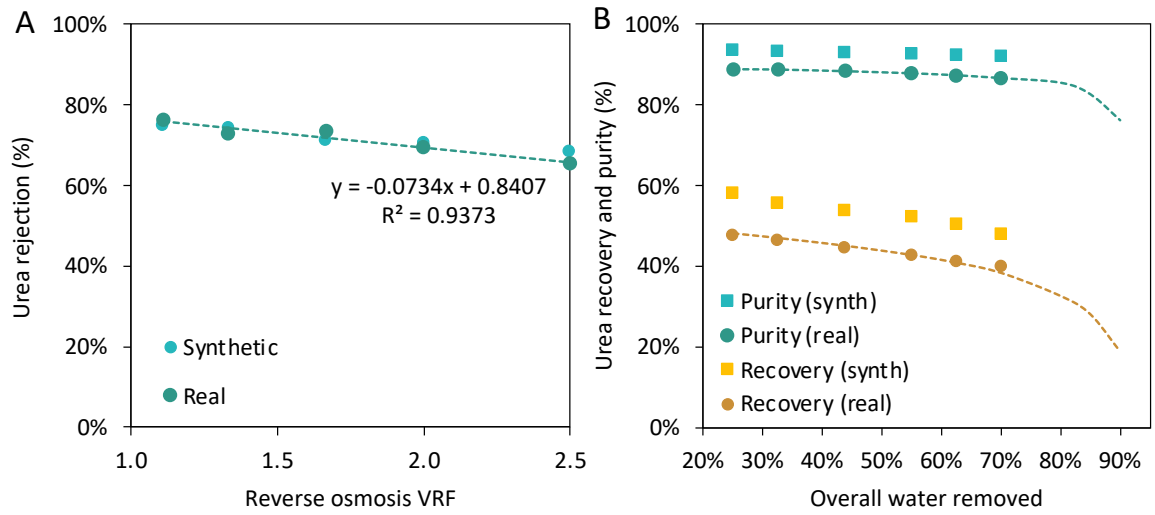

the simplified concentration of organics used in the synthetic urine recipe. It is advised that overall water removal for the hybrid NF-RO system should be limited to 80% since above this, both urea purity and recovery decrease substantially.

Figure 8-3: Concentration of NF90 permeate via SWRO, urea rejection as a function of VRF (A), predicted urea recovery and purity as overall water removal increases.

Figure 8-4 gives a summary mass balance for the tight NF-RO process with an overall volume reduction of 80%. The final concentrated liquid fertilizer would have a urea purity of 89% with an overall urea recovery of 32.7%. In comparison to a different process to recover and purify urea from urine, Marepula et al. (2021) used an evaporation and ethanol purification process and they were able to recover a dry product that contained 67% of the original urea with a purity of 76%. In addition, there is still

considerable urea in the NF concentrate stream that could also be further treated to recover more urea. As the NF brine still contains the majority of the organics, further treatment with a membrane process (forward osmosis, membrane distillation, or RO) would likely result in fouling. Further concentration with a process such as evaporation or freeze concentration would be suitable as these processes are not affected by fouling. A process such as the one developed by Marepula et al. (2021) could also be used as there is a much smaller volume of water to remove by evaporation. This would increase the overall urea recovery to 67%. A freeze concentration process, such as the one developed by (Noe-Hays et al., 2021) could also be used. Their process treated hydrolyzed urine and achieved a nitrogen recovery of 92% with a VRF of 5.8. However, ss this process treated hydrolyzed urine, it is unclear what the urea recovery would be if stabilized urine was treated with a freeze concentration process.

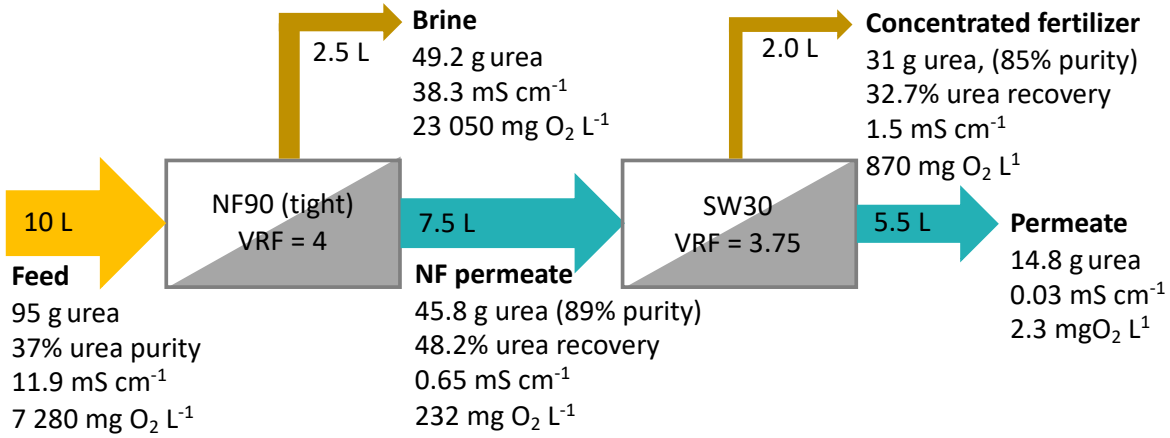

Figure 8-4: Summary mass balance for the hybrid NF90-SW30 treatment process assuming an overall water removal of 80%.

Whilst almost 68% of the urea would be lost using an NF-RO treatment process, this process cannot be directly compared to studies that investigated nutrient recovery from hydrolyzed or fresh (non-stabilized) urine as many of these previous studies did not account for N lost through ammonia volatilization during the urine collection or storage phase. An analysis of at least 10 studies using hydrolyzed urine estimated that the N losses due to volatilization could range anywhere from 0 – 44% (see Appendix E). Nitrogen loss from non-stabilized urine will vary significantly depending on collection methods (urinals/toilets with in-situ collection tanks vs. piped systems) (Udert et al., 2003a), whether collection tanks are sterilized (presence of urease-producing bacteria), storage duration, whether or not storage tanks are sealed (potential for ammonia to escape), and if the pH is adjusted (NH_3 is volatile, whilst NH_4^+ ions are not).

8.3.4 Treatment process decision tree

The optimal treatment process of urine to recover nutrients will vary depending on the desired end product and its use. A decision tree is shown in Figure 8-5 that can be used to decide which membrane treatment option to use. Whilst a treatment process with only high-pressure SWRO offers the highest urea recovery, the value and use of the product may be limited as it can only be used as a fertilizer on non-edible plants (to reduce pharmaceutical uptake concerns) with some level of salt tolerance. The final product value can be increased by recovering urea in a purer form; however, it ultimately comes at the cost of urea recovery. Although the loose NF-RO configuration provided better urea recovery (and reasonable pharmaceutical removal) compared to the tight NF-RO configuration the purity was significantly lower (56% compared to 85%). As the aim is to produce a purer urea product the additional treatment cost may not be worth the small improvement in purity. The loose NF membrane is advantageous for its higher permeate flux (Figure E-1) and it is advised that ion exchange resins be investigated to replace monovalent ions in urine with divalent ones to improve salt rejection. A detailed economic analysis would be required to determine feasibility based on the product use and value. Whilst these scenarios would still need to be tested at a pilot scale level and beyond, this study provides a proof of concept for producing different urea streams directly from stabilized urine.

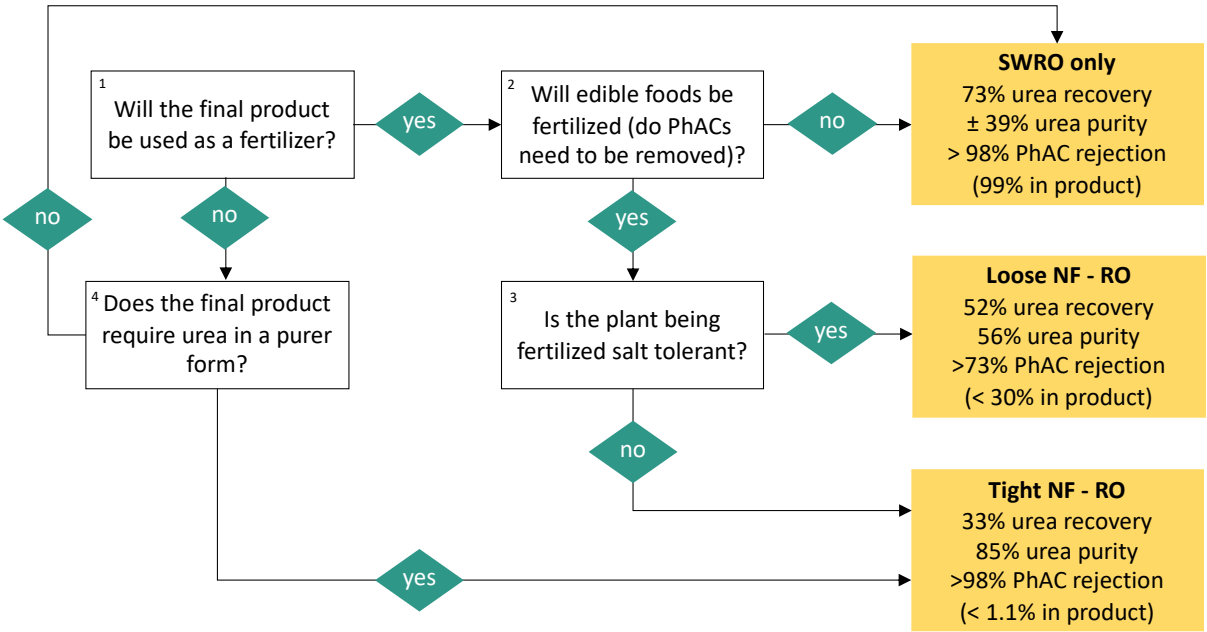

Figure 8-5: Decision tree to determine the preferred treatment process based on the desired final product. Recoveries and purities were calculated assuming all streams were treated such that for the overall process 80% of the water was removed. Results were calculated by extrapolating data from this study (NF90 and NF270) and from the RO experiments in Chapter 7. Purity was determined based on urine composition U5. Importantly, purity will vary slightly for different urine compositions. Pharmaceutical rejection by SWRO was assumed to be comparable to (if not greater than) the NF90 membrane based on similar observations by Radjenović et al. (2008).

The advantage of a hybrid NF-RO process is that it recovers urea in a purer form. Other membrane processes such as forwards osmosis (FO) and membrane distillation (MD) would also result in salts and pharmaceuticals being concentrated along with the nutrients such as with the RO process. It is also important to note that as MD operates at elevated temperatures fresh or stabilized urine would undergo chemical urea hydrolysis and therefore can't be used If the aim is to recover urea. However, NF could be used as a pre-treatment step before FO or MD to also remove salts and pharmaceuticals. It is likely that it would also optimize both processes as the fouling compounds would be removed. And in the case of FO, as the NF permeate has a lower osmotic pressure the concentration of draw solution required to achieve a defined flux would not have to be as high. Ray et al. (2020) compared the cost of ammonia recovery for RO, NF, and FO and found that FO cost 2 to 13 times more than RO and NF (depending on the treatment scenario). Whilst this comparison was for hydrolyzed urine it is likely that the comparative costs would be similar for stabilized urine

8.4 CONCLUSIONS

Both a loose (NF270) and tight (NF90) NF membrane can be used to physically remove pharmaceuticals from stabilized urine. At 75% water removal (as permeate), more than 70% (NF270) and 99% (NF90) of the pharmaceuticals would be removed and recovered in the brine stream. Urine pre-treatment with tight NF recovered 48% of the urea in the permeate (75% water removal). The NF90 pre-treatment increased the purity of the urea from 37% to 89% in the permeate, removing 90% of the organics and 96% of the ions present in the urine. Pre-treatment with a loose NF270 membrane recovered more urea in the permeate (78%) with a 75% water removal. Removal of organics and ions was limited to 78% and 44%, respectively. This resulted in a final urea purity of 56%.

The NF pre-treatment step only purifies the urea and does not significantly concentrate it. Using the NF90 membrane the total volume was only reduced by 25% and further concentration would still be required to reduce transportation costs. The permeate can be further treated with high-pressure SWRO. At an overall water removal of 80%, the urea recovery would be 32.7%. Further concentration of the loose NF permeate (to 80% overall water removal) would increase the overall urea recovery to 52% (compared to the tight NF process), however, this concentrated stream would be less pure (56% purity) and contain undesirable salts.

A decision tree was also developed that can be used to determine the optimal treatment train based on the desired product. A detailed evaluation of the final products formed is still required to determine if the increased product value gained by purification is worth the offset in overall urea lost during the purification process.

REFERENCES

BergmanBergman, R. 2007. Reverse osmosis and nanofiltration, 2nd edition, American Water Works Association, Colorado, USA.

Eyni, H., Jahangiri, M., Kiani, F. and Tahermansouri, H. 2018. Investigation of Solution pKa and Thermodynamic Values of Lamivudine and Pefloxacin Drugs by Ab initio and DFT Methods. Journal of Solution Chemistry 47(6), 1079-1095.

Ferreira, L., Sánchez-Juanes, F., González-Ávila, M., Cembrero-Fuciños, D., Herrero-Hernández, A., González-Buitrago, J.M. and Muñoz-Bellido, J.L. 2010. Direct identification of urinary tract pathogens from urine samples by matrix-assisted laser desorption ionization-time of flight mass spectrometry. Journal of clinical microbiology 48(6), 2110-2115.

Foureaux, A.F.S., Reis, E.O., Lebron, Y., Moreira, V., Santos, L.V., Amaral, M.S. and Lange, L.C. 2019. Rejection of pharmaceutical compounds from surface water by nanofiltration and reverse osmosis. Separation and Purification Technology 212, 171-179.

Hilal, N., Kochkodan, V., Al Abdulgader, H., Mandale, S. and Al-Jlil, S.A. 2015a. A combined ion exchange–nanofiltration process for water desalination: I. sulphate–chloride ion-exchange in saline solutions. Desalination 363, 44-50.

Hilal, N., Kochkodan, V., Al Abdulgader, H., Mandale, S. and Al-Jlil, S.A. 2015b. A combined ion exchange–nanofiltration process for water desalination: III. Pilot scale studies. Desalination 363, 58-63.

Hilt, E.E., McKinley, K., Pearce, M.M., Rosenfeld, A.B., Zilliox, M.J., Mueller, E.R., Brubaker, L., Gai, X., Wolfe, A.J. and Schreckenberger, P.C. 2014. Urine is not sterile: use of enhanced urine culture techniques to detect resident bacterial flora in the adult female bladder. Journal of clinical microbiology 52(3), 871-876.

Lienert, J., Bürki, T. and Escher, B.I. 2007. Reducing micropollutants with source control: substance flow analysis of 212 pharmaceuticals in faeces and urine. Water Science and Technology 56(5), 87-96.

Marepula, H., Courtney, C. and Randall, D. 2021. Urea recovery from stabilized urine using a novel ethanol evaporation and recrystallization process. Chemical Engineering Journal Advances, 100174.

Mnkeni, P.N., Kutu, F.R., Muchaonyerwa, P. and Austin, L.M. 2008. Evaluation of human urine as a source of nutrients for selected vegetables and maize under tunnel house conditions in the Eastern Cape, South Africa. Waste management & research 26(2), 132-139.

Noe-Hays, A., Homeyer, R.J., Davis, A.P. and Love, N.G. 2021. Advancing the Design and Operating Conditions for Block Freeze Concentration of Urine-Derived Fertilizer. ACS ES&T Engineering 2(3), 446-455.

Pandorf, M., Hochmuth, G. and Boyer, T.H. 2018. Human urine as a fertilizer in the cultivation of snap beans (Phaseolus vulgaris) and turnips (Brassica rapa). Journal of agricultural and food chemistry 67(1), 50-62.

Patterson, C., Anderson, A., Sinha, R., Muhammad, N. and Pearson, D. 2012. Nanofiltration membranes for removal of color and pathogens in small public drinking water sources. Journal of Environmental Engineering 138(1), 48-57.

Pronk, W., Palmquist, H., Biebow, M. and Boller, M. 2006. Nanofiltration for the separation of pharmaceuticals from nutrients in source-separated urine. Water Research 40(7), 1405-1412.

Radjenović, J., Petrović, M., Ventura, F. and Barceló, D. 2008. Rejection of pharmaceuticals in nanofiltration and reverse osmosis membrane drinking water treatment. Water Research 42(14), 3601-3610.

Ray, H., Perreault, F. and Boyer, T.H. 2020. Rejection of nitrogen species in real fresh and hydrolyzed human urine by reverse osmosis and nanofiltration. Journal of Environmental Chemical Engineering, 103993.

Schäfer, A.I. and Fane, A.G. (2021) Nanofiltration: Principles, applications, and new materials, John Wiley & Sons, New York, USA.

Thamaraiselvan, C., Michael, N. and Oren, Y. 2018. Selective separation of dyes and brine recovery from textile wastewater by nanofiltration membranes. Chemical Engineering & Technology 41(2), 185-293.

Udert, K.M., Larsen, T.A., Biebow, M. and Gujer, W. 2003. Urea hydrolysis and precipitation dynamics in a urine-collecting system. Water Research 37(11), 2571-2582.

Wishart, D.S., Guo, A., Oler, E., Wang, F., Anjum, A., Peters, H., Dizon, R., Sayeeda, Z., Tian, S. and Lee, B.L. 2022. HMDB 5.0: the Human Metabolome Database for 2022. Nucleic acids research 50(D1), D622-D631.

CHAPTER 9: EUTECTIC FREEZE CRYSTALLIZATION

CHAPTER 9: EUTECTIC FREEZE CRYSTALLIZATION

This chapter is based on Paper 5 which is currently in preparation for submission for possible publication.

9.1 INTRODUCTION

In Chapter 7 it was demonstrated that reverse osmosis (SWRO membrane, 55 bar) can remove at least 60% (although, it is hypothesized that further water removal is possible) of the water from stabilized urine pre-treated with air bubbling to remove excess calcium, recovering 85.5% of the urea and 98.5% of the potassium in the brine stream. However, urine treatment using RO alone has its limitations. If membrane fouling and scaling occur it significantly reduces RO operation efficiency (Bergman, 2007). Whilst microfiltration (Ray et al., 2022) and air bubbling (Chapter 6) pre-treatment can reduce the potential for fouling and scaling, there is a limit to their effectivity as the urine becomes more concentrated. In addition, high concentration factors are constrained by the feed pump and membrane's operating design pressure. The osmotic pressure of a feed stream increases as it is concentrated, thus resulting in a decreased driving force and permeate flux. Whilst the development of new ultra-high pressure RO membranes that can operate up to 120 bar (Dupont, 2020) may increase the feasible concentration factor, there will still be a limit to the maximum water removal. Furthermore, salts present in urine are also concentrated along with the urea and potassium ions in the RO brine stream. Fertilizer application rates would therefore require adjustment based on a crop's salt sensitivity (Mnkeni et al., 2008). A technique for further concentrating the stream, while also removing salt(s), would be beneficial and help tailor the composition of fertilizers recovered from human urine for targeted use.

Various studies investigating different forms of freeze concentration (FC) have shown promise as a urine concentration method and their results are summarized in Table 3. However, freeze concentration, like RO, concentrates salts along with fertilizer nutrients in the brine stream. Eutectic freeze crystallization (EFC) is an extension of FC and was identified as a potential method to simultaneously concentrate the urine while also precipitating out salt(s) (described in detail in Chapter 3). Furthermore, eutectic freeze crystallization is advantageous compared to RO because it is not affected by membrane scaling. In theory, complicated separation techniques to recover pure ice are not required because the salts formed during EFC can be separated by gravity. This is because salts (e.g. $Na_2SO_4 \cdot 10H_2O$ – 1.46 g cm^{-3}, (Haynes et al., 2016)) are typically denser than ice (0.92 g cm^{-3}, (Haynes et al., 2016)).

Previous studies investigating whether salts can be recovered from urine using EFC have only been theoretical and examined hydrolyzed urine (Randall and Nathoo, 2018). Proof of technical feasibility, in this case using stabilized urine that has been pre-concentrated using RO, is still required. Randall and Nathoo (2018) used a thermodynamic model to show that hydrolyzed urine would produce different salts at varying temperatures using EFC. Thermodynamic models are useful as they can be used to

predict which salts will form and at what temperatures (Lewis et al., 2010). Urine contains many organics (such as creatine, creatinine, and uric acid) which are not present in the databases of thermodynamic modelling software (OLI Systems Inc, 2022). It is therefore unclear how accurate a thermodynamic model will be for simulating real urine treatment under EFC conditions.

The overarching aim of this chapter was therefore to investigate the feasibility of using EFC to further concentrate stabilized urine that had already been concentrated using RO. The objectives of this chapter were to:

1. Thermodynamically determine how much more water needs to be removed before salts will form, the temperatures at which they form as well as the identify the salt(s) that form.
2. Compare the thermodynamic modelling results to experimental data in terms of the equilibrium ice crystallization temperature and the mass of ice formed after cooling to a fixed temperature, specifically for freeze crystallization conditions (i.e., no salt crystallization).
3. Experimentally show that salt and ice form in synthetic and real urine at eutectic conditions, determine the operating temperature range and identity of the first salt to form at these conditions.

9.2 MATERIALS AND METHODS

9.2.1 Urine collection and preparation

Urine stabilization with $Ca(OH)_2$ results in the precipitation of >98% of the phosphorus as calcium phosphate (Flanagan and Randall, 2018). Therefore, the recovery of fertilizer nutrients in this work focused on the recovery of urea (N) and potassium (K^+).

Real urine

Real urine was collected in waterless urinals pre-dosed with 10 g L^{-1} $Ca(OH)_2$. The stabilized urine was then filtered (1.2µm) and pre-treated with air bubbling as per the method described in Section D.1. The pre-treated urine was then concentrated via RO using the same method given in Chapter 8. A SW30 FilmTec membrane operating at 55 bar was used to achieve a volume reduction factor of 3.33 (70% water removal). The water removal was limited at 70% due to the increase in the urine's osmotic pressure as it was concentrated, resulting in a decrease in driving force for the permeate flux. At a VRF of 3.33, the permeate flux was 30% of the initial flux. The collected RO brine was then used in the real urine EFC experiments. A detailed composition of the real urine is available in Table F-6.

Synthetic urine

The generic synthetic urine recipe, described in Chapter 3, was used for this work. The recipe was adjusted to mimic a 70% water removal using RO. This was achieved by extrapolating the rejection rates as a function of the concentration factor achieved in Chapter 7 for air bubbled urine. A detailed method for the development of the synthetic urine recipe is available in Appendix F along with the recipes for each synthetic urine composition (Table F-1).

9.2.2 Thermodynamic modeling

The thermodynamic software OLI stream analyzer (OLI Systems Inc, 2022) was used to model the RO urine brine after 70% water removal (as this was the water removal achieved with real urine). The model was used to determine the temperature at which the first ice crystal formed, the mass of ice formed before any salts crystallized, the type of salts that formed, the temperature at which each salt formed, and the total mass of salts formed at a given temperature. The model was then used to inform the experimental method and operating temperature set point.

9.2.3 Experimental setup and methods

Experiments were conducted in jacketed glass crystallizers (GlassChem, South Africa) of varying sizes (500, 1000, and 2000 mL). The crystallizers were insulated with bubble wrap, and the temperature was controlled using a chiller (Proline RP855, Lauda, Germany) and circulating Kry40 coolant. To prevent ice formation on the inner walls of the crystallizers, the liquid was mixed with an overhead stirrer at 200 rpm. The solution temperature was continually monitored with a PT-100 temperature probe and data logger (176 T4, Testo, Lenzkirch). A cascading EFC process as described by Randall et al. (2011) was used to reach EFC conditions. The ice product was filtered using a Buchner funnel connected to a 1 L filtration flask. The ice collected was then immediately weight before it began melting. A portion of the ice (40g) was separately washed with de-ionized water (40g) that was pre-cooled to 4°C. Each stage involved cooling the liquid to a fixed temperature and holding the solution at that fixed temperature for 30 minutes. The liquid was then cooled at a fixed cooling rate (CR) until the desired end liquid temperature was reached. During the EFC experiments, samples of the liquid were taken and filtered at different temperatures throughout the cooling process. For the EFC experiments, ice seeds were added at -10.25°C for synthetic urine and -9.4°C for real urine. Approximately 0.1to 0.15 g of Na_2SO_4 (>97% purity, Merck, Germany) was added as the salt seed at -10.5°C. The anhydrous form of Na_2SO_4 was used for seeding as $Na_2SO_4 \cdot 10H_2O$ is thermally unstable and the waters of hydration quickly evaporate (Reddy et al., 2010). All experiments were conducted in triplicate with synthetic urine and then validated once with real urine.

9.3 RESULTS AND DISCUSSION

9.3.1 Thermodynamic model

A thermodynamic model was used to determine the operating conditions required to achieve eutectic conditions by assessing if and how much more water needs to be removed before salts will form, the temperatures at which they form as well as the identify the salt(s) that form. Figure 9-1 shows the mass percent of ice and mass of salt formed as urine (70% pre-concentration with RO) is cooled from 0 to -50°C for the generic synthetic urine composition (Figure 9-1A) and the real urine composition (Figure 9-1B). The model showed that both urine composition were not near eutectic conditions and further water removal as ice after RO would be required before salts would crystallize. For the synthetic urine composition, an additional 68% water removal (90% overall water removal) would be required and for the real urine composition, an additional 65% water removal (89% overall water removal) would be required before salt crystallization would occur. For both urine compositions, the first salt predicted to crystallize was $Na_2SO_4 \cdot 10H_2O$, which would be beneficial to remove as not all plants have a high Na^+ tolerance (Mnkeni et al., 2008).

The synthetic and real urine compositions include the same group of ions but in varying concentrations. Both compositions have similar ice crystallization temperatures (-2.93 vs. -2.96°C) and will form the same types of salts. However, the temperatures at which each salt forms and the amount of salt that can form differ slightly. For the synthetic urine composition, KCl and urea crystallize at -25 and -29.2°C respectively, whereas for the real urine composition KCl and urea crystallize much closer together at -27.2 and -27.6°C respectively. Varying urine compositions and the choice of operating temperatures would therefore require consideration when designing a full-scale EFC system.

Whilst a multi-stage EFC system could be employed to recover KCl, and then urea (in each stage for the synthetic composition), the salts formed would not be pure. The KCl would be contaminated with $Na_2SO_4 \cdot 10H_2O$ and in stage two, urea would be contaminated with both $Na_2SO_4 \cdot 10H_2O$ and KCl. However, Randall et al. (2009) showed that selective salt seeding could be used to promote the crystallization of only one salt, provided operation occurred within the meta-stable zone width. Theoretically, operating the system at eutectic conditions of -25°C would produce 8.73 g of $Na_2SO_4 \cdot 10H_2O$ from 1 L of urine pre-concentrated with RO (assuming a generic synthetic urine composition). This would remove 15.7% of the Na^+ ions and 82.8% of the SO_4^{2-} ions. Removal percent would vary based on initial urine composition.

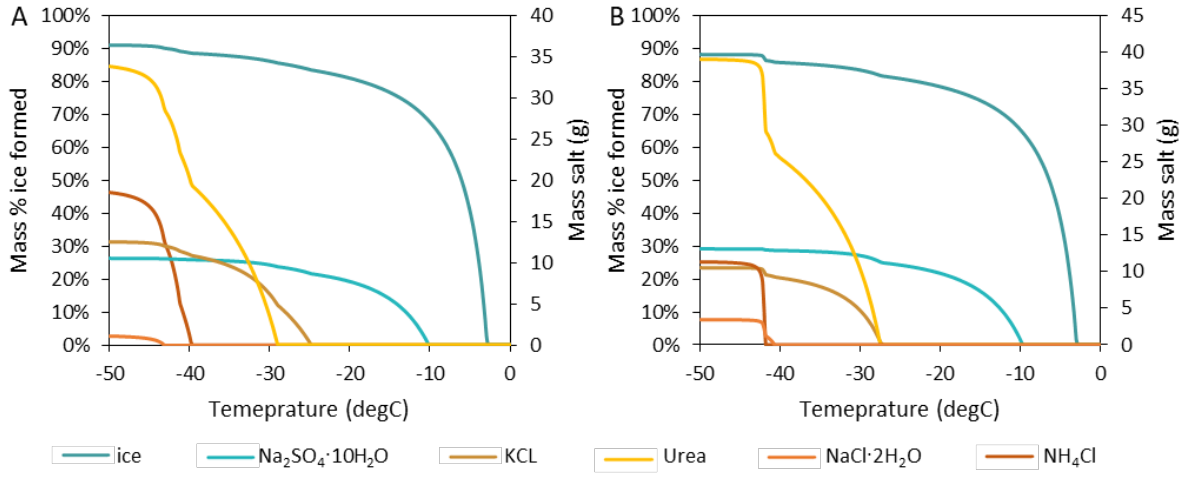

Figure 9-1: Mass % of ice formed, and mass of salt formed when freezing urine that has been pre-concentrated (70% water removal) using RO. The model was based on the generic synthetic urine composition (A), and the composition of the real urine used in this study (B).

9.3.2 Comparison of thermodynamic modelling results and experimental data

Figure 9-2 compares the modelled and experimental results for the ice equilibrium temperature (IET) and mass % of ice formed for synthetic and real urine. The model provides a good prediction of IET for both synthetic and real urine despite the model not accounting for many of the organics present in real urine. However, the accuracy of the IET prediction decreases as the solution becomes more concentrated. For example, for FC1 there is only a 0.02°C difference between the predicted and measured IET while this difference increases to 0.45 °C for EFC conditions.

The mass % of ice recovered for both synthetic and real urine was also greater than the predicted values with up to a 10% difference for synthetic urine and 5% for real urine. This likely occurred for two reasons. Firstly, when the ice slurry is filtered, a small amount of liquid remains entrapped within the ice increasing the measured ice mass. Secondly, the model predicts perfect ice separation, whereas in practice small concentrations of the solute are trapped in the ice as it freezes. This means that at a fixed temperature the liquid is marginally less concentrated than predicted by the model, which allows more ice to form at the respective temperature. A mass balance (in Appendix F) showed that the percentage of impurities in the ice varied but increased when the mass % of ice removed increased and when the feed became more concentrated (Figure F-3A). Commercial freeze concentrators would remove impurities and entrapped liquid from the ice using washing columns and recycle streams (van der Ham et al., 2004). Randall et al. (2011) showed that solute concentrations in ice decreased by a factor of up to 10 after one washing cycle. Figure F-3B in the appendices shows that after washing the concentration of impurities in the ice decreased by a factor of 8 to 20. In general, the experimental data matched the results predicted by the thermodynamic model.

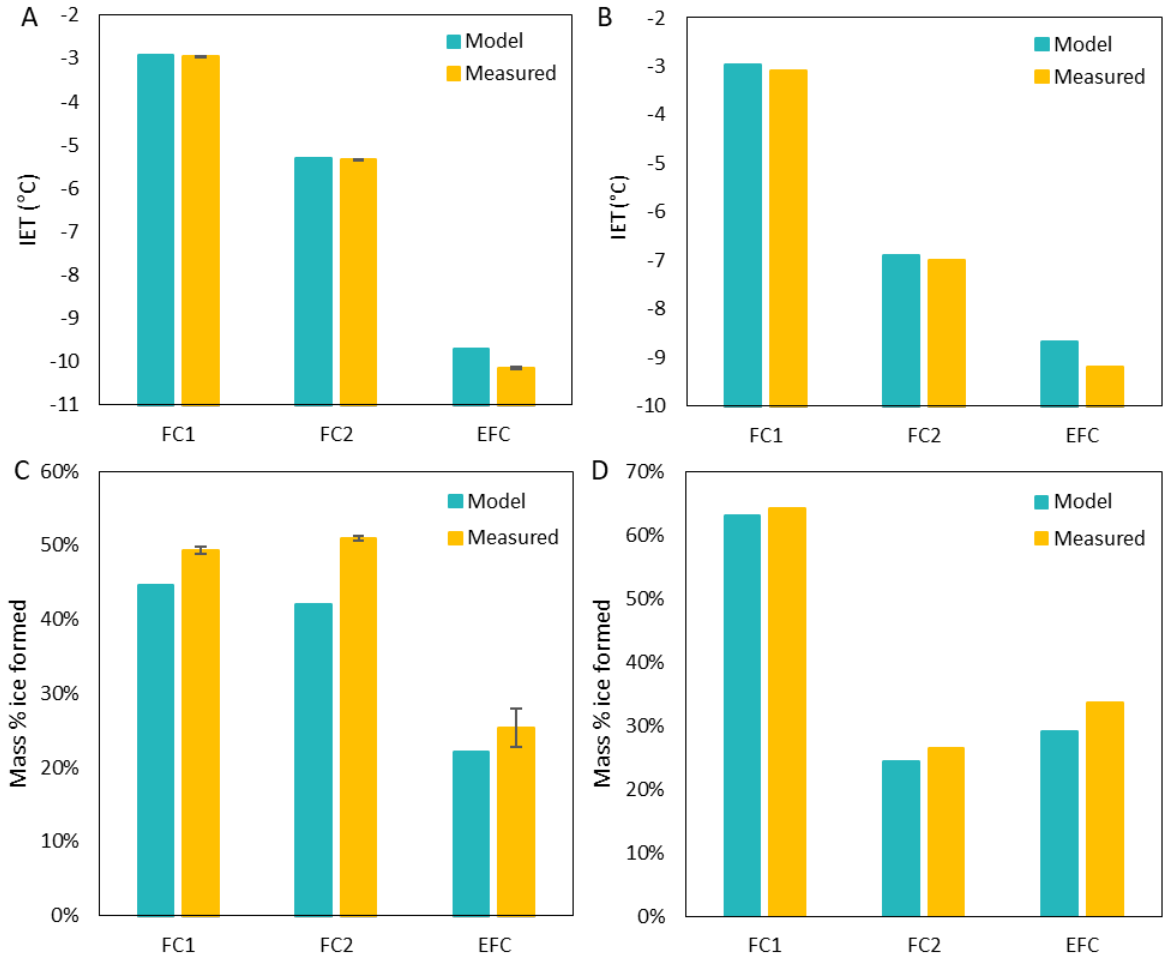

Figure 9-2: Comparison of the predicted and measured ice equilibrium temperature for the generic synthetic and real urine compositions (A, B) and the mass % ice formed at the set operating temperature versus the measured % of ice (C, D) for generic synthetic (A, B) and real urine (C, D) compositions.

9.3.3 Salt precipitation at eutectic conditions for synthetic and real urine

Figure 9-3 shows the anion (SO_4^{2-} and Cl^-) and cation (Ca^{2+} and Na^+) concentrations in the liquid as a function of temperature during ice and salt crystallization for synthetic and real urine. Ice seeds were added at -10.25°C for synthetic urine and -9.4°C for real urine. Salts seeds were added at -10.5°C for both synthetic and real urine. The first salt predicted to form by the thermodynamic model was $Na_2SO_4 \cdot 10H_2O$. Chloride (Cl^{-1}) and calcium (Ca^{2+}) ions were measured as spectator ions for comparison. For both the synthetic and real urine, the Cl^{-1} and Ca^{2+} concentrations remained constant before ice crystallization and then increased as ice formed, and the solution became more concentrated. The concentration continued to increase even after the Na_2SO_4 salt seed was added. The sulfate ion concentration for both synthetic and real urine was constant before ice crystallization. The concentration increased after ice crystallization but decreased after the salt seed was added. This indicates that a salt (containing SO_4^{2-}) had begun to crystallize. The Na^+ ion concentration remained constant before ice

crystallization, and then began to increase after ice crystallization and a salt seed was added. However, if the Na^+ and Ca^{2+} ion concentration at -10.5°C is compared to the concentration at -12.5°C, the Na^+ ion concentration only increased by 2.7% while the Ca^{2+} ion concentration increased by 11.4% (for real urine). A similar trend was observed in the synthetic urine experiment. This suggests that a sodium-based salt was also crystallizing. The model predicted that salt would first form at -9.82°C (synthetic urine composition) and -9.65°C (real urine composition), however, salt formation was only observed after a salt seed was added at -10.5 °C. This experimental method confirms that eutectic conditions were reached and that a salt crystallized, however, it does not confirm the exact eutectic temperature of the system and only indicates a range.

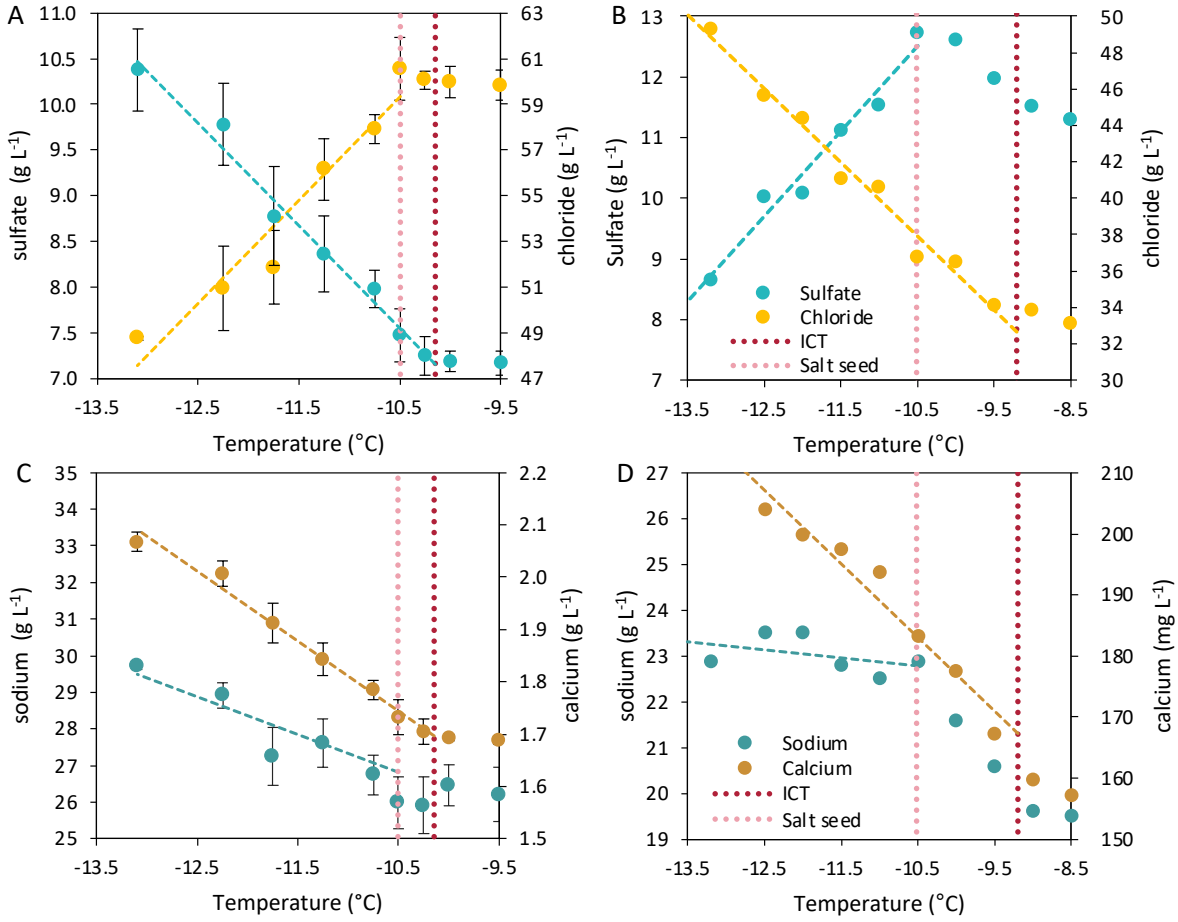

Figure 9-3: Anion (A,B) and cation (C,D) concentrations as a function of temperature for synthetic (A, C) and real (B, D) urine. Ice and salt seeds were added to ensure consistent ice and salt crystallization.

After the liquid temperature reached -13.2°C the stirrer was turned off to allow the ice and salt to separate by gravity. The ice and salt were then recovered separately. For the real urine experiments, more ice formed than anticipated and it filled the entire crystallizer. This meant that gravity separation

could not be used and the salt that crystallized remained trapped in the ice during filtration. Analysis of the salts recovered from the synthetic urine showed that of the 610 mg L^{-1} dissolved; 405 mg L^{-1} was SO_4^{2-} and 191 mg L^{-1} was Na^+. This accounts for 97.7% of the mass of salt dissolved. The model predicted that $Na_2SO_4 \cdot 10H_2O$ would form, however, analysis of the salt indicated no waters of hydration. $Na_2SO_4 \cdot 10H_2O$ is thermally unstable and has a melting point of 32.1°C (Haynes et al., 2016) and therefore during drying the waters of hydration will evaporate (Hamilton and Menzies, 2010). Previously, both Reddy et al. (2010) and (Randall et al., 2011) confirmed that Na_2SO_4 with 10 waters of hydration does crystallize under EFC conditions and they showed that the mass lost during drying accounted for 10 waters of hydration. The small concentrations of other ions measured are likely due to liquid entrapment during the filtration of the salt. Figure 9-4A shows the mass % of various ions recovered in the ice (the measured concentrations are available in Appendix F). More Na^+ and SO_4^{2-} were recovered in the ice than other ions, indicating the presence of $Na_2SO_4 \cdot 10H_2O$ in the ice as a result of salt entrapment because of inefficient separation (Reddy et al., 2009). The moles of Na^+ and SO_4^{2-} ions in the ice are also equal (Figure 9-4B), which further indicates the crystallization of $Na_2SO_4 \cdot 10H_2O$.

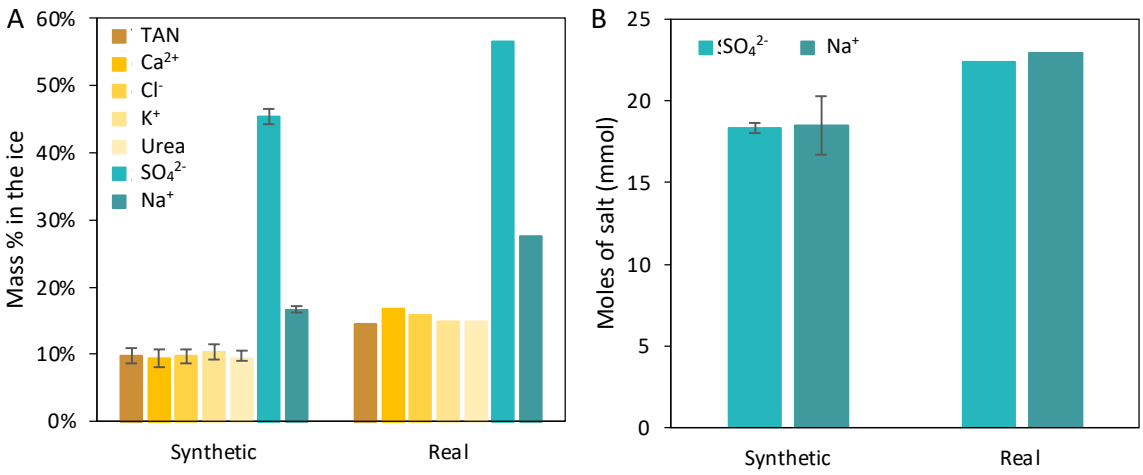

Figure 9-4: Mass % of various ions in the ice after EFC and filtration (A) and the moles of Na^+ and SO_4^{2-} ions in the ice after EFC and filtration (B). Real urine results do not have error bar as only synthetic urine experiments were conducted in triplicate because the composition of real urine is never the same.

After the set temperature was reached the stirrer speed was reduced to gently agitate the salt-ice mixture and assist with separation as advised by Reddy et al. (2009). However, poor salt-ice separation occurred, and in the case of the real urine, no salt-ice separation occurred. Poor separation can occur for multiple reasons. If too much ice has formed there will be no distinct region between the ice and the liquid to allow the salt to settle into. Reddy et al. (2009) advise that during EFC conditions the total ice volume should only be 30% of the reactor volume. During the filtration process if there is no distinct ice and liquid layer the settled salt may accidentally become re-mixed with the ice as it is removed. Good separation also requires controlling crystal size as large particles fall more freely whilst fine powders

tend to stick (Myerson, 2002). Vaessen et al. (2003) advised that residence time should be controlled for optimal crystal growth. In this current work, the fast-cooling rate of ± 2°C hr^{-1} may have promoted fine salt crystals rather than large crystals, making gravitational separation difficult. However, the objective of this research was to confirm the precipitation of a salt at eutectic conditions rather than optimize the salt-ice separation.

9.3.4 Optimizing nutrient recovery

The aim of this research was to show experimentally that salt will crystallize in urine at eutectic conditions. In the freezing stages, before eutectic conditions were reached, as much as 24% of the ions were recovered in the ice. This ice was not further treated, however, industrial EFC systems are designed to include wash columns and recycle streams to reduce the concentration of impurities in the ice (van der Ham et al., 2004). Without ice washing and recycling the overall urea recovery after RO, FC, and EFC for real urine was only 49%. The EFC experiments were conducted at a temperature of -13.2°C, whereas full-scale operation to maximize $Na_2SO_4 \cdot 10H_2O$ recovery would be conducted at approximately -27°C (the temperature at which next salt begins to form (Figure 9-1B)) and an overall water recovery of 95% based on the real urine composition (Figure 9-1B) b. A Theoretical mass balance (based on a real urine composition) was conducted to determine a more realistic recovery rate for urea and K^+ ions. Figure 9-5 shows the process flow diagram used for the theoretical mass balance including recoveries and stream concentrations. A detailed summary of the assumptions used for the mass balance is given in Appendix G (Table G-2).

The mass balance showed that by including washing and a recycle stream, the urea recovery would increase from 49 to 77%, with 96% K^+ recovery. The final brine (liquid fertilizer) would contain 309 g L^{-1} urea and 43.5 g L^{-1} K^+ (11.5% N, 3.5% K by weight). Approximately 3.5 kg of $Na_2SO_4 \cdot 10H_2O$ salt would be recovered from 1 m^3 of fresh, untreated urine, representing a 24.9% Na^+ and 87.3% SO_4^{2-} ion removal. The removal of $Na_2SO_4 \cdot 10H_2O$ during EFC would result in an end product with 3.05 wt% Na^+, which is lower than using an alkaline dehydration process, where the final product would contain 4.6 wt% Na^+ (Simha et al., 2020a). The permeate and ice streams combined contain approximately 4 g L^{-1} of urea, which would not be suitable to be used as drinking water. However, this stream could be used for non-potable purposes such as watering plants, cleaning, and flushing toilets. The concentration of urea means that the permeate would provide some fertilization properties, however, since the stream is even more dilute than urine, it would not be feasible to sell as a commercial fertilizer because of the low N content. Whilst it is possible to treat the stream further using RO, it is unlikely that this would be cost-effective since the main contaminant of the water is urea and this cannot be perfectly removed using RO (see Chapter 7). The energy requirements for the process are analyzed in Chapter 10.

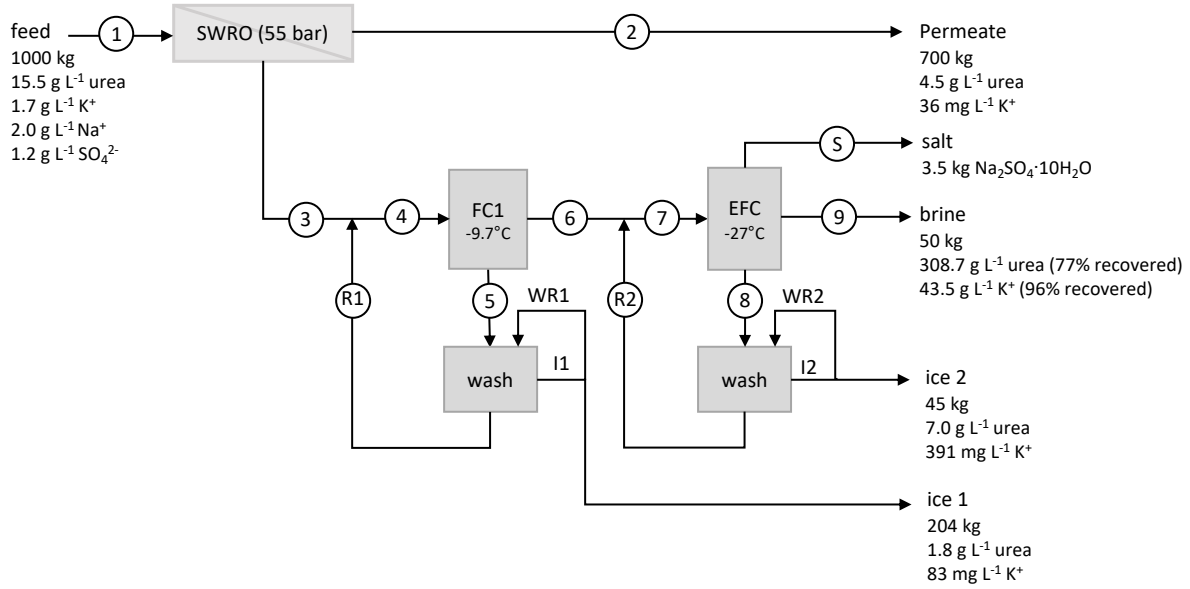

Figure 9-5: Process flow diagram for a mass balance assuming the ice recovered was purified in a washing column that uses a portion of the melted purified ice as a wash-liquor. The basis was 1000 kg of urine (based on the real urine composition). Operating temperatures are estimations based on the thermodynamic model predictions.

9.3.5 Final liquid fertilizer comparison to commercial fertilizers

Figure 9-6 compares the N and K composition of the product streams from various urine concentration technologies (with varying water removals) to four commercially available liquid fertilizers with similar N-content. Phosphorus content was excluded from this analysis as some treatment methods recover P separately as calcium phosphate (RO, RO-FC, RO-EFC, NF-RO) during the collection phase, other methods partially recover P as struvite (ND), and with other methods, the P is recovered in the liquid product (FC) and solid product (AD). It is therefore difficult to make an equivalent comparison. The final fertilizer compositions were determined using an initial composition of 15.5 g-urea L^{-1} and 1.7 g-K L^{-1}. As the input urine composition for the ND fertilizer is unknown, the final product composition could not be adjusted to an equivalent input. The urine concentration technologies include: RO only (70% water removal), RO followed by FC (no salt formation, calculated theoretically) with an overall water removal of 80% (calculated theoretically), multi-stage block FC with recycles (Noe-Hays et al., 2021), RO followed by FC and EFC (calculated theoretically), nitrification and distillation (ND) (Udert and Wächter, 2012), and alkaline dehydration (AD). Alkaline dehydration has been investigated using a variety of substrates and operating temperatures and each variation in method results in a different N-recovery and a product with a slightly different nutrient composition (Simha et al., 2021; Simha et al., 2020a; Simha et al., 2020b; Vasiljev et al., 2022). The nutrient content for AD reported in Figure 9-6 is the average from the four studies.

An RO-EFC (11.5% N, 3.5% K) process and AD (10.5% N, 1.5% P, 4.2% K-average composition) produce the products with the highest nitrogen content composition. The dry fertilizer product produced by Simha et al. (2020a) has a higher K content because the drying medium contained K. Fertilizer application rates are based on kg of nutrient per area rather than fixed masses of fertilizer. Freeze concentration (3.9% N, 0.5% P, 0.9% K) (Noe-Hays et al., 2021) and ND (4.2% N, 0.2% P, 1.5% K) (VUNA GmbH, 2020) had a product with a similar nutrients content. It was expected that the nutrient content of fertilizer made using RO (< 70% water removal) or NF-RO (low N recovery) would be too low and further concentration would be required to increase the nutrient content to that comparable with commercially available fertilizers. However, a comparable commercial fertilizer could be found for each of the fertilizers produced from the different treatment methods. The context of fertilizer use is also important, fertilizers with lower nutrient content would need to be applied in larger volumes to meet required nutrient application rates. This is further investigated in the economic analysis of Chapter 10.

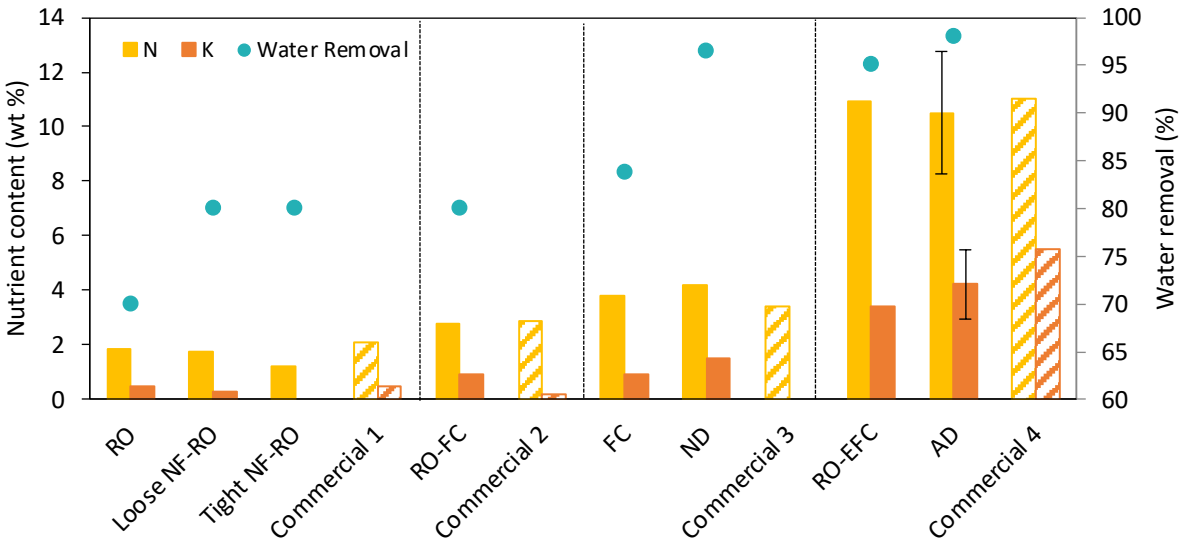

Figure 9-6: Nitrogen and potassium content (weight %), and water removal (%) of the different fertilizers produced using different treatment methods compared to commercially available liquid fertilizers with comparable nitrogen content. Commercial 1 (Protek, 2022), commercial 2 (Rolfes Agri, 2022b), commercial 3 (Rolfes Agri, 2022a), commercial 4 (Bonsai Tree, 2022). Fertilizer compositions reported in literature include freeze concentration (FC) (Noe-Hays et al., 2021), nitrification and distillation (ND) (VUNA GmbH, 2020), and alkaline dehydration (Simha et al., 2020a).

9.4 CONCLUSIONS

This research showed for the first time that it is possible to use EFC to further concentrate human urine after pre-concentration with RO. Urine pre-concentrated with RO (70% water removal) was thermodynamically modelled and the model predicted that $Na_2SO_4 \cdot 10H_2O$ would be the first salt to crystallize at EFC conditions (-9.8°C). However, a further 68% water removal would be required before

reaching EFC conditions. Using EFC to further concentrate urine would remove 82.8% of the SO_4^{2-} ions and 15.7% of the Na^+ ions from the solution, resulting in an overall water removal of 95% and a more concentrated liquid fertilizer product (for the generic synthetic urine composition).

A comparison of the experimental and modelled results showed that the model was able to accurately predict the ice formation temperature (< 0.5°C difference), however, it was less accurate at predicting the mass of ice formed (±10% difference) due to the presence of entrapped liquid and imperfect ice separation. The thermodynamic model was accurate in predicting the ice crystallization temperature, water removal required before salt formation, and the type of salt that will precipitate, which can then be used to design an EFC process.

To confirm that $Na_2SO_4 \cdot 10H_2O$ was crystallizing at eutectic conditions, the concentration of Ca^{2+}, Cl^-, Na^+, and SO_4^{2-} was measured as the solution temperature was incrementally decreased. The concentration of Na^+ and SO_4^{2-} in the liquid decreased after a Na_2SO_4 salt seed was added at -10.5°C, whilst the concentration of Ca^{2+} and Cl^{-1} continued to increase. This indicated that eutectic conditions had been reached for ice-$Na_2SO_4 \cdot H_2O$. Whilst the model predicted that salt would crystallize at -9.82°C (generic synthetic urine composition) and -9.65°C (real urine composition), this did not occur, and Na_2SO_4 seeds needed to be added to induce salt crystallization. It was therefore only possible to determine a eutectic temperature range, which was between the ice crystallization temperature (-10.15°C for synthetic and -9.19°C for real urine) and the ice seeding temperature (-10.5°C).

A theoretical mass balance of RO followed by FC and EFC for stabilized urine concentration, including ice washing and recycle streams, was conducted with a 95% water removal (by mass). The overall urea and K^+ recovery was calculated to be 77% and 96%, respectively. Over 98% of the phosphorus would be recovered as calcium phosphate during the urine stabilization step. The final liquid fertilizer would have a urea concentration of 304g L^{-1} and 42.8 g L^{-1} K^+ (11.5% N, 3.5% K) and 3.5 kg of $Na_2SO_4 \cdot 10H_2O$ could theoretically be recovered from 1000 kg of urine. The urea and K^+ concentration in the liquid fertilizer product stream is comparable to commercially available all-purpose liquid fertilizers.

REFERENCES

Bergman, R. 2007. Reverse osmosis and nanofiltration, 2nd edition, American Water Works Association, Colorado, USA.

Bonsai Tree. 2022. Hortisol 200 mL [Online]. Available: https://www.bonsaitree.co.za/products/hortisol-200ml [Accessed 25 August 2022].

Dupont. 2020. DuPont™ XUS180808 Reverse Osmosis Element: Product Data Sheet [Online]. Dupont. Available: https://www.dupont.com/content/dam/dupont/amer/us/en/water-solutions/public/documents/en/45-D01736-en.pdf [Accessed 15/09/2021].

Flanagan, C.P. and Randall, D.G. 2018. Development of a novel nutrient recovery urinal for on-site fertilizer production. Journal of Environmental Chemical Engineering 6(5), 6344-6350.

Hamilton, A. and Menzies, R.I. 2010. Raman spectra of mirabilite, Na2SO4· 10H2O and the rediscovered metastable heptahydrate, Na2SO4· 7H2O. Journal of Raman Spectroscopy 41(9), 1014-1020.

Haynes, W.M., Lide, D.R. and Bruno, T.J. 2016. CRC handbook of chemistry and physics, 95th edition, CRC Press, Florida, USA.

Lewis, A.E., Nathoo, J., Thomsen, K., Kramer, H., Witkamp, G., Reddy, S. and Randall, D.G. 2010. Design of a Eutectic Freeze Crystallization process for multicomponent waste water stream. Chemical Engineering Research and Design 88(9), 1290-1296.

Mnkeni, P.N., Kutu, F.R., Muchaonyerwa, P. and Austin, L.M. 2008. Evaluation of human urine as a source of nutrients for selected vegetables and maize under tunnel house conditions in the Eastern Cape, South Africa. Waste management & research 26(2), 132-139.

Myerson, A. 2002. Handbook of industrial crystallization, Butterworth-Heinemann.

Noe-Hays, A., Homeyer, R.J., Davis, A.P. and Love, N.G. 2021. Advancing the Design and Operating Conditions for Block Freeze Concentration of Urine-Derived Fertilizer. ACS ES&T Engineering 2(3), 446-455.

OLI Systems Inc. 2022. OLI Stream Analyzer, version 11.0, OLI Systems Inc, New Jersey, USA.

Protek. 2022. Product Catalogue [Online]. Available: https://www.proteksa.co.za/Protek-Product-Catalogue-EN.pdf [Accessed 25 August 2022].

Randall, D., Nathoo, J. and Lewis, A. 2009 Seeding for selective salt recovery during eutectic freeze crystallization, pp. 639-646, Pretoria, South Africa.

Randall, D., Nathoo, J. and Lewis, A. 2011. A case study for treating a reverse osmosis brine using Eutectic Freeze Crystallization—Approaching a zero waste process. Desalination 266(1-3), 256-262.

Randall, D.G. and Nathoo, J. 2018. Resource recovery by freezing: A thermodynamic comparison between a reverse osmosis brine, seawater and stored urine. Journal of Water Process Engineering 26, 242-249.

Ray, H., Perreault, F. and Boyer, T. 2022. Ammonia recovery and fouling mitigation of hydrolyzed human urine treated by nanofiltration and reverse osmosis. Environmental Science: Water Research & Technology 8(2), 429-442.

Reddy, S., Kramer, H., Lewis, A. and Nathoo, J. 2009. Investigating factors that affect separation in a eutectic freeze crystallisation process. International Mine Water Conference, Document Transformation Technologies. Pretoria, South Africa, 19-23 October. 649-655.

Reddy, S., Lewis, A., Witkamp, G., Kramer, H. and Van Spronsen, J. 2010. Recovery of Na2SO4· 10H2O from a reverse osmosis retentate by eutectic freeze crystallisation technology. Chemical engineering research and design 88(9), 1153-1157.

Rolfes Agri. 2022a. CARBology Induce [Online]. Available: https://rolfesagri.co.za/wp-content/uploads/2021/02/Carbology-induce.pdf [Accessed 25 August 2022].

Rolfes Agri. 2022b. Ocean Plus [Online]. Available: https://rolfesagri.co.za/wp-content/uploads/2021/02/Ocean_Plus_New-Inteligro-Label.pdf [Accessed 25 August 2022].

Simha, P., Friedrich, C., Randall, D.G. and Vinnerås, B. 2021. Alkaline dehydration of human urine collected in source-separated sanitation systems using Magnesium Oxide. Frontiers in Environmental Science 8, 9.

Simha, P., Karlsson, C., Viskari, E.-L., Malila, R. and Vinnerås, B. 2020a. Field testing a pilot-scale system for alkaline dehydration of source-separated human urine: a case study in Finland. Frontiers in Environmental Science 8, 168-178.

Simha, P., Lalander, C., Nordin, A. and Vinnerås, B. 2020b. Alkaline dehydration of source-separated fresh human urine: Preliminary insights into using different dehydration temperature and media. Science of the Total Environment 733, 139313.

Udert, K.M. and Wächter, M. 2012. Complete nutrient recovery from source-separated urine by nitrification and distillation. Water Research 46(2), 453-464.

Vaessen, R., Seckler, M. and Witkamp, G.J. 2003. Eutectic freeze crystallization with an aqueous KNO3− HNO3 solution in a 100-L cooled-disk column crystallizer. Industrial & engineering chemistry research 42(20), 4874-4880.

van der Ham, F., Seckler, M.M. and Witkamp, G.J. 2004. Eutectic freeze crystallization in a new apparatus: the cooled disk column crystallizer. Chemical Engineering and Processing: Process Intensification 43(2), 161-167.

Vasiljev, A., Simha, P., Demisse, N., Karlsson, C., Randall, D.G. and Vinnerås, B. 2022. Drying fresh human urine in magnesium-doped alkaline substrates: Capture of free ammonia, inhibition of enzymatic urea hydrolysis & minimisation of chemical urea hydrolysis. Chemical Engineering Journal 428, 131026.

VUNA GmbH. 2020. Aurin Recycled Fertilizer [Online]. Available: https://vuna.ch/en/aurin-recycling-dunger/ [Accessed 21 August 2022].

CHAPTER 10: ECONOMIC ANALYSIS

CHAPTER 10: ECONOMIC ANALYSIS

10.1 INTRODUCTION

Reverse osmosis (RO) was identified as a promising urine concentration technology. In Chapter 5 and Chapter 6 two different pre-treatment methods (chemical addition and aeration) were investigated. Both methods successfully reduced Ca^{2+} ion concentrations by more than 95%. In Chapter 7, RO was used to concentrate acid and base (pre-treated) stabilized urine. During acid stabilization, the formation of uric acid dihydrate (UAD) crystals and an organic compound was observed. All urine was pre-treated with microfiltration (MF) before RO. During MF of the acid stabilized urine, the filter paper became blocked with organic compounds and UAD crystals. Significant scaling of the RO membrane also occurred during operation. Whilst high urea recovery was achieved using RO, it was determined that acid stabilization is not a suitable stabilization method if the urine is to be concentrated using RO. Aeration and chemical addition as pre-treatment methods were found to be equally effective, however, aeration was chosen as the preferred pre-treatment method as this method does not add additional ions (Na^{+}), it reduces the urine pH to within the operating range of most common RO membranes, and it would also sequester CO_2 from the atmosphere and partially offset CO_2 produced during traditional $Ca(OH)_2$ production (Ellis et al., 2020).

Nanofiltration (NF) treatment prior to RO was investigated as a method to produce a purer product by removing pharmaceuticals and salts from urine. Both loose and tight NF membranes were investigated. Loose NF membranes could remove pharmaceuticals but had limited efficiency with salt removal. Whilst the tight NF membrane effectively removed both pharmaceuticals and salts and produced a purer urea stream, the recovery of urea was lower. The maximum water removal achievable with RO is limited by osmotic pressures and therefore further concentrating using eutectic freeze crystallization (EFC) was investigated as this method can simultaneously remove salts and water. Even after RO treatment, additional water needs to be removed to reach eutectic conditions where both ice and salt can crystallize. This can be achieved using freeze concentration, in which only ice crystallizes (Randall and Nathoo, 2015).

Figure 10-1summarizes the different treatment options tested in this study. Each method would result in a different water removal and final composition. The fertilizer products produced will therefore have different values in different markets and the cost for each treatment process will also differ in terms of operating and capital costs. Chipako and Randall (2020a) investigated the feasibility and logistics of a decentralized urine treatment and resource recovery system. However, the urine treatment system modelled was theoretical and the technical feasibility of operation had not yet been proven experimentally. This research investigated a variety of treatment options and, whilst all proved technically feasible, the economic feasibility of the different treatment methods needs to also be considered. For example, whilst NF pre-treatment prior to RO might recover urea in a purer form (without undesirable salts and pharmaceuticals) the decrease in urea recovery and additional capital and

operational costs may not be economically feasible. Currently, the different treatment options exist only at a laboratory scale and full capital expenditure (CAPEX) is not within the scope of this work. However, high-level operating cost analysis, such as the final fertilizer value, was considered together with the estimated energy costs for the pre-treatment, membrane, and freezing processes.

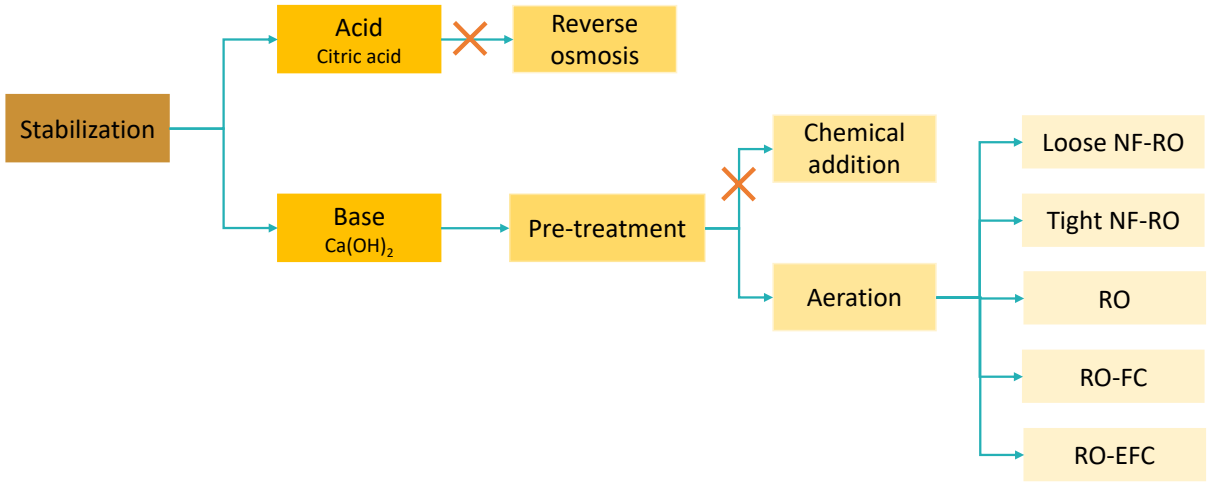

Figure 10-1:Summary of tested and preferred treatment process options.

The five different treatment processes all require the same pre-treatment inputs ($Ca(OH)_2$ stabilization and air bubbling). The most significant difference in operating costs would be the energy requirements of the different processes. The gross value of the fertilizer produced is a function of the fertilizer selling price and the volume produced. Therefore, although a process might have a higher operating cost, the final product value might justify the increased treatment costs.

There are many scales at which urine can be collected and treated. For example, urine could be collected and treated at the toilet/bathroom scale (Riechmann et al., 2021b; Simha et al., 2020a), at a building scale (Fumasoli et al., 2016), or at a decentralized treatment facility (Chipako and Randall, 2020a). Chipako and Randall (2020a) compared on-site treatment for several shopping centres (for an RO system) to treatment at a decentralized facility and found that the cost of transporting the untreated urine to a decentralized treatment facility was more favorable in terms of CAPEX. Chipako and Randall (2020a) estimated that it is possible to collect 7 500 L of urine per week from 8 shopping centers in the Cape Town region. The amount of fertilizer produced from 7 500 L would vary based on the treatment method used. They estimated that the market for niche liquid fertilizers is approximately 2 L per week per nursery/garden center in the Cape Town region. They reported that there are approximately 70 nurseries in Cape Town, which would mean a sales potential of 140 L of liquid fertilizer per week. Niche fertilizers (typically used for domestic garden use) are usually sold at a premium compared to commercial synthetic fertilizers which are sold in bulk for agricultural use. For example, a commercially available niche fertilizer, which contains 2.4% N (Makhro, 2022), is typically sold for R220 L^{-1}

(Takealot, 2022). This liquid fertilizer is equivalent to R8 292 per kg-N compared to synthetic urea (used in commercial farming), which costs approximately R32 kg^{-1} or R68.7 per kg-N (ChemLab Supplies, 2022). The gross fertilizer value is therefore highly dependent on the product end use, e.g., domestic/home gardening versus commercial farming, and the size of each market. Whilst E-commerce platforms could increase the market size for niche fertilizers, it is likely that depending on the treatment method used, not all the fertilizer produced would be able to be sold at a premium price.

In commercial agricultural settings, fertilizer is applied on a kg-nutrient per hectare basis. The fertilizers produced using the different treatment processes all have varying nutrient content and therefore the volume required to apply a certain kg-N ha^{-1} may vary significantly based on how dilute the fertilizer is. The fertilizer would also need to be stored at the treatment facility as farmers typically only apply fertilizer once or twice a season. The fertilizer also needs to be transported from the treatment facility to the farm which would increase operating costs. Trimmer and Guest (2018) analyzed the average distance that would need to be travelled to apply 5% of a city's recoverable fertilizer nutrients. The travel distance required is related to cropland density and will differ for cities. For example, for Rome only 6 km travel was required whilst for Boston it was 329 km (Trimmer and Guest, 2018).

Margins on fertilizer sales at bulk prices would therefore be much smaller. It is therefore important to determine if the fertilizers produced would be profitable if also sold at bulk prices. Chipako and Randall (2020a) showed that the decentralized collection and treatment of urine is feasible. However, the type of treatment method and end-product composition has not yet been investigated. The objective of this chapter was therefore to:

1. Asses how the different treatment configurations, as well as established urine treatment technologies (alkaline dehydration and nitrification and distillation), compare in terms of energy requirements.
2. Compare the value of the fertilizer produced using the different treatment configurations in the context of the niche fertilizer market.
3. Considering the size of the niche fertilizer market, determine how the value of the products compare if the fertilizers produced are sold at bulk commercial prices and whether the fertilizer produced can be profitable at a commercial scale.

10.2 METHODS

10.2.1 System boundaries

Figure 10-2 shows the process flow diagram (PFD) for a potential urine source-separation, transportation, and treatment system. For this analysis, a decentralized urine treatment model was

chosen as Chipako and Randall (2020a) showed that the cost of transporting urine to a decentralized treatment facility was cheaper than on-site treatment (for an RO system). The decentralized system is based on the work of (Chipako and Randall, 2020a), which identified eight shopping centers in the Cape Town area from which 7 500 L of urine per week could be collected and then transported to a decentralized facility for treatment. Five different treatment configurations were identified, and the nutrient recoveries and water removals of each treatment configuration were experimentally determined. Regardless of treatment configuration, the urine would be stabilized with $Ca(OH)_2$ and pre-treated with air bubbling before concentration. The operational cost of pre-treatment is discussed in Chapter 5 and Chapter 6.

The system boundary used for the analysis of the different treatment methods, therefore, considers only the treatment process and transport of the final fertilizer product as the inputs for all five different treatment methods would be the same. The treatment methods in this study were also compared to three additional urine treatment technologies: freeze concentration (FC) (Noe-Hays et al., 2021), alkaline dehydration (AD), and nitrification and distillation (ND) (Udert and Wächter, 2012). Five studies investigated AD of urine (Riechmann et al., 2021b; Simha et al., 2021; Simha et al., 2020a; Simha et al., 2020b; Vasiljev et al., 2022), each system operated at various temperatures and used different alkaline substrates. The ND system was designed to be used at the building scale and the AD system at the bathroom scale. This analysis considers urine collection and treatment at a decentralized facility (which was the most suitable for an RO process). Although this is at a different scale to what ND and AD systems were designed for, it was still deemed important to include these technologies in the analysis for comparison purposes.

The five AD studies all had comparable water removal, however, the nitrogen recovery and content in the final product varied between studies due to the different operating conditions. Riechmann et al. (2021b) operated their AD system at ambient temperatures rather than at 50-60 °C (Simha et al., 2020a). Nitrogen recovery achieved during short-term (3-4 days) laboratory experiments was high (97%), however, this was not the case during long-term(10-20 days) pilot-scale experiments where N-recovery was only 20%. This process still requires further optimization and for this reason, it was excluded from the fertilizer market analysis. An average N-content from the remaining four studies was used in the market analysis.

Phosphorus was excluded from this analysis as some treatment methods recover P separately as calcium phosphate (RO, RO-FC, RO-EFC, NF-RO) during the collection phase, other methods recover P as struvite (ND), and with other methods, the P is recovered in the liquid (FC) and solid (AD) products. It would therefore be difficult to make an equivalent comparison. However, the P recovered in the stabilization step could be added to the final product to meet the desired P concentrations. However, as

the P is recovered as a solid it would need to be digested first and then added as an aqueous solution at an additional expense. This aspect was not considered in the economic analysis.

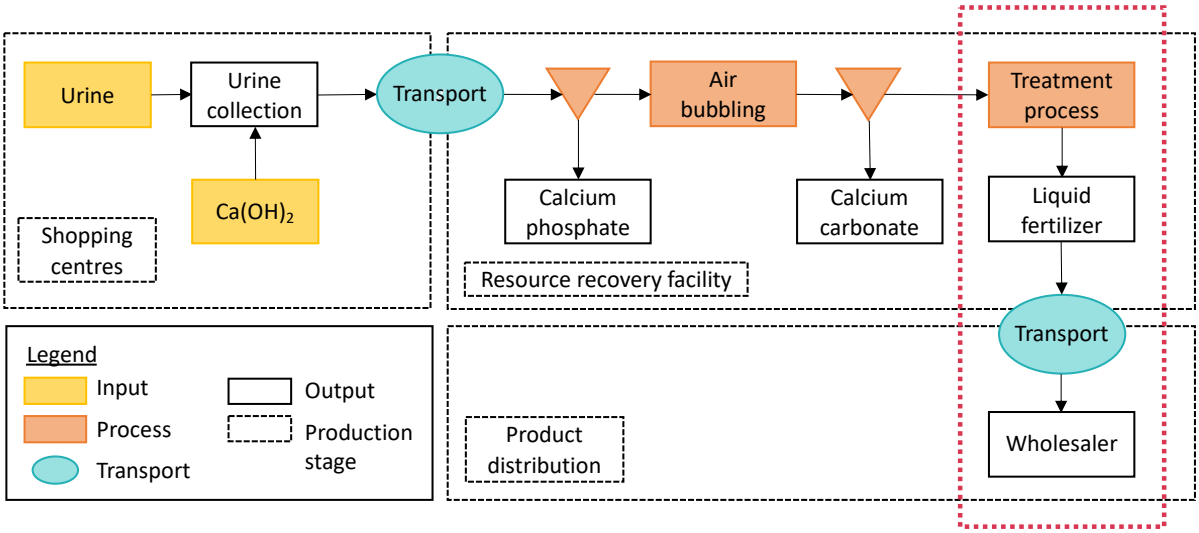

Figure 10-2: Process diagram for a potential urine source-separation, transport, and treatment system, where the red line indicates the boundaries for the system investigated in this analysis, adapted from (Chipako and Randall, 2020a).

10.2.2 Mass and energy balance

Process flow diagrams for each treatment option were developed (Appendix G) and from this mass and energy balances were conducted. The energy balance considered the energy required for pre-treatment (air bubbling). Energy is reported as kWh (electrical energy) required to treat 1 m^3 of fresh urine. A summary of the assumptions used for the mass balances is available in the appendices. The energy requirements of the lab-scale equipment are not an accurate reflection of a full-scale plant and therefore the energy requirements for RO, NF, and freezing were calculated using the energy requirements of full-scale systems obtained from the literature. The energy requirements for an FC process (with varying water recovery) were calculated in this study rather than using the energy requirements reported by Noe-Hays et al. (2021) as this is a theoretical value and not realistic of a full-scale FC treatment process. The energy requirements for AD (Simha et al., 2020a) and ND (Udert and Wächter, 2012) were reported by the authors of those studies and are presented with the calculated energy requirements for the treatment configurations investigated in this study.

10.2.3 Fertilizer sales value

The two markets for fertilizer are typically commercial agricultural use and household fertilizer use. The sales price for niche liquid and dry fertilizers was calculated using a least square regression analysis of the fertilizer sales price as a function of nutrient content (by weight) according to (Chipako and Randall, 2020a) and updated for fertilizer prices in 2022. The commercially available fertilizers chosen

included those designed for use on ornamental vegetation, as well as vegetation intended for human consumption. All prices for niche liquid fertilizers were collected from the Stark Ayres Nursery in Rondebosch, Cape Town (18 August 2022). This ensured a similar pricing comparison was used.

A comparison of the UBFs to commercial fertilizers was based on an N-cost analysis as this is the main component of all the UBFs. The bulk fertilizer (25-50 kg bags) value was calculated based on a farmer using a 50/50 split of synthetic urea (R32 kg^{-1}, (ChemLab Supplies, 2022)) and limestone ammonium nitrate (LAN) 28% N granular fertilizer (R23.57 kg^{-1}, (Tack'nTogs, 2022)). The price that the urine-based fertilizer (UBF) can be sold for (in bulk) was based on the average Rand per kg-N that the synthetic fertilizer is sold for. For the AD fertilizer product, an average N-content (based on the compositions from four studies) was used to calculate the bulk price. A summary of the assumptions and values from the literature used for these calculations is available in Table G-2.

10.2.4 Niche fertilizer market

Gross fertilizer sales were calculated based on an input of 7 500 L per week as a case study for the Cape Town region. The volume and sales value of each fertilizer varied based on the treatment method and nitrogen content. A sensitivity analysis was conducted that compared gross fertilizer sales as a function of the niche fertilizer market size. Fertilizers not sold at niche prices were assumed to be sold at bulk prices. The system boundary was fixed to an input of 7 500 L of urine per week from which each treatment method produced a different amount of final product. The maximum revenue possible occurs if the total volume of fertilizer produced is sold at niche prices, after which, maximum revenue is fixed by the volume of fertilizer produced even if the niche fertilizer market would have allowed for more product to be sold. For the AD process, it was assumed that the mass of fertilizer produced from 1 L of urine was fixed regardless of operating conditions.

10.2.5 Bulk fertilizer market

Fertilizer is typically applied by calculating the kg-N required per hectare and then the appropriate amount of fertilizer is applied based on its N-content (Heyns, 2016). In this analysis, a basis of 1000 kg-N was used. As an example, a typical nitrogen application in a mature vineyard is 50-60 kg-N ha^{-1} (AWRI, 2010). An application of 1000 kg-N would therefore be sufficient for a 20 ha vineyard (which would be considered a small farm), however, maize requires approximately 100 kg-N ha^{-1} (FERTASA, 2016) and therefore 1000 kg-N would only be sufficient for a 10 ha farm. A sensitivity analysis was conducted to determine how the cost of transporting the fertilizer to the farm (as a percentage of the gross fertilizer value) varied by distance travelled. Liquid fertilizers are typically transported using tanker trucks and then stored in fertilizer tanks on the farm (Heyns, 2016). Granular fertilizers would

be transported and stored in bags. It was assumed, based on the volume of fertilizer required, that it would be transported using either a 4, 8, 14, or 18-ton truck. For the AD system, the transport costs were calculated based on the average N-content of the fertilizer produced in the four studies. A list of assumptions used is available in Table SX.

10.3 RESULTS AND DISCUSSION

A comparison of the energy requirements and nitrogen recoveries of different urine treatment processes was conducted in Paper 3 and the results of that analysis are included in Table 13. This section further expands on that analysis including the energy requirements of the different treatment process configurations investigated in this study.

10.3.1 Energy requirement

Figure 10-3 shows the energy requirements of different urine treatment methods with varying total water removals as a function of 1 m^3 of fresh urine (A) and per kg-N recovered (B). Each treatment method has a different N recovery, by adjusting the energy requirements to a kg-N basis they can be more fairly compared. Whilst AD provides high water removal and NPK recoveries at an operating temperature range of 50 – 60°C (Simha et al., 2020b), the energy requirements are 12 times greater than RO (16 kWh m^{-3}, including air bubbling pre-treatment), even with energy recovery (AD-198 kWh m^{-3}). Riechmann et al. (2021b) used forced air convection in their AD system and, even though they operated at ambient temperatures, the overall energy requirements reported were still greater than RO at 150 kWh m^{-3} water evaporated. Although the air was not heated, energy was still required to operate fans that provide the air convection. Since evaporation is slower at ambient temperatures the fans needed to operate for longer to evaporate the same amount of liquid which could explain the higher energy requirements.

Industrial seawater desalination using evaporative processes such as multi-stage flash distillation or multi-effect distillation typically has lower energy requirements (14-28 kWh m^{-3}) (Abdelkareem et al., 2018) compared to AD and ND. However, these processes are also designed to operate at temperatures of 70 to 110°C (Hore-Lacy, 2007). At this temperature range, chemical urea hydrolysis would occur (Randall et al., 2016) and it is unclear what N-recovery would be achievable. The effect of operating these systems at lower temperatures would also reduce the rate of evaporation and therefore require more total energy to remove the same amount of water. These aspects should be considered if large-scale evaporation systems are to be used for concentrating stabilized human urine.

Reverse osmosis required the least amount of energy even with air bubbling, which contributed 63% of the total energy requirements. NF-RO requires an additional treatment step (compared to RO), however, because only 0.8 m^3 (loose NF) and 0.75 m^3 (tight NF) is treated by RO post NF treatment, the overall energy requirement would only be 1.1 kWh m^{-3} (loose NF-RO) more than RO-only treatment. The NF-RO energy requirements calculations do not consider the fact that the NF pre-treatment step removes a significant amount of salt (44% - loose NF, 96% tight NF) and organics (78 loose NF, 90% tight NF) (Chapter 8) and would make the operation of the RO more efficient. The energy calculations for RO processes do not consider the indirect energy costs to remove the remaining N from the non-potable water stream produced. For example, the 20% N recovered in the permeate of an RO process (70% water removal) would still need treatment at a WWTP if this stream was used for toilet flushing. Only the AD process would have no additional indirect energy costs as this method produces a dry product and no water is recovered that requires further treatment.

It was expected that the energy requirements for FC-only would be lower than evaporative processes, however, for comparable water removal (95%), FC (162 kWh m^{-3}) has a similar energy requirement to AD (198 kWh m^{-3}) and ND (154 kWh m^{-3}). Importantly, the energy requirements for AD and ND included energy recovery, while no energy recovery was considered for FC. Without energy recovery, the electricity required would be 1320 kWh m^{-3} (AD) (Simha et al., 2020a) and 710 kWh m^{-3} (ND) (Udert and Wächter, 2012). Many studies investigating FC typically report the energy requirement as the theoretical energy required to freeze ice, however, this is an over-simplification. For example, Noe-Hays et al. (2021) estimated an energy requirement of 11 Wh to freeze 1 kg of ice, while Best and Vasavada calculated an energy requirement of 154 kWh per kg water removed for an actual full-scale FC plant that concentrated skim milk (Best and Vasavada, 1993a).

Apart from these, the above-mentioned treatment methods, a hybrid forward osmosis–membrane distillation (FO-MD) process could also be used. However, whilst the energy requirements for FO are low (0.27 kWh m^{-3}, (Iskander et al., 2017)), the thermal energy requirements which drive the separation process in MD (103 kWh m^{-3}, (Ullah et al., 2018) are 6 times more than RO. In addition, the nutrient recovery results have been mixed (discussed in detail in Chapter 2) and nutrients that permeate through the membrane will build up in the draw solution as it is continuously regenerated (Liu et al., 2016). In general, progress in establishing FO for commercial and industrial applications has also been slow (Francis et al., 2020).

When accounting for the energy required as a function of nitrogen recovered, a different outcome is observed. Freezing processes (using a per m^3 treated basis) have similar energy requirements to evaporative processes. However, when considering nitrogen recovery, the energy requirement significantly decreases. For example, at 70% water removal, FC requires 7 times more energy than RO per m3 urine treated but the FC process has a higher nitrogen recovery of 92% (Noe-Hays et al., 2021)

compared to 79.5% for RO (this study). This means, that per kg-N recovered, FC processes only use approximately twice as much energy as RO. Conversely, for ND, based on the nitrogen in the product (50 g-N L^{-1}, 30 L product from 1000 L urine (Etter et al., 2015)) the energy requirement per kg-N (102 kWh $kg\text{-}N^{-1}$) is almost three times more than AD (35 kWh $kg\text{-}N^{-1}$).

Biological nitrogen removal (BNR) at a wastewater treatment plant requires approximately 14.6 kWh $kg\text{-}N^{-1}$ (Panepinto et al., 2016). Whilst advancements in wastewater treatment technologies, such as anammox, can reduce energy requirements for aeration by up to 60% (Winkler and Straka, 2019), BNR is still the most widely used treatment method in South Africa (WRC, 2016). Electric ammonia plants have an estimated energy consumption of 12 kWh $kg\text{-}N^{-1}$ (Brown, 2019), thus resulting in a combined energy requirement of 26 kWh $kg\text{-}N^{-1}$. Nitrification and distillation was the only urine treatment method that required more energy than the energy for WWTPs and urea production combined. Essentially, for all treatment processes, the energy required is offset by the energy that would have been used to create synthetic N fertilizer and treat the urine at conventional WWTPs. This analysis shows why it is important to compare energy requirements on a per N basis (Figure 10-3B) and not only on a m^3 feed basis (Figure 10-3A).

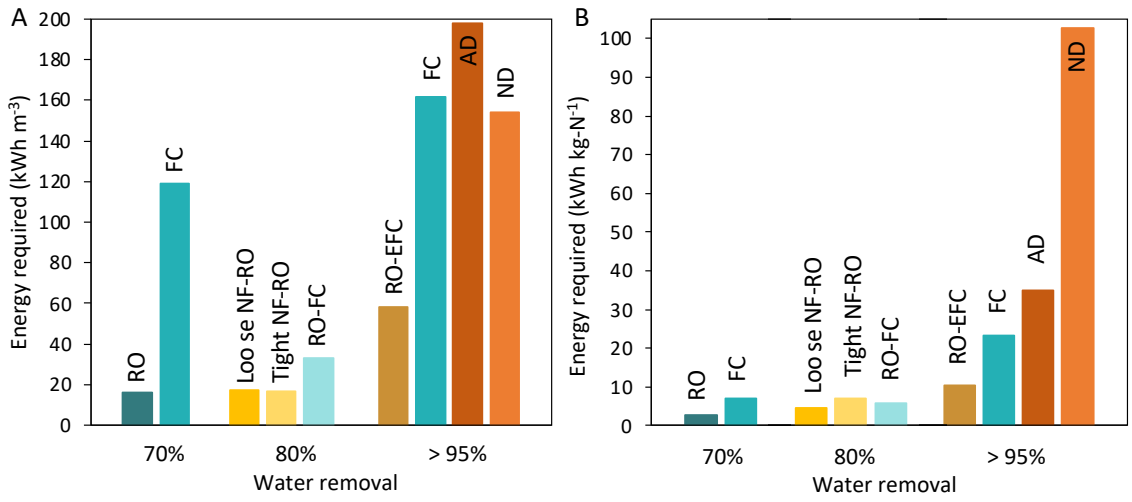

Figure 10-3: Energy required to treat 1 m^3 urine (A) and the energy required per kg-N recovered (B) for urine treated with different concentration technologies and varying water recoveries. The energy requirements for all RO and FC-related treatments were calculated using values from the literature for similar processes, whilst the energy requirements for alkaline dehydration (AD) (Simha et al., 2020a) and nitrification and distillation (ND) (Udert and Wächter, 2012) were other urine treatment investigations. For both AD and ND, the energy requirements include energy recovery, while no energy recovery was included for FC.

10.3.2 Fertilizer sales price

Figure 10-4 shows the trend between niche fertilizer sales price and nitrogen content. For liquid fertilizers (Figure 10-4A) the nitrogen content provided a reasonably accurate predictor for the fertilizer price with an R^2 value of 0.933. The sales price as a function of P-content, K-content, and total nutrient

was also compared (Figure G-4A), however, nitrogen content was the most accurate indicator for liquid fertilizer price. The sales price of different dry niche water soluble fertilizers was also investigated (Figure 10-4B). In general, there was no trend in terms of price as a function of nutrient content (this was also the case for P, K, and total nutrient content, Figure G-4B). The fertilizer produced using AD is a dry product and therefore the sales price of this fertilizer was determined by taking an average of the sales price of fertilizers in Figure 10-4B.

This method to determine the sales value of fertilizers does have its limitations. For example, each of the final products produced using different concentration methods have varying final compositions. In some cases, all the salts remain concentrated with the nitrogen and potassium, in other cases, there is partial salt removal, and in some cases, there is also pharmaceutical removal. A more detailed market analysis should be conducted for different fertilizer compositions produced from human urine. However, for this analysis, a least squares regression for liquid fertilizer and an average price for dry fertilizer was determined to be sufficiently accurate as a method to estimate the final fertilizer value as a first estimation of market value.

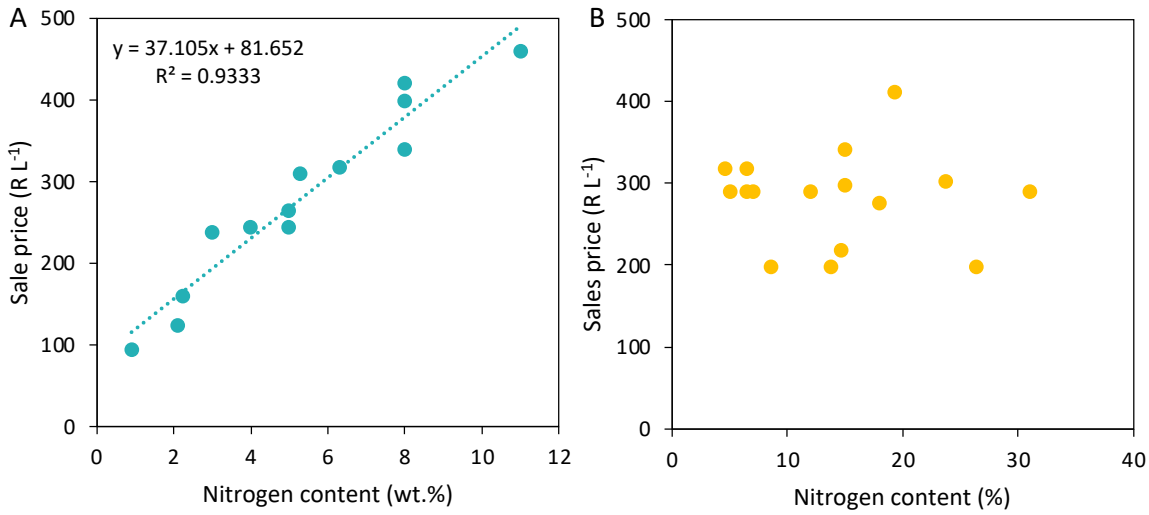

Figure 10-4: Fertilizer price as a function of nitrogen content (weight %) available at a local garden center in Cape Town, South Africa for different niche liquid (A) and dry (B) fertilizers.

Chipako and Randall (2020a) identified that the niche fertilizer market size is limited in the Cape Town region, and some of the fertilizer produced would likely need to be sold at bulk processes if only this region was considered as the market. Figure 10-5A shows the water removal achieved using each treatment process and the N-content of the fertilizer produced. Figure 10-5B shows the estimated sales price for the niche and bulk fertilizers produced using the different treatment methods. Although the N-content in a fertilizer produced using AD has shown to vary from 7.8 to 13.2%, the sales price would be fixed as it was observed, that for dry niche fertilizer, the price is not a function of nutrient content.

This analysis suggests that recovering a completely dry product is less desirable if the product is to be sold as a niche fertilizer, at least in the South African market. If the product from an AD process was instead liquid (with the same nutrient content), it could theoretically be sold for R 471 L^{-1} compared to R 283 kg^{-1} for the dry product. Both the niche and bulk fertilizer sales prices are linked to the nitrogen content. The fertilizer values shown in Figure 10-5 are used in the analysis in the following two sections. In Chapter 9, an analysis of commercially available fertilizers revealed that commercial fertilizers exist with similar nutrient contents for each of the fertilizers produced using different treatment methods Figure 9-6 In reality, UBFs contain other key fertilizer components, (P and K) would also influence the bulk sales price. However, this was not considered in the analysis as the primary focus was on the N content of the UBFs. These aspects should be considered in future work through a more detailed market and economic analysis.

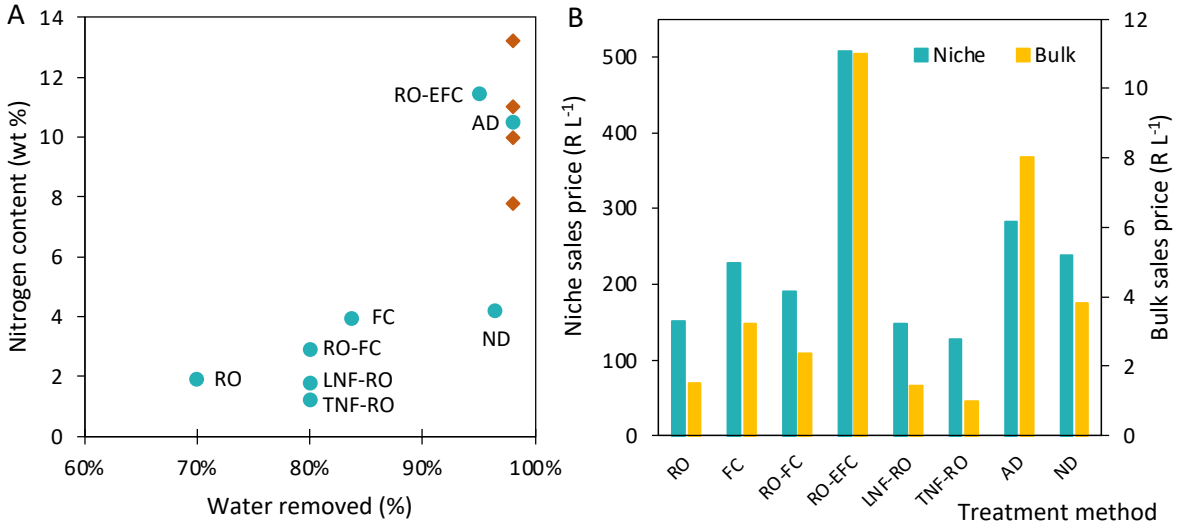

Figure 10-5: Nitrogen content of the fertilizers produced as a function of water removed for the different treatment methods (A) and sales price for 1 L of niche or bulk fertilizer products made using different urine treatment methods (B). The sales price for the alkaline dehydration product is R kg^{-1}, as this method produces a dry product. Variation in nitrogen content for AD (♦).

10.3.3 Niche fertilizer market

The gross value of UBFs produced is a function of the fertilizer market size, its sales price, and the volume of fertilizer produced from each treatment method. An analysis of the fertilizer market was conducted assuming a feed of 7 500 L of urine per week would be collected and treated to produce fertilizers. Figure 10-6A shows the nitrogen content and volume of fertilizer produced using each treatment method. Chipako and Randall (2020a) estimated the niche liquid fertilizer market in Cape town was 140 L per week. For all treatment methods, the volume of fertilizer produced is more than the market for niche fertilizers if only Cape Town was considered as the market. For example, RO (with 70% water removal) would be able to produce 2171 L of fertilizer from 7 500 L of urine. Whilst E-

commerce platforms could increase the market size, it is likely that, depending on the treatment method used, there might not be a market to sell all the fertilizer as a niche product and at a premium price.

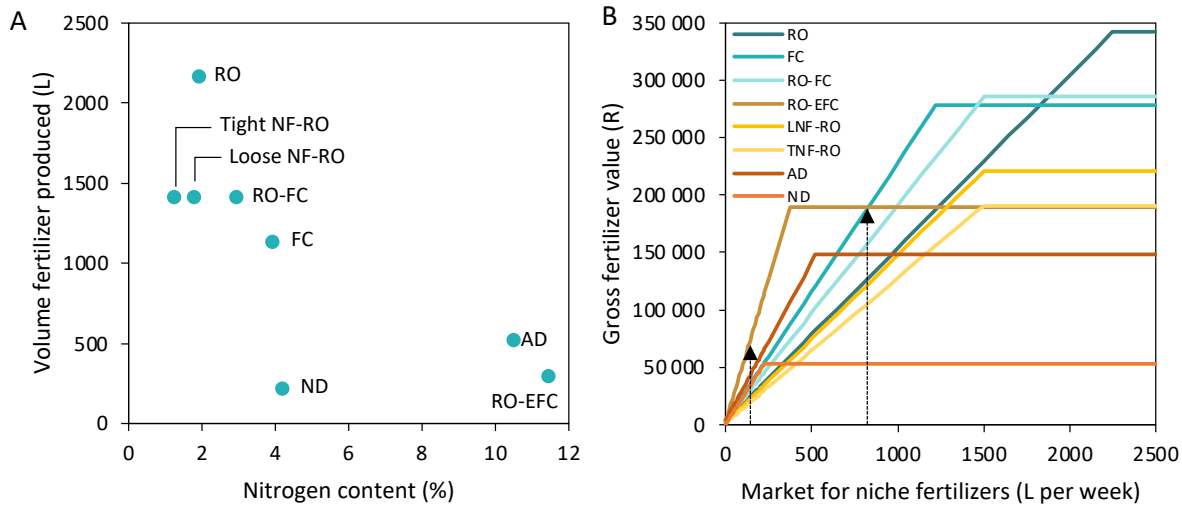

Figure 10-6: Nitrogen content (weight %) and volume of fertilizer produced from 7 500 L of feed urine using different treatment methods (A), and the gross value of the different fertilizer products as a function of the size of the niche fertilizer market (B). Gross value plateaus when all fertilizer produced from 7 500 L of input urine is sold at the niche fertilizer sales price. Values for AD are in kg and the volume produced was assumed to be fixed regardless of N-content.

Figure 10-6B shows the gross value of the fertilizer product as a function of the niche fertilizer market size (assuming an input of 7 500 L per week). If more fertilizer is produced than the niche market size, then it was assumed that the remaining fertilizer was sold at bulk prices. The gross value of the fertilizer produced is fixed by the volume of fertilizer produced and is reached when all fertilizer produced from 7 500 L of input urine is sold at the niche fertilizer sales price. Figure 10-6B shows that if the niche fertilizer market was infinitely large, the UBF produced using RO would have the highest gross value. However, assuming a more realistic market of 140 L per week it is evident that the UBF produced using RO-EFC is the most valuable. This is because only 375 L of fertilizer is produced with RO-EFC and therefore 37% of the fertilizer produced can be sold at a niche price (R487 L^{-1}) compared to RO where 6% of the fertilizer produced can be sold at a niche price (R150 L^{-1}), where the prices are based on the final N content and RO-EFC produces a product with a higher N-content.

The RO-EFC treatment method would result in the highest gross value up until a niche fertilizer market size of 814 L per week. For example, if the market size was increased from Cape Town to South Africa, and the market for niche fertilizers in South Africa was 814 L per week, then FC would produce a product with the highest gross value. In general, the treatment method that results in the highest gross sales value is dependent on the niche fertilizer market size. Although the tight NF-RO and loose NF-RO treatment produce a purer product with less salts and pharmaceuticals the gross value of the fertilizers is low due to their low N-content. However, this analysis does not consider operating costs and net

profit as a function of fertilizer market size may differ. In addition, this analysis does not consider that each UBF has a different composition and that the market size for each composition may vary significantly. For example, if there is a large market for fertilizers used for ornamental plants or lawns (> 2000 L per week) then the additional treatment costs of NF do not add value to the product and using RO would be more profitable. Nonetheless, this economic analysis provides a good summary of the products that can be produced together with their potential value. It is recommended that a more detailed market and economic analysis be conducted to obtain more accurate results.

10.3.4 Bulk fertilizer market

The previous analysis assumed that the excess fertilizer produced (not sold as a niche product) could be sold as a bulk fertilizer. However, many of the fertilizers have a much lower N content than commercial synthetic fertilizers and would significantly larger volumes would need to be applied. Figure 7A shows the feed urine input required, and end fertilizer product required to supply 1000 kg of Nitrogen which would cover approximately 20 ha of vineyards. This was compared to a commercial synthetic fertilizer which has a 50/50 mix of urea and LAN. The volume of feed urine required varies from 145 to 406 m^3, which would be the equivalent of between 19 and 54 weeks of urine collection using the 8 shopping centers as a basis. For UBF produced using tight NF membrane and RO, the urine input required would take one year to collect and the product produced would only be able to meet the fertilizer requirements of one small wine farm. Using dried UBF product as an example, and a basis of 1000 kg-P and 1000 kg-K, 625 m^3 and 239 m^3 feed urine would be required. All other treatment methods would require even more feed urine. This example illustrates the large volumes of urine required to only produce 1000 kg of P or K-based fertilizers.

To apply 1000 kg-N only 2.8 tons of commercial fertilizer would be required compared to 52.48 m^3 of UBF produced using RO, and 6.9 m^3 (8.7 tons) of the UBF produced using EFC-RO. This is significantly more product that needs to be stored and transported and considering the low price at which bulk fertilizer is sold it is important to consider how the cost of transport compares to the gross value of the product (shown in Figure 7B). For the AD processes, depending on the N-content of the final product, the amount of fertilizer required (to apply 1000 kg-N) would vary from 7.5 to 12.8 tons.

Depending on the location of the urine collection and treatment operation, the product might need to travel far distances to reach the end user (Trimmer and Guest, 2018). It is therefore important to consider how distance affects operating costs. For the Cape Town region, the average travel distance is approximately 75 km (Trimmer and Guest, 2018). As expected, the UBFs with lower N-content have the highest transport cost as a percent of gross value which could be as much as 5% for tight NF-RO if the UBF needs to be transported 75 km, this increases to 13% at 200 km. These results suggest that low N-content UBFs would likely not be as profitable, especially in regions where agricultural fields are far

away from the urine collection operation. However, regardless of cropland location, the practical aspect of use and storage should also be considered. Further research and engagement with commercial farmers

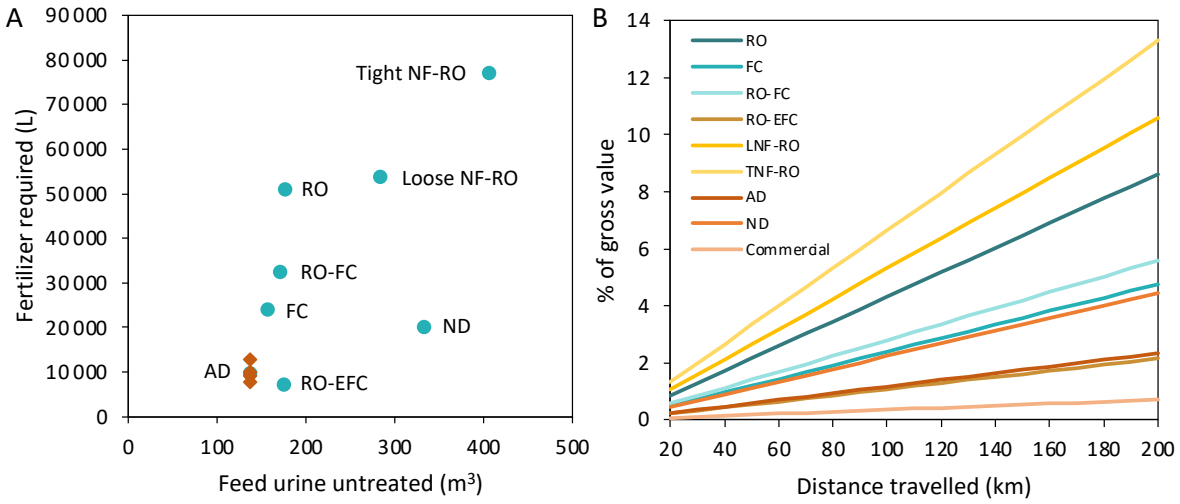

and their perceptions of the practicalities and quality of UBFs should be investigated.

Figure 10-7: Untreated urine input (m^3) and fertilizer application required to apply 1000 kg-N for different fertilizer production methods (A) and the cost of transporting the fertilizer product between 20 and 200 km as a percentage of the product's gross value (B). Variation in the amount of AD fertilizer required (kg) based on N-content (♦).

10.3.5 Niche versus bulk fertilizer markets

Based on the analysis from this study, there are two major conclusions about the niche and bulk fertilizer markets. Niche fertilizers have a significantly higher sales price than bulk fertilizers (R152 vs R1.5 for RO, 70% water removal) and at the collection scale of 8 shopping centers, marketing to the commercial agricultural market would not be profitable. For example, if the entire population of Cape Town's (4.168 million people) urine was collected and treated (with AD) it would take 6 days to collect enough urine to produce the fertilizer required to meet the application rates required to add fertilizer to South Africa's 3.1 million hectares of maize (du Plessis, 2003). This illustrates the scale of urine collection and treatment required to replace commercial fertilizers for just one crop. Comparatively, one week of urine collection and treatment with RO-EFC, for example, would produce almost two times the amount needed to supply the predicted Cape Town niche fertilizer market. At this stage, focusing on the niche fertilizer market would be more profitable but could also expose a wider range of people to the concept of UBFs and the normalization of urine recycling.

10.3.6 Analysis summary

Each treatment method has advantages and disadvantages, which are summarized in Table 12. As a result, the choice of preferred treatment methods will be ultimately defined by several factors. A summary of the different urine treatment methods in terms of water removal, NPK recovery, fertilizer NPK content, process energy requirements, and transport cost per km as a percentage of bulk fertilizer sales price are summarized in Table 13.

Reverse osmosis can be used to remove the bulk component of water from human urine using minimal energy; however, urea recovery will always be limited by the membrane separation efficiency. Long-term operation of a urine RO concentration system is also required using pilot and full-scale systems. For RO processes, acid stabilization was determined to be unsuitable. Base stabilization with $Ca(OH)_2$ results in the precipitation of almost all the phosphorus (>98%) as calcium phosphate (Flanagan and Randall, 2018). This results in a final liquid product with limited P as it is recovered separately. Depending on the fertilizer composition desired, the P might need to be supplemented. However, the calcium phosphate formed during stabilization could potentially be digested and added to the liquid product to match the desired P concentration. The treatment cost of RO decreases as the treatment capacity increases (Wittholz et al., 2008) and the CAPEX required for an RO system at the toilet or even building scale would therefore not be economically feasible. Treatment methods incorporating RO are best suited to be used for large-scale treatment at a decentralized facility.

All treatment methods, except NF-RO, concentrate salts along with nutrients. Although NF-RO can be used to remove pharmaceuticals and salts, it comes at the cost of nutrient recovery. For example, tight NF-RO increases urea purity from 39% (RO-only) to 85% but urea recovered was only 32.8% for this configuration. The concentration of inorganic species is only a concern if the species is high in proportion to the nutrient content. In addition, If the RO product (which contains salts and fertilizer components) can be sold for use on ornamental vegetation and lawns only, then there would be no requirement for additional treatment and the associated costs. Whilst NF-RO produces a purer urea product, that could potentially be used in other products such as cosmetics (Andersson et al., 1999) or diesel engines (Baker, 2012), it is unlikely that the product could be produced at a price competitive with synthetic urea at this stage.

Freeze concentration processes are promising as they have shown high nutrient recovery and water removal and would not be affected by scaling such as with RO. Industrial freeze concentration is also well established and widely used in the juice (Sánchez et al., 2009) and dairy industries (Best and Vasavada, 1993a). Unlike evaporation, FC can be used to concentrate either stabilized or hydrolyzed urine as chemical urea hydrolysis and loss of volatile NH_3 would not occur at low operating temperatures. The type of freeze concentration method (block-freeze versus suspension-freeze) may influence the nutrient recovery and energy requirements. The one downside of FC is that, for a similar

level of separation to RO, the capital costs of a large system are typically much higher (Rodriguez et al., 2000). Williams et al. (2015) reviewed the cost of water production for different desalination technologies and found RO to be between 30-60% cheaper than freezing and distillation processes.

Evaporative crystallization processes are advantageous as they can remove all the water from urine without the potential for scaling, thus significantly reducing transport costs. However, they can be energy intensive. The scalability of the processes is also limited. For example, the alkaline dehydration system is designed to be operated at the toilet scale treating 30 L of urine per day (Simha et al., 2020a) and it is not clear what the energy requirements would be for large-scale systems. Monitoring of evaporation temperature is also important, as Simha et al. (2020a) observed that a temperature overshoot to 90°C instead of 60°C resulted in an average N recovery of 30% when up to 70% recovery was expected. During AD, excess substrate or base stabilizer is required as a buffer to keep the urine pH high during evaporation and prevent urea hydrolysis. In addition, during dehydration, CO_2 dissolution from the air into the urine occurs which decreases the solution pH (Randall et al., 2022), this would not be the case for RO or FC. Continuous or batch operation of an AD system could also impact N-recovery. Any hydrolysis (chemical or enzymatic) that occurs in a continuous system would be compounded as the mass of urea builds up and re-dissolves with each new batch of urine added.

Bulk collection and evaporation would require large surface areas. Industrial scale evaporation is possible using distillation; however, the high operating temperatures and continuous operation may lead to significant nitrogen loss due to chemical urea hydrolysis (Randall et al., 2022). Successful distillation of urine was achieved when the nitrogen was first nitrified and converted to nitrate which reduces volatilization (Udert and Wächter, 2012). Large-scale evaporative crystallizers should be investigated to evaluate the potential of this concentration method at scale.

Hybrid processes, such as RO-EFC are promising because they take advantage of the positive aspects of each treatment method. Reverse osmosis is used to remove the bulk of the water making the EFC process more efficient as the solution is closer to eutectic conditions and uses almost three times less energy than FC (for a similar water removal). Operation at eutectic conditions also allows for the removal of undesirable ions such as Na^+ and SO_4^{2-} by crystallizing $Na_2SO_4 \cdot 10H_2O$.

The preferred treatment method may also be influenced by the urine collection method. If urine is collected in the basement of a building and treated on-site, the volume of urine available for treatment will influence the capital costs of the treatment equipment installed. Whereas, if urine is collected on a larger scale from multiple sources and treated at a decentralized treatment facility the economies of scale and capital costs could favor a different treatment method

Table 12: Advantages and disadvantages of different urine treatment technologies.

Process	Advantages	Disadvantages
RO	Low energy requirements, scalable, and lower capital investment than other methods.	Limited water removal, and potential for membrane scaling or fouling.
RO-FC	Improved water removal without membrane scaling or fouling.	Lower urea recovery in the membrane treatment step (79.5%).
RO-EFC	Reduces sodium and sulfate ion concentrations in the fertilizer product (removes undesirable salts).	A complex system which is likely to require high capital investment.
Loose NF-RO	Removes pharmaceuticals.	Low urea recovery (52%) and minimal salt removal.
Right NF-RO	Removes salts and pharmaceuticals.	Potassium is removed with salts and has a low urea recovery (32.8%).
Freeze concentration	High nutrient recovery (92%), not affected by chemical urea hydrolysis.	High capital investment is required.
Alkaline dehydration	Recovers a dry product and all key nutrients (NPK) appear in the final product.	High energy requirement, salts concentrated with fertilizer nutrients.
Nitrification & distillation	Nitrification and distillation treatment steps have high nutrient recovery and water removal.	Highest energy requirement per kg-N. Urine is not stabilized, therefore there is a potential for N-loss during collection and storage.

Table 13: Comparison of different urine concentration methods in terms of water removal, NPK recovery, NPK content, process energy requirements, and transport cost per km as a % of bulk fertilizer sales price.

Process	Urine type	Water removed	Recovery (%) N	P	K	NPK (wt. %)	Energy requirement ($kWh\ m^{-3}$)[c]	($kWh\ kg\text{-}N^{-1}$)	Transport cost (% value/km)	Reference
RO	$Ca(OH)_2$ Stabilized[h]	70%	80	98	99	1.9: 0: 0.5	16.0	2.8	0.043	This study
RO-FC		80%	77	98	95	2.9: 0: 0.9	33.0	5.9	0.028	
RO-EFC		95%	75	98	96	11.5: 0: 3.5	58.3	10.5	0.011	
Loose NF-RO		80%	52	98	39	1.8: 0: 0.3	17.1	4.6	0.053	
Right NF-RO		80%	33	98	4.1	1.2: 0: 0:	16.8	7.0	0.066	
Freeze concentration	Hydrolyzed	83.7%	92	92	92	3.9: 0.5: 0.9	(14)[d] 143	21.5	0.024	(Noe-Hays et al., 2021)
Alkaline dehydration	Base stabilized	>98%	70	100	100	13.2: 2.3: 6	198[f]	34.8[f]	0.012[g]	(Simha et al., 2020a)
			90			10: 1: 4				(Simha et al., 2020b)
			80			7.8: 0.7: 3.9				(Simha et al., 2021)
			98			11: 2: 3				(Vasiljev et al., 2022)
Nitrification & distillation	Hydrolyzed	>95%[e]	99[b]	99	100	4.2: 0.1: 1.5	154	92.4	0.022	(Etter et al., 2015; Udert and Wächter, 2012)

All RO processes include air bubbling pre-treatment which requires 10 $kWh\ m^{-3}$ (Paper 2).

[a]Urine is mixed with a variety of substrates that raises the pH to prevent urea hydrolysis.

[b]Values are for N and P recovered in the nitrification/distillation process and do not account for loss during storage and collection. Accounting for 11% urea hydrolysis (Udert et al., 2003a) and P precipitation (Barbosa et al., 2016) adjusted N and P recovery is 87.7%, and 69.7%, respectively.

[c]Energy requirements for RO processes determined by (Abdelkareem et al., 2018)

[d]Noe-Hays et al. (2021) reported the theoretical energy requirement for freezing. This value was updated to account for a more realistic full-scale operation based on the work of Best and Vasavada (1993a), but using the water removal achieved by Noe-Hays et al. (2021)

[e]Etter et al. (2015) report that 30 L of product is made from 1000L of urine.

[f]Energy requirement based on (Simha et al., 2020a).

[g]Transport cost is based on an average nutrient content of these four studies.

[h]Membrane treatment process (RO, RO-FC, RO-EFC, loose NF-RO, and tight NF-RO) recover P separately from the liquid fertilizer, as it is precipitated as calcium phosphate during stabilization.

10.4 CONCLUSIONS

Commercially available organic fertilizers have a wide variety of nutrient compositions, as do the products produced from each urine treatment method investigated in this work. A commercial fertilizer with a comparable nitrogen content could be found for each UBF regardless of the urine treatment method used. Therefore, theoretically, there is a market for all the UBFs produced, however, the market size for the fertilizers produced may not result in the highest profitability for the same volume of feed urine to the process.

Treatment methods that incorporated RO had the lowest energy requirements, followed by FC, and AD processes had the highest energy requirements. An RO-EFC process with 95% water removal required 2.8 times less energy than if FC had been used alone and 3.4 times less energy than AD to concentrate the same volume of feed urine. Converting the energy requirements to a kWh kg-N^{-1} recovered improved the comparative energy requirements of FC and AD as these typically have higher nitrogen recovery (96% and 90% N recovery, respectively) compared to RO-EFC (77% N recovery).

Niche fertilizers are more valuable than bulk fertilizers and can be sold for more than R8 292 kg-N^{-1} compared to R68.7 kg-N^{-1} for bulk fertilizers. Based on the estimated niche fertilizer market of 140 L per week, the UBF produced using RO-EFC had the highest gross value of R73 000 (produced from 7 500 L of feed urine). This converts to a gross value of R9 700 m^{-3} feed urine. However, if the niche fertilizer market is larger (2 000 L per week for example) the RO fertilizer would have the highest gross value (R304 000) whilst the RO-EFC fertilizer's gross value would remain at R69 800. This analysis only considers gross value and does not account for the cost of production. The UBF produced using RO-EFC or AD would be the most practical for bulk sale as these two treatment methods would have the lowest transportation costs (as they have the highest N-content). For example, to supply 1000 kg of N, 2.8 tons of commercial fertilizer are required and only 7.5 m^3 of UBF is produced using RO-EFC compared to 51 m^3 of the UBF produced using RO-only with a 70% water removal. The net cost of decreased transportation costs versus increased operational costs to further reduce the fertilizer volume requires additional analysis though, especially considering the capital costs that would be required for the RO-EFC process. In addition, the volume of urine that needs to be collected and treated to meet agricultural requirements is significant. Wide-spread urine collection would be required. At this stage, the business model favors producing UBFs for the niche liquid fertilizer market.

This research showed the technical feasibility of concentrating stabilized urine using a suite of different treatment technologies. In general, the final choice of treatment method will depend on several factors and not only the gross product value. These include the product end-use (ornamental plants versus edible crops), plant nutrient requirements and desired nutrient ratios, and the method of urine collection (plumbed versus free-standing systems) as well as the scale of treatment required (toilet, building,

centralized). A detailed economic analysis comparing multiple different system boundary options would likely yield different preferred treatment options for each scenario.

Further testing using a pilot-scale plant is necessary to obtain more accurate operational costs (energy requirements, product transportation costs, nutrient recovery, water removal, and practicality of operation) that can be used to determine a net profit rather than gross sales value. Future work should investigate fertilizer licensing and ensuring the product meets local fertilizer regulations. A detailed market analysis should also be conducted of the different potential fertilizer products. A comparison of capital and operating expenses for each treatment method is also required to determine the financial feasibility of each treatment method.

REFERENCES

Abdelkareem, M.A., Assad, M.E.H., Sayed, E.T. and Soudan, B. 2018. Recent progress in the use of renewable energy sources to power water desalination plants. Desalination 435, 97-113.

Andersson, A., Lindberg, M. and Lodén, M. 1999. The effect of two urea-containing creams on dry, eczematous skin in atopic patients. I. Expert, patient and instrumental evaluation. Journal of dermatological treatment 10(3), 165-169.

AWRI. 2010. Grapevine nutrition: nitrogen fertilization, pp. 1-4, Adelaide, Australia.

Baker, M. 2012. Overview of Industrial Urea Markets: Application and Opportunities. TFI Fertilizer Technology and Outlook Conferences. Philadelphia, USA, 13-15 November.

Barbosa, S.G., Peixoto, L., Meulman, B., Alves, M.M. and Pereira, M.A. 2016. A design of experiments to assess phosphorous removal and crystal properties in struvite precipitation of source separated urine using different Mg sources. Chemical Engineering Journal 298, 146-153.

Best, D. and Vasavada, K. 1993. Freeze concentration of dairy products Phase 2: Final report, Dairy Research Foundation, Illinois, USA.

Brown, T. 2019. Renewable hydrogen for sustainable ammonia production. Chemical Engineering Progress 115(8), 47-53.

ChemLab Supplies. 2022. Urea Prills [Online]. Available: https://chemlabsupplies.co.za/product/urea-prills/ [Accessed 24 August 2022].

Chipako, T. and Randall, D. 2020. Investigating the feasibility and logistics of a decentralized urine treatment and resource recovery system. Journal of Water Process Engineering 37, 101383.

du Plessis, J. 2003. Maize Production. Services, D.A.I. (ed), Directorate Agricultural Information Services, Pretoria, South Africa.

Ellis, L.D., Badel, A.F., Chiang, M.L., Park, R.J.-Y. and Chiang, Y.-M. 2020. Toward electrochemical synthesis of cement—An electrolyzer-based process for decarbonating CaCO3 while producing useful gas streams. Proceedings of the National Academy of Sciences 117(23), 12584-12591.

Etter, B., Udert, K.M. and Gounden, T. 2015 VUNA: Valorisation of Urine Nutrients. Promoting Sanitation & Nutrient Recovery through Urine Separation. Final Project Report 2015, ETH Zurich.

FERTASA. 2016. Fertilizer Handbook, FERTASA, Pretoria, South Africa.

Flanagan, C.P. and Randall, D.G. 2018. Development of a novel nutrient recovery urinal for on-site fertilizer production. Journal of Environmental Chemical Engineering 6(5), 6344-6350.

Francis, L., Ogunbiyi, O., Saththasivam, J., Lawler, J. and Liu, Z. 2020. A comprehensive review of forward osmosis and niche applications. Environmental Science: Water Research & Technology 6(8), 1986-2015.

Fumasoli, A., Etter, B., Sterkele, B., Morgenroth, E. and Udert, K.M. 2016. Operating a pilot-scale nitrification/distillation plant for complete nutrient recovery from urine. Water Science and Technology 73(1), 215-222.

Heyns, E. 2016. When and how to fertilizer: Winetech technical [Online]. WineLand Media. Available: https://www.wineland.co.za/when-and-how-to-fertilise/ [Accessed 23 August 2022].

Hore-Lacy, I. 2007. Nuclear Energy in the 21st Century. Hore-Lacy, I. (ed), pp. 93-110, Academic Press, Burlington.

Iskander, S.M., Zou, S., Brazil, B., Novak, J.T. and He, Z. 2017. Energy consumption by forward osmosis treatment of landfill leachate for water recovery. Waste Management 63, 284-291.

Liu, Q., Liu, C., Zhao, L., Ma, W., Liu, H. and Ma, J. 2016. Integrated forward osmosis-membrane distillation process for human urine treatment. Water research 91, 45-54.

Makhro. 2022. GroBest Liquid Fish Fertilizer Label [Online]. Available: https://makhro.co.za/wp-content/uploads/2021/03/Grobest-Label_compressed.pdf [Accessed 24 Agust 2022].

Noe-Hays, A., Homeyer, R.J., Davis, A.P. and Love, N.G. 2021. Advancing the Design and Operating Conditions for Block Freeze Concentration of Urine-Derived Fertilizer. Environmental Science & Technology Engineering 2(3), 446-455.

Panepinto, D., Fiore, S., Zappone, M., Genon, G. and Meucci, L. 2016. Evaluation of the energy efficiency of a large wastewater treatment plant in Italy. Applied Energy 161, 404-411.

Randall, D.G., Brison, A. and Udert, K.M. 2022. High temperatures and CO2 dissolution can cause nitrogen losses from urine stabilized with base. Frontiers in Environmental Science 10.

Randall, D.G., Krähenbühl, M., Köpping, I., Larsen, T.A. and Udert, K.M. 2016. A novel approach for stabilizing fresh urine by calcium hydroxide addition. Water Research 95, 361-369.

Randall, D.G. and Nathoo, J. 2015. A succinct review of the treatment of Reverse Osmosis brines using Freeze Crystallization. Journal of Water Process Engineering 8, 186-194.

Riechmann, M.E., Ndwandwe, B., Greenwood, E.E., Reynaert, E., Morgenroth, E. and Udert, K.M. 2021. On-site urine treatment combining Ca(OH)2 dissolution and dehydration with ambient air. Water research X 13, 100124.

Rodriguez, M., Luque, S., Alvarez, J. and Coca, J. 2000. A comparative study of reverse osmosis and freeze concentration for the removal of valeric acid from wastewaters. Desalination 127(1), 1-11.

Sánchez, J., Ruiz, Y., Auleda, J., Hernández, E. and Raventós, M. 2009. Freeze concentration in the fruit juices industry. Food Science and Technology International 15(4), 303-315.

Simha, P., Friedrich, C., Randall, D.G. and Vinnerås, B. 2021. Alkaline dehydration of human urine collected in source-separated sanitation systems using Magnesium Oxide. Frontiers in Environmental Science 8, 9.

Simha, P., Karlsson, C., Viskari, E.-L., Malila, R. and Vinnerås, B. 2020a. Field testing a pilot-scale system for alkaline dehydration of source-separated human urine: a case study in Finland. Frontiers in Environmental Science 8, 168-178.

Simha, P., Lalander, C., Nordin, A. and Vinnerås, B. 2020b. Alkaline dehydration of source-separated fresh human urine: Preliminary insights into using different dehydration temperature and media. Science of the Total Environment 733, 139313.

Tack'nTogs. 2022. Fertiliser LAN [Online]. Available: https://tackntogs.co.za/products/fertilizer-lan-50kg?variant=30271928172599 [Accessed 24 August 2022].

Takealot. 2022. Grobest FH100 500ml - Organic fertilizer [Online]. Available: https://www.takealot.com/grobest-fh100-500ml-organic-fertilizer/PLID72013635 [Accessed 24 August 2022].

Trimmer, J.T. and Guest, J.S. 2018. Recirculation of human-derived nutrients from cities to agriculture across six continents. Nature Sustainability 1(8), 427-435.

Udert, K.M., Larsen, T.A., Biebow, M. and Gujer, W. 2003. Urea hydrolysis and precipitation dynamics in a urine-collecting system. Water Research 37(11), 2571-2582.

Udert, K.M. and Wächter, M. 2012. Complete nutrient recovery from source-separated urine by nitrification and distillation. Water Research 46(2), 453-464.

Ullah, R., Khraisheh, M., Esteves, R.J., McLeskey Jr, J.T., AlGhouti, M., Gad-el-Hak, M. and Tafreshi, H.V. 2018. Energy efficiency of direct contact membrane distillation. Desalination 433, 56-67.

Vasiljev, A., Simha, P., Demisse, N., Karlsson, C., Randall, D.G. and Vinnerås, B. 2022. Drying fresh human urine in magnesium-doped alkaline substrates: Capture of free ammonia, inhibition of enzymatic urea hydrolysis & minimisation of chemical urea hydrolysis. Chemical Engineering Journal 428, 131026.

Williams, P.M., Ahmad, M., Connolly, B.S. and Oatley-Radcliffe, D.L. 2015. Technology for freeze concentration in the desalination industry. Desalination 356, 314-327.

Winkler, M.K. and Straka, L. 2019. New directions in biological nitrogen removal and recovery from wastewater. Current opinion in biotechnology 57, 50-55.

Wittholz, M.K., O'Neill, B.K., Colby, C.B. and Lewis, D. 2008. Estimating the cost of desalination plants using a cost database. Desalination 229(1-3), 10-20.

WRC. 2016. Wastewater Treatment Technologies – A basic guide, Water Research Commision, Pretoria, South Africa.

CHAPTER 11: CONCLUSIONS AND FUTURE WORK

CHAPTER 11: CONCLUSIONS AND FUTURE WORK

11.1 CONCLUSIONS

Human urine can be used as a more sustainable alternative to synthetic fertilizers. Source-separation and nutrient recovery from urine also reduces the nutrient loads and treatment requirements at traditional wastewater treatment plants. Despite this, the widespread use of urine as fertilizer is not yet commonplace. Whilst methods for separate urine collection and stabilization (to prevent urea degradation and the resulting malodor) are well established, urine is 97% water and the cost of large-scale collection and transportation from urban to agricultural areas is not economically feasible. This has led to the investigation of a variety of methods (of varying complexity) to remove the water and concentrate urine. However, many of these technologies are still being tested at the laboratory scale or are being designed for treatment at the individual toilet/household scale. To be truly revolutionizing, a urine concentration method that can operate at a significant scale and which is energy efficient is required.

Reverse osmosis (RO) was identified as a promising, yet understudied, concentration technique because it is energy efficient when compared to other urine concentration methods. Full-scale RO has been proven to be commercially viable as it is widely used to desalinate seawater. In typical RO processes, the brine produced is a waste stream that requires disposal. When concentrating urine with RO there is zero waste as the brine is the product fertilizer and the permeate can be used as a non-potable water source. Limited research into urine concentration using RO was attributed to the potential for membrane scaling, low urea recovery, and unknown concentration limits. In addition, if urine is not stabilized the urea breaks down into ammonia, which is lost to the atmosphere through volatilization. The use of an RO process therefore also had to consider how stabilization affects the treatment process.

Chapter 5 and Chapter 6 focused on pre-treatment methods for $Ca(OH)_2$ stabilized urine. Bicarbonate salt addition reduced the Ca^{2+} concentration to less than 10 mg L^{-1}. Air bubbling removed between 85% and 98% of the Ca^{2+} (depending on operating time, air flow rate, and initial concentration). Although air bubbling reduced the urine pH to 8.5 (which is below the threshold for urea hydrolysis prevention), no urea hydrolysis was observed for at least 18 hours after the pH reached 8.5.

In Chapter 7, urine pre-treated with air bubbling and bicarbonate salt addition was concentrated using RO and the effectiveness of the pre-treatment methods were compared to a process with no pre-treatment. Both pre-treatment methods were equally effective. Air bubbling was chosen as the preferred pre-treatment method as it does not require salt addition and the associated greenhouse gas emissions associated with the salt's production. In addition, air bubbling sequesters CO_2 from the atmosphere. Air bubbling resulted in a pH (8.0-8.5) which was within the membrane design operating parameters unlike with $NaHCO_3$ addition (pH-11.0), and it did not add additional Na^+ ions.

CHAPTER 11: CONCLUSIONS AND FUTURE WORK

Stabilization of urine with an acid (citric acid) resulted in the formation of uric acid dihydrate crystals and an unidentified organic compound during concentration. Neither could be removed with a pre-treatment step, and it was concluded that concentration of acidified urine should be achieved using evaporation or freeze concentration instead. Real urine, stabilized with $Ca(OH)_2$ and pre-treated with air bubbling, was concentrated using a seawater RO membrane operating at 55 bar. Water removal of 60% was achieved and 85.5% of the urea and 98.5% of the potassium was recovered in the brine, and more than 99% of the phosphorus was recovered as a separate solid phosphate-based fertilizer. The final liquid had a concentration of 11.2 g-N L^{-1} and 3.66 g-K L^{-1}, however, the final composition will depend on the feed urine composition.

Pharmaceuticals and salts present in urine are concentrated with the nutrients using RO. In Chapter 8, a hybrid NF-RO process was tested to purify the urea-rich stream further. Both loose and tight NF membranes could be used to remove pharmaceuticals (loose > 70%, and tight > 99% removal) at a 75% water removal (as permeate). The permeate from the tight NF membrane (75% water removal) contained 48% of the urea and the permeate from the loose NF membrane contained 78% of the urea. Urea purity was increased from 37% to 89%, removing 90% of the organics and 96% of the ions present in the urine using the tight NF membrane. Using the loose NF membrane, the purity increased to 56%, and 78% of the organics and 44% of the ions were removed.

The permeate from a tight NF membrane was further treated with a high-pressure SWRO membrane. An overall water removal of 80% resulted in a urea recovery of 32.7%. Further concentration of the permeate using loose NF membranes (to 80% overall water removal) would increase the overall urea recovery to 52%. Based on this analysis, a decision tree was developed that can be used to determine the optimal treatment train based on the desired product. In general, the increased purity comes at the cost of urea recovery. Water removal in the RO step was limited to an overall water removal of 80% as a significant decrease in urea recovery was observed as the water removal increased beyond this percentage.

Water removal achieved using RO will have a limit as the osmotic pressure of the feed increases to the point that it is equal to the pump's operating pressure. As the urine becomes more concentrated there is also the potential for fouling and scaling as solubility limits of different aqueous species are reached. In Chapter 9, EFC was investigated to further concentrate the urine as freezing processes are not affected by membrane scaling and the technology has the potential to simultaneously remove undesirable salts. A thermodynamic model was first used to predict crystallization temperatures, water removal (as ice) before salt crystallization began, and the types of salts that would crystallize. The experimental analysis determined that the model accurately predicted ice crystallization temperatures (< 0.5°C difference). The model also predicted the mass of ice formed at a fixed temperature with a ±10% accuracy since the model did not account for impurities trapped in the ice.

CHAPTER 11: CONCLUSIONS AND FUTURE WORK

Overall, this research was the first to show experimentally that $Na_2SO_4 \cdot 10H_2O$ crystallizes from urine at eutectic conditions. A theoretical mass balance (including ice-washing and recycle streams) was used to show that the liquid fertilizer composition after RO-EFC (95% water removal) would be 304 g urea L^{-1} and 42.8 g K L^{-1} (11.5% N, 3.5% K), and 3.5 kg of $Na_2SO_4 \cdot 10H_2O$ could theoretically be recovered from 1000 kg of urine. The system would have an overall urea and potassium recovery of 77.1% and 96%, respectively.

An economic analysis comparing the different treatment methods was conducted in Chapter 10. The analysis showed that treatment processes using RO for the bulk of the water removal have the lowest energy consumption (16 kWh m^{-3}, 70% water recovery), followed by freeze concentration (119-162 kWh m^{-3}, 70-95% water removal), and evaporative processes (154 -198 kWh m^{-3}, >95% water removal) was the most energy intensive. The value of each product produced was estimated based only on the N-content of the final product. Using a basis of 7.5 m^3 input urine per week and a niche fertilizer market size of 140 L per week for the Cape Town region only, RO-EFC produced the product with the highest gross value. FC had the highest value if the market size increased to 0.81 m^3 per week, and RO-only had the highest value for a market size > 0.2 m^3 per week. However, this analysis did not include capital and operating expenses, therefore the net value as a function of market size remains uncertain. It is, however, evident that an accurate market size will influence the preferred treatment method. The use of urine-based fertilizers (UBF) for commercial use may require transport up to 200 km from the treatment facility to the end-user. The volume of UBF transported increases as N-content decreases. Transport costs as a percentage of the product's gross value could account for between 0.8% (RO-EFC – 11.5% N) and 3.2% (RO – 1.9% N) of the fertilizer's gross value (75 km) depending on the product composition.

In conclusion, membrane and hybrid freezing processes can be used to produce different liquid fertilizers with comparable compositions to commercially available fertilizers. Different process configurations can be used to remove pharmaceuticals and salts as well as to further concentrate the product. The choice of treatment configuration will be influenced by the size of the urine collection system since the capital costs for different treatment methods will vary based on the feed volume. In addition, the treatment method will also depend on the niche fertilizer market size, the fertilizer use (ornamental plants versus edible crops), and the associated fertilizer regulations for each type of product. This novel work ultimately offers new urine concentration methods for fertilizer production.

11.2 FUTURE WORK

After assessing the results of this study, including the scope and limitations, the following recommendations for future research are suggested:

1. The RO experiments were conducted with a pressure limitation of 55 bar. The use of new ultra-high pressure SWRO membranes and pumps should be investigated to determine if urea rejection and water removal rates can be improved further at even higher operating pressures (120 bar).
2. The rejection of a wider range of pharmaceuticals by loose NF and tight NF membranes should be investigated to better understand how rejection is affected by the molecular mass, the charge of the pharmaceuticals, and how the pharmaceuticals interacts with the urine chemistry matrix.
3. Nanofiltration physically removes pharmaceuticals, however, pharmaceuticals can also be degraded. Advanced oxidation processes such as hydrodynamic cavitation, UV, electrochemical, and hydrogen peroxide systems should also be considered for use in conjunction with, or as an alternative pharmaceutical removal options to NF.
4. The use of ion exchange resins should be considered to replace the monovalent ions in urine (such as chloride ions) with divalent ions (such as sulfate ions). This would potentially increase the ion rejection with loose NF membranes and produce a higher purity urea product. This approach would also reduce the overall osmotic pressure of the urine and therefore improve flux. This pre-treatment could also be used before SWRO membranes to improve operation.
5. A hybrid NF-FC process should be experimentally investigated as an alternative to an NF-RO system to determine if a higher N-content product can be produced by increasing both urea recovery and water removal.
6. The results presented in this study are based on the use of laboratory scale equipment operated in a batch configuration. The next phase should be conducted using a pilot-scale plant. More information on the long-term operation of the processes is also required to better understand what operational challenges might be encountered.
7. The effectiveness of the different fertilizer products (produced from the different treatment methods) should be tested on various crops to establish how the nutrient and salt concentrations in each product affects various plants. This will help determine specific fertilizer markets.
8. A more nuanced understanding of the legislative environment in South Africa regarding fertilizer production from human urine is necessary as this is currently a hurdle to entrepreneurship activities in this space. Legislation may also influence the preferred treatment configuration if full pharmaceutical removal is legally required.

9. An estimation of the CAPEX and OPEX for different treatment methods, as well as for different treatment volumes (e.g., 100 L per day versus 1 000 L per day), should be determined. This can then be used in a more detailed economic analysis to compare how treatment methods compare in terms of net profit rather than gross sales only. The preferred method will also likely be influenced by the scale of urine treatment and collection (e.g., toilet-level, building scale, or collection and transport to a decentralized treatment facility).
10. A detailed fertilizer market analysis is required to help better understand the market size, consumer requirements, and a realistic sales price. Each treatment method produces a product with a varying composition, which influences its use (for example, ornamental plants versus edible crops). The market size within each niche fertilizer category should therefore be considered.

APPENDICES

APPENDICES

APPENDIX A: LITERATURE DATA ANALYSIS

A.1 Energy calculations

Nitrification Distillation

Primary energy demand (PED): Nitrification 8.9 W Cap^{-1} (Udert and Wächter, 2012)

Urine production = 1.5 L Cap^{-1} day^{-1}, Total nitrogen concentration of 8.8 g-N Cap day^{-1} (Maurer et al., 2003)

Primary energy conversion factor (PECF) 31% used. (UCPTE, 1994)

$$\text{Energy requirement (nitrification)} = \frac{8.9\ \text{W}}{\text{Cap}}\,\text{PED} \times 0.31\ \text{PECF} \times \frac{\text{Cap. day}}{1.5\ \text{L}} \times \frac{24\text{h}}{\text{day}} = \frac{44\ \text{kWh}}{\text{m}^3\ \text{urine}}$$

Energy required for distillation was 710 kWh L^{-1-} (Udert and Wächter, 2012)

Vapour compression can be used to recover 85% of the energy requirements for distillation which would reduce the energy consumption to 110 Wh L^{-1}.

Total energy requirement = 710 + 44 = 754 kWh m^{-3} urine

Total energy requirement with energy recovery = 110+ 44 = 154 kWh m^{-3}

Alkaline dehydration

Dry toilet optimum PED = 10 MJ L^{-1} urine (Simha et al., 2020a) and 1.5 MJ L^{-1} with 85% energy recovery using a heat pump (Simha, 2021). Energy recovery with a heat pump reduced the energy required to 198 kWh m^{-3} urine.

PECF = 47.6% (Simha, 2021)

$$\text{Energy requireent} = \frac{10\ \text{MJ}}{\text{L urine}}\,\text{PED}\ \times 0.476\ \text{PECF} \times \frac{\text{kWh}}{3.6\ \text{MJ}} \times \frac{1000\ \text{L}}{\text{m}^3} = \frac{1320\ \text{kWh}}{\text{m}^3\ \text{urine}}$$

Freeze concentration

Iterative mass balance for a two-stage block freeze concentration process with recycle streams produced 22.9kg of ice for every 15.4 kg of urine feed.

The formation of 1 kg of ice requires the removal of 334 kJ (92.8 Wh) of heat,41 which would consume 39 kJ (11 Wh) of electricity if performed using a heat pump with a COP of 8.5 (Noe-Hays et al., 2021)

$$\text{Energy requirement} = \frac{11\ \text{kWh}}{1000\text{kg ice}} \times 17.9\text{kg ice} \div 15.4\ \text{kg urine} = \frac{16.35\ \text{kWh}}{1000\ \text{kg urine}}$$

Urea production

Patyk and Reinhardt (1997) reported that urea production required 54 MJ kg-N^{-1}.

Converting this based on the 5.86 g N L^{-1} of urine (Maurer et al., 2003) to determine the energy required to produce the equivalent amount of urea present in urine.

$$\text{Urea production energy} = \frac{54\ \text{MJ}}{\text{kgN}} \times \frac{\text{kWh}}{3.6\text{MJ}} \times \frac{5.86\ \text{g N}}{\text{L urine}} = \frac{87.9\ \text{kWh}}{\text{m}^3\ \text{urine}}$$

Denitrification at a WWTP

Maurer et al. (2003) reported that N treatment at a WWTP using denitrification requires 45 MJ kg-N^{-1}

Converting this based on the equation above would require 73.25 kWh to treat the N in 1 m^3 of urine

APPENDICES

APPENDIX B: CHEMICAL ADDITION PRE-TREATMENT

B.1 Real urine composition

(Table B-1 below summarizes the compositions of the different real and synthetic urines used in Chapter 5.

(Table B-1: Composition of different stabilized urine samples used in this Chapter 5.

Measured	Units	U1	U2	U3	U4	U5	Synthetic
Urea-N	mmol L^{-1}	415 ± 24.9	845 ± 4.08	468 ± 7.67	1123 ± 8.22	1154 ± 1.80	422 ±19.1
Ammonia-N	mmol L^{-1}	10.1 ± 0.68	19.6 ± 2.7	16.7 ± 0.23	32.3 ± 2.77	16.4 ± 1.58	27.7 ± 0.67
Total phosphate-P	mmol L^{-1}				n/d		
Chloride	mmol L^{-1}	50.9 ± 1.60	98.1 ± 0.31	72.0 ± 4.71	191 ± 1.32	151 ± 0.71	125 ± 1.64
Sulfate	mmol L^{-1}	4.51 ± 0.16	9.36 ± 0.04	4.0 ± 0.37	17.5 ± 0.17	13.1 ± 0.12	6.20 ± 0.25
Magnesium	mmol L^{-1}	0.41 ± 0.04	0.33 ± 0.01	0.32 ± 0.00	1.04 ± 0.07	0.66 ± 0.01	0.41 ± 0.00
Calcium	mmol L^{-1}	23.7 ± 1.01	29.7 ± 0.33	29.7 ± 0.20	52.8 ± 0.34	34.4 ± 0.57	33.5 ± 0.33
Sodium	mmol L^{-1}	41.7 ± 0.79	67.3 ± 0.94	45.7 ± 1.26	106 ± 1.90	117 ± 2.51	97.3 ± 2.51
Potassium	mmol L^{-1}	30.5 ± 1.86	74.6 ± 1.19	33.0 ± 1.21	117 ± 1.71	76.7 ± 2.64	66.0 ± 9.32
COD	mg O_2 L^{-1}	4540 ± 70.7	7710 ± 70.7	3625 ± 21.2	10595 ±163	8715 ± 148.5	-
pH	-	12.53	12.53	12.52	12.46	12.52	12.59

n/d – not detected

APPENDIX C: AERATION PRE-TREATMENT

C.1 Experimental Setup

A visualization of the apparatus setup is presented in Figure C-1. The total liquid height in the reactor was 9.5 cm. A cylindrical air stone, with a diameter of 13 mm and a height of 27 mm, was used. The bottom of the air stone sat approximately 1 cm from the bottom of the vessel.

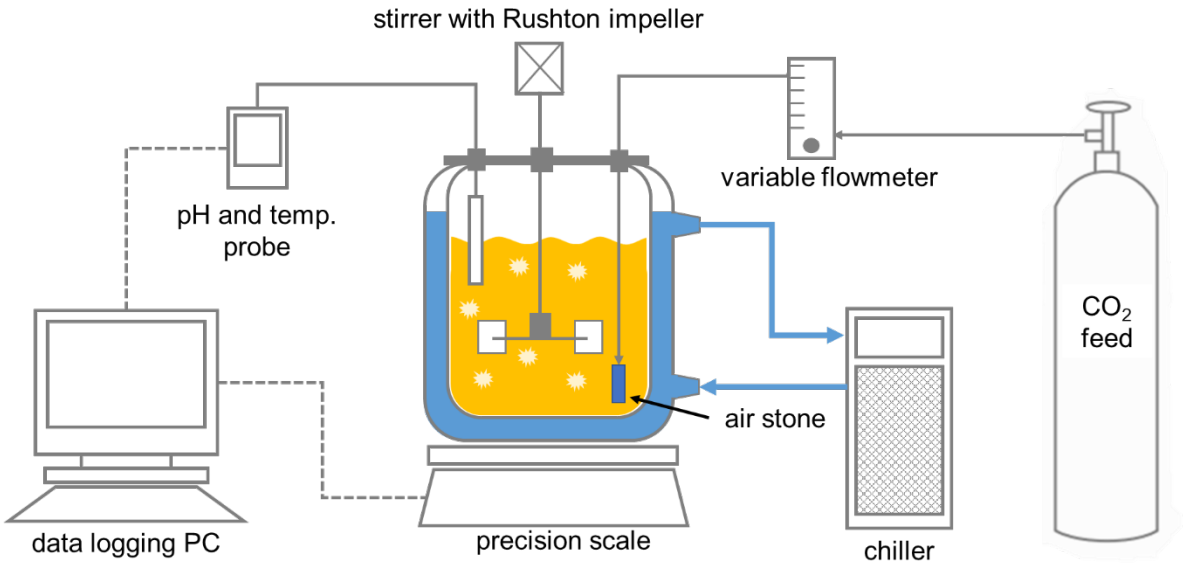

Figure C-1: Experimental setup including temperature-controlled reactor; stirrer with Rushton impeller; variable flowmeter for air/CO_2 flowrate control; pH, temperature, mass measurement, and CO_2 tank which was replaced by an air pump for air bubbling experiments.

C.2 Urine compositions

Table C-1 summarises the composition of the different stabilized urine samples used in Chapter 6.

Table C-1: Composition of different stabilized urine samples used in this Chapter 6.

Measured	Units	U1	U2	U3	U4	U5
Urea-N	mg L^{-1}	8568	9451	4178	5176	6638
Ammonia-N	mg L^{-1}	273	225	245	294	229
Total phosphate-P	mg L^{-1}	0.13	n/d	3.00	0.03	10.93
Chloride	mg L^{-1}	3614	2886	2779	3060	3789
Sulfate	mg L^{-1}	1516	1583	826	979	1018
Magnesium	mg L^{-1}	12.3	13.4	9.7	10.6	15.92
Calcium	mg L^{-1}	1216	1292	1039	1297	1054
Potassium	mg L^{-1}	2543	1804	1902	1866	1610
COD	mg L^{-1}	n/m	n/m	4214	5183	5267
pH	-	12.63	12.52	12.57	12.55	12.53

n/d – not detected, n/m – not measured

C.3 Simulation Improvements

The model developed by Udert (2002) was adapted by Brison (2016) to include ammonia stripping and enzymatic urea hydrolysis. Equation C-1 was used to model the NH_3 stripping rate where; S_{NH_3} is the NH3 concentration in the reactor [mol L^{-1}] and H_{NH_3} is the Henry constant for NH3 in water [$mol_{(g)}$ $mol^{-1}_{(aq)}$]. The solubility of NH3 in water at 20°C is 5.6E-4 $mol_{(g)}$ $mol^{-1}_{(aq)}$ (Montgomery, 1985).

$$V \cdot \frac{dS_{NH_3}}{dt} = Q_{air} \cdot H_{NH_3} \cdot S_{NH_3} \qquad \text{(Equation C-1)}$$

Equation C-2 (Fidaleo and Lavecchia, 2003) was used to model the pH-dependent rate of enzymatic urea hydrolysis where; μ_{max} is the maximum hydrolysis rate [mol d^{-1}], $K_{ES,1}$ and $K_{ES,2}$ are the molecular dissociation constants [mol L^{-1}], K_M is the Michaelis constant [mol L^{-1}], and S_{urea} is the urea concentration in the reactor [mol L^{-1}]. As no urea hydrolysis was observed it was assumed that there was no urease activity.

$$V \cdot \frac{dS_{urea}}{dt} = \mu_{max} \cdot \frac{1}{\left(1+\frac{10^{-pH}}{K_{ES,1}}+\frac{K_{ES,2}}{10^{-pH}}\right)} \cdot \frac{S_{urea}}{K_M+S_{urea}} \qquad \text{(Equation C-2)}$$

In addition, the dissociation constants for the inorganic carbon system were adjusted to account for the urine salinity and temperature according to Millero et al. (2006). It was assumed that all urine samples had a constant salinity of 10%. Urine contains several amino acids including creatinine, creatine, glycine, histidine, etc (Putnam, 1971). These compounds all have a dissociation constant in the range of 9.06 – 9.9 (Haynes et al., 2016). The model was updated to account for these amino acids, for simplification creatinine was used to represent all of the amino acids as it is present in the highest concentration (670 -2150 mg L^{-1}) (Putnam, 1971). Creatinine has a dissociation constant of 9.2 (Haynes et al., 2016). For simplicity, the same concentration of creatinine was used to model every experimental condition and a concentration of 0.05 mol L^{-1} was selected based on the combined concentrations of amino acids present in urine. It was also assumed that any inorganic carbon present in the urine would react with the calcium present in the stabilized urine to form calcium carbonate and therefore the initial concentration of inorganic carbon ($H_2CO_3/HCO_3^-/CO_3^{-2}$) was zero.

C.4 Analysis of precipitates

The concentration of PO_4^{3-}, Mg^+, SO_4^{2-}, Cl^-, and K^+ in the liquid were measured at the start and end of each experiment to determine if any other ions were precipitated during the air bubbling processes. In all cases, the final PO_4^{3-} concentrations were below the accurately detectable level. Figure C-2 shows the percentages of Mg^+, SO_4^{2-}, Cl^-, and K^+ that were removed during air bubbling. There is no significant observable trend between air flow rate and the removal of any of the ions. In all conditions, more than 94% of the magnesium present was removed from the liquid phase. The percentage removal of sulfate

and chloride falls within the margin of error and it is therefore unlikely that any sulfate or chloride compounds formed during the air bubbling processes. Potassium removal was between 15-19% with an error of between 4-8%.

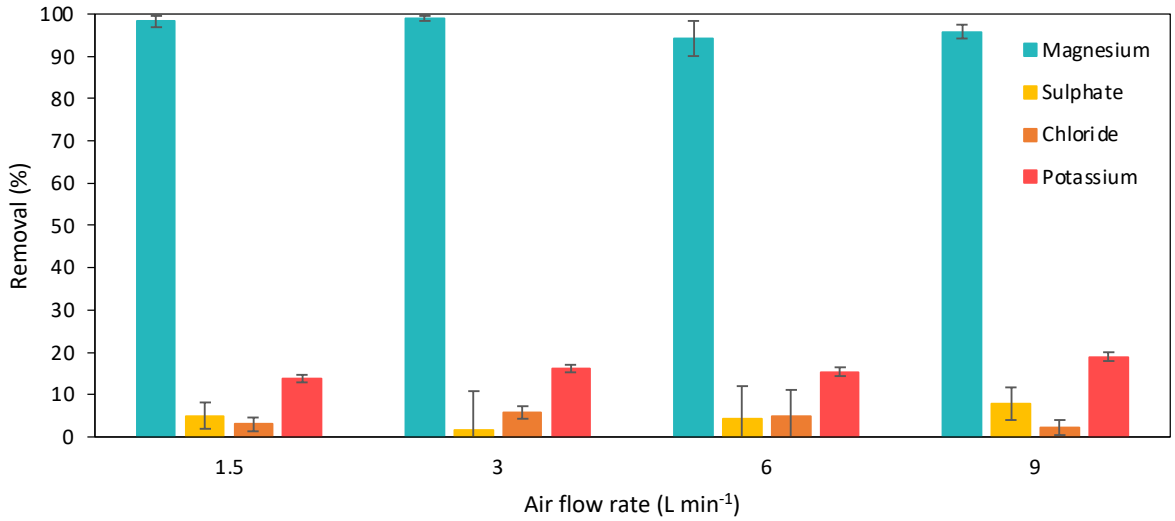

Figure C-2: Removal of magnesium, sulfate, chloride, and potassium for air flowrates varying between 1.5 and 9 L min^{-1}.

Elemental analysis via the SEM confirmed that no potassium was present in the precipitant. It was therefore assumed that the 15-19% potassium removal observed was due to experimental error in the analysis process. Figure C-3 displays the scanning electron microscope imagery of the precipitant sample prepared at a 3 L min^{-1} air flow rate, shown at a scale of 50, 10, 5, and 2 µm. The precipitant appears to have a cube-like morphology.

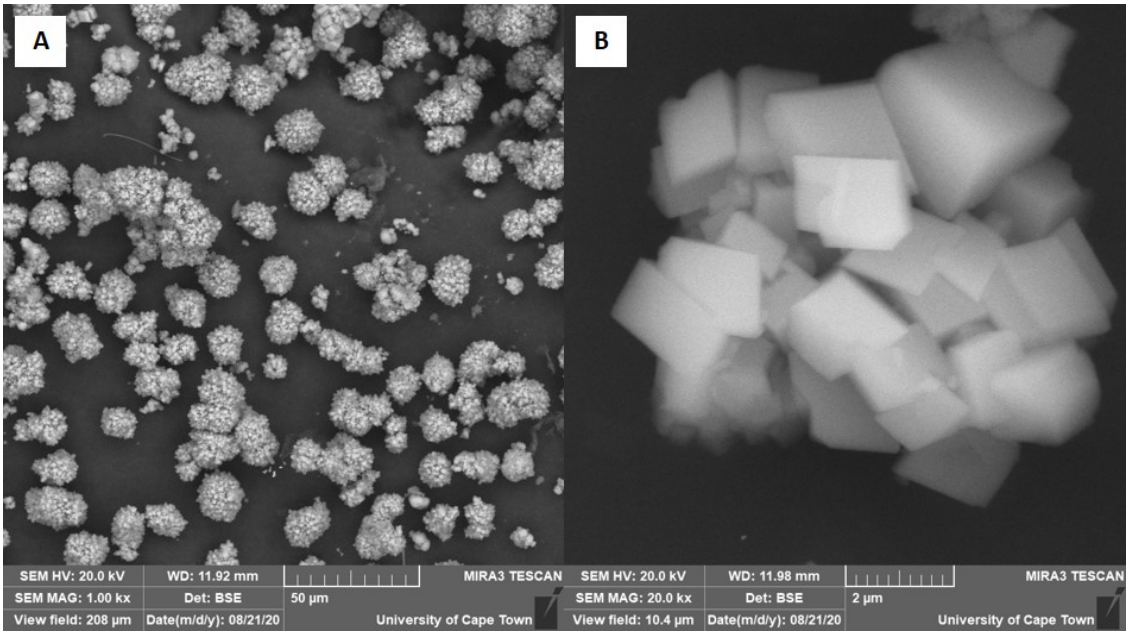

Figure C-3: SEM photograph of precipitants prepared using 3 L min^{-1} air at 50 µm (A) and 2 µm (B) scale.

C.5 Model Fit

The model was fit by first adjusting the initial OH^- concentration to match the initial pH measured experimentally. The simulated data were then fitted to the experimental data by adjusting the mass transfer coefficient (k_{La}), the calcite precipitation rate constant (k_{CaCO_3}). Table C-2 summarizes the values of the key parameters for each experimentally investigated flow rate that were inputted into the model. A comparison of the experimental and simulated results for the 9, 6, and 1.5 $L.min^{-1}$ air flow rates are shown in Figure C-4. The figures also include the Nash-Sutcliff model efficiency (NSE) coefficient. A value of 1 indicates a perfect fit, 0.5-0.65 indicates sufficient fit, and 0 indicates that the mean of the experimental values is as good a fit as the model. In the simulation of most air flow rates, an oscillation pH is observed at a pH of approximately 11. The cause of the oscillation is unknown; however, the model still provides a sufficient fit to accurately represent the experimental data. The oscillation also does not impact the conclusions drawn regarding the kinetics and different operating mechanisms.

Table C-2: Fitted values of the key parameters for each experimentally investigated air flow rate.

Exp. No.	Units	A1	A2	A3	A4	C1	C2
Flow rate	$L.min^{-1}$	1.5	3	6	9	1.5	1.5
CO_2 Conc.	%	0.04	0.04	0.04	0.04	1.0	100
k_{La}	d^{-1}	34 971	21 940	13 544	10684	34971	2180
OH^- initial	$mol\ L^{-1}$	0.056	0.049	0.048	0.044	0.041	0.061
k_{CaCO_3}	d^{-1}	139	139	139	139	584	584
TIC initial	$mol\ L^{-1}$			Assumed to be zero			
Urease Activity	$mol\ d^{-1}$			Assumed to be zero			

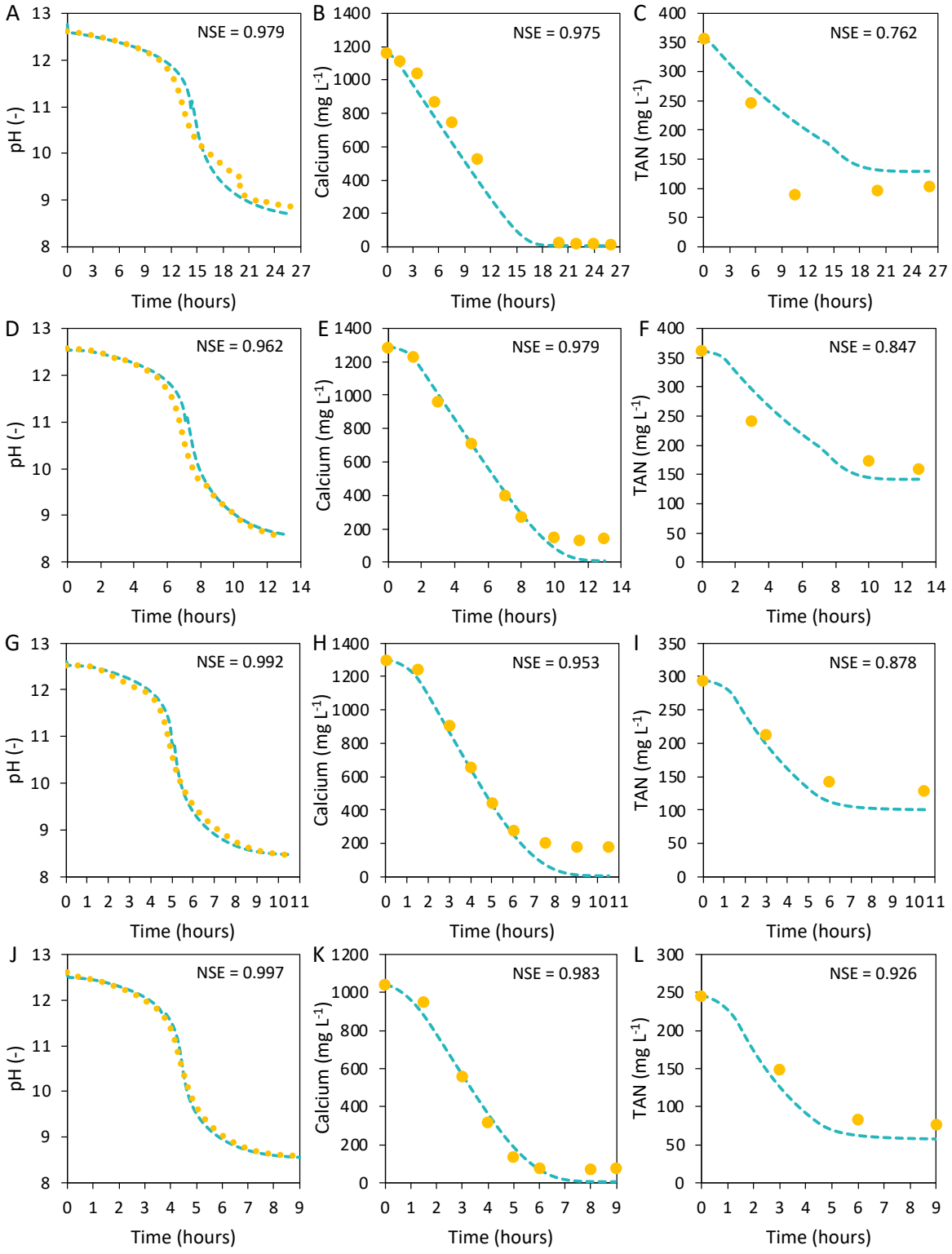

Figure C-4: Comparison of simulated (- - -) and experimental (• • •) results for an air flowrate of 1.5 L min^{-1} (A-C), 3 L min^{-1} (D-F), 6 L min^{-1} (G-I), and 9 L min^{-1} (J-L), where A, D, G, and J compare pH; B, E, H, and K compare calcium concentration; and C, F, I, and L compare the total ammoniacal nitrogen concentration (TAN). The Nash-Sutcliff model efficiency coefficient is also provided.

Figure C-5A and Figure C-5B compare the experimental data for 100% CO_2 at 1.5 L min^{-1} to the model if the dissociation constant for the inorganic carbon system was not adjusted for salinity and if creatinine was not included, respectively. Correction of the inorganic carbon system dissociation constants improved the NSE coefficient from 0.972 to 0.985 and the inclusion of creatinine improved the NSE coefficient from 0.848 to 0.985. It is evident that creatinine provides buffering capacity in the pH range of 8-9.

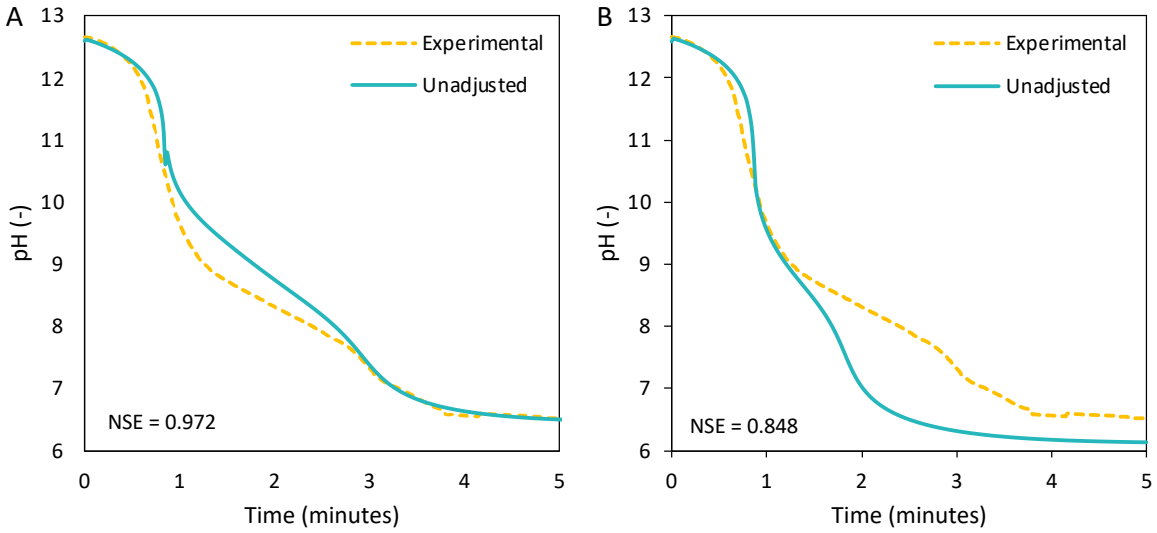

Figure C-5: Comparison of the experimental (- - -) and simulated data (—) if the bicarbonate and carbonate dissociation constants were not adjusted for salinity and temperature (A) and if creatinine was not included in the model's urine composition (B).

C.6 Impact of urine composition

Aquasim was used to simulate how different urine compositions would impact the pH (A) and calcium (B) and the results are shown in Figure C-6. From the simulation, it was observed that the initial composition will impact the rate at which the pH decreases and there is a correlation between the initial pH and the time required to reach equilibrium. Solutions with a higher pH require the addition of more CO_2 to reach the final pH. The simulation estimated an equilibrium calcium concentration of 5.9 ± 2.3 mg L^{-1}. The urine composition, therefore, has minimal impact on the final concentration but will influence the required operating time to reach X % calcium removal.

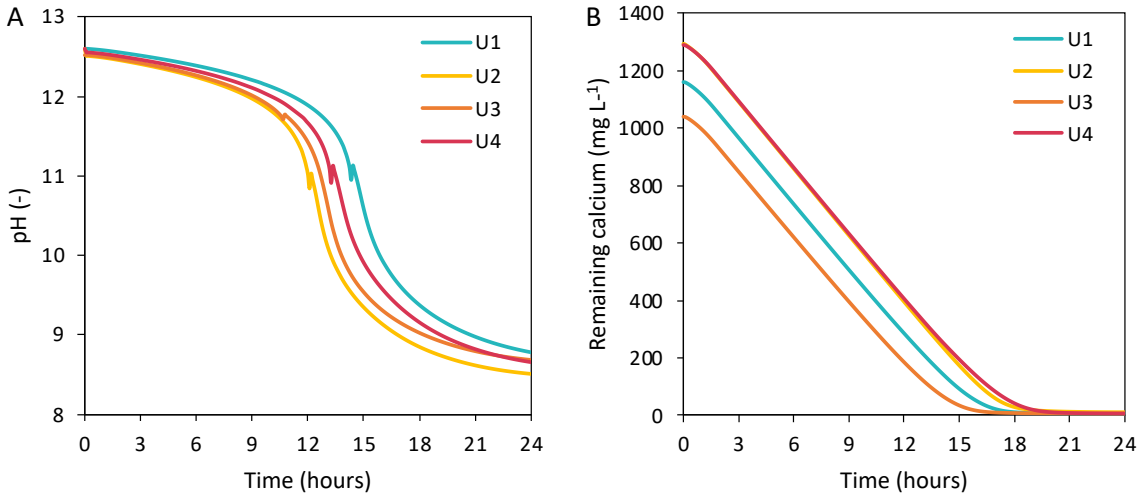

Figure C-6: Simulated impact of urine composition on the pH (A) and calcium concentration (B) at an air flow rate of 1.5 L min^{-1}.

C.7 Effect of treatment on concentration via reverse osmosis

The mass of solids formed during water removal for untreated and treated stabilized urine was simulated as shown in Figure C-7. The concentration of stabilized urine results in immediate precipitation of solids as the solution is saturated with $Ca(OH)_2$. The simulation did not account for any potential reactions with CO_2 present in the air and therefore the majority of the solid formed (up to 90%) water removal is $Ca(OH)_2$. This would not be the case in reality as CO_2 permeation in RO systems is common and this would result in the formation of $CaCO_3$ (Mitsoyannis and Saravacos, 1977).

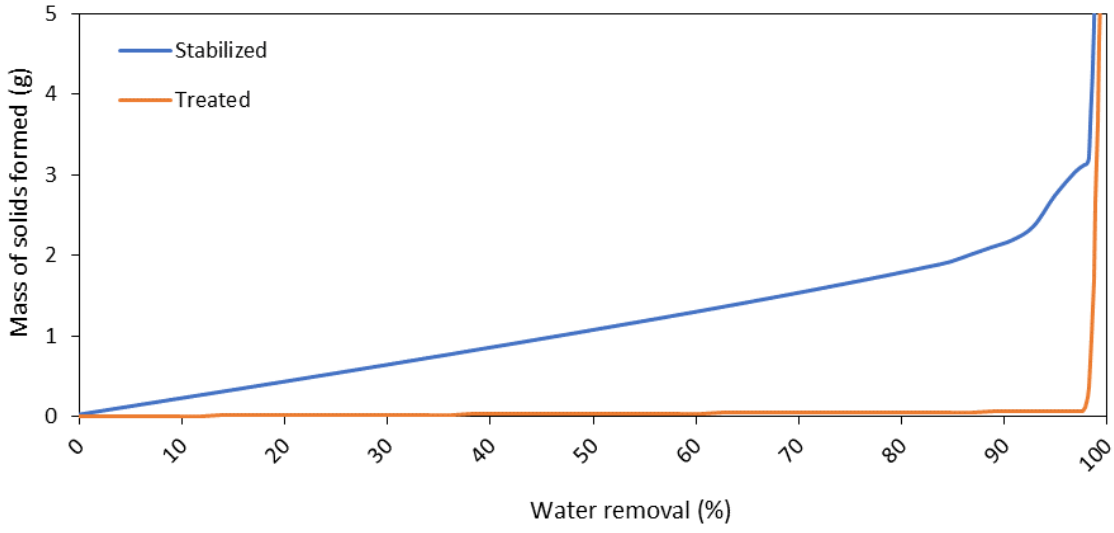

Figure C-7: Mass of solids formed as a function of water removal for $Ca(OH)_2$ stabilized urine and stabilized urine treated with air/CO_2 bubbling.

C.8 Power requirement calculations

The power requirements for each air flow rate were calculated according to Equation C-3 (Sierra et al., 2008). Where P_G/V_L is the power requirement per cubic meter of urine (W m^{-3}), ρ_L is the density of the liquid (kg m^{-3}), g is the rate of gravitational acceleration (9.8 m s^{-2}), and U_{sg} is the superficial gas velocity (m s^{-1}).

$$P_G/V_L = \rho_L g U_{sg} \qquad \text{(Equation C-3)}$$

The superficial gas velocity is a function of the gas flow rate (m^3 s^{-1}) and the cross-sectional area (m^2) as per Equation C-4.

$$U_{sg} = V_G/A \qquad \text{(Equation C-4)}$$

The reactor dimensions were calculated according to Hulatt (Hulatt and Thomas, 2011). A column configuration was used with a height of 2 m. Based on a total reactor volume of 1 m^3 the column diameter was determined to be 0.8 m. The cost of electricity was assumed to be \$0.06 kWh^{-1} (E.I.A, 2020).

C.9 Economic considerations

The operating time required to reach 95% calcium removal for different flow rates for 1% and 5% CO_2 was modelled and is presented in Figure C-8A. The precipitation rate constant determined by Velts et al. (2011) was used to model the 5% CO_2. Figure C-8B depicts how the operating time impacts the total operating costs. The flow rate can be increased to decrease the operating time required to reach 95% calcium removal. However, as the flow rate increases, the efficiency of the CO_2 used decreases, resulting in an exponentially increasing cost. The optimum operating flow rates were determined to be 0.75 and 0.1875 L min^{-1} L^{-1} for 1% and 5% CO_2 respectively.

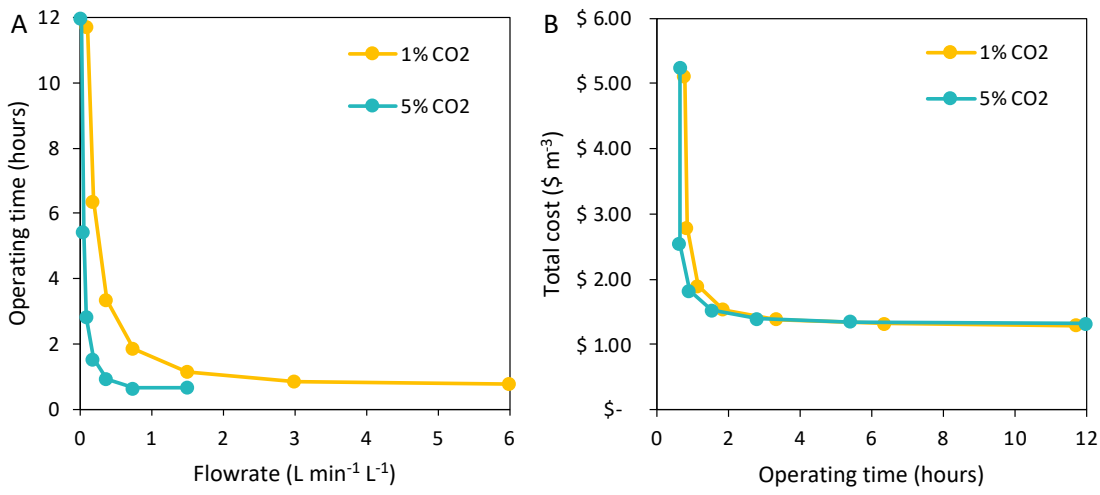

Figure C-8: Effect of flow rate on the operating time required for 95% calcium removal using 1% and 5 % CO_2 (A), and the total cost as a function of operating time (B).

APPENDIX D: CONCENTRATION USING REVERSE OSMOSIS

D.1 Air bubbling pre-treatment method

Treatment of $Ca(OH)_2$ stabilized urine (synthetic or real) using the air bubbling pre-treatment method involved weighing out 6 000 g of 1.2 µm filtered stabilized urine into a 10 L container. A cylindrical air stone (6 x 1.5 cm) was placed vertically in the solution and the air flow rate was 12 L min^{-1}. A stirrer (Hei-TORQUE Core, Heidolph Instruments, Germany) operating at 550 rpm was used to improve the mass transfer of CO_2 bubbles to the liquid phase. The pH of the solution was continuously monitored and when a pH of 8.5 was reached, the air bubbling was deemed to be complete. The treated urine was further filtered to 0.45 µm before beginning any membrane separation experiments.

D.2 Chemical addition pre-treatment method

The pretreatment of $Ca(OH)_2$ stabilized urine (synthetic or real) with the addition of $NaHCO_3$ or NH_4HCO_3 involved measuring out 5.1 L of stabilized urine and adding the relevant salt. Whilst only 5 L was required for the membrane experiments, an additional 100 mL was measured to account for any loss during the later filtration step. The calcium concentration of the stabilized urine was measured and the molar equivalent of $NaHCO_3$/NH_4HCO_3 plus 5% was calculated as per Equation D-1 and Equation D-2. An additional 5% of the carbonate salt was added to ensure complete calcium removal. The solution was mixed with a magnetic stirrer (F-13, Freed Electric, Israel) for at least 30 minutes to ensure complete conversion of calcium to $CaCO_3$ after which the solution was filtered to 0.45 µm before beginning any membrane experiments.

$$\text{Mass } NaHCO_3(\text{mg}) = \frac{1.05 \times Ca^{2+}\left(\frac{\text{mg}}{\text{L}}\right)}{40.08\left(\frac{\text{mg } Ca^{2+}}{\text{mmol}}\right)} \times 84.007\left(\frac{\text{mg } NaHCO_3}{\text{mmol}}\right) \times 5.1 \text{ L} \qquad \text{(Equation D-1)}$$

$$\text{Mass } NH_4HCO_3(\text{mg}) = \frac{1.05 \times Ca^{2+}\left(\frac{\text{mg}}{\text{L}}\right)}{40.08\left(\frac{\text{mg } Ca^{2+}}{\text{mmol}}\right)} \times 79.06\left(\frac{\text{mg } NH_4HCO_3}{\text{mmol}}\right) \times 5.1 \text{ L} \qquad \text{(Equation D-2)}$$

D.3 Real urine compositions

Measured	Units	Citric acid	$Ca(OH)_2$	Air bubbled
Urea-N	mg L-1	5 351	5 734	5 505
Ammonia-N	mg L-1	233	206	68.8
Total phosphate-P	mg L-1	418	n/d	n/d
Chloride	mg L-1	3 316	3 657	3 515
Sulfate	mg L-1	912	929	892
Magnesium	mg L-1	52.9	12.7	0.68
Calcium	mg L-1	51.9	1 200	42.1
Potassium	mg L-1	1 536	1 624	1 543
COD	mgO2 L-1	12 000	7 400	7 288
pH	-	3.35	12.45	8.45

Table D-1 summarizes the ion compositions, COD, and pH for the real urine stabilized with either citric acid or calcium hydroxide used in Chapter. The fresh urine used for both stabilization methods was the same composition, however, as fresh urine was stabilized immediately, the composition of the fresh urine before stabilization could not be measured. The concentrations measured in the citric acid and air bubbled urine were slightly lower than the $Ca(OH)_2$ stabilized urine because they were the concentrations measured after slight dilution caused by de-ionized water in the pipes of the RO system after cleaning.

Table D-1: Composition of the real urine stabilized with citric acid or calcium hydroxide, respectively. All experiments were conducted at 25°C.

Measured	Units	Citric acid	$Ca(OH)_2$	Air bubbled
Urea-N	$mg\ L^{-1}$	5 351	5 734	5 505
Ammonia-N	$mg\ L^{-1}$	233	206	68.8
Total phosphate-P	$mg\ L^{-1}$	418	n/d	n/d
Chloride	$mg\ L^{-1}$	3 316	3 657	3 515
Sulfate	$mg\ L^{-1}$	912	929	892
Magnesium	$mg\ L^{-1}$	52.9	12.7	0.68
Calcium	$mg\ L^{-1}$	51.9	1 200	42.1
Potassium	$mg\ L^{-1}$	1 536	1 624	1 543
COD	$mgO_2\ L^{-1}$	12 000	7 400	7 288
pH	-	3.35	12.45	8.45

n/d – not detected

D.4 Effect of pre-treatment method on sodium and chloride ion rejection

Effect of pre-treatment method on sodium and chloride ion rejection (Figure D-1) shows the rejection of sodium and chloride ions as a function of volume reduction factor (VRF) for synthetic urine stabilized with $Ca(OH)_2$. This urine had either no pre-treatment, or it was pre-treated with $NaHCO_3$ addition, NH_4HCO_3 addition, or air bubbling. The results show comparable sodium and chloride ion rejections for all three pre-treatment methods, remaining relatively constant with increasing VRF. The rejection of sodium and chloride ions for synthetic urine with no pre-treatment was comparable up to a VRF of 1.33, after which the rejection decreased significantly.

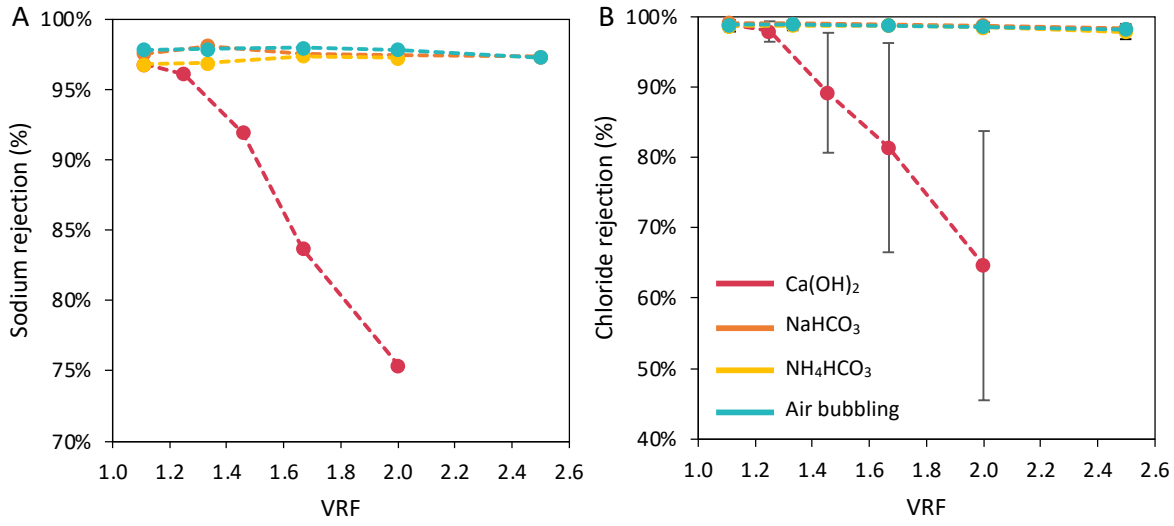

Figure D-1:Sodium (A), and chloride (B) rejection for synthetic urine stabilized with $Ca(OH)_2$ and then pre-treated with $NaHCO_3$, NH_4HCO_3, or air bubbling.

D.5 Ion rejection with real urine

Figure D-2 compares sodium and chloride ion rejection as a function of VRF for both real and synthetic urine. The real urine was either stabilized with citric acid or $Ca(OH)_2$ and pre-treated with air bubbling. For both sodium and chloride ions, the rejection was higher for real urine than for synthetic urine. Sodium and chloride ion rejection decreased after a VRF of 2.5. This could be an indication that concentration polarization was occurring. In all cases, rejection was greater than 97%.

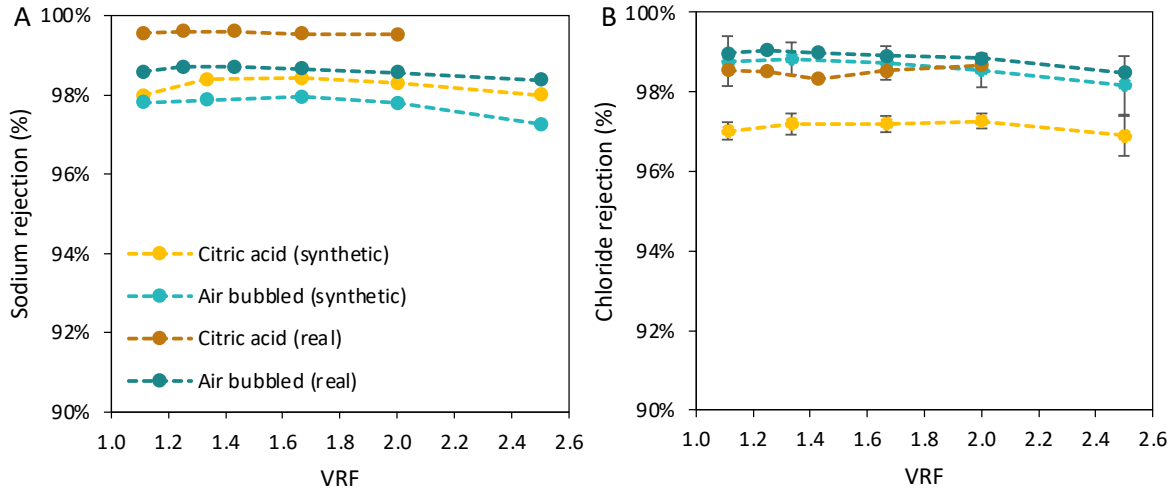

Figure D-2: Sodium (A), and chloride (B) rejection for real and synthetic urine stabilized with citric acid or with Ca(OH)2 and then pre-treated with air bubbling.

D.6 Effect of stabilization method on flux

Figure D-3A compares the normalized flux of real and synthetic urine stabilized with citric acid. Real urine shows a much steeper flux decline up to a VRF of 1.11, after which the flux decline follows a similar gradient. This suggests that a fouling layer may have built up quickly for the real urine run thus causing a steeper initial flux decline. However, for $Ca(OH)_2$ stabilized urine pre-treated with air bubbling (Figure D-3B), the flux decline as a function of VRF was the same regardless of whether real or synthetic urine was used. Figure D-3C compares the normalized flux for synthetic urine stabilized with citric acid and $Ca(OH)_2$ stabilized synthetic urine pre-treated with air bubbling. The citric acid stabilized urine shows a steeper flux decline which suggests that membrane scaling may have occurred. Figure D-3D compares the absolute flux for both real and synthetic urine. The absolute flux for acidified urine (synthetic and real) is lower and is likely due to the addition of citric acid which would increase the feed osmotic pressure.

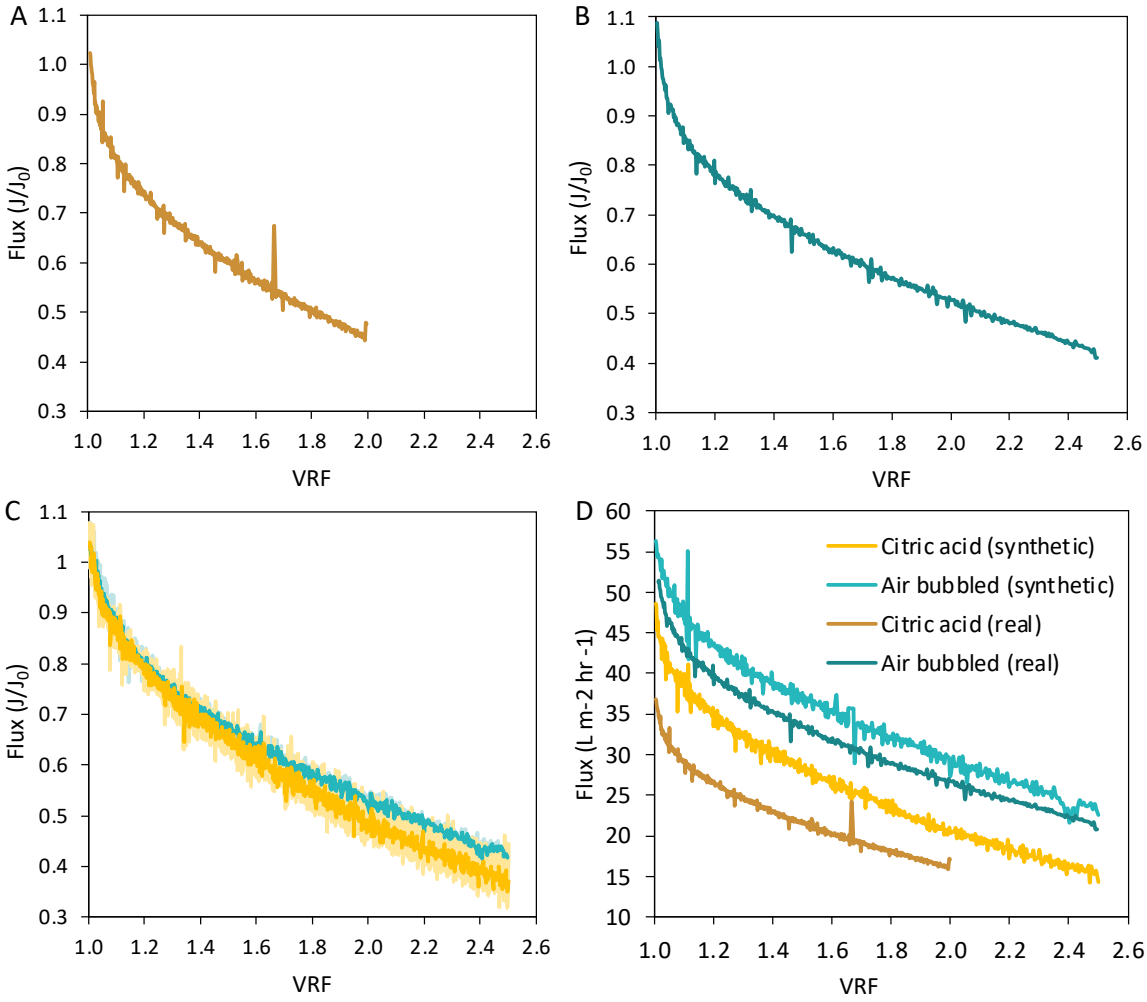

Figure D-3: Comparison of the normalized flux for synthetic and real urine stabilized with citric acid (A), stabilized with Ca(OH)2 and pre-treated with air bubbling (B), comparison of the normalized flux for synthetic urine stabilized with citric acid and synthetic urine stabilized with Ca(OH)2 and pre-treated with air bubbling (C), and comparison of the absolute flux for both real and synthetic urine stabilized with citric acid or stabilized with Ca(OH)2 and pre-treated with air bubbling (D).

D.7 Real urine mass balance

Figure D-4 shows the mass balance for the ions measured in real urine stabilized with $Ca(OH)_2$, pre-treated with air bubbling, and concentrated via RO (VRF = 2.5). Figure D-4 shows the mass balance for the ions measured in real urine stabilized with citric acid and concentrated via RO (VRF = 2).

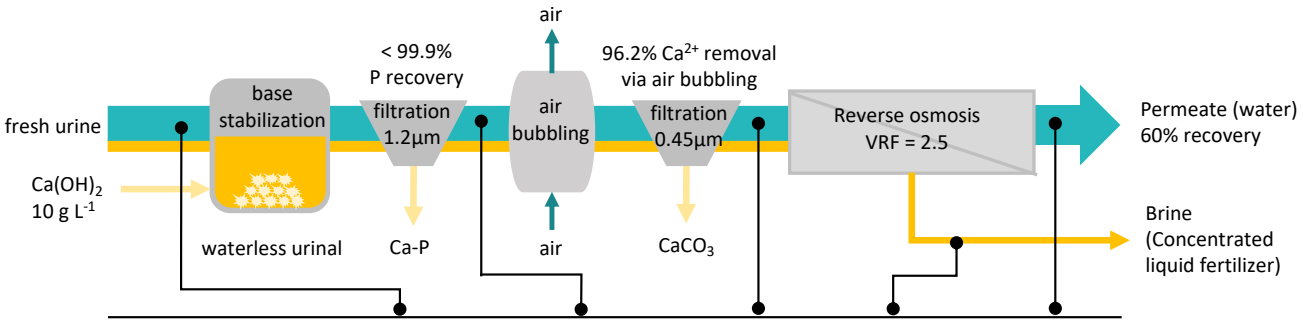

Compound	Fresh	$Ca(OH)_2$ stabilized	Pre-treated	Concentrate	Permeate
Urea-N (mg)	28 671	28 671	29 505	24 038	3 986
TAN (mg)	1 152*	1 028	369	195	32
Cl^- (mg)	18 286	18 286	18 838	17 441	191
SO_4^{2-} (mg)	4 644	4 644	4 780	4 610	29
Na^+ (mg)	10 688	10 688	10 747	10 077	102
K^+ (mg)	8 122	8 122	8 271	7 480	78
Ca^{2+} (mg)	281*	6 000	226	249	4.86
Mg^{2+} (mg)	280*	63.5	3.64	2.47	0.39
PO_4-P (mg)	2 226*	n/d	0.10	1.08	0.03
COD (mg O_2)	35 250	35 250	39 061	31 088	174
Conductivity (mS/cm)	n/m	20.9	13.1	29.4	0.28
pH (-)	n/m	12.45	8.45	8.55	9.85

**Masses based on concentrations measured in the real urine stabilized with citric acid.*

Figure D-4: Mass balance for ions present in real urine stabilized with $Ca(OH)_2$ pre-treated with air bubbling and then concentrated via RO to remove 60% of the water.

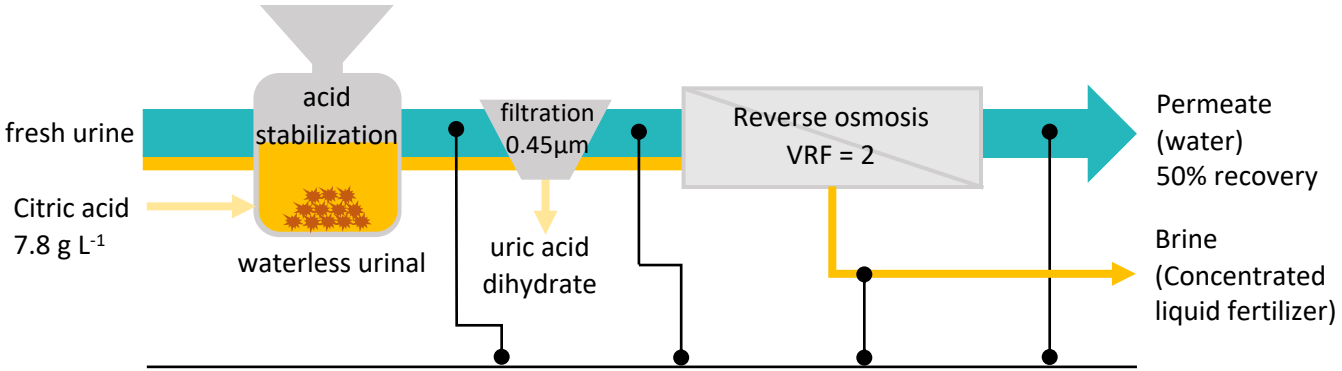

Compound	Fresh	Acidified	Concentrate	Permeate
Urea-N (mg)	28 143	28 680	27 513	1 831
TAN (mg)	1 276	1 248	1 244	6
Cl^- (mg)	17 510	17 771	20 494	184
SO_4^{2-} (mg)	4 914	4 888	5 239	12
Na^+ (mg)	10 688	10 278	10 519	25
K^+ (mg)	7 937	8 233	7 681	33
Ca^{2+} (mg)	281	278	209	4
Mg^{2+} (mg)	280	283	277	n/d
PO_4-P (mg)	2 226	28 680	27 513	1 831
COD (mg O_2)	n/m	64 320	63 248	218
Conductivity (mS/cm)	n/m	14.8	27.2	0.61
pH (-)	n/m	3.35	3.32	2.97

Figure D-5: Mass balance for ions present in real urine stabilized with citric acid and then concentrated via RO to remove 50% of the water.

D.8 Analysis of membrane surface

A scanning electron microscope (SEM) was used in conjunction with Energy dispersive X-ray spectroscopy (EDS) to analyze the RO membrane surface after concentrating synthetic urine stabilized with either citric acid or $Ca(OH)_2$ stabilized with either no pre-treatment, or pre-treatment with $NaHCO_3$ addition, NH_4HCO_3 addition, or air. Analysis of a membrane used to concentrate a low scaling potential urea, NaCl, and KCl solution is also included as a control. Figure D-6 displays the SEM images of the membrane surfaces after treatment with synthetic urine and Figure D-7 shows the membrane surface after treatment with real urine.

The RO membrane surface after treating base stabilized and air bubbled Figure D-7A urine is similar to the control Figure D-6A. However, there were a few small organic solids present Figure D-7B). Overall, minimal membrane scaling was observed. The RO membrane after treating citric acid stabilized urine showed both the presence of inorganic solids (Figure D-7C) and organic fouling (Figure D-7D).

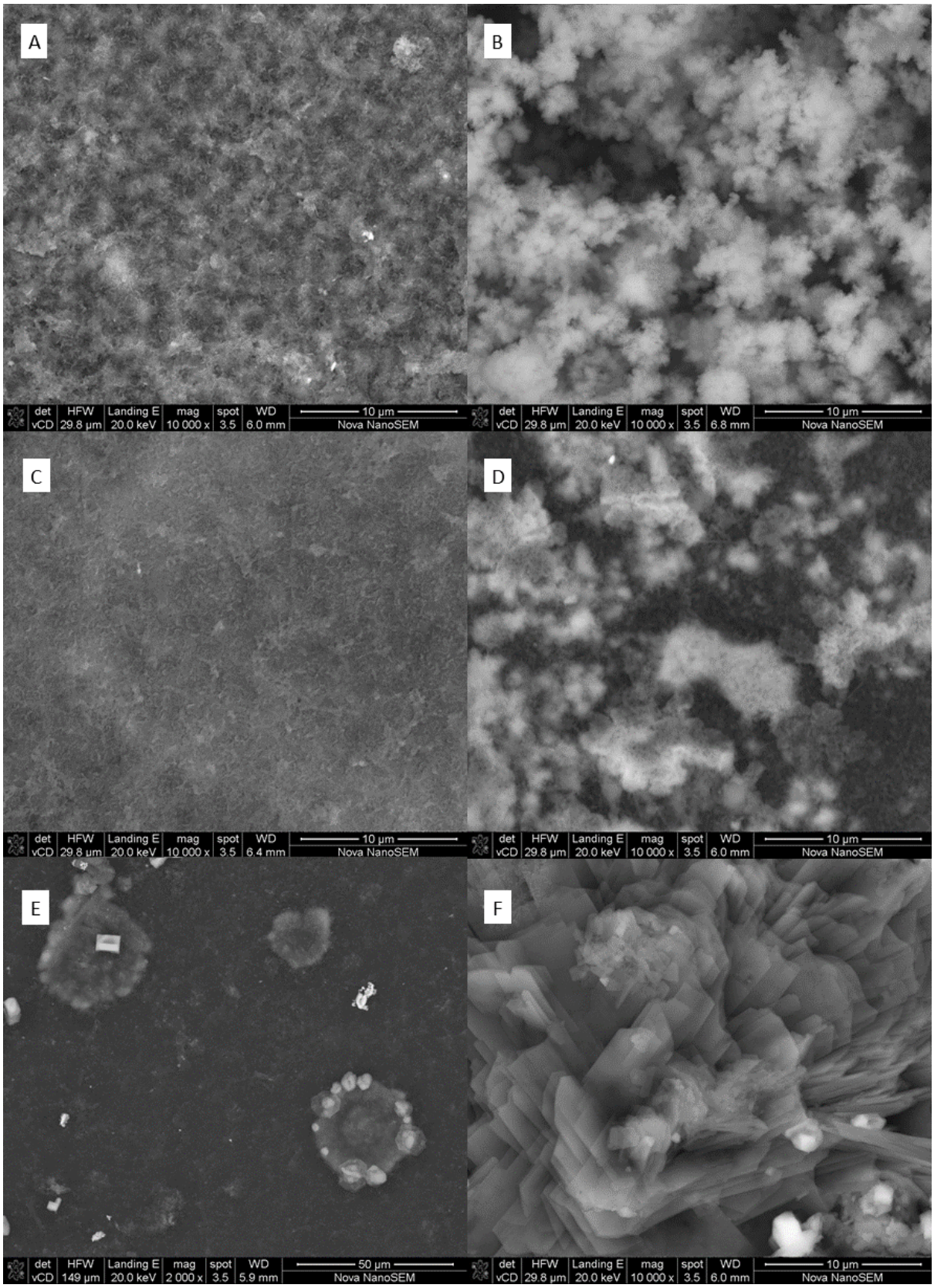

Figure D-6: SEM images of RO membrane surface after water removal from synthetic urine stabilized and pre-treated via control (A), $Ca(OH)_2$ (B), $NaHCO_3$ (C), NH_4HCO_3 (D), air bubbling (E), citric acid (F), with magnification varying from 10 – 50 µm.

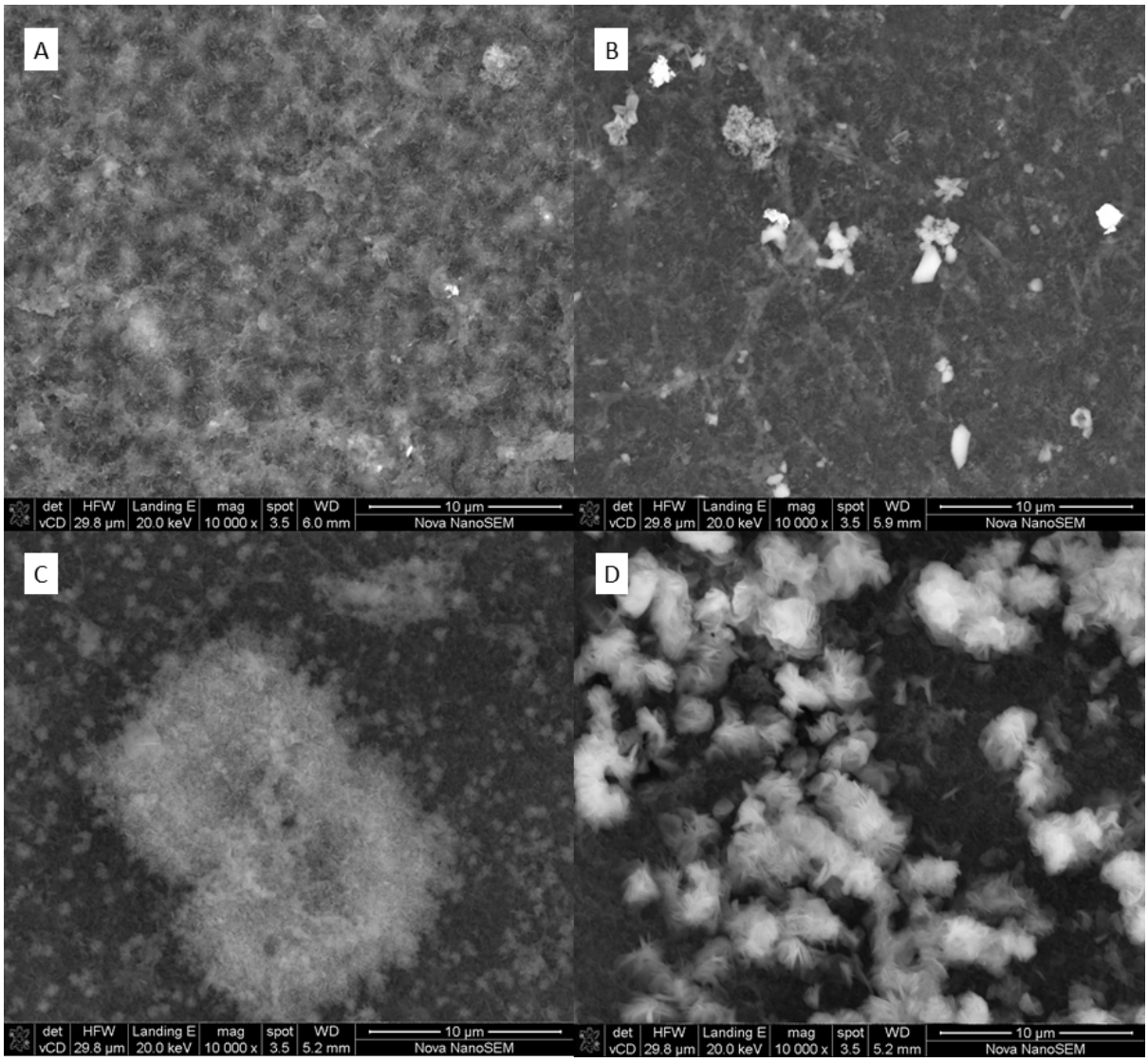

Figure D-7: SEM images of RO membrane surface after water removal from real urine stabilized with $Ca(OH)_2$ and pre-treated with air bubbling (A, B), real urine stabilized with citric acid (C, D) at a magnification scale of 10 µm.

D.9 Filtration of real urine

Before RO or pre-treatment, all urine was filtered with filter paper with a pore size of 1.2µm. Figure D-8 shows the filter paper after the filtration of real urine stabilized with citric acid (A, B), and real urine stabilized with $Ca(OH)_2$ (C, D). Where Figure D-8A and Figure D-8C were after the filtration of the supernatant and Figure D-8B and Figure D-8D were after the filtration of the settled solids. Filtration of the supernatant of acidified urine was challenging as the filter paper was quickly blocked, this was clear from the discoloration of the filter paper most likely caused by an undissolved compound (Figure D-8A). Filtration of the supernatant of $Ca(OH)_2$ stabilized urine was much quicker. There was only a small amount of residue on the filter paper caused by a slight overflow of undissolved $Ca(OH)_2$ (Figure D-8C).

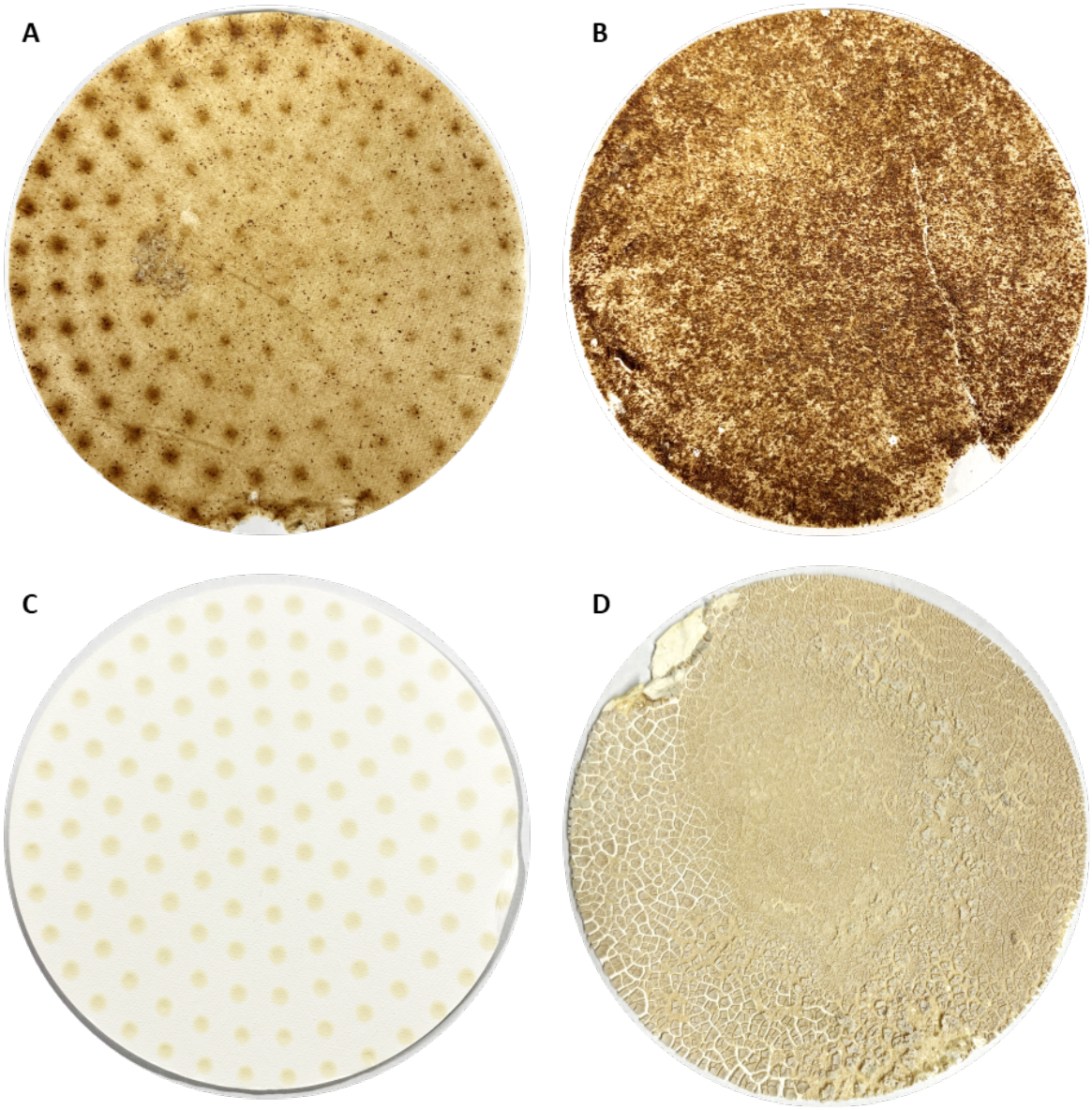

Figure D-8: Filter paper (1.2 µm) after the filtration of real urine stabilized with citric acid (A, B), and real urine stabilized with Ca(OH)2 (C, D). Where A and C is after the filtration of the supernatant and B and D is after the filtration of the settled solids.

D.10 Analysis of precipitates

The precipitates collected from the real urine stabilized with citric acid were analyzed using single crystal x-ray diffraction (XRD). Data were collected on a Bruker ApexII DUO diffractometer using graphite-monochromated Mo-Kα radiation (χ = 0.71073 Å). Data collection was carried out at 173(2) K. Temperature was controlled by an Oxford Cryostream cooling system (Oxford Cryostat). Cell refinement and data reduction were performed using the program SAINT (SAINT, 2003). The data was scaled, and absorption correction was performed using SADABS (Atwood and Barbour, 2003).

The structure was solved by direct methods using SHELXS-97 (Sheldrick, 2015) and refined by full-matrix least-squares methods based on F^2 using SHELXL-2014 and using the graphics interface program X-Seed (Barbour, 2001). The programs X-Seed and POV-Ray (Persistence of Vision Pty. Ltd., 2014) were used to prepare molecular graphic images. The analysis confirmed that the crystals were uric acid dihydrate and the ellipsoidal structure is shown in Figure D-9. Figure D-10 shows microscopic images (DM750 microscope with an ICC50 W camera, LEICA, Germany) taken of the crystals. Not all crystals had a defined shape. However, the crystals in the top-left have a shape very similar to uric acid dihydrate crystals documented by Herring (1962).

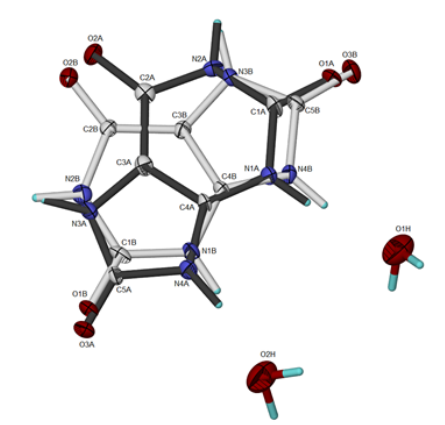

Figure D-9: Ellipsoidal structure of uric acid dehydrate.

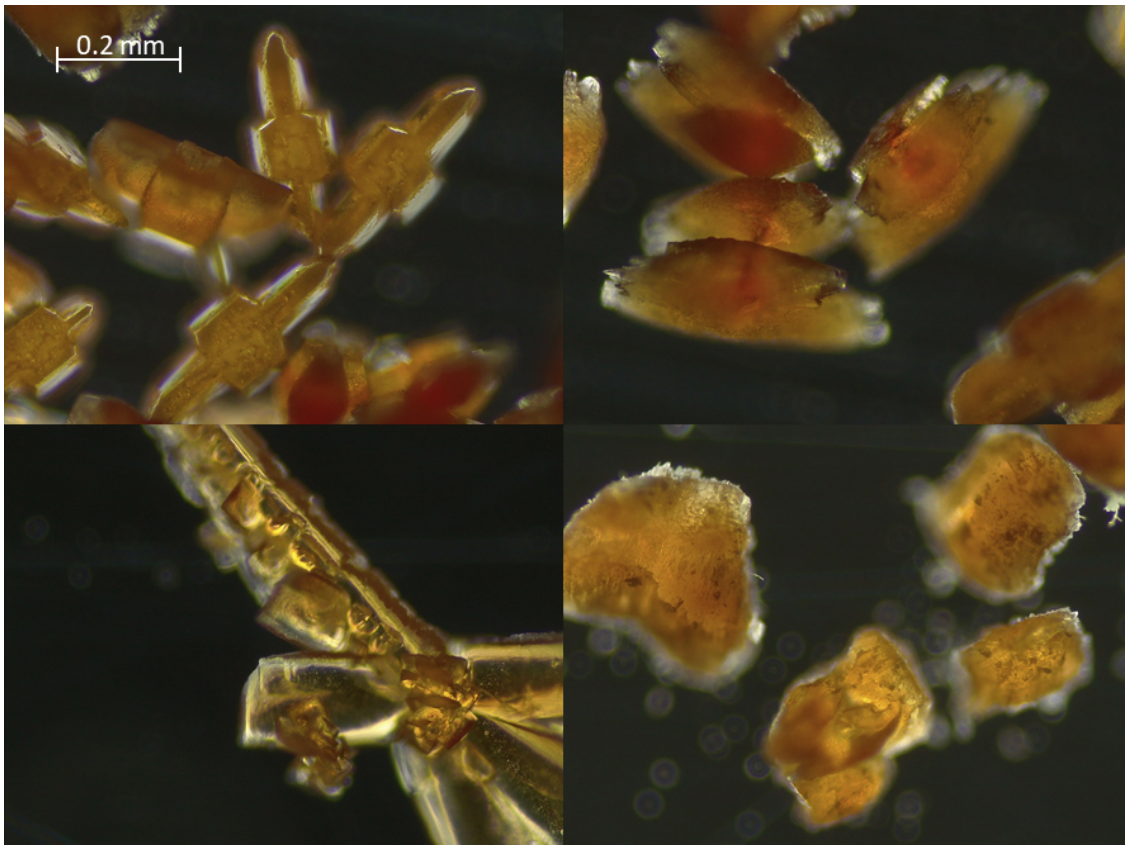

Figure D-10: Microscopic images of precipitates formed in real urine stabilized with citric acid.

D.11 Effect of pH on the performance of the RO membrane

Each stabilization method and pre-treatment option resulted in a different solution pH. The rejection of chloride, sodium, potassium, and urea achieved from each stabilization method and pre-treatment at a VRF of 2 was plotted to determine if there was a correlation between pH and rejection (Figure D-11). The red shaded region indicates a pH range outside the membrane's designed operating range (>11). The feed pH appears to have no significant effect on ion rejection (Na+, Cl-, K+) within the designed membrane operating pH range. However, feed pH does appear to affect urea rejection which decreases by 13% between a pH of 3.4 and 11.4. Ozaki and Li (2002) observed a similar trend with a 6% decrease in urea rejection between a pH of 3 and 9 using a low-pressure RO membrane. Berg et al. (1997) suggest that this phenomenon may be caused by electrostatic repulsion between the membrane's acidic functional groups that result in increased pore size and therefore decreased rejection. Outside the designed pH range a sharp decrease in rejection (up to 34%) for all compounds was observed. This indicates the importance of operating within the membrane's designed pH range to ensure the membrane lifespan is not affected (Franks et al., 2009).

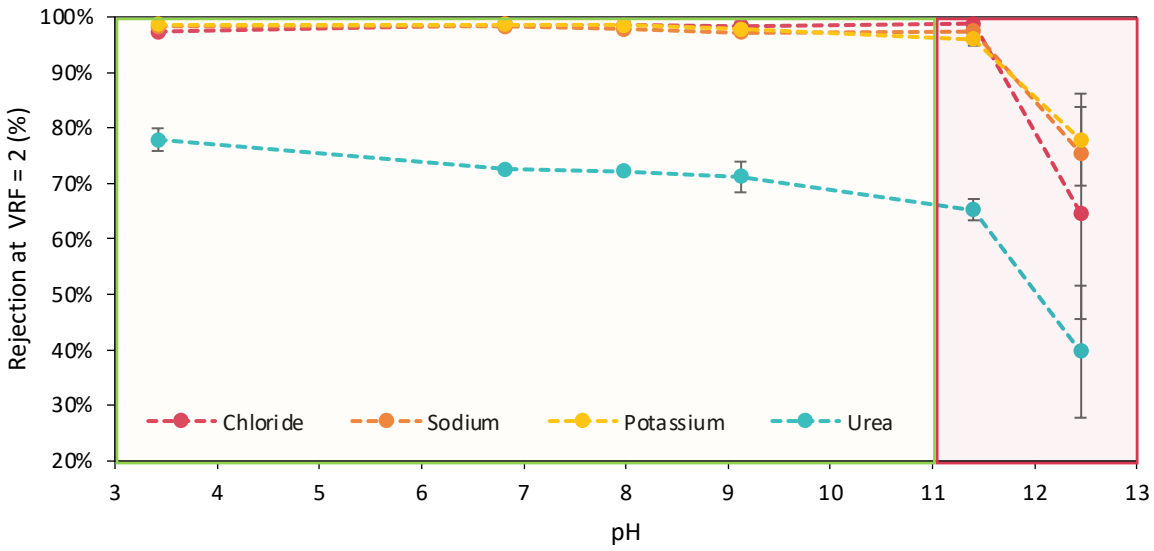

Figure D-11: Rejection of urea, chloride, potassium, and sodium at VRF = 2 as a function of brine pH. The shaded area indicates a pH outside the designed operating range of the membrane.

APPENDIX E: HYDRBID NANOFILTRATION

E.1 Real urine compositions

Table E-1 is a summary of the real urine compositions used in Chapter 8.

Table E-1: Composition of different stabilized urine samples used in this Chapter 8.

Measured	Units	U1	U2	U3	U4	U5
Urea	mg L^{-1}	11 506	11 288	9 640	11 175	9 241
Ammonia-N	mg L^{-1}	87	337	74	144	109
Total phosphate-P	mg L^{-1}			BDL		
Chloride	mg L^{-1}	3 077	3 376	2 806	3 606	2 771
Sodium	mg L^{-1}	1680	2050	1525	1780	1565
Sulfate	mg L^{-1}	854	1 048	796	904	918
Magnesium	mg L^{-1}			BDL		
Calcium	mg L^{-1}	107	49	118	142	193
Potassium	mg L^{-1}	1 394	1 404	1 229	1858	1 251
COD	mg L^{-1}	6 125	6 325	6 075	5625	7 063
pH	-	9.0	8.6	8.4	8.5	8.4
Experiment	-	NF270 (1&2)	NF270 (3)	NF90 (1)	NF90 (2)	NF90 (3)

BDL – Below detection limit.

E.2 Effect of operating pressure

To determine the effect of operating pressure on rejection and flux, 5 L of urine was circulated through a pre-compacted NF90 and NF270 membrane at a fixed pressure. When 5% of the water had been removed (as permeate) it was returned to the feed tank to keep the concentration of the feed constant. The permeate flux was monitored until it reached steady state. Once steady state was reached, permeate was collected until a 10% water removal (as permeate) or a VRF of 1.11 was achieved. Samples of the permeate and brine were then taken for analysis. This process was repeated at four additional feed pressures ranging from 15 to 35 bar.

E.3 Ion concentration as an indication of urea concentration

Previous studies that recovered nutrients from hydrolyzed urine often did not (or were not able to) measure the initial urea concentration before urea hydrolysis. It is therefore difficult to calculate the true loss of nitrogen due to ammonia volatilization. Only four studies could be found, that measured the initial urea concentration before hydrolysis had occurred. Urea hydrolysis does result in the precipitation

of compounds such as struvite and calcium phosphate, however, sulfate ions do not precipitate during this process. It was hypothesized that there may be a correlation between the concentration of sulfate and urea and that this correlation could then be used to determine the original urea concentration of hydrolyzed urine. The calculated initial urea concentration could then be used to determine N losses due to volatilization. The urea and sulfate concentrations measured in either fresh or stabilized urine from 10 different studies were compared to determine if there was any significant correlation. Table E-2 summarizes the values collected.

Table E-2: Urea and sulfate concentrations measured in real fresh or stabilized urine from varying studies.

Urea-N (mg-N L^{-1})	Sulfate (mg-SO_4 L^{-1})	Reference
5 362	886	Chapter 8 urine compositions
5 260	1083	
4 496	796	
5 207	991	
2 713	433	Chapter 5 urine compositions
5 516	899	
3 058	388	
7 539	1 255	
8 568	1 516	Chapter 6 urine composition
9 451	1 583	
4 178	826	
5 176	979	
6 638	1 018	
5 292	864	(Pronk et al., 2006b)
5 810	748	(Udert et al., 2003a)
6 475	1 095	(Wei et al., 2018)
5 420	825	(Randall et al., 2016)
5 935	1 014	(Vasiljev et al., 2022)
4 217	723	(Volpin et al., 2019c)
3 090	508	(Riechmann et al., 2021a)

E.4 Rejection as a function of transmembrane pressure

Nanofiltration is typically used to treat brackish water and is operated at low pressures (5-20 bar) to minimize energy consumption. However, urine has a much higher TDS and therefore osmotic pressure. Permeate flux is also a function of the difference between the operating and feed osmotic pressure. Higher operating pressures are therefore required to allow for sufficient driving force for permeation to occur. Filmtec NF membranes have a maximum design operating pressure of 41 bar. The effect of feed pressure between 15 and 35 bar was investigated to determine its effect on urea rejection, flux, and the rejection of other ions as shown in Figure E-1. Feed pressure had a more significant effect on urea rejection for the NF90 membrane than for the NF270 membrane. These results suggest that the NF90 membrane should be operated at a lower pressure to maximize the urea recovery, however, this would

limit overall water removal (as permeate) potential due to a decrease in driving force as the urine is concentrated which may cancel out the effect on overall urea recovery. Whilst the concentration of urea in the permeate may be higher (at lower operating pressure), the overall volume collected will be less.

Increasing the operating pressure resulted in a linear increase in permeate flux (Figure E-1B). This is advantageous as it also reduces the total membrane area, and therefore equipment capital costs, required or it reduces the operating time required to treat a fixed volume of urine, and therefore operating costs. Increasing the pressure improved ion rejection for both the NF90 and NF270 membranes. The increase in rejection was most significant for monovalent ions using the NF270 membrane. This supports the recommendation to use a higher operating pressure to improve the urea purity.

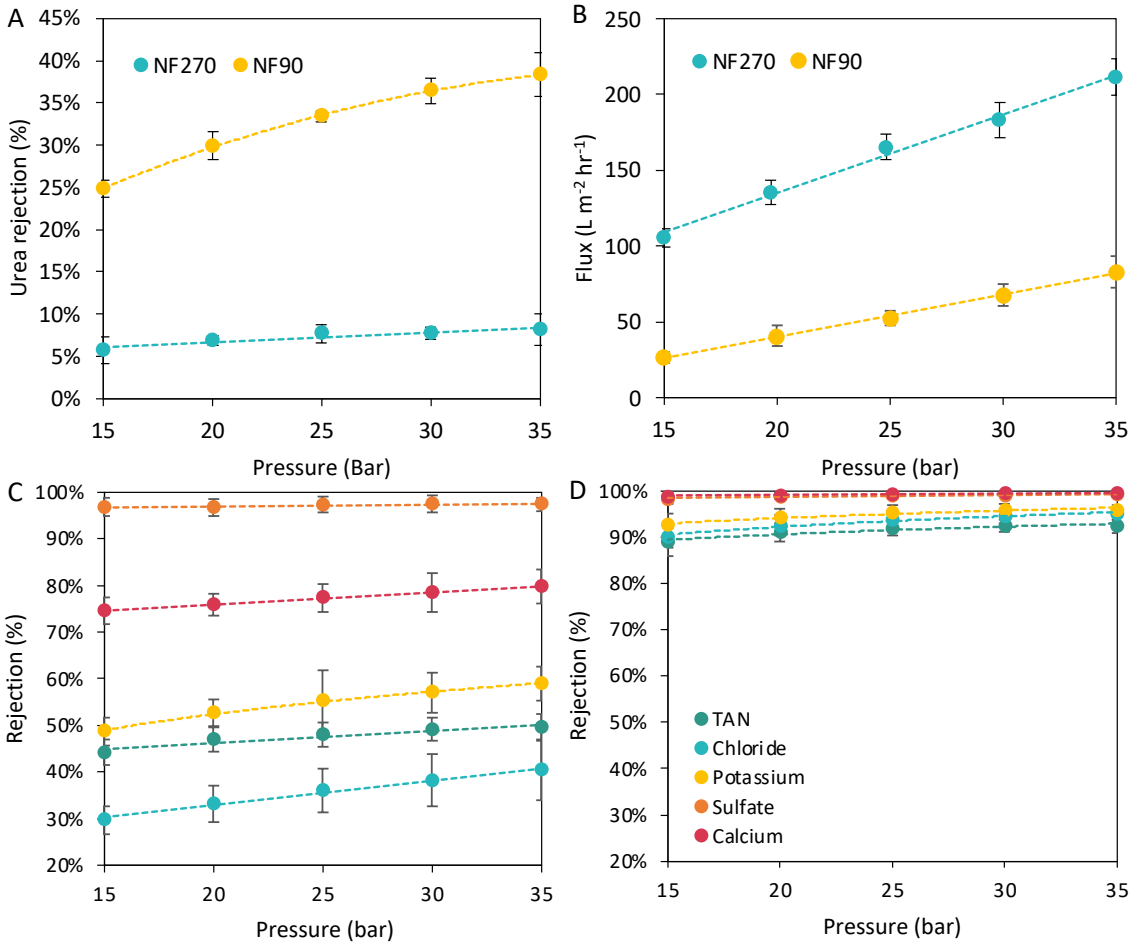

Figure E-1: Effect of transmembrane pressure on urea rejection (A), permeate flux (B), NF270 ion rejection (C), and NF90 ion rejection (D).

E.5 Ion rejection of the NF270 and NF90 membranes

Figure E-2 compares the ion rejection capabilities of the NF90 and NF270 membranes for both real and synthetic urine as a function of volume reduction factor (VRF). No significant difference in the rejection of ions was observed for real and synthetic urine for either membrane, except for the rejection of calcium

by the NF270 membrane. Calcium removal during air bubbling for synthetic urine is not as effective as with real urine. Synthetic air bubbled urine, therefore, has a much higher initial calcium concentration (312 ± 63 vs. 130 ± 44 mg L^{-1}) which may result in the differences in rejection. As expected, the rejection of monovalent ions by the NF270 membrane was poor. However, the rejection of divalent ions sulfate and calcium was much higher (>94% and >66%, respectively). Due to the poor ion rejection, the purity of the urea collected in the permeate does not improve much.

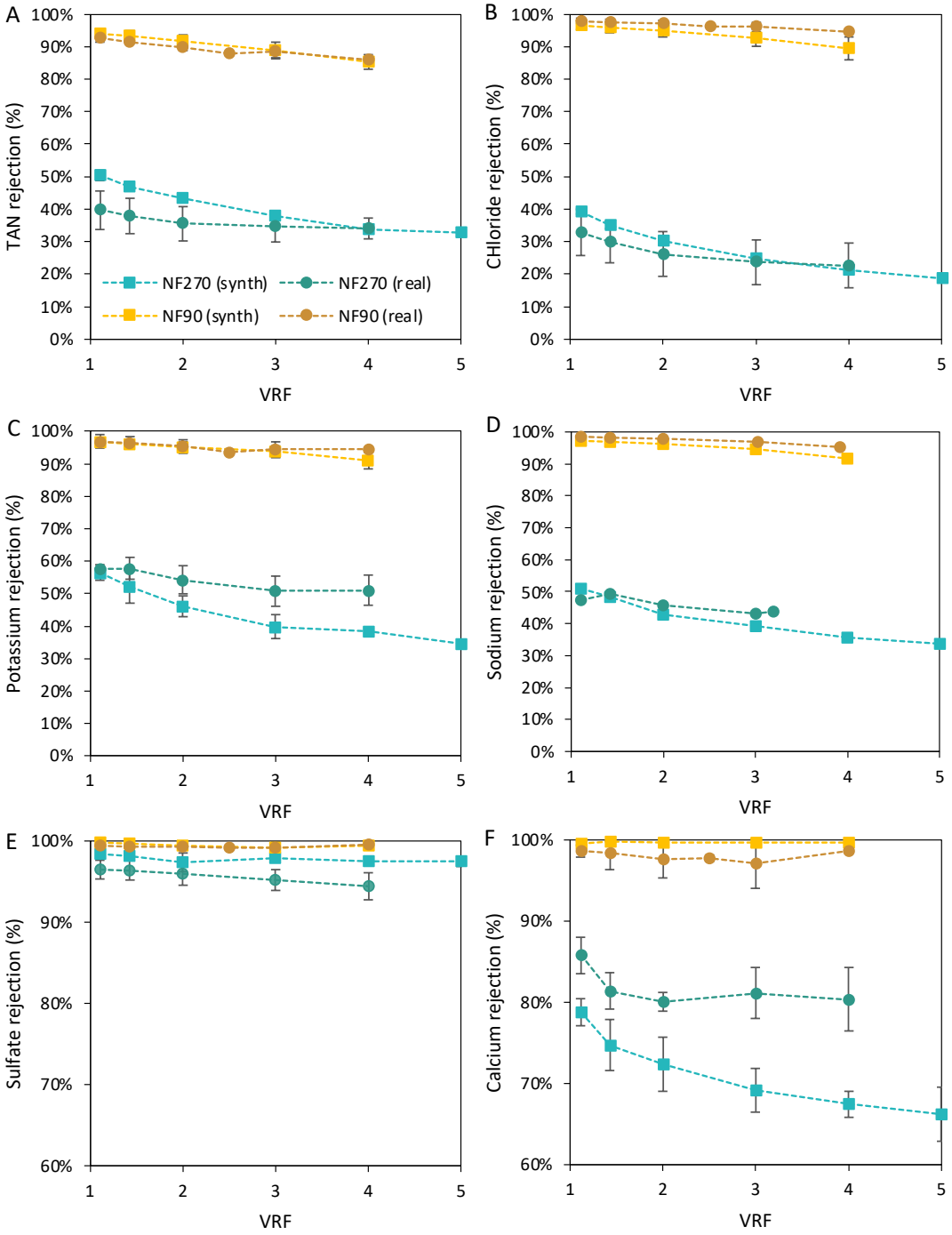

Figure E-2: Rejection of TAN (A), chloride (B), potassium (C), sodium (D), sulfate (E), and calcium (F) as a function of VRF for the NF270 and NF90 membranes using synthetic and real urine.

The NF90 membrane also provided better rejection of divalent ions compared to monovalent ions. However, in general, all ions were well rejected (>86%). The pH of air bubbled urine is approximately 8.5 (for real urine, and 8.0 for synthetic urine). The pKa for the ammonia/ammonium system is 9.25 therefore the majority of ammoniacal nitrogen present in both synthetic and real urine will be in the form of charged ammonium. This explains the much higher rejection of total ammoniacal nitrogen (TAN) when compared to urea.

E.6 Permeate flux

Figure E-3 depicts the permeate flux for the NF90 and NF280 membranes for both real and synthetic urine. There are two factors that caused the flux to decline. As the brine is continuously circulated it becomes more concentrated and its osmotic pressure increases resulting in a decrease in permeate flux. Membrane fouling can also result in flux decline. It is clear when comparing the synthetic and real urine (for both the NF90 and NF270 membranes) that membrane fouling occurred as the flux decline is much steeper. The flux decline was also steeper for the NF270 real urine compared to the NF90 membrane. In Chapter 7, no fouling was observed when concentrating real urine ($Ca(OH)_2$ stabilized, air bubbling pre-treatment) with an SW30 membrane. It is likely that differences in fouling between the three membranes are due to differences in urine composition. Further investigation into how urine composition and membrane type affects the potential for membrane fouling is therefore required.

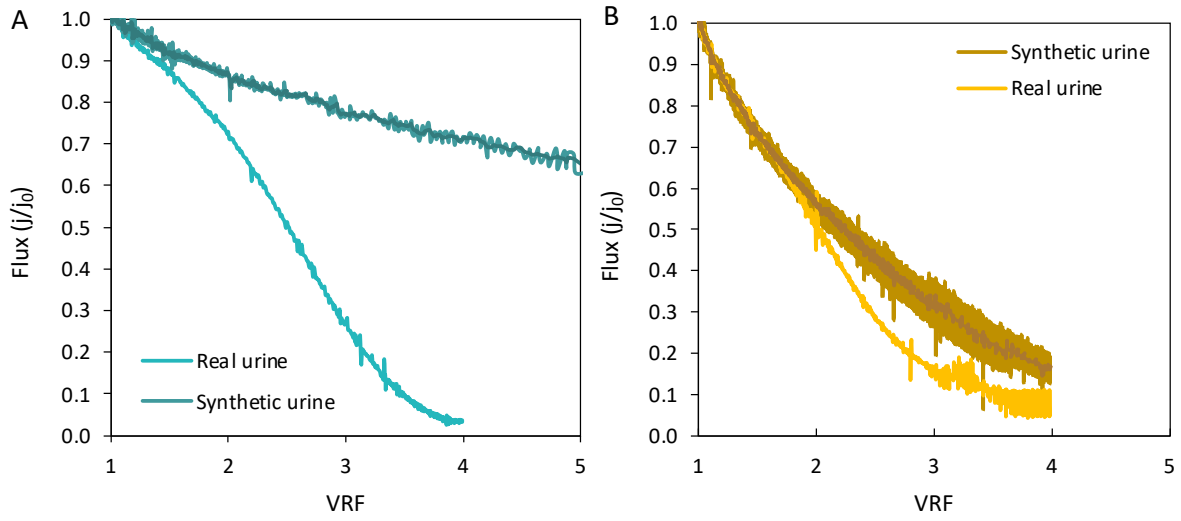

Figure E-3: Normalized permeate flux as a function of VRF for the NF270 (A), and NF90 (B) membranes for both synthetic and real urine. The light area indicates the variation between the experimental runs and the darker line is the average.

E.7 Relationship between urea and sulfate concentration

Figure E-4 plots the concentration of urea versus the concentration of sulfate. A linear trendline explained 90.2% of the correlation between the data. Whilst the sulfate concentration is not a perfect

predictor of the urea concentration in fresh or stabilized urine it was determined that the correlation was sufficient such that it could be used to estimate an initial urea concentration in hydrolyzed urine. The relationship between chloride and sodium, and urea concentration was also investigated, however, the correlation using sulfate was more statistically significant.

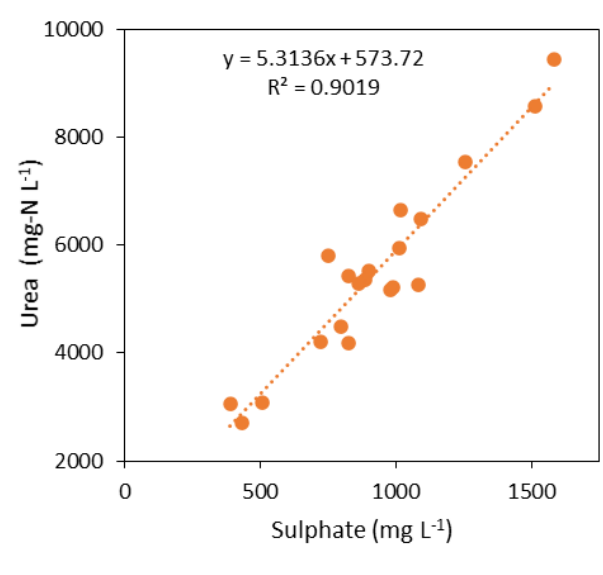

Figure E-4: Correlation between sulfate and urea concentration in real fresh or stabilized urine.

E.8 Nitrogen loss during urea hydrolysis

Ten studies using real hydrolyzed urine were analyzed to determine if the N lost during urea hydrolysis, and subsequent ammonia volatilization could be quantified. If an initial fresh urine total nitrogen concentration was available then this was used to calculate N-loss, however, if not the initial nitrogen concentration was estimated using the sulfate concentration. The results of this analysis are summarized in Table E-3. Measured N loss varied from 9-29%, and predicted N loss had a larger range (0 – 49%). The average N-loss was 24 ± 15%. This large variation in N loss during urea hydrolysis was expected as there are many factors that would influence the potential for ammonia volatilization (as discussed in the main paper). For example, a treatment process may recover 90% of the N from hydrolyzed urine but accounting for N-loss during urea hydrolysis and storage (assuming 24%) would reduce the overall recovery to 68%. This distinction is important when comparing processes that treat hydrolyzed urine versus stabilized urine to ensure that all nitrogen has been accounted for.

Table E-3: Calculated and predicted nitrogen loss during the hydrolyzation of real urine.

Sulfate (mg L^{-1})	Initial N (mg L^{-1})	N after hydrolysation (mg L^{-1})	N-Loss (%)	Reference
993	5 850	3 576	38%	(Jönsson et al., 1997)
748	5 810[a]	5 020	17%[a]	(Udert et al., 2003a)
778	4 708	2 390	49%	(Udert and Wächter, 2012)
721	4 336	2 450	44%	(Hug and Udert, 2013)
308	2 210	1 990	10%	(Fumasoli et al., 2016)
708	4 336	4 140	5%	
822	4 941	2 790	44%	(Zöllig et al., 2017)
234	1 817	1 860	-2%	
1 223	7 072	5 037	29%	(Jagtap and Boyer, 2018)
1 095	6 475[a]	6 159	5%[a]	(Wei et al., 2018)
n.m	7 284[a]	6 619	9%[a]	(Xu et al., 2019)
n.m	7 284[a]	5 203	29%[a]	
955	5 648	3 745	34%	(Ray et al., 2020)
998	5 877	4 330	26%	
925	5 489	4 375	20%	
957	5 659	4 415	22%	

a – fresh/initial nitrogen concentrations were measured in the study and N-loss is based on measured values rather than predicted values. n.m – not measured.

E.9 Complete treatment process mass balance

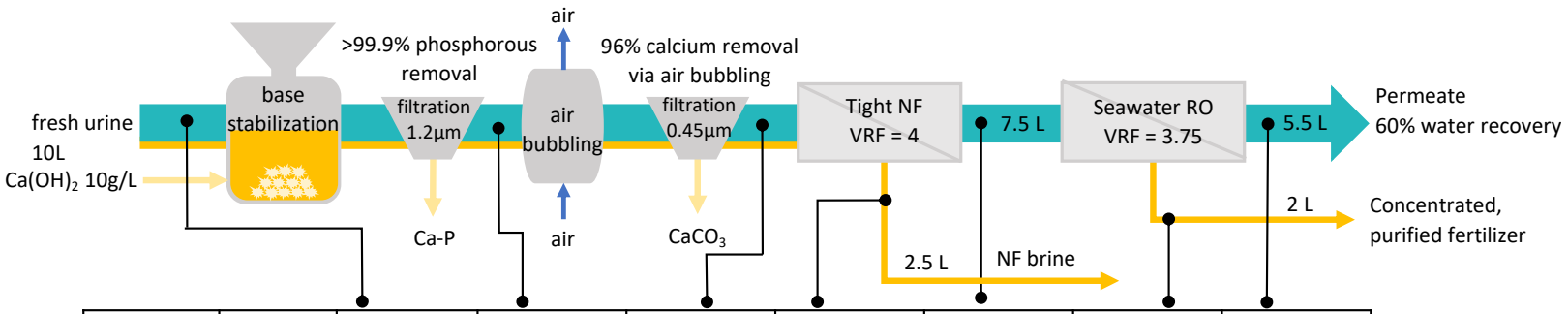

Compound	Units	Fresh	Stabilized	Pre-treated (NF feed)	NF brine	NF permeate	RO brine (End product)	RO permeate
Urea-N	g	92 410			48 303	44 558	30 218	14 340
TAN		3 187*	2 855	1 140	858	113	92.2	9.35
Cl^-		27 710			25 310	990	789	178
SO_4^{2-}		9 180			9 150	30	24.2	5.8
Na^+								
K^+		12 510			11 280	443	322	131
Ca^{2+}		520*	13 143	1 930	1 475	9.15	BDL	BDL
Mg^{2+}		530*	179	BDL	BDL			
PO_4-P		4 180*	0.01		BDL			
COD	mg O_2	n.M	70 630		57 625	1 740	1 731	8.70
Conductivity	mS cm^{-1}		-	11.9	38.3	0.65	1.50	0.03
pH	-		12.45	8.4	8.4	9.1	8.3	8.7
Volume	L	10	10	10	7.5	2.5	2	5.5

	$Ca(OH)_2$	Ca-P	$CaCO_3$	Units
Ca^{2+}	541	343	382	g/kg solid
Mg^{2+}	5.3	12.2	3.4	
PO_4-P	-	20.1	-	

Figure E-5 is the complete mass balance for a hybrid NF-RO process using a tight NF membrane and assuming overall water removal of 80%.

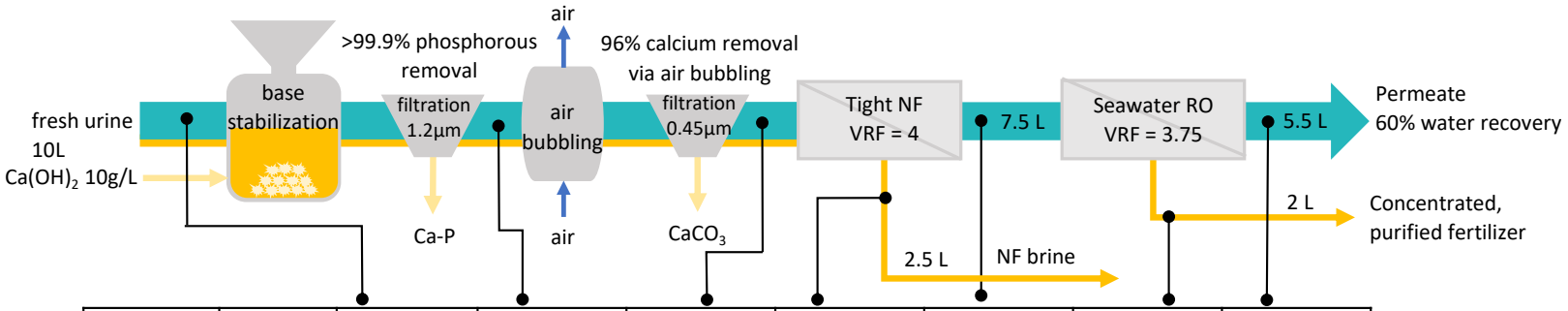

Compound	Units	Fresh	Stabilized	Pre-treated (NF feed)	NF brine	NF permeate	RO brine (End product)	RO permeate
Urea-N	g	92 410			48 303	44 558	30 218	14 340
TAN		3 187*	2 855	1 140	858	113	92.2	9.35
Cl^-		27 710			25 310	990	789	178
SO_4^{2-}		9 180			9 150	30	24.2	5.8
Na^+								
K^+		12 510			11 280	443	322	131
Ca^{2+}		520*	13 143	1 930	1 475	9.15	BDL	BDL
Mg^{2+}		530*	179	BDL	BDL			
PO_4-P		4 180*	0.01		BDL			
COD	mg O_2	n.M	70 630		57 625	1 740	1 731	8.70
Conductivity	mS cm^{-1}		-	11.9	38.3	0.65	1.50	0.03
pH	-		12.45	8.4	8.4	9.1	8.3	8.7
Volume	L	10	10	10	7.5	2.5	2	5.5

	$Ca(OH)_2$	Ca-P	$CaCO_3$	Units
Ca^{2+}	541	343	382	g/kg solid
Mg^{2+}	5.3	12.2	3.4	
PO_4-P	-	20.1	-	

Figure E-5: Complete mass balance for a hybrid NF-RO process including $Ca(OH)_2$ stabilization and air bubbling pre-treatment. Mass balance for calcium phosphate is based on the work of Flanagan and Randall (2018). *Values estimated from Chapter

APPENDIX F: EUTECTIC FREEZE CRYSTALLIZATION

F.1 Synthetic pre-concentrated urine recipes

Table 6 shows the salt concentrations required for the synthetic post-RO and pre-concentrated urine recipes. For the freezing experiments, two synthetic urine recipes were used. One was developed to represent the urine concentration post-RO (70% water removal) and the second was developed to represent the urine pre-concentrated to just before the eutectic point. Both synthetic recipes assumed that air bubbling treatment had already occurred.

Table F-1: Recipe for synthetic urine that mimics RO and pre-concentration with FC.

Compound		Post-RO ($g\ L^{-1}$)	Pre-concentrated ($g\ L^{-1}$)
Urea	$CO(NH_2)_2$	35.06	105.4
Sodium chloride	NaCl	12.80	42.25
Potassium chloride	KCl	12.55	41.81
Sodium dihydrogen phosphate	NaH_2PO_4	-	-
Sodium sulfate	Na_2SO_4	4.793	15.97
Ammonium acetate	CH_3OONH_4	1.815	5.569
Calcium chloride dihydrate	$CaCl_2{\cdot}2H_2O$	1.791	5.951
Magnesium chloride	$MgCl_2$	-	-
Sodium Acetate	NaC_2H_3O	4.863	16.39

F.2 Cascading freeze concentration procedure

For the concentration of real urine (post-RO, 70% water removal), a cascading concentration procedure (Figure F-1) was used. For synthetic urine, this procedure was only used for FC1 and FC2. For EFC, the pre-concentrated synthetic urine composition (Table F-1) was used. In a cascading procedure, the liquid from the previous step was used as the feed for the next FC step.

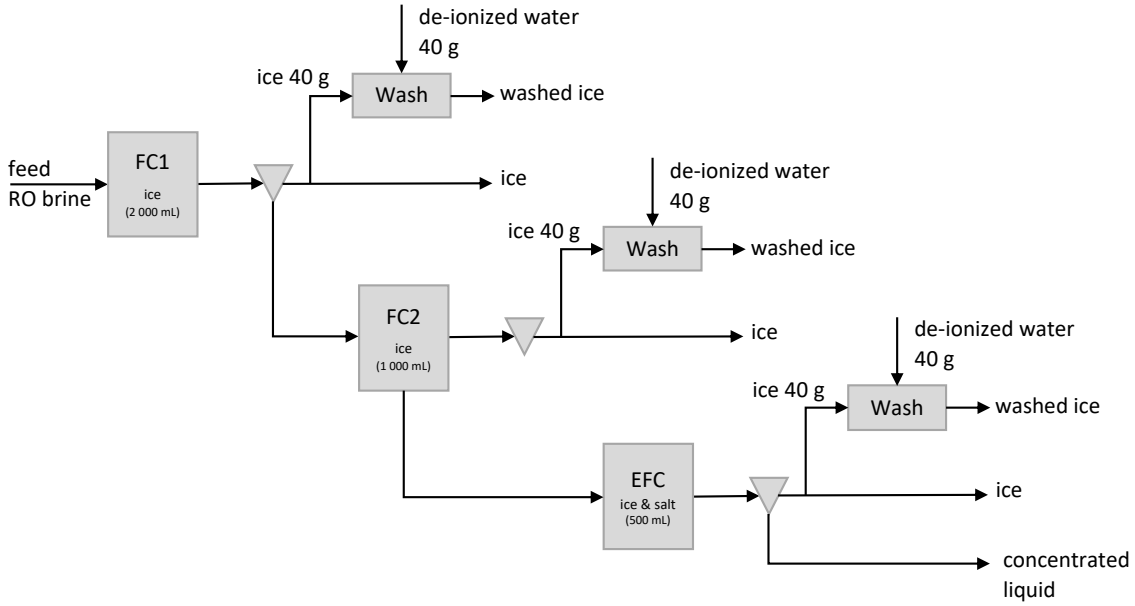

Figure F-1: Cascading EFC procedure.

Table F-2 summarizes the experimental conditions used for each freezing process, including the chiller temperature setpoints, the resulting liquid temperature, and the cooling rate. The determined ICT for each stage is also included.

Table F-2: Summary of experimental conditions

Parameter		Synthetic			Real		
		FC1	FC2	EFC	FC1	FC2	EFC
ICT		-2.95	-5.35	-10.15	-3.1	-6.99	-9.2
Start T_{Liq}		-2.8	-5.2	-9.9	-3.0	-6.9	-9.0
End T_{Liq}	(°C)	-5.5	-9	-13.2	-9.2	-9.5	-13.2
Start $T_{chiller}$		-3.45	-5.75	-10.45	-3.45	-7.45	-9.55
End $T_{chiller}$		-6.05	-10.75	-13.95	-9.95	-10.45	-14.05
Cooling rate	(°C hr^{-1})	0.2	0.5	2	0.5	0.2	2.57

F.3 Salt seeding

Figure F-2 shows the temperature profile when synthetic urine (pre-concentrated) was cooled past the predicted eutectic temperature. In Figure F-2A only ice seeds were added at -10.25°C. In Figure F-2B ice seeds were added at -10.25°C and approximately 0.15 g of Na_2SO_4 salt seeds were added at -10.5°C. The small kink in the temperature curves indicates that salt crystallization had occurred. Without salt seeding, the temperature at which salts began to crystallize was much lower and there was more variation in the crystallization temperatures. In the cases where a salt seed was added, the crystallization occurred consistently at -10.6°C. This indicates how seeding can be used to control the operation of an

EFC system. The crystallization of salts after the seeds were added does not confirm that the eutectic point of this solution was -10.6°C. This is because between the ICT and seeding a meta-stable zone exists. To determine the exact eutectic temperature further analysis would be required by adding salt crystals at different intervals between the ICT and -10.5°C. Salt seeding was used in the main EFC experiment to ensure that crystallization occurred at a consistent temperature.

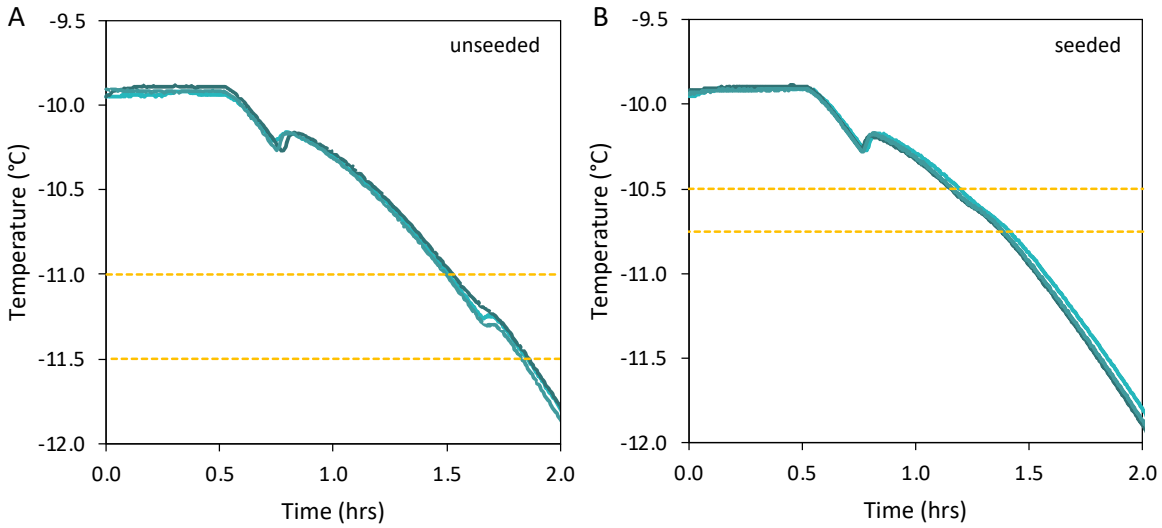

Figure F-2: Comparison of the temperature profile for the pre-concentrated synthetic urine as it is cooled without Na_2SO_4 seeding (A) and with Na_2SO_4 seeding.

F.4 Ice separation efficiency

Figure F-3A shows the mass percentage of dissolved solids recovered in the ice for real and synthetic urine and compares it to the mass percentage of the feed removed as ice in each stage, as well as the feed conductivity at the start of each stage. The figure shows that both the mass percentage of feed recovered as ice and the feed conductivity influences the mass percentage of dissolved solids recovered in the ice. Figure F-3B shows the ratio of the dissolved solids concentrations of the unwashed ice to washed ice. The unwashed ice contained between 6 and 12 times more dissolved solids. The ratio of unwashed ice to washed ice concentration for FC1-synthetic is most likely higher than for FC1-real because more dissolved solids (24%) were recovered in the real urine ice compared to the synthetic urine ice (11%). Based on these results ice washing can reduce the concentration of dissolved solids entrapped in the ice by a factor of 10.

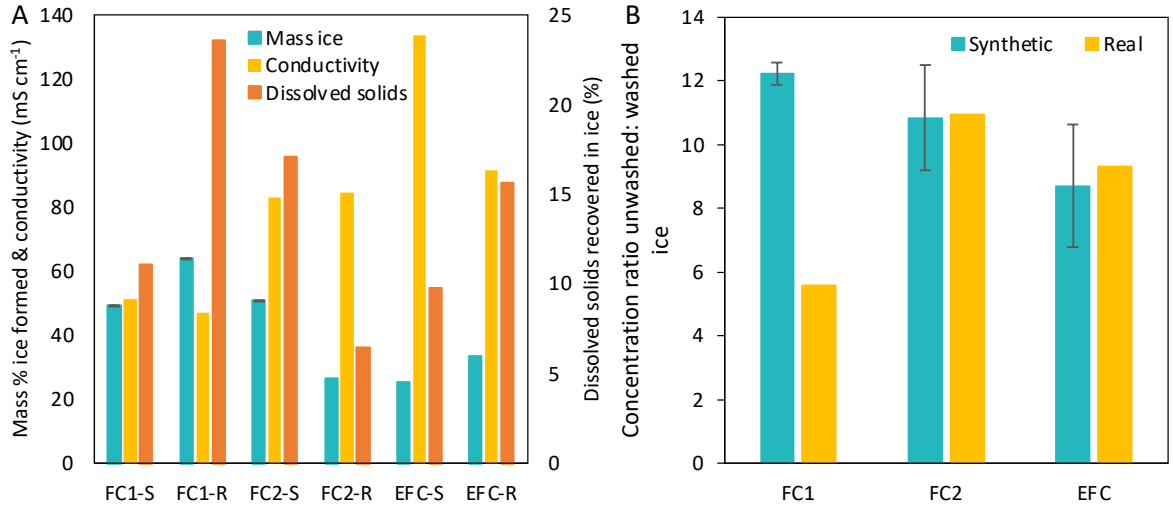

Figure F-3: Feed conductivity, mass % of feed recovered as ice, and the mass % of dissolved solids recovered in the ice (A). The ratio of the average ion concentration in the unwashed ice to the washed ice (B). For synthetic (S) and real (R) urine.

F.5 Visual representation of increasing concentration

Figure F-4 shows visually how the solution colour changed as it was concentrated using RO, FC, and then EFC. It also shows the colour of the unwashed and washed ice which gives a good visual indication of how washing removed entrapped liquid and impurities to improve the ice purity.

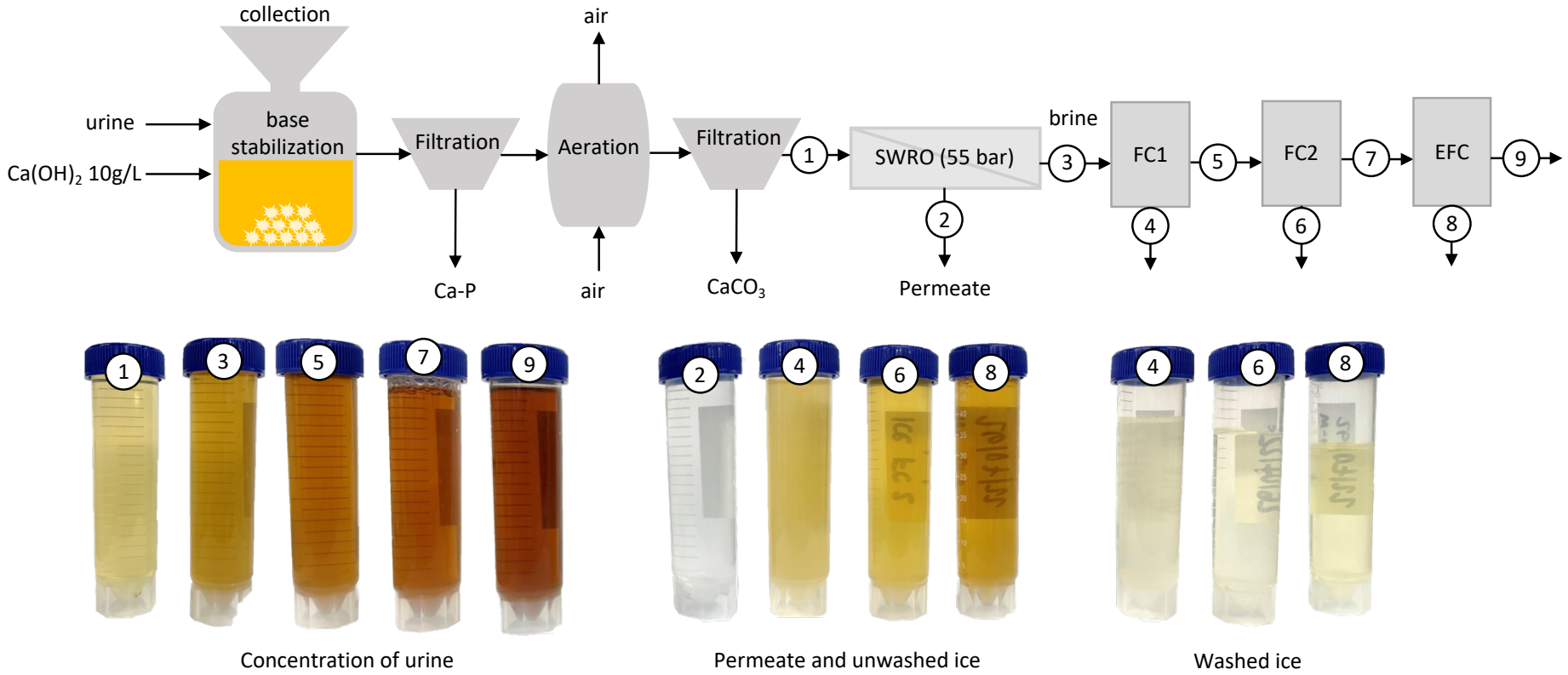

Figure F-4: Visual representation of the urine concentration and ice washing process in terms of solution colour.

F.6 Mass balance

Table F-3, Table F-4, and Table F-5 are summaries of the stream masses, volumes, densities, conductivities, and ion concentrations measured during FC1, FC2, and EFC using synthetic urine post-RO.

Table F-3: Concentration of ions measured during FC1 using synthetic urine.

Synthetic urine		FC1			
		Feed	Liquid	Unwashed ice 1	Washed ice 1
Stream mass	(g)	2057 ± 3.6	1030 ± 9.8	1 015 ± 7.0	-
Stream volume	(mL)	2000	877 ± 6.7	1 013 ± 7.6	-
Density	(g mL^{-1})	1.03	1.05	1.00	-
Conductivity	(mS cm^{-1})	51.33 ± 0.4	82.87 ± 0.9	12.94 ± 0.7	1.08 ± 0.3
TAN	(mg-N L^{-1})	384 ± 72	656 ± 69	81.4 ± 2.9	10.6 ± 1.5
Ca^{2+}	(mg L^{-1})	491 ± 4.0	879 ± 3.6	108 ± 8.7	6.1 ± 1.8
Cl^-		14 584 ± 146	25 414 ± 170	3 226 ± 123	232 ± 62
K^+		6 885 ± 177	12 497 ± 34	1 552 ± 85	118 ± 29
SO_4^{2-}		3 171 ± 72	5 746 ± 77	691 ± 45	48.4 ± 15
Urea		35 749 ± 1 294	63 787± 1 343	7 254 ± 388	526 ± 154
Na^+		7725	13 625	1763	138

Table F-4: Concentration of ions measured during FC2 using synthetic urine.

Synthetic urine		FC 2			
		Feed	Liquid	Unwashed ice 2	Washed ice 2
Stream mass	(g)	2057 ± 15.8	488 ± 2.6	521.7 ± 8.9	-
Stream volume	(mL)	2000 ± 6.1	445 ± 0.6	519.9 ± 12	-
Density	(g mL^{-1})	1.05	1.09	1.00	-
Conductivity	(mS cm^{-1})	82.9 ± 0.9	121.0 ± 1.4	32.08 ± 0.45	1.87 ± 1.1
TAN	(mg-N L^{-1})	677 ± 43	1 067 ± 50	205 ± 12	20.8 ± 9.4
Ca^{2+}	(mg L^{-1})	882 ± 3.2	1 563 ± 13.3	286 ± 3.1	18.0 ± 11.4
Cl^-		26 575 ± 511	47 935 ± 1 031	8 460 ± 212	645 ± 340
K^+		12 566 ± 52.8	22 245 ± 579	3 968 ± 113	282 ± 149
SO_4^{2-}		5 787 ± 118	10 277 ± 114	1 826 ± 42	131 ± 74
Urea		64 731 ± 792	117 825 ± 3 215	20 803 ± 469	1 452 ± 829
Na^+		14 175	24 800	4 500	38.7

Table F-5: Concentration of ions measured during EFC using synthetic urine.

Synthetic urine		EFC			
		Feed	Liquid	Unwashed ice 3	Washed ice 3
Stream mass	(g)	546.7 ± 7.2	380.9 ± 9.9	134.9 ± 5.8	-
Stream volume	(mL)	495.7± 5.6	340.3 ± 9.1	128.2 ± 4.8	-
Density	(g mL^{-1})	1.10	1.12	1.05	-
Conductivity	(mS cm^{-1})	133.4 ± 0.4	149.3 ± 1.2	69.56 ± 3.6	-
TAN	(mg-N L^{-1})	928 ± 14.4	1 154 ± 15.4	338 ± 28	50.8 ± 18.7
Ca^{2+}	(mg L^{-1})	1 632 ± 12.3	2 703 ± 26.8	568 ± 65	84.5 ± 41
Cl^-		48 691 ± 1 065	60 069 ± 492	17 468 ± 1 444	2 378 ± 1 124
K^+		21 753 ± 151	27 486 ± 1 012	8 539 ± 652	1 115 ± 526
SO_4^{2-}		10 435 ± 84	7 573 ± 212	17 535 ± 450	4 787 ± 1 367
Urea		109 987 ± 3 504	140 578 ± 4 885	38 171 ± 4 088	4 889 ± 2 133
Na^+		26 000 ± 450	32 625 ± 4 980	16 042± 72	3 390 ± 1 178

Figure F-5 shows the mass balance for the real urine treatment including stabilization, air bubbling, and RO (70% water removal).

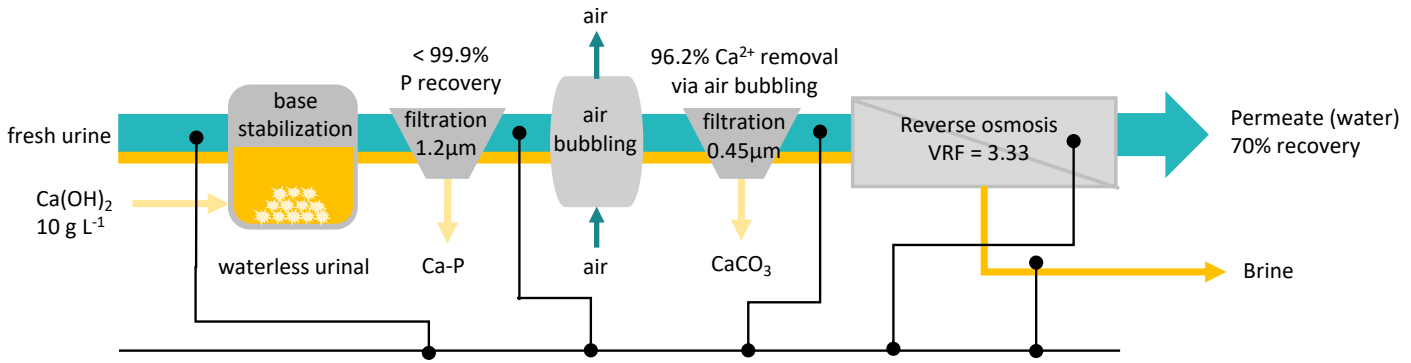

Compound	Fresh	$Ca(OH)_2$ stabilized	Pre-treated	Permeate	Concentrate
Stream vol. (L)	12.36	12.36	12.36	8.65	3.57
Urea-N (mg)	183 309	183 309	192 002	47 488	15 0897
TAN (mg)	-	95 400	1 229	178	3 137
Cl^- (mg)		44 091	44 091	487	44 184
SO_4^{2-} (mg)	14 841	14 841	14 841	29	15 387
Na^+ (mg)	24 967	24 967	24 967	231	25 158
K^+ (mg)	21 130	21 130	21 130	343	19 923
Ca^{2+} (mg)	-	18 045	2 451	0	587
Mg^{2+} (mg)	-	185.5	1	0	0
PO_4-P (mg)	-		not detectable		
COD (mg O_2)	89 919	89 919	89 919	467	80 917
Conductivity (mS/cm)	n/m	20.67	13.67	0.38	47.17

**Concentration of TAN, Ca^{2+},Mg^{2+},PO_4-P, change during stabilization and the fresh urine is stabilized during collection.*

Figure F-5: Mass balance for the treatment of the real urine with stabilization, air bubbling, and RO (70% water removal

Table F-6 is a summary of the stream masses, volumes, densities, conductivities, and ion concentrations measured during FC1, FC2, and EFC using real urine post-RO (70% water removal).

Table F-6: Concentration of ions measured during FC1, FC2, and EFC in real urine.

Real urine		FC1				FC2				EFC			
		Feed	Liquid	Unwashed ice 1	Washed ice 1	Feed	Liquid	Unwashed ice 2	Washed ice 2	Feed	Liquid	Unwashed ice 3	Washed ice 3
Mass	(g)	2084	724.9	1 337	-	709.7	515.4	187.5	-	510.8	303.7	179.1	
Vol	(mL)	2000	667	1 323	-	653.5	465.0	184.8	-	460	270	175.3	
Density	(g mL^{-1})	1.04	1.09	1.01	-	1.09	1.11	1.01	-	1.11	1.12	1.07	
Conductivity	(mS cm^{-1})	47.17	82.68	17.67	3.41	84.41	94.77	25.93	2.68	91.77	105.5	62.12	12.16
TAN	(mg-N L^{-1})	916	1 941	339	59	2 003	2 486	464	50	2 486	3 192	897	102
Ca^{2+}	(mg L^{-1})	53	121	21	9	123	158	29	n.d.	158	201	66	3
Cl^-		11.91	26.58	4.16	0.754	27.46	34.66	6.049	558	34.66	49.36	13.70	1 466
K^+		7.404	15.51	2.394	0.46	16.79	21.17	3.700	371	21.17	29.89	7.870	904
SO_4^{2-}	(g L^{-1})	4.048	8.971	1.36	0.256	9.285	12.08	2.053	181	12.08	8.658	16.95	3.836
Urea		40.32	90.79	13.95	2.372	93.37	117.7	21.14	1.827	117.7	164.1	43.71	4.199
Na^+		7.05	15.1	2.398	0.423	16.18	20.2	3.75	318	20.2	22.88	13.88	2.420
COD	(g O_2 L^{-1})	22.63	48.75	8.295	1.06	48.8	63.6	13.05	1.114	63.6	89.63	26.45	2.836

APPENDIX G:ECONOMIC ANALYSIS

G.1 Mass and energy balance

Energy requirements

Table G-1 shows the energy requirements of different treatment processes. The energy required for air bubbling was calculated and is shown in more detail in Appendix C. The energy required for NF was taken as the average value presented in three NF studies.

Table G-1: Energy requirements of different urine treatment processes used to determine the overall process energy requirements.

Treatment	Energy (kWh m^{-3})	Reference
Air bubbling	10	Calculated, Appendix C
RO	6	(Abdelkareem et al., 2018)
NF	2.3	(Liikanen et al., 2006; Mendret et al., 2019; Wafi et al., 2019)
Freezing	154.5	(Best and Vasavada, 1993b)

Mass balance assumptions

Table G-2 shows a summary of assumptions used for the energy balance calculations. The percentage water removed in each FC stage was adjusted to achieve the desired overall water removal. The urea and ion recovery in the brine was based on measured values (Figure F-5). The mass percentage of ions in the recovered ice was estimated based on the water removed in each FC step as well as the initial liquid concentration (Figure F-3). The concentration of ions in the washed ice as a function of the concentration of the ions in the unwashed ice was estimated based on the average values measured in the EFC experiments (Figure F-3). In commercial freeze concentration processes, a portion of the washed ice is melted and recycled to be used as washing liquor. Qin et al. (2009) had a wash liquid height of 8 cm in a 50 cm ice column, which is the equivalent to a recycle of 16%. However, Johnson (1976) stated that typically 5% of the washed ice is recycled as wash liquor. Therefore, an average of 10% was used.

Table G-2: Summary of assumptions for the RO-FC, RO-EFC, and FC mass balance.

Parameter		RO-FC	RO-EFC	FC (70%)	FC (95%)
Water removed (%)	Total	80%	95%	70%	95%
	RO	70%	70%	-	-
	FC1	36%	70%	48%	79%
	FC2	-	-	48%	79%
	EFC	-	50%	-	-
RO mass % ions in the brine	Urea	79.5%	79.5%	N/A	N/A
	Other	98.5%	98.5%	N/A	N/A
Mass % ions recovered in ice	FC1	25%	25%	15%	25%
	FC2	-	-	20%	30%
	EFC	-	22%	-	-
Washed ice ion concentration as a % of unwashed ice concentration				10%	
% washed ice recycled as washing liquor				10%	

As urine is concentrated its density increases. As a theoretical mass balance was conducted the density of all the streams was not known. The theoretical density was predicted using a thermodynamic model (OLI Systems Inc, 2022) as a function of water removed (Figure G-1). The water removal model was based on the generic synthetic urine composition. The predicted density was also used to convert concentration values from literature to mass percentages.

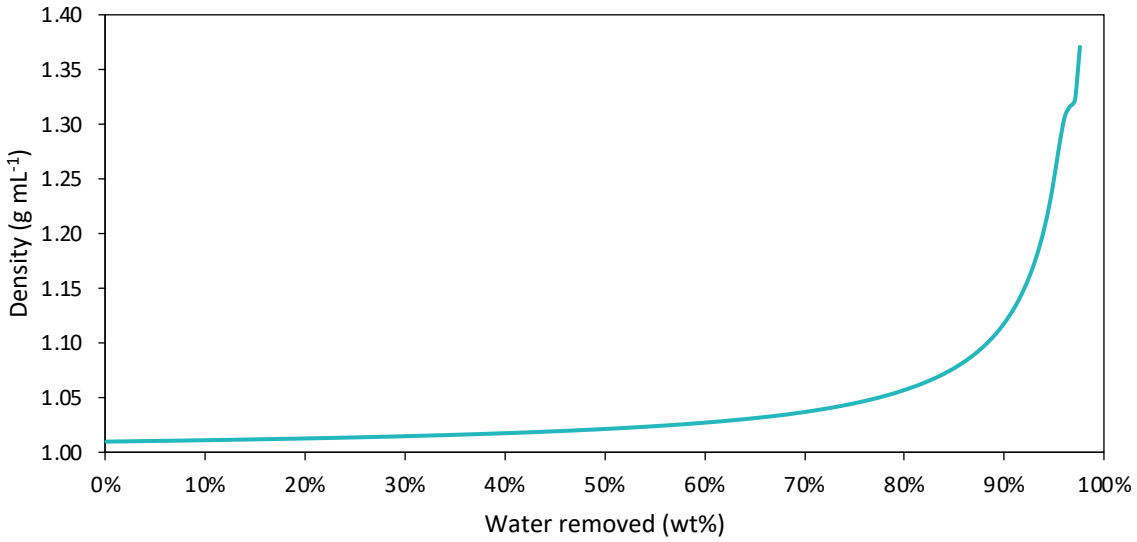

Figure G-1: Predicted urine density as a function of water removal.

Process flow diagrams and mass balances

Figure G-2 and Table G-3 show the process flow diagram (PFD) and mass balance (MB) for an RO-FC process with an overall water removal of 70%. Table G-4 shows the MB for and RO-EFC process with an overall water removal of 95%. The PFD for the RO-EFC process is available in Chapter 9 (Figure 9-5). Figure G-3 shows the PFD for an FC process and Table G-5 and Table G-6 show the mass balances for an overall water removal of 70% and 95%, respectively. The initial feed masses of urine used for each mass balance vary, however, the overall energy requirements calculated were all converted to a basis of $1m^3$ urine feed. For the FC mass balances, only a mass balance on urea was conducted. During the FC experiments, it was observed that all ions were recovered in the same proportions in the ice (if no crystallization occurred). Therefore, a mass balance on only one compound needed to be conducted as recoveries, and concentrations of other compounds could be calculated based on those determined for urea.

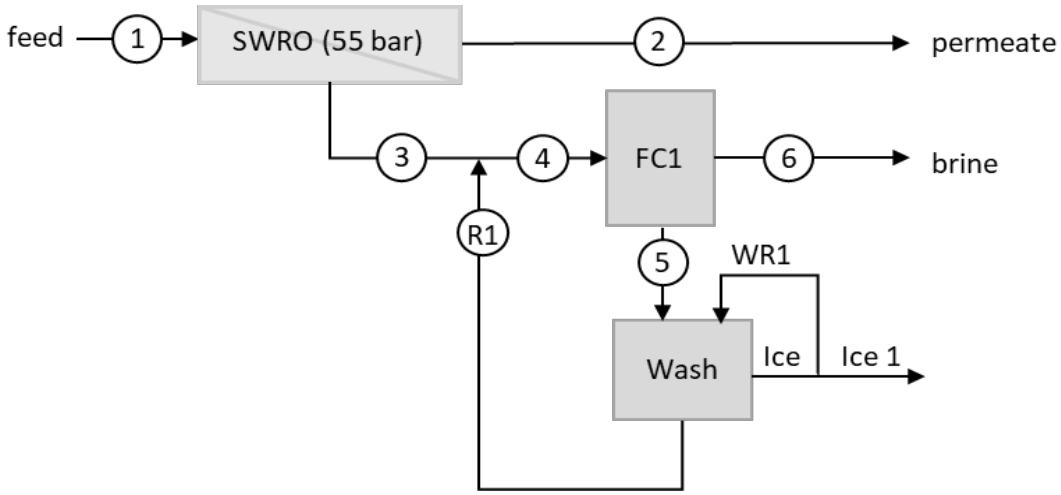

Figure G-2: Process flow diagram for the RO-FC configuration (80% water removal).

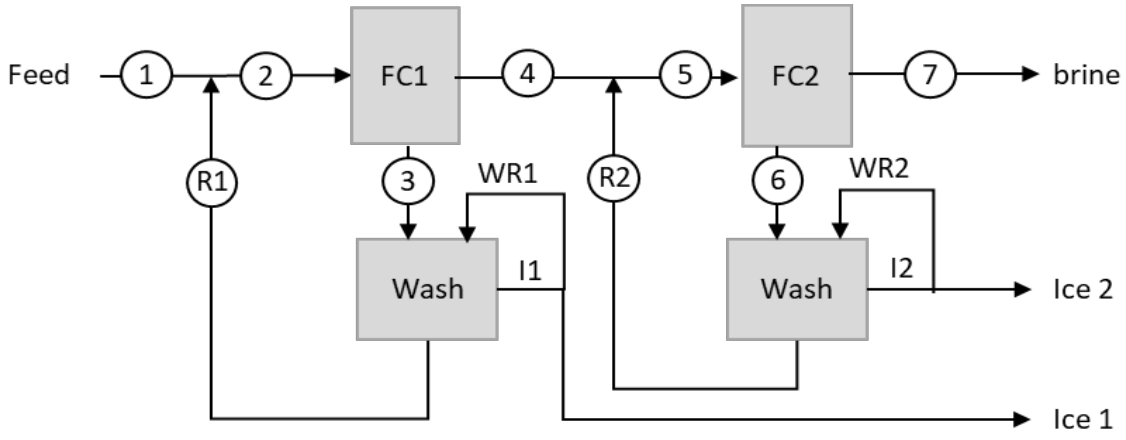

Figure G-3: Process flow diagram for the FC configuration for both 70% and 95% water removal.

Table G-3: RO-FC (80% water removal) mass balance.

Stream		1	2	3	4	5	6	R1	Ice 1	WR1	Ice
Total	g	100	70	30	31	11	20	1.0	10	1.12	11.16
	L	99	70	29	30	11	18	1.0	10	1.0	11
	g mL^{-1}	1.01	1.00	1.04	1.04	1.01	1.11	1.15	1.00	1.00	1.00
Urea	g L^{-1}	15.5	4.5	42.6	53.3	36.6	66.4	415	3.7	3.7	3.7
	g	1 552	318	1 234	1 596	399	1 197	362	36.7	4.1	40.8
Potassium	g L^{-1}	1.7	0.6	5.7	7.2	4.9	8.9	55.8	0.5	0.5	0.5
	g	169	3	166	215	54	161	49	4.9	0.5	5.5

Table G-4: RO-EFC (95% water removal) mass balance.

Stream		1	2	3	4	5	6	7	8	9	R1	R2	Ice 1	Ice 2	Salt	WR1	I1	WR2	I2
Total	g	3 215	2 250	964	1 030	721	309	324	160	152	66	15	655	146	11.3	72.8	728	16	162
	mL	3 186	2 250	927	990	712	279	292	150	121	52	13	655	146	-	73	728	16	162
	g mL^{-1}	1.01	1.00	1.04	1.04	1.01	1.11	1.11	1.07	1.26	1.26	1.15	1	1	-	1	1	1	1
Urea	g L^{-1}	15.5	4.5	42.7	51.7	18.0	137.9	164.3	70.5	308.7	222.7	752.3	1.8	7.0	-	1.8	1.8	7.0	7.0
	kg	49.83	10.22	39.62	51.25	12.81	38.44	47.96	10.55	37.41	11.63	9.525	1.179	1.026	-	0.131	1.310	0.114	1.140
Potassium	g L^{-1}	1.7	0.041	5.7	5.9	0.8	18.9	19.8	3.9	43.0	10.2	41.3	0.082	0.387	-	0.1	0.1	0.4	0.4
	g	5 416	92	5 324	5 856	586	5 271	5 794	579	5 214	532	523	53.9	56.3	-	6.0	59.9	6.3	62.6
Sodium	g L^{-1}	2.0	0.05	6.8	7.0	1.0	22.5	23.6	4.6	37.8	12.1	49.1	0.1	0.5	-	0.1	0.1	0.5	0.5
	g	6 436	109	6 327	6 958	696	6 263	6 884	688	4 581	632	621	64	67	1 614	7	71	7	74
Sulfate	g L^{-1}	1.2	0.03	4.1	4.2	0.6	13.3	14.0	2.7	2.6	7.2	29.2	0.1	0.3	-	0.1	0.1	0.3	0.3
	g	3 823	65	3 758	4 134	413	3 720	4 090	409	312	375	369	38.0	39.8	3 369	4.2	42.3	4.4	44.2

Table G-5: FC (70% water removal) mass balance.

Stream		1	2	3	4	5	6	7	R1	R2	Ice 1	Ice 2	I1	WR1	I2	WR2
Total	g	100	105	50	55	57	27	30	5	2	45	25	50.25	5.03	27.52	2.75
	L	99.0	105	50	51	54	27	27	4	2	45	25	50.25	5.03	27.52	2.75
	g mL^{-1}	1.01	1.00	1.00	1.07	1.07	1.00	1.12	1.07	1.09	1.00	1.00	1.00	1.00	1.00	1.00
Urea	g	990	1 125	149	977	1 194	239	955	135	217	14	22	15	2.0	24	2.0
	g L^{-1}	10.0	10.76	2.99	19.08	22.3	8.76	35.1	31.9	95.5	0.30	0.88	0.30	0.30	0.88	0.88

Table G-6: FC (95% water removal) mass balance.

Stream		1	2	3	4	5	6	7	R1	R2	Ice 1	Ice 2	I1	WR1	I2	WR2
Total	g	3 185	3 432	2 718	714	769	609	160	247	55	2471	554	2746	276	615	61.5
	L	3 153	3 432	2 718	667	719	609	142	231	51	2471	554	2746	276	615	61.5
	g mL^{-1}	1.01	1.00	1.00	1.07	1.07	1.00	1.12	1.07	1.09	1.00	1.00	1.00	1.00	1.00	1.00
Urea	kg	31.53	38.70	7.883	30.82	42.37	12.71	29.66	7.167	11.56	0.717	1.156	0.796	0.080	1.284	0.128
	g L^{-1}	10.00	11.28	2.90	46.19	58.94	20.87	208.6	31.03	227.4	0.29	2.09	0.29	0.29	2.09	2.09

G.2 Niche fertilizer prices

Table G-7 gives a summary of the prices of different commercially available niche liquid fertilizers used in this work. The price of the fertilizer was analyzed in terms of nutrient content to determine if there was a trend between nutrient content and price. Table G-8 gives the price per kg for various dry niche fertilizers as well as the nutrient content in each product.

Table G-7: Nutrient composition and sales price of commercially available niche liquid fertilizers found at the Stark Ayres garden center in Rondebosch, Cape Town.

Brand	Product name	N	P	K	NPK	Cost	Quantity
		(weight %)				(R L^{-1})	(mL)
Makhro	Go Organic	0.91	0.15	0.23	1.29	95	2000
Protek	Guano Flo	2.1	0.4	0.4	2.9	124.5	2000
Biogrow	Biotrissol	3.0	7.2	5.0	15.2	238	500
EHG	Grow	2.25	0.78	4	7.03	160	1000
Garden Centre	Sea Secret	5.0	0.9	2.2	8.1	264	500
Talborne	Buds and flowers	4.0	1.0	6.0	11	244	500
Efekto	SeaGro	5.3	0.7	1.7	7.7	310	500
Pokon	Geranium	6.3	2.3	5.5	14.1	318	500
Talborne	Multi Plant	5.0	1.0	2.0	8.0	244	500
Efekto	Nitrosol	8.0	2.0	5.8	15.8	399	1000
Margaret Roberts	Organic Super Charger	8.0	2.0	6.0	16	420	500
Pokon	Universal	8.0	3.0	6.0	17	340	500
Makhro	Hortisol	11	1.8	5.5	18.3	460	200

Table G-8: Nutrient composition and sales price of commercially available niche dry fertilizers found at the Stark Ayres garden center in Rondebosch, Cape Town.

Brand	Product name	N	P	K	NPK	Cost	Quantity
		(weight %)				(R kg^{-1})	(kg)
Wonder	Shake n grow	23.75	4.75	9.5	38	302	0.5
	Rose colour burst	18	9	15	42	276	
	Blue hydrangea	15	10	13	38	342	
Dr Fishers	Multifeed	19.3	8.3	15.8	43.4	412	
Culterra	Multi sol N	26.4	4.6	13.2	44.2	198	
	Multi Sol P	8.6	4.3	8.6	21.5	198	
	Multi Sol K	13.8	4.6	27.6	46	198	
	Plant food	4.6	13.8	27.6	46	318	
Garden care	Nutrifeed	6.5	2.7	13	22.2	318	
	Flowering orchid	7	9.3	24.8	41.1	290	
	Growing orchid	31	4.9	9.1	45	290	
	Hydrangea food	15	4.3	27.4	46.7	298	
	Nutrifeed	6.5	2.7	13	22.2	290	
	Plant food	14.6	4.5	27.4	46.5	218	
	Rose food	12	8.3	14.7	0	290	
	Organic 315	5	1.7	8.3	0	290	

Figure G-4A compares the fertilizer sales price as a function of the different nutrients present in niche liquid fertilizers. There was no statistically significant correlation between P and K content and the fertilizer sales price. Figure G-4B assesses dry niche fertilizers. The correlation between the sales price and the total nutrient content (NPK) improved, with an R^2 value of 0.76. However, using N-content as an indicator for sales prices had the highest correlation ($R^2 = 0.93$). For the dry niche fertilizers, there was no observable trend regardless of nutrient content and there appeared to be a relatively fixed average price. Various dry fertilizers had differing core nutrients (Table G-8). Even when only fertilizer brands with the same core nutrients were compared, there was no trend between price and nutrient content. Urine-based liquid fertilizers produced using membrane processes do not contain any P as this is recovered separately during the collection step. Therefore, if the sum of the N, P, and K content was used to calculate the fertilizers value, as there is no P, it would underpredict the sales price. This is because in a full-scale treatment process, the recovered P would be further treated and then added to the liquid fertilizer to increase the nutrient content. It was for these reasons that N content was used to predict the sales price rather than other values.

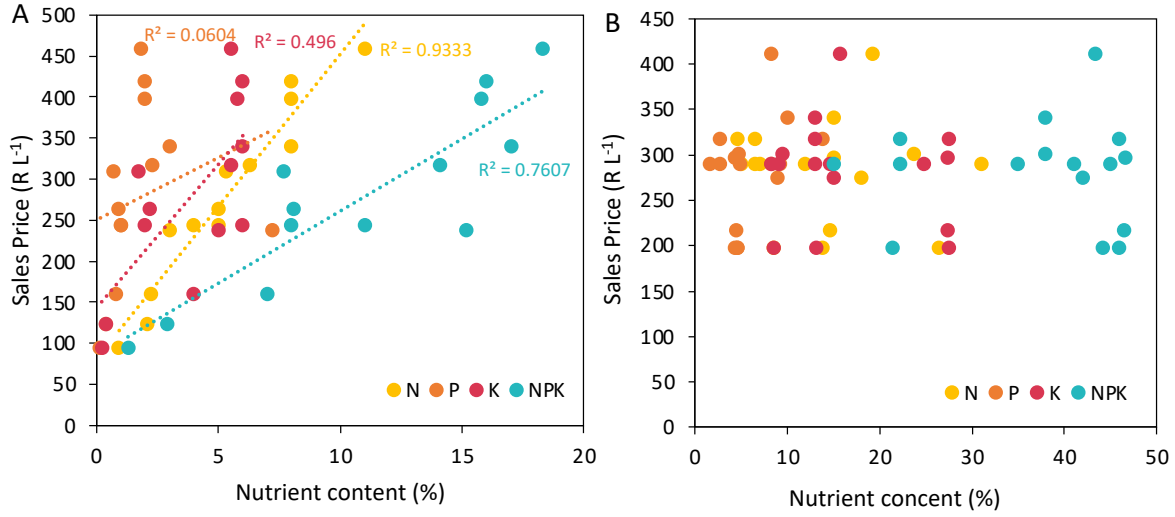

Figure G-4: Comparison of fertilizer price as a function of different nutrients in fertilizers, where NPK is the sum of different nutrients for different niche liquid (A) and dry (B) fertilizers.

G.3 Bulk fertilizer market

Table G-7 gives a summary of the assumptions used for the bulk fertilizer analysis. The assumptions in this table were used to calculate the cost of transporting fertilizer (of varying distances) as a percentage of the gross sales value.

Table G-9: Assumptions used to calculate the cost of transporting fertilizer as a percentage of its gross value.

Parameter		Value	Units	Reference
Nitrogen required		1000	kg-N per application	Basis of analysis
Petrol price		25	R L^{-1}	(AA, 2022)
Truck fuel efficiency	4-ton	6.67	km L^{-1}	(Lubbe et al., 2013)
	8-ton	3.33		
	14-ton	2.50		
	18-ton	2.22		

APPENDICES

REFERENCES

AA. 2022. Fuel Pricing [Online]. Available: https://aa.co.za/fuel-pricing/ [Accessed 15 August 2022].

Abdelkareem, M.A., Assad, M.E.H., Sayed, E.T. and Soudan, B. 2018. Recent progress in the use of renewable energy sources to power water desalination plants. Desalination 435, 97-113.

Atwood, J.L. and Barbour, L.J. 2003. Molecular graphics: from science to art. Crystal growth & design 3(1), 3-8.

Barbour, L.J. 2001. X-Seed—A software tool for supramolecular crystallography. Journal of Supramolecular Chemistry 1(4-6), 189-191.

Berg, P., Hagmeyer, G. and Gimbel, R. 1997. Removal of pesticides and other micropollutants by nanofiltration. Desalination 113(2-3), 205-208.

Best, D. and Vasavada, K. 1993. Freeze concentration of dairy products Phase 2. Final report, Dairy Research Foundation, Elk Grove Village, IL (United States).

Brison, A. 2016. Understanding the processes involved during the stabilization of urine with calcium hydroxide, ETH Zürich Zürich

E.I.A 2020 Electric Power Monthly, U.S. Department of Energy, Washington, DC.

Fidaleo, M. and Lavecchia, R. 2003. Kinetic study of enzymatic urea hydrolysis in the pH range 4-9. Chemical and biochemical engineering quarterly 17(4), 311-318.

Flanagan, C.P. and Randall, D.G. 2018. Development of a novel nutrient recovery urinal for on-site fertilizer production. Journal of Environmental Chemical Engineering 6(5), 6344-6350.

Franks, R., Bartels, C. and Nagghappan, L. 2009. Performance of a reverse osmosis system when reclaiming high pH-high temperature wastewater. American Water Works Association Membrane Technology Conference. Memphis, USA, 15-18 March. 1-16.

Fumasoli, A., Etter, B., Sterkele, B., Morgenroth, E. and Udert, K.M. 2016. Operating a pilot-scale nitrification/distillation plant for complete nutrient recovery from urine. Water Science and Technology 73(1), 215-222.

Haynes, W.M., Lide, D.R. and Bruno, T.J. 2016. CRC handbook of chemistry and physics, 95th edition, CRC Press, Florida, USA.

Herring, L.C. 1962. Observations on the analysis of ten thousand urinary calculi. The Journal of urology 88(4), 545-562.

Hug, A. and Udert, K.M. 2013. Struvite precipitation from urine with electrochemical magnesium dosage. Water Research 47(1), 289-299.

Hulatt, C.J. and Thomas, D.N. 2011. Productivity, carbon dioxide uptake and net energy return of microalgal bubble column photobioreactors. Bioresource technology 102(10), 5775-5787.

Jagtap, N. and Boyer, T.H. 2018. Integrated, multi-process approach to total nutrient recovery from stored urine. Environmental Science: Water Research & Technology 4(10), 1639-1650.

Johnson, W.E. 1976. State-of-the-art of freezing processes, their potential and future. Desalination 19(1-3), 349-358.

Jönsson, H., Stenström, T.-A., Svensson, J. and Sundin, A. 1997. Source separated urine-nutrient and heavy metal content, water saving and faecal contamination. Water science and technology 35(9), 145-152.

Liikanen, R., Yli-Kuivila, J., Tenhunen, J. and Laukkanen, R. 2006. Cost and environmental impact of nanofiltration in treating chemically pre-treated surface water. Desalination 201(1-3), 58-70.

Lubbe, P.A., Archer, C.G. and Whitehead, E.N.C. 2013. Guide to machinery costs, Department of agriculture, forestry, and fisheries, Pretoria, South Africa.

Maurer, M., Schwegler, P. and Larsen, T.A. 2003. Nutrients in urine: energetic aspects of removal and recovery. Water Science and Technology 48(1), 37-46.

Mendret, J., Azais, A., Favier, T. and Brosillon, S. 2019. Urban wastewater reuse using a coupling between nanofiltration and ozonation: Techno-economic assessment. Chemical Engineering Research and Design 145, 19-28.

Millero, F.J., Graham, T.B., Huang, F., Bustos-Serrano, H. and Pierrot, D. 2006. Dissociation constants of carbonic acid in seawater as a function of salinity and temperature. Marine Chemistry 100(1-2), 80-94.

Mitsoyannis, E. and Saravacos, G.D. 1977. Precipitation of calcium carbonate on reverse osmosis membranes. Desalination 21(3), 235-240.

Montgomery, J.M. 1985. Water treatment: principles and design, John Wiley & Sons.

Noe-Hays, A., Homeyer, R.J., Davis, A.P. and Love, N.G. 2021. Advancing the Design and Operating Conditions for Block Freeze Concentration of Urine-Derived Fertilizer. Environmental Science & Technology Engineering 2(3), 446-455.

OLI Systems Inc. 2022. OLI Stream Analyzer, version 11.0, OLI Systems Inc, New Jersey, USA.

Ozaki, H. and Li, H. 2002. Rejection of organic compounds by ultra-low pressure reverse osmosis membrane. Water Research 36(1), 123-130.

Patyk, A. and Reinhardt, G.A. 1997. Düngemittel-Energie-und Stoffstrombilanzen, Springer.

Persistence of Vision Pty. Ltd. 2014 Persistence of Vision Raytracer (V3.6).

Pronk, W., Palmquist, H., Biebow, M. and Boller, M. 2006. Nanofiltration for the separation of pharmaceuticals from nutrients in source-separated urine. Water Research 40(7), 1405-1412.

Putnam, D.F. 1971 Composition and concentrative properties of human urine, p. 112, NASA, Washington, D.C.

Qin, F.G., Yang, M.L., Yang, X.X., Chen, X.D. and Abeynaike, A. 2009. Experimental and thermal analysis of washing the packed ice bed in wash columns. AIChE journal 55(11), 2835-2847.

Randall, D.G., Krähenbühl, M., Köpping, I., Larsen, T.A. and Udert, K.M. 2016. A novel approach for stabilizing fresh urine by calcium hydroxide addition. Water Research 95, 361-369.

Ray, H., Perreault, F. and Boyer, T.H. 2020. Rejection of nitrogen species in real fresh and hydrolyzed human urine by reverse osmosis and nanofiltration. Journal of Environmental Chemical Engineering, 103993.

Riechmann, M.E., Ndwandwe, B., Greenwood, E.E., Reynaert, E., Morgenroth, E. and Udert, K.M. 2021. On-site urine treatment combining $Ca(OH)_2$ dissolution and dehydration with ambient air. Water research X 13, 100124.

SAINT. 2003. Bruker AXS Inc., p. 112, Wisconsin, USA.

Sheldrick, G.M. 2015. Crystal structure refinement with SHELXL. Acta Crystallographica Section C: Structural Chemistry 71(1), 3-8.

Sierra, E., Acién, F., Fernández, J., García, J., González, C. and Molina, E. 2008. Characterization of a flat plate photobioreactor for the production of microalgae. Chemical Engineering Journal 138(1-3), 136-147.

Simha, P. 2021. Alkaline Urine Dehydration: how to dry source-separated human urine and recover nutrients?, Swedish University of Agricultural Sciences.

Simha, P., Karlsson, C., Viskari, E.-L., Malila, R. and Vinnerås, B. 2020. Field testing a pilot-scale system for alkaline dehydration of source-separated human urine: a case study in Finland. Frontiers in Environmental Science 8, 168-178.

UCPTE. 1994 Yearly Report. 1993. UCPTE (Union pour la coordination de la production et du transport de l'électricité), Vienna, Austria.

Udert, K. 2002. The fate of phosphorus and nitrogen in source-separated urine, PhD thesis. Swiss Federal Institute of Technology, Zurich, Switzerland.

Udert, K.M., Larsen, T.A., Biebow, M. and Gujer, W. 2003. Urea hydrolysis and precipitation dynamics in a urine-collecting system. Water Research 37(11), 2571-2582.

Udert, K.M. and Wächter, M. 2012. Complete nutrient recovery from source-separated urine by nitrification and distillation. Water Research 46(2), 453-464.

Vasiljev, A., Simha, P., Demisse, N., Karlsson, C., Randall, D.G. and Vinnerås, B. 2022. Drying fresh human urine in magnesium-doped alkaline substrates: Capture of free ammonia, inhibition of enzymatic urea hydrolysis & minimisation of chemical urea hydrolysis. Chemical Engineering Journal 428, 131026.

Velts, O., Uibu, M., Kallas, J. and Kuusik, R. 2011. CO2 mineral trapping: Modeling of calcium carbonate precipitation in a semi-batch reactor. Energy Procedia 4, 771-778.

Volpin, F., Yu, H., Cho, J., Lee, C., Phuntsho, S., Ghaffour, N., Vrouwenvelder, J.S. and Shon, H.K. 2019. Human urine as a forward osmosis draw solution for the application of microalgae dewatering. Journal of hazardous materials 378, 120724.

Wafi, M.K., Hussain, N., El-Sharief Abdalla, O., Al-Far, M.D., Al-Hajaj, N.A. and Alzonnikah, K.F. 2019. Nanofiltration as a cost-saving desalination process. SN Applied Sciences 1(7), 1-9.

Wei, S.P., van Rossum, F., van de Pol, G.J. and Winkler, M.-K.H. 2018. Recovery of phosphorus and nitrogen from human urine by struvite precipitation, air stripping and acid scrubbing: A pilot study. Chemosphere 212, 1030-1037.

Xu, K., Qu, D., Zheng, M., Guo, X. and Wang, C. 2019. Water reduction and nutrient reconcentration of hydrolyzed urine via direct-contact membrane distillation: ammonia loss and its control. Journal of Environmental Engineering 145(3), 04018144.

Zöllig, H., Remmele, A., Morgenroth, E. and Udert, K.M. 2017. Removal rates and energy demand of the electrochemical oxidation of ammonia and organic substances in real stored urine. Environmental science: water research & technology 3(3), 480-491.